

From THE DEPARTMENT OF MICROBIOLOGY, TUMOR AND CELL BIOLOGY
Karolinska Institutet, Stockholm, Sweden

**IMMUNE REGULATION
DURING PULMONARY TB AND
DURING *M. TUBERCULOSIS*/
HIV-1 CO-INFECTION**

Chaniya Leepiyasakulchai



**Karolinska
Institutet**

Stockholm 2013

All previously published papers were reproduced with permission from the publisher.

Figure 5,6 and 14 were produced using Sevier Medical Art.

Published by Karolinska Institutet. Printed by Larserics Digital Print AB.

© **Chaniya Leepiyasakulchai**, 2013

ISBN 978-91-7549-276-6

“We enjoy the process far more than the proceeds”

Warren Buffett

ABSTRACT

Individually, tuberculosis (TB) and acquired immunodeficiency syndrome (AIDS) pose major global health problems and together, they form a deadly liaison. Preventive vaccines for any of the diseases are not yet available. Therefore, better understanding of protective immunity to each pathogen that cause the diseases and how co-infection influences host immune responses are urgently needed. The overall aim of this thesis was to increase our understanding of immune regulation and protective immune responses during pulmonary TB and during *Mycobacterium tuberculosis* (Mtb)/ human immunodeficiency virus-1 (HIV-1) co-infection in the mouse model.

In **study I**, we explored CD103⁺ dendritic cell (α E-DC) and CD4⁺Foxp3⁺ regulatory T (Treg) cell function during pulmonary TB. We showed that in mice resistant to Mtb infection the number of α E-DCs increased dramatically in response to Mtb infection. In contrast, highly susceptible mice failed to recruit α E-DCs even during chronic infection. Instead of producing TNF α , α E-DCs preferentially produced TGF β . In contrast to resistant mice, the Treg cell population was diminished in the lungs, but not in the draining pulmonary lymph node (PLN) of highly susceptible DBA/2 mice during chronic infection. Further, we showed that Treg cells produced IFN γ in response to infection with a virulent clinical Mtb isolate. The reduced number of lung α E-DCs and Treg cells in susceptible mice coincided with severe lung inflammation and increased bacterial burden. Our results indicated that α E-DCs and Treg cells may play a role in regulating the host immune response during pulmonary TB.

In **study II**, we further investigated the origin, tissue localization, infection rate and cytokine profile of α E-DCs during pulmonary TB. We showed that alveolar epithelial cells support monocyte survival and differentiation *in vitro*. We demonstrated that bone marrow-derived monocytes were precursors of α E-DCs in the lungs and PLN during pulmonary TB. We confirmed the localization of α E-DCs beneath the bronchial epithelial cell layer and near the vascular wall during steady state conditions, and showed that α E-DCs had a similar localization in the lungs during pulmonary TB. In addition, α E-DCs were detected in the bronchoalveolar lavage during the infection. In contrast to other DC subsets, we found that only a minor fraction of lung α E-DCs was infected with the bacterium. We also showed that virulent Mtb did not significantly alter the cell surface expression level of MHC II on infected cells *in vivo* and that α E-DCs contain the highest frequency of IL-12p40⁺ cells among the myeloid cell subsets in infected lungs. Our results support a model in which inflammatory monocytes are recruited into the Mtb-infected lung tissue and, depending on which non-hematopoietic cells they interact with, differentiate along different paths to give rise to multiple monocyte-derived cells, including DC with a distinctive α E-DCs phenotype.

In **study III**, we determined the impact of chronic Mtb infection on the immunogenicity of a HIV vaccine candidate. We found that, depending on the vaccination route, Mtb-infected mice displayed impairment in both the magnitude and in the quality of both antibody- and T cell responses to the vaccine components p24Gag and gp160Env. Mtb-infected and HIV-vaccinated mice exhibited reduced p24Gag-specific serum IgG and IgA titers, and suppressed gp160Env-specific serum IgG titers compared to uninfected HIV-1-vaccinated controls. Importantly, the virus neutralizing activity in serum of intramuscular HIV-vaccinated Mtb-infected mice was significantly decreased relative to the uninfected controls. In addition mice concurrently infected with Mtb had fewer p24Gag-specific IFN γ -expressing T cells and multifunctional T cells in the spleen. These results suggested that Mtb infection may interfere with the effectiveness of HIV vaccines in humans.

In **study IV**, we established a mouse model for Mtb/HIV-1 co-infection by utilizing the chimeric EcoNDK virus. During the time-course of the experiment, we did not detect signs of immunodeficiency. However, we confirmed that the virus was present in Mtb/EcoNDK co-infected mice at least 14 days after a single injection of the virus. In fact, the viral load was significantly higher in the lungs and in the spleen of Mtb/EcoNDK co-infected mice compared to animals infected with the virus alone. We showed that EcoNDK influence the adaptive T cell response directed towards the bacterium. We observed that the number of Mtb-specific CD8⁺ T cells was significantly increased in the spleen compared to Mtb-infected animals. Furthermore, we characterized the cell surface expression profile of T cell immunoglobulin and mucin domain-3 (Tim-3) and Program Death 1 (PD-1) on T cell subsets during TB and during Mtb/EcoNDK co-infection. Even though we did not detect any significant difference between Mtb-infected and co-infected mice, we did find that Tim-3 and PD-1 were utilized differently by CD4⁺ T cells and CD8⁺ T cell subsets. Finally, we showed that TB10.4-specific CD8⁺Tim-3⁺ T cells were enriched for both TNF α - and IFN γ -producing cells. Our murine co-infection model may be a useful tool to elucidate why pulmonary TB is such a problem in patients with HIV-1/AIDS.

LIST OF PUBLICATIONS

- I. **Failure to recruit anti-inflammatory CD103⁺ dendritic cells and a diminished CD4⁺ Foxp3⁺ regulatory T cell pool in mice that display excessive lung inflammation and increased susceptibility to *Mycobacterium tuberculosis***
Chaniya Leepiyasakulchai, Lech Ignatowicz, Andrzej Pawlowski, Gunilla Källenius and Markus Sköld
Infect Immun 2012, **80**:1128-1139.
- II. **Infection rate and tissue localization of murine IL-12p40-producing monocyte-derived CD103⁺ lung dendritic cells during pulmonary tuberculosis**
Chaniya Leepiyasakulchai, Chato Taher, Olga D. Chuquimia, Jolanta Mazurek, Cecilia Söderberg-Naucler, Carmen Fernández and Markus Sköld
PLoS One 2013, **8**:e69287.
- III. ***Mycobacterium tuberculosis* infection interferes with HIV vaccination in mice**
Lech Ignatowicz, Jolanta Mazurek, Chaniya Leepiyasakulchai, Markus Sköld, Jorma Hinkula, Gunilla Källenius, Andrzej Pawlowski
PLoS One 2012, **7**:e41205.
- IV. **A murine model of *Mycobacterium tuberculosis*/HIV-1 co-infection for studies on pathogen-specific T cell responses *in vivo***
Chaniya Leepiyasakulchai, Lech Ignatowicz, Lalit Rane and Markus Sköld
Manuscript.

TABLE OF CONTENTS

1	Introduction	1
1.1	<i>Tuberculosis (TB) and Human Immunodeficiency Virus Infection (HIV-1): Major Global Health Concerns</i>	1
1.2	<i>Primary and Latent TB</i>	5
1.3	<i>Experimental Model for TB</i>	6
1.4	<i>Pathogenesis and Immune Responses to Mtb</i>	8
1.5	<i>Immune Regulation During TB</i>	16
1.6	<i>Pulmonary DCs in Mice and Their Role in TB</i>	23
1.7	<i>Human Immunodeficiency Virus (HIV) -1</i>	25
1.8	<i>Mtb and HIV-1 Co-infection</i>	26
2	Aims of the thesis	30
3	Materials and Methods	31
3.1	<i>Study I</i>	31
3.2	<i>Study II</i>	32
3.3	<i>Study III</i>	32
3.4	<i>Study IV</i>	32
4	Results and discussion	33
4.1	<i>The Role of αE-DC during Pulmonary TB - Paper I & II</i>	33
4.2	<i>Ongoing Mtb Infection Interferes with The HIV Vaccine Response in Mice - Paper III</i>	42
4.3	<i>A Murine Model of Mtb/HIV-1 Co-infection for Studies on Pathogen-Specific T Cell Responses in vivo -Paper IV</i>	45
5	Acknowledgements	49
6	References	52

LIST OF ABBREVIATIONS

AEC	Alveolar epithelium cell
AIDS	Acquired immunodeficiency syndrome
APC	Antigen-presenting cell
BCG	Bacillus Calmette Guerin
BSL-3	Biosafety level 3
CCR5	Cysteine-cysteine chemokine receptor type 5
CD	Cluster of differentiation
CFU	Colony forming unit
COX2	Cyclooxygenase2
CXCR4	Chemokine (C-X-C motif) receptor type 4
DC	Dendritic cell
DC-SIGN	Dendritic cell-specific intercellular adhesion molecule-3-grabbing non-integrin
GFP	Green fluorescent protein
GM-CSF	Granulocyte-macrophage colony-stimulating factor
HIV	Human immunodeficiency virus
IDO	Indoleamine-2,3-dioxygenase
IFN γ	Interferon gamma
IL	Interleukin
iNOS	Inducible nitric oxide synthase
LN	Lymph node
LXA4	Lipoxin A4
ManLam	Mannose-capped lipoarabinomannan
MHC	Major histocompatibility complex
Mtb	<i>Mycobacterium tuberculosis</i>
NHP	Non human primate
NOS	Nitric oxide synthase
PBMC	Peripheral blood mononuclear cells
PD-1	Program death 1
PGE2	Prostaglandin E2
pi	Post infection

LIST OF ABBREVIATIONS (CONTINUED)

PIM	Phosphatidylinositol mannoside
PLN	Pulmonary lymph node
PPD	Purified protein derivative
RA	Rheumatoid Arthritis
SIV	Simian immunodeficiency virus
TGFβ	Transforming growth factor beta
Th	T helper cell
Tim-3	T cell immunoglobulin and mucin domain-3
TNFα	Tumor necrosis factor alpha
Treg	Regulatory T cell
TST	Tuberculin skin test
WHO	World health organization
WT	Wild type
αE	Alpha E- integrin

1 INTRODUCTION

1.1 TUBERCULOSIS (TB) AND HUMAN IMMUNODEFICIENCY VIRUS INFECTION (HIV-1): MAJOR GLOBAL HEALTH CONCERNS

Infectious diseases, particularly, HIV-1/AIDS (Acquired Immunodeficiency Syndrome) and tuberculosis (TB) are among the top ten causes of death in low and middle-income countries. TB ranks as the second cause of death from infectious disease worldwide after HIV-1 [1]. Individually, HIV-1 and TB pose major global health challenges and together, they form a deadly liaison. Either individually or synergistically, these two diseases cause substantial morbidity, mortality, negative socioeconomic impact and human suffering worldwide [2].

Mycobacterium tuberculosis (Mtb) has infected mankind for more than 4000 years. Mtb is able to cause disease in many organs but the most common form of TB is pulmonary TB. TB is a curable disease, even though drug resistance is an emerging problem. The global TB incidence declined gradually since the discovery of antibiotics against Mtb in 1940s and disappeared from the world public health agenda in the 1960s and 1970s [3]. However, resurgence of TB cases began in the early 1990s for many reasons, including the emergence of the HIV-1/AIDS and the increase in incidence of multidrug resistant (MDR) and extensively drug resistant (XDR) Mtb strains. The HIV-1/AIDS pandemic produced a sharp increase in notifications of TB cases, particularly in sub-Saharan Africa and South East Asia [4]. In parallel, TB started to re-emerge in several industrialized countries including USA [5], most western European countries and in Eastern Europe [6].

Despite attempts to stop the global TB burden by implementing TB control programs, including the Directly Observed Treatment, Short-course (DOTS) by the World Health Organization (WHO), TB remains a major global health problem especially in areas where resources are limited. Even though the number of new TB cases have been falling gradually since 2006 (Figure 1), there were an estimated 8.7 million new cases of TB and 1.4 million people died from TB in 2011 worldwide [1]. According to a WHO report, 82% of this global burden is distributed among 22 high-burden countries [1]. The highest prevalence was estimated in African, and Southeast Asian countries (Figure 2). India holds the global rank-one position in the number of incident cases of TB, followed by China, South Africa, Indonesia and Pakistan [1]. In addition, it has been estimated that 2 billion people are infected by TB and are living with latent TB.

Bacillus Calmette Guérin (BCG) is attenuated live *Mycobacterium bovis*, was first used as TB vaccine in 1921 and it is the only vaccine against TB available globally today. Unfortunately, the vaccine only protects infants from tuberculous meningitis and against miliary TB [7], and has limited protective efficacy in adolescents and adults. Finding a better vaccine is needed for global TB

prevention. Development of new vaccines, including modified and strengthened BCG vaccines, as well as novel vaccines designed for prime-boost vaccination strategies, are in the pipeline and involves several academic groups, research institutions and public-private partnerships such as AERAS and the TB Vaccine Initiative [3]. To date, there are at least 12 new vaccine candidates at different phases of clinical trial [8]. Unfortunately, no vaccine candidate has so far succeeded in providing efficient protection. This indicates that we need better understanding of the components of protective immune responses against Mtb.

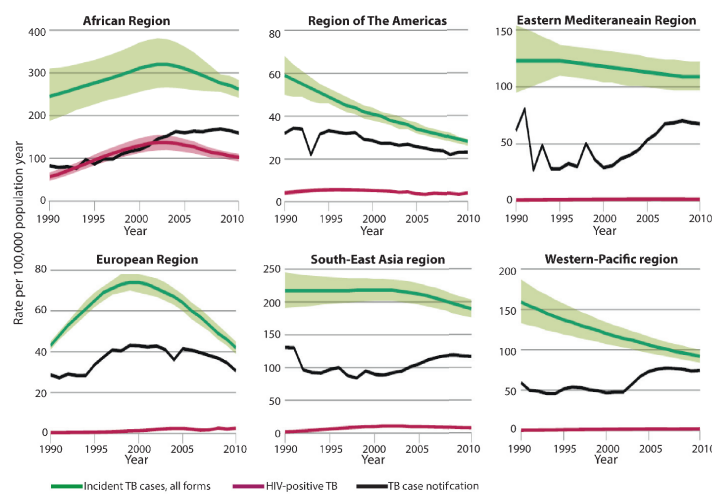


Figure 1. Recent trends in TB incidence and case notification rates data. *Adapted from Ref[1].*

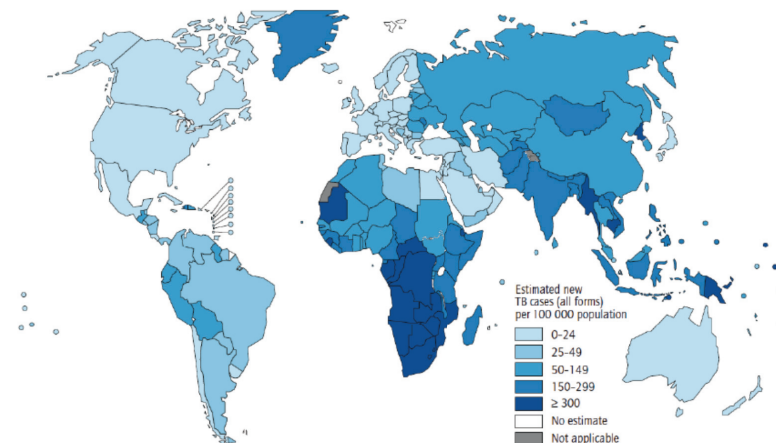


Figure 2. Estimate TB incident rate, 2011. *Adapted from ref [1].*

HIV-1 is a lentivirus and was recognized as the etiologic agent of AIDS more than 30 years ago, a century after the identification of Mtb. HIV-1 is transmitted by blood, semen, vaginal fluids and breast milk. HIV-1 preferentially infects immune cells, especially CD4⁺ T cells, and causes a significant reduction in the number of CD4⁺ T cells resulting in serious weakening of the immune system. AIDS is a lethal disease associated with opportunistic infections, i.e. viral infections, fungal and bacterial infections, particularly Mtb. In addition, due to the immunosuppressive condition, AIDS patients develop autoimmune diseases and endocrine disturbances [9].

The global AIDS epidemic peaked in 1999 and has been steadily declining. According to UNAIDS, the Joint United Nations Program on HIV-1/AIDS, the overall growth of the global aids epidemic appears to have stabilized. This is due to various factors including preventive efforts, behavioural change, and better access to treatment. Even though the number of new infection has been falling in many countries, the number of new infections overall are still high with approximately 2.5 million new cases of HIV-1 infection in 2011 [10]. This was 20% lower than that in 2001. The HIV-1 incidence declined in 39 countries by more than 25% between 2001 and 2011 (Figure 3), most of which are in sub Saharan Africa. Despite the appreciated decrease in infection rates, sub-Saharan Africa continues to be heavily affected by HIV-1 and accounted for 72 % of all new HIV-1 infections in 2011. Although there are improvements in most countries, there were still at least 9 countries; most are in Asia and South East Asia, where the incidence increased by more than 25 % from 2001 to 2011 (Figure 3). Since the first cases were reported in 1981, the global HIV-1 epidemic has caused over 30 million deaths and left an estimated 34 million individuals living with HIV-1 at the end of 2011. In addition, due to the significant scale up of antiretroviral therapy in low- and middle-income countries over the past few years, the number of AIDS related deaths has been falling. Approximately, 1.7 million people died due to HIV-1/AIDS in 2011, down 24% from the peak in 2005 [10].

Many advances have been made in the prevention of HIV-1 transmission and management of HIV-1/AIDS, i.e. the development of highly sensitive and specific HIV-1 screening tests [11] which could successfully eliminate HIV-1 transmission by blood transfusion, antiretroviral drugs [12, 13] which can stop the replication of HIV-1 and delay the symptoms, turning HIV-1 infection into a chronic condition instead of a rapidly terminal illness. Despite the advances, HIV-1 remains a major public health challenge.

There is strong evidence that the risk of TB among HIV-1 infected individuals is significantly higher than the general population. A WHO report with data from 64 countries revealed that HIV-1-infected people are over 20 times more likely to develop active TB than HIV-1 negative individuals in settings with a generalized HIV-1 epidemic. In countries with low HIV-1 prevalence, the risk was 26–37 times that of HIV-1 negative individuals. Globally, about 13% of TB cases occur among people infected with HIV-1 (>50%) in some African countries [1].

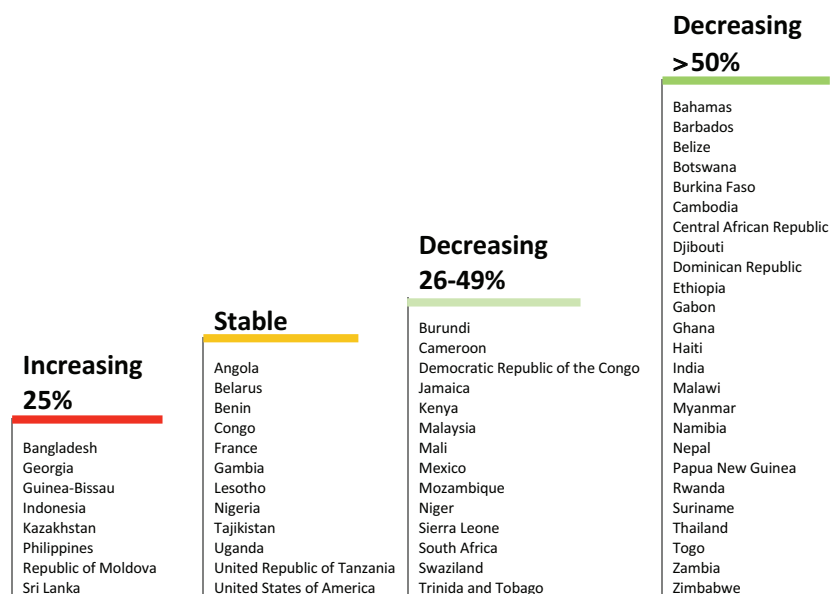


Figure 3. Change in TB incidence rate of HIV-1 infection among adults 15-49 years old, 2001-2011, selected countries. *Redrawn from ref [10].*

The burden of co-infection is particularly high in sub-Saharan Africa, and is of growing concern in Asia. TB is a major cause of death among people living with HIV-1, whose impaired immune systems make them particularly susceptible to TB. Co-infection with both microorganisms accelerates disease development, worsens the pathogenesis and amplifies the transmission of TB. 430,000 of the 1.4 million people that died from TB in 2011 were HIV-1 positive (30%) [1].

In conclusion, despite the significant increase in financial support and recent progress addressing HIV-1 and Mtb, these two pathogens continue to be linked in a global pandemic and a global health concern. Preventive vaccines are not yet available for any of the pathogens. The current challenge is to find ways of controlling both TB and HIV-1, and to improve diagnosis and management of co-infection. Therefore, better understanding of how Mtb and HIV-1 interacts individually, or synergistically, with the host immune system is urgently needed.

1.2 PRIMARY AND LATENT TB

The acid-fast bacillus, *Mycobacterium tuberculosis*, was first identified by Robert Koch in 1882 as the causative agent for TB. TB is an airborne disease transmitted through inhalation of air droplets containing Mtb that are expelled when a patient with active TB coughs or sneezes. Various outcomes following exposure to Mtb can be predicted as shown in Figure 4 [14]. After Mtb exposure, only about 30% of individuals become infected [14, 15]. Approximately, 5–10% of infected individuals subsequently develop clinical disease (Primary TB) within 1 or 2 years, whereas the rest (90%–95%) will contain the bacteria and present no disease symptom, which is defined as latent TB. This latent state is maintained by host immune responses initiated after Mtb exposure. Reactivation of latent TB, or post-primary TB, develops later in life and can be caused either by reactivation of bacteria persisting from the initial infection or by failure to control a subsequent reinfection. The lifetime reactivation risk is about 10% in healthy adults and can occur at any time in life, but usually occurs within 2–5 years after infection. The risk factors such as malnutrition, diabetes, aging, smoking, alcohol, chronic diseases, and HIV-1 infection greatly contribute to the reactivation of the disease [1].

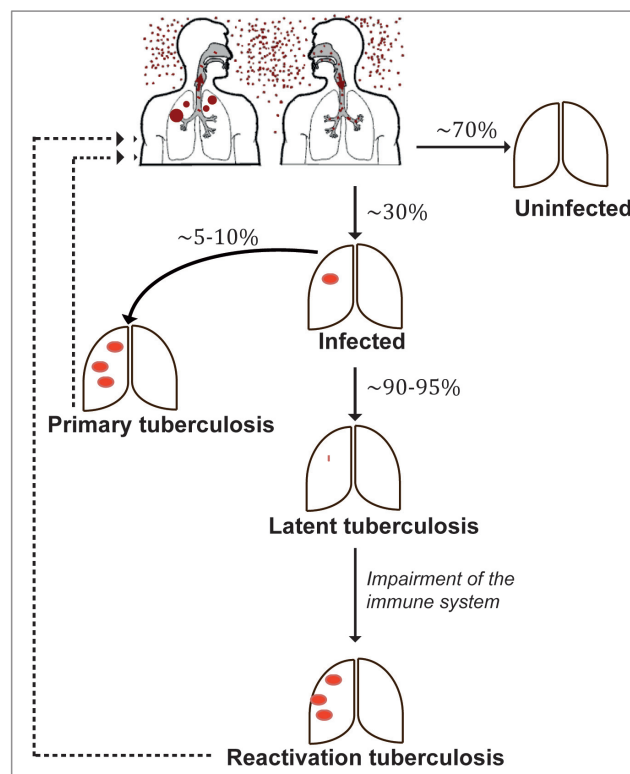


Figure 4. Outcome after Mtb exposure. *Adapted from ref [14].*

Primary and post primary TB may have distinct clinical presentations. The combination of symptoms and examination findings may range from systemic responses such as fever, weight loss and night sweats, to local consequences of the infection in the lungs such as cough and hemoptysis. Chest X-ray shows radiological abnormalities such as hilar lymphadenopathy and lung cavities or densities due to pathogenesis in the lungs [16]. Post primary TB is predominantly a pulmonary disease, involving extensive damage to the lungs and efficient aerosol transmission of bacteria, but can also present as extrapulmonary, or miliary TB. On the other hand, patients with latent TB are asymptomatic and cannot spread Mtb to other persons [14, 17].

Diagnosis of latent TB has been attempted by using the tuberculin skin test (TST) where the cell-mediated immune response can be determined after intradermal injection of purified protein derivative (PPD) antigens. A positive response leads to an induration in the skin due to a delayed-type hypersensitivity reaction, 48-72 hours after the injection. However, the TST test gives low specificity since BCG-vaccinated individuals, or environmental mycobacterial exposed individuals, also respond to PPD. This is because PPD antigens are prepared from culture filtrates of Mtb, which are also found in the attenuated BCG vaccine and in many environmental mycobacteria [18]. More recently, the IFN γ release assay (IGRA) was developed to determine immune responses that are specific against Mtb. Early secretory antigen target-6 (ESAT-6) and culture filtrate protein (CFP-10), that are absent in BCG and most environmental mycobacteria, are proteins used in IGRAs to determine IFN γ production by antigen-specific T cells [19]. The IGRA test offers improved specificity and sensitivity [18]. In addition, it is a non-invasive test compare to TST test since the IGRA only requires whole blood or peripheral blood mononuclear cells (PBMCs).

1.3 EXPERIMENTAL MODEL FOR TB

Animal models have contributed greatly to our understanding of TB. No single animal model can completely mimic human TB since human TB exhibits a complex disease spectrum. Each animal model provides pros and cons. The choice of which model to use for these studies depends on the research questions, as well as on practical issues i.e., cost, availability, biosafety level 3 (BSL3) animal housing, ethical considerations and reagent availability. Several excellent animal models are available including mice, guinea pigs, rabbits, non-human primates (NHP) and fish.

1.3.1 The mouse model

Mice are widely used to study various aspects of TB: the study of Mtb mutants, host immune responses and to determine the effectiveness of drugs and vaccine candidates. This is because mice offer ease of manipulation and housing,

numerous inbred strains, availability of mutants and genetically altered strains, as well as a wide range of available reagents.

Mice on the C57BL/6 and BALB/c genetic backgrounds are most commonly used in mycobacterial research. The most physiologically relevant way, which mimics the natural route of infection in human, is by aerosolization of the microorganism for respiratory infection. Aerosol infection is performed by exposing the mice to air droplets containing Mtb, which is generated by a nebulizer. The dose of infection can be manipulated by varying the concentration of bacteria in the nebulizer or time of exposure. Following low dose aerosol infection (50-200 colony forming units (CFU) per mouse) there is an increase in the number of live bacteria in the lungs that reaches a peak by week 4 post infection (pi) (10^5 - 10^7 CFU) and then plateaus for several months [20]. The bacteria first disseminate to the mediastinal lymph nodes [21] and then to other organs. Eventually, with slow progression of pathogenesis, even resistant mice succumb to the infection within a year [22, 23]. Studies on the induction of the adaptive immune response are usually performed during the first 3-4 weeks after infection when the number of CD4⁺ and CD8⁺ T cell reaches a peak in the lungs [20].

Following low dose Mtb aerosol infection, different mouse strains display various degree of susceptibility to TB. C57BL/6 and BALB/c mice are considered relatively resistant to Mtb infection whereas DBA/2 mice and other strains are more susceptible (Table 1). However, when the bacteria is given systemically to BALB/c mice via the intravenous route, and not localized to the lungs, BALB/c mice are considered susceptible to Mtb. Susceptible mice succumb to Mtb infection rapidly due to extensive lung tissue damage and inability to control bacterial growth. In contrast, resistant mice control bacterial growth better, display less lung tissue damage, form granuloma-like structures and live longer after Mtb exposure [24].

Table 1. Inbred mouse strains used in tuberculosis research. *Adapted from ref [24].*

Resistant	Intermediate	Susceptible
A/Sn	BALB/c	129/Sv
BALB/c		A/I
C57BL/10		C3Hc *
C57BL/6		CBA
		DBA/2
		I/St

*Including C3H/HeJ, C3H/SnJ, C3H/ HeOuJ, C3HeB/FeJ and C3H.SW-H2b

The mouse model has contributed immensely to our understanding of the immune mechanisms that control Mtb infection. For example, studies using inbred mice with deletions in genes encoding the cytokines IL-12, IFN γ [25, 26], or TNF α [27] showed that these immune factors are essential for controlling Mtb infection. These findings in the mouse model have been translated into patient studies where TNF α [28], IL-12, and IFN γ have been shown to be critical for preventing TB in humans [17].

Although the advantages of using mice in TB studies are pronounced, there are limitations. For example, latent Mtb infection is difficult to model in mice. In humans, the initial infection is usually controlled by host immune responses resulting in no detectable bacteria and no symptoms. In resistant mice, although the infection is controlled for some time, bacterial numbers are not reduced and remain relatively high. Also, the pathogenesis in the lungs is progressive throughout the course of infection. However, a latent model (the *Cornell* model) in mice was developed in the 1950s and is still being used today. The *Cornell* model is an attempt to mimic latent Mtb infection in mice in which the animals are infected with Mtb, followed by a short antibiotic treatment regimen (isoniazid and pyrazinamide), resulting in no detectable bacilli by culturing tissue lysates [29]. After antibiotic treatment, reactivation of the infection can occur spontaneously, or in response to immunosuppressive agents [29-31]. There is little evidence that this model actually reflects human latent TB [32].

TB pathology in mouse lungs is different from the pathology observed in humans. The human granuloma is usually a well-circumscribed structure composed of lymphocytes surrounding macrophages. In contrast, the mouse granuloma comprises loose non-necrotic aggregates of macrophages and lymphocytes and do not form into the classical granuloma structure seen in human TB. The granuloma in mice although progressive, does not result in caseous necrosis and cavity formation. However, some susceptible mouse strains such as C3HeB/FeJ [33-35], inducible nitric oxide synthase (*NOS*) 2^{-/-} mice develop highly organized encapsulated necrotic lesions [36].

1.4 PATHOGENESIS AND IMMUNE RESPONSES TO MTB

The outcome of Mtb infections depends on the interaction between the bacteria and the host immune system. During the infection, these interactions can lead to pathogen control and establishment of latent infection, or progressive disease. Based on experimental models, Zuniga *et al* [37] have proposed that TB pathogenesis can be divided in four well-defined events.

1. **Inhalation of the mycobacteria:** interaction with resident macrophages through cellular receptors and internalization of the bacteria.
2. **Inflammatory cell recruitment:** recruitment of immune cells and induction of the production of pro-inflammatory cytokines.

3. **Control of mycobacteria proliferation:** arrival of adaptive immune cells to the site of infection.
4. **Post primary TB:** mycobacteria persistence associated with a failure in the immunosurveillance system.

1.4.1 Mtb enters into the host cells and arrests phagosome maturation

Once the bacteria reach the lung parenchyma, it is generally accepted that resident alveolar macrophages encounter and take up the bacteria first [38]. After this, dendritic cells (DCs), macrophages, and neutrophils also take part in the phagocytic process [39-41]. In fact, in low dose aerosol-infected mice, Wolf AJ *et al* showed that Mtb can infect various myeloid cell subsets and that CD11b⁺/CD11c⁺ cells [39], which contains both myeloid DC and activated macrophages [42], contained the highest percentage of infected cells. The result from our study (Study II) revealed that the dominant infected population in the lungs was CD11b⁺/CD11c⁺ cells, which contains neutrophils and small macrophages [43]. Although Mtb preferentially infects phagocytic cells, it may also interact with nonprofessional phagocytic cells, such as alveolar epithelial cells [44] and mesenchymal stromal cells [45].

Endocytosis of Mtb involves numerous receptors such as macrophage mannose receptor (MMR), the main receptor on macrophages, recognizes mycobacterial cell wall components like lipoglycan, mannose-capped lipoarabinomannan (ManLAM) and phosphatidylinositol mannosides (PIM) [46]; Complement receptor (CR) on phagocytic cells such as CR3 and CR1 involved in complement-opsonized Mtb uptake by which Mtb cell wall components activate the alternative complement pathway and are opsonized by C3b and iC3b; DC-specific intercellular adhesion molecule 3-grabbing nonintegrin (DC-SIGN), a major uptake receptor in human DC, recognizes ManLAM, PIMs, arabinomannan and lipomannan (reviewed in reference [46] and [47]). In addition, Scavenger receptors (SRs) also play a role in Mtb binding and uptake [48].

Once the bacteria are internalized, the phagosome fuses with a lysosome to digest the bacteria. The dogma is that Mtb is an intracellular bacillus able to manipulate, persist and replicate within infected cells, particularly professional phagocytes. Virulent Mtb is able to arrest phagosomal maturation by preventing phagolysosomal fusion, inhibiting acidification of the phagosomal compartments [38] and thereby adapting to the intracellular environment of the macrophages and creating a niche for survival. However, there is evidence showing that the bacteria escape into the cytosol [49-51]. It was recently emphasized by Houben and colleagues that translocation from phagolysosomes into the cytosol compartment of human macrophages and DCs requires the ESX-1 (type VII) secretion system expressed by virulent Mtb [52]. ESX-1 has been proposed to be a bacterial virulent factor that helps disseminate the bacterium by causing phagosomal rupture, inhibiting cell apoptosis and promoting necrosis of the cell and enhancing cell-to-cell spread [53].

In addition, much research is focusing on how Mtb modulates host macrophages to benefit the bacterium itself. One interesting finding is that virulent Mtb strains could inhibit apoptosis and promote necrosis of infected macrophages [54]. Apoptosis is a form of cell death in which plasma membrane integrity is preserved and so called apoptotic vesicles are formed. It is considered an innate host defence mechanism that allows DC to take up the infected apoptotic body and prime naive T cells through a process known as cross-priming/cross-presentation, which may stimulate naive CD8⁺ T cells more efficiently. In contrast, necrosis is the process of cell death characterized by plasma membrane disruption that induces inflammation. In the context of Mtb infection, necrosis of the infected macrophages releases the bacteria that can infect neighbouring cells (Figure 5). The inhibition of apoptosis by virulent Mtb strains was later found involve the balance in biosynthesis of prostaglandin E2 (PGE2) and Lipoxin A4 (LXA4) in the host cells. PGE2 acts as a pro-apoptotic lipid mediator, which protects against necrosis and it is important for stimulation of membrane repair mechanisms. In contrast, LXA4 is a pro-necrotic lipid mediator that suppresses PGE2 synthesis, resulting in mitochondrial damage and inhibition of plasma membrane repair mechanisms and leads to the induction of necrosis [55]. Virulent Mtb inhibits apoptosis and promotes necrosis of infected macrophages by stimulating the production of LXA4 that inhibits the cyclooxygenase (COX2) production and thus effectively shuts down PGE2 biosynthesis [56, 57]. In conclusion, three major outcomes following Mtb infected human or murine macrophages can be predicted, namely necrosis, apoptosis, and survival of infected macrophages [58].

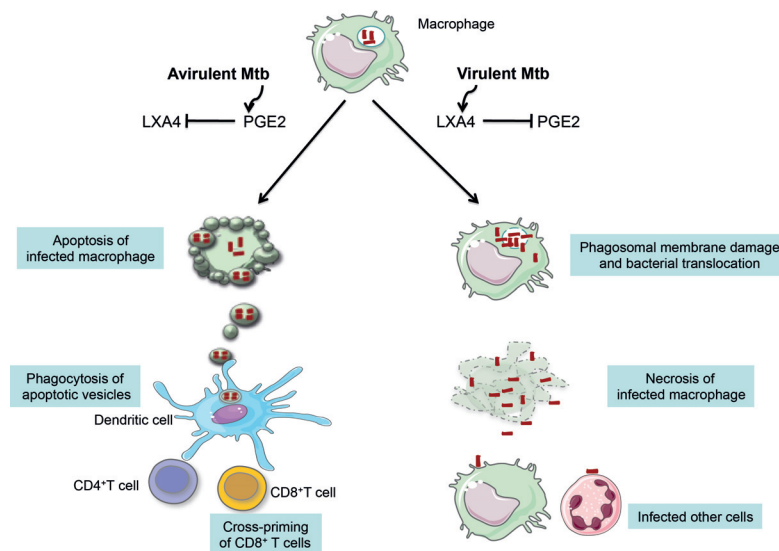


Figure 5. Mycobacterium modulate the host macrophage. *Adapted from ref [57].*

1.4.2 Innate immune response in TB

A study using the mouse model indicated that early innate immunity (within the first 3 weeks of infection) could kill a substantial number of mycobacteria despite unsuccessful complete clearance of the pathogen [59]. The bacteria that escape the initial intracellular destruction can multiply and disrupt the cells, after which chemokines attract uninfected monocytes and other inflammatory cells to the lungs [38]. These recruited monocytes give rise to various myeloid cell types, i.e. macrophages and DCs [42] and are ready to take up the bacterium [39, 60]. IL-8, which attracts neutrophils and monocytes [61], monocyte chemoattractant protein 1 (MCP-1), which acts on monocytes, macrophages and NK cells [62], are examples of important chemokines that help inflammatory cell-trafficking upon Mtb infection. Eventually, newly recruited cells are infected by Mtb at the site of infection. Studies using the zebrafish model have shown that bacteria that are released from the cell that was initially infected can infect more than two previously uninfected cells and amplifying the number of infected cells *in vivo* [63]. The zebrafish model has also provided data showing that recruited innate immune cells are able to form the initial granuloma-like structure without involving adaptive immune cells [64].

The initial immune activation starts with recognition of Mtb products by pattern recognition receptors (PRRs). PRRs are the primitive part of the innate immune system and could identify pathogen-associated molecular patterns (PAMPs), which are associated with microbial product or cellular stress. Mycobacterial products can be recognized by both extracellular and intracellular PRRs. Toll-like receptors (TLR), membrane-bound PRRs, are essential for microbial recognition on macrophages and DCs [65]. Of the 11 TLRs identified to date, TLR-2, TLR-4, TLR-9 are involved in recognition of Mtb products. TLR-2 recognizes cell wall glycolipids such as ManLAM and PIMs, while TLR-4 and TLR-9 recognize heat shock protein 60/65 and unmethylated CpG motifs in bacterial DNA, respectively. In addition, the intracellular receptors nucleotide-binding oligomerization domain (NOD) 1 and NOD2 are able to recognize bacterial peptidoglycan. C-type lectins and DC-SIGN, other important receptors in the PRR family, serve both as receptors for bacterial recognition and uptake [66].

Following recognition of Mtb antigens, the intracellular signalling cascades are activated and lead to activation of the transcriptional factor NF- κ B. Finally, cytokines are released, which in itself triggers further cell activation and cytokine production.

1.4.3 Adaptive immune response to Mtb infection

As mentioned earlier, Mtb can infect many myeloid cell subsets soon after aerosol infection. Animal models have shown that lung DCs can be infected *in vivo*. Migratory DCs could transport live mycobacteria or apoptotic vesicles containing mycobacterial antigens to the draining pulmonary lymph node (PLN) and prime naïve T cells [21, 67, 68]. T cell priming requires expression of peptide antigen in

the context of MHC, co-stimulatory molecules, and the necessary cytokines, i.e. IL-12 that promote the induction of a Th-1 phenotype. Since the cell wall of mycobacteria contains lipids and glycolipids, in addition to presentation of peptide antigens via the MHC pathways, various lipid antigens could be presented by CD1 molecules to CD1-restricted T cells [69-71]. As a result of priming, by DCs, effector T cells develop in the PLN and migrate to the site of infection where they can exert their functions to control Mtb infection [21, 72].

In humans, the onset of adaptive immune responses in TB is considerably delayed compared to other pathogens [73]. Studies of TB in isolated communities, where naïve populations were briefly (≤ 24 h) exposed to a patient with active pulmonary TB, showed that immune responses to Mtb (measured as skin test reactivity using the Pirquet test) occurred on an average 42 days after exposure [16, 74]. Experimental animal models suggest that, depending on the mouse strain, DCs requires 8-9 days to migrate to the draining lymph node (LN) after aerosol infection [21, 67]. Priming of T cells in the draining PLN does not occur before day 10 pi [21, 67, 68], and the migration of effector T cells to the site of infection requires 15–18 days [68]. This delay is greatly different from other lung infections such as influenza, where virus-specific cytotoxic T cells were seen as early as 2-3 days pi in the mediastinal LN [75]. The reason for the delayed T cell response is unclear. However, the delay in the CD4⁺ T cell response is likely to allow the bacteria sufficient time to establish persistent infection. Multiple possible explanations for the delayed T cell response have been proposed:

- Delayed migration of professional antigen-presenting cells (APCs) from the infected lungs to PLNs [67].
- Mtb interferes with antigen presentation by down modulating the co-stimulatory molecule CD86 on macrophages [76]. The Mtb lipid cell wall component Trehalose 6,6'-dimycolate (TDM) was found to reduce the expression of MHC-II, CD1d and CD40 on mouse bone marrow-derived macrophages *in vitro*. Also, TDM suppressed macrophage presentation of the Mtb antigen Ag85B [77].
- Mtb inhibits macrophage and neutrophil apoptosis [55-58] that delays activation of naïve antigen-specific T cells.
- Foxp3⁺CD4⁺ regulatory T (Treg) cells can inhibit [78, 79] and delay the arrival of effector T cells in the lungs during early TB [78].
- IL-10: study from BCG infected IL-10^{-/-} animals demonstrated that IL-10 inhibited the migration of BCG infected DCs to the draining LN and suppressed IL-12 production [80].

Once the onset of adaptive immune response is established, it is clear that there is an influx of effectors cell in the lungs [81].

1.4.3.1 CD4⁺ T cells

It is well established that CD4⁺ T cells are crucial in the control of TB infection in both humans and mice [82, 83]. Experimental data from the murine model revealed that MHC-II-deficient mice, and *in vivo* CD4⁺ T cell-depleted mice, rapidly succumbed to infection [26, 84-86]. This is further validated by the fact that HIV-1-infected individuals, with associated loss of CD4⁺ T cells, are at an increased risk of TB reactivation and new Mtb infection. Several CD4⁺ T cell subsets play a role in immune responses against Mtb infection. For example, Th1, Th2, Th17 and Treg cells [78, 79]. The best characterized are Th1 cells, which depend on the cytokine IL-12 and the transcription factor T-bet. The primary effector function of Th1 cells is to produce IFN γ , TNF α , IL-2, which are important for macrophage activation by induction of nitric oxide synthesis and potentiating the killing ability of the macrophages [26, 83, 87]. Interestingly, effector Th1 cells can also produce multiple cytokines (IFN γ , IL-2, TNF α) at the same time and are referred to as multifunctional T cells. These cells are thought to be functionally superior to T cells that only produce one of the cytokines [88]. The exact role of multifunctional T cells in TB is unclear. They are thought to be associated with better control of Mtb growth in humans [89]. However, patient studies have shown that TB patients with active disease elicited a significantly greater number of multifunctional T cells compared to latently infected individuals, or household contacts [90, 91]. In addition, these cells were induced in many murine TB vaccine studies [88, 92] and were found associated with better protection. Not only are they able to produce protective cytokines, human CD4⁺ T cells are also able to secrete granulysin, and perforin to perform cytolytic function [93]. Furthermore, CD4⁺ T cells help maintain optimal cytotoxic CD8⁺ T cell responses [94].

Another CD4⁺ T cell subset that produce the signature cytokine IL-17, Th17 cells, are also induced during mycobacterial infections [95]. IL-17 is a pro-inflammatory cytokine driving the recruitment of effector cells, such as neutrophils, and participating in the activation of macrophages. IL-17-producing CD4⁺ T-cells are present in mycobacterial granulomas [96]. Published data indicated that repetitive subcutaneous BCG vaccination in Mtb-infected mice results in an enhanced IL-17 response, which was accompanied by extensive tissue damage and neutrophil accumulation [97]. In addition, mice with non-hematopoietic cells unable to respond to IFN γ elicited excessive IL-17 levels with neutrophilic inflammation in the lungs and poor bacterial control [98]. Collectively, these data suggest a detrimental role for Th17 cell during the chronic phase.

1.4.3.2 CD8⁺ T cells

In addition to CD4⁺ T cells, the importance of CD8⁺ T cells in optimal immunity to TB has been shown in animal models. Mice lacking CD8⁺ T cells succumbed earlier than wild-type (WT) mice following the low dose aerosol infection [99], and susceptibility was even more pronounced if Mtb was given by the intravenous

route [100]. Mice deficient in molecules such as transporter associated with antigen processing (TAP), CD8, and perforin were shown to be more susceptible to Mtb infection [101]. A critical role of CD8⁺ T cell in immunity to Mtb has been also shown in non-human primates. Depletion of CD8⁺ T cells in BCG-vaccinated rhesus macaques led to a significant decrease in vaccine-induced immunity against TB [102]. Little is known about the role of CD8⁺ T cells in human. However, infected people generate Mtb-specific CD8⁺ T cells [103-105] that express effector functions that can suppress bacterial growth *in vitro* [106].

Priming of naïve CD8⁺ T cells requires peptide antigens presented by MHC-I, which requires an endogenous antigen. Two possible mechanisms for the presentation of Mtb antigens to CD8⁺ T cells have been proposed: first, Mtb translocates into the cytosol of infected DCs [50], or Mtb antigens leak from phagolysosome [107, 108], leading to processing of the antigens via the cytosolic pathway [109]. Second, DCs take up apoptotic vesicles from Mtb-infected cells and then process and present antigens on MHC-I via cross-presentation [110, 111]. Antigen-specific CD8⁺ T cell responses to various Mtb-derived peptides have been identified both in human and mice [105, 112, 113]

One of the effector functions of activated CD8⁺ T cells is the production of IFN γ and TNF α , which could activate macrophages to suppress bacterial growth [114]. In addition to the production of cytokines, CD8⁺ T cells mediate cellular cytotoxicity. CD8⁺ T cells from Mtb-infected humans express granulysin and can directly kill intracellular Mtb [115, 116]. Even though mice lack granulysin, a study showed that antigen-specific CD8⁺ T cells generated following infection have cytotoxic activity *in vivo* [117]. This cytolytic activity has been shown to involve perforin-mediated cytolysis [118]. Many investigators now believe that CD8⁺ T cells are important to control Mtb growth and should be considered new vaccine design [112, 119, 120]

1.4.4 Humoral immune response

The numerous studies on antibody-mediated immunity against Mtb over the past 100 years have resulted in contradictory results (extensive review in [121]). This has led to general neglect of this area of investigation. Recently, B cell function during TB has gained attention due to the role for B cells in host immunity against other intracellular microbes [122], the understanding that B cells are required for immune regulation, and the correlation of specific antibodies and protection in some studies [121].

B cells are found abundantly within the lymphocytic cuff of granulomas in humans and NHP [123, 124] and in the granulomatous lesion in mice [124]. Hence, B cells may have a role in maintaining the granuloma structure. However, the definitive mechanism remains to be defined. A study by Chan and colleagues has shown that B cell-deficient mice have exacerbated immunopathology, including accumulation of neutrophils and elevated IL-10 levels in the lungs. This phenotype was reversed by B cell adoptive transfer [125]. A dramatic increase in the bacterial

load was observed in the lungs and spleen of B cell-deficient mice [126]. In contrast, another study has shown that B cell-deficiency resulted in a delay in inflammatory progression [127]. This discrepancy has no reasonable explanation except for the difference in the Mtb strains used in the experiments. The role of B cell in TB is still unclear and remains to be fully delineated.

1.4.5 Granuloma formation and function

The characteristic lesions of TB are granulomas, which have long been considered a host defence mechanism for containing persistent pathogens. Primary granulomas start with the aggregation of infected macrophages, usually in the lungs. Infected macrophages produce soluble mediators that recruit macrophage and other cell types to the site of infection to form the granulomas. The basic structure of granuloma composes of many cell types as shown in Figure 6 [128]. Macrophages can undergo additional changes: they can fuse and form multinucleated giant cells or differentiate into foam cells, and can transform into epithelioid cells. Other cell types that engage in the granuloma structure are neutrophils, DCs, B and T cells, natural killer cells, fibroblasts and cells that secrete extracellular matrix components, i.e. collagens, laminin, fibronectin and matrix metalloproteinases [129]. The granuloma in humans with active TB, demonstrates central necrosis that grossly has a “cheese-like” appearance, so called the caseous granuloma.

Due to the difficulties in obtaining granulomas in lung tissue biopsies from TB patients, this has led to the widespread use of animal models, which have been improved over the years to reproduce more closely the progression of the disease observed in humans. As mentioned earlier, granulomas in most mouse strains are comprised of loose non-necrotic aggregates, but a mouse strain that develops necrotic granulomas has been identified. *NOS 2*^{-/-} mice infected with Mtb develop lung granulomas similar to those of humans [36]. In addition, Harper *et al* and Driver ER *et al* recently reported that C3HeB/FeJ mice develop necrotic lesions in response to Mtb infection [34, 35]. Furthermore, lung tissue sections from mice with reactivation TB (the *Cornell* model: see section 1.3.1) demonstrate multiple similarities to early post-primary TB in humans [130]. Guinea pigs and rabbits produce necrotic granulomas, which are more human-like [118]. NHPs (rhesus monkeys and macaques) have the additional advantage of presenting various outcomes to infection, similarly to humans [118, 131-133]. However, cost, availability of reagents and ethical considerations limit the widespread use of NHPs in TB research. In addition, zebrafish larvae infected with marine mycobacterium (*Mycobacterium marinum*) has been proposed as a model for study primary role of innate immunity in initiation of granuloma formation solely in the context of innate immune response since the adaptive immune response has not yet developed in the embryos state [64].

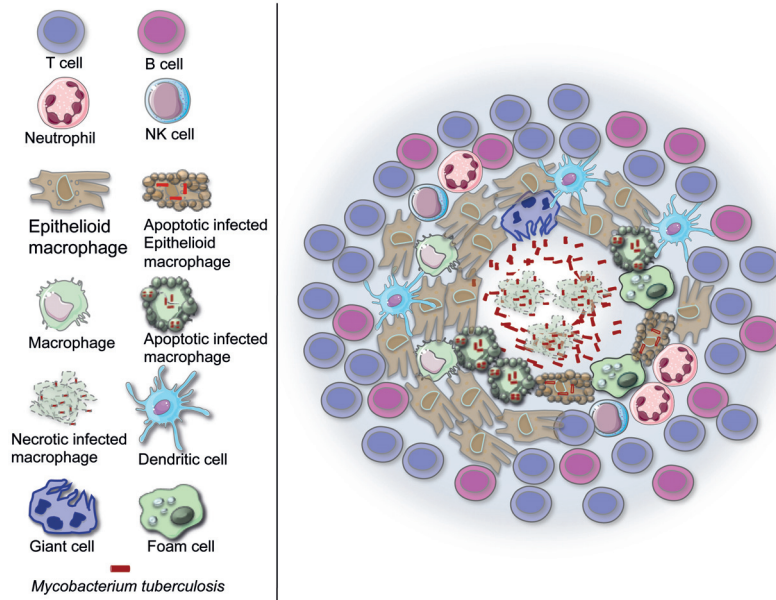


Figure 6. Structure and cellular constituents of the tuberculous granuloma. *Redrawn from [128].*

There is still debate on the role and function of granulomas as to whether such a structure benefits the host or the pathogen. On one hand, granuloma formation seems to be primarily a host-defence mechanism for containing the bacteria. In humans and NHPs, granulomas can become calcified; with the calcification process beginning within the caseous center and this type of granuloma is capable of limiting the growth and spread of Mtb [134]. On the other hand, the granuloma also shelters the bacteria, providing them with a niche in which they can persist in a latent form until an opportunity arises for re-activation. In addition, a study from the zebra fish model suggested that the granuloma help spread infected macrophages that can form secondary granulomas. The granulomas thereby promote bacterial spread in the tissue and even systemically [63].

1.5 IMMUNE REGULATION DURING TB

Generally, when our body encounters a pathogen, the innate immune response is triggered, resulting in the production of various pro-inflammatory cytokines and chemokines that regulate the adaptive branch of the immune system, i.e. humoral- and cell-mediated immune responses. The adaptive immune response responds to infection by clonal expansion of antigen-specific cells. Effector cells exert their

functions, i.e. secrete soluble mediators such as cytokines and chemokines, or via direct cell-cell interactions, that orchestrate appropriate immune responses in a complex system to control the infection. Eventually, the immune system needs to shut down after clearance of the microorganism [65].

In the context of Mtb infection, a quick and robust immune response is needed to control bacterial growth and dissemination. Partial successful immunity is shown in latent TB where bacterial growth is being controlled [14, 17]. Impaired immune function could lead to failure to control the bacteria, resulting in reactivation of latent TB and rapid progression to active disease. High antigenic load due to bacterial replication could induce strong pro-inflammatory immune responses and lead to excessive inflammation, lung tissue damage and loss of function [97]. Therefore, the immune response needs to be finely tuned to minimise tissue destruction while maintaining the effector functions that control bacterial growth. Several mechanisms that involve cells, cytokines and inhibitory molecules have been reported.

1.5.1 Participation of Treg cells

Treg cells are characterised by the expression of the Foxp3 transcription factor and the CD4 molecule. Treg cells suppress the immune system and play a pivotal role in immune tolerance that prevents autoimmune diseases in humans and in animal models [135]. In infection, Treg cell expansion occurs and suppresses the intensity of effector immune responses, which may result in pathogen persistence and chronic infection. On the other hand, Treg cells can potentially minimise tissue damage caused by strong immune responses directed towards the pathogens [136].

The Treg cell compartment expands both in patients with active TB [137-139] and in experimental animal models of TB [79, 140, 141], and these cells have also been shown to accumulate in both human and mouse lung granulomas [79, 139]. However, it is not known whether such an increase contributes to the development of TB or is a result of increasing responses to inflammation or tissue damage. The mechanism how Treg cells contribute to immune regulation in TB remains to be fully characterised. Further, there is lack of conclusive data showing that Treg cells play a detrimental or protective role during the inflammatory response.

Recently, Urdahl *et al* provided some insights into the role of Treg cells in Mtb-infected mice. The authors found that the induction of Treg cells occurred in the PLN in an antigen-specific manner. Antigen-specific Treg cells recognized Mtb antigens presented by DCs in PLN and proliferated at this site [78, 79, 142]. The expansion of antigen-specific Treg cells in the PLN and the arrival of Treg cells in the lungs were also delayed, similar to what has been observed for effector T cells [79]. Moreover, Treg cells limited the rate of effector T-cell priming and expansion [78]. The role of Treg cells during pulmonary TB is still under debate. While Scott-Browne *et al* demonstrated that depletion of Treg cells in Mtb infected

mice resulted in decreased bacterial load in the lung but not in the spleen [79], the observation by Quinn *et al* showed that inactivation Treg cells *in vivo* prior to Mtb infection did not alter lung bacterial load or lung pathology [143]. Interestingly, Ozeki *et al* demonstrated that during the early stage of infection, depletion of Treg cells in Mtb-infected mice reduced both the bacterial load and the granuloma lesions in the lungs compared to untreated Mtb-infected mice. In contrast, there was no difference in bacterial burden and lung histopathology between Treg cell-depleted mice and untreated animals at a later stage of the infection, suggesting different roles for Treg cells at early and late stages of Mtb infection [144]. In addition, a study from Chen *et al* has shown that following IL-2 treatment in the early stage of Mtb infection in macaques, the expansion of Treg cells occurred simultaneously with CD4⁺/CD8⁺/γδ T effector cell expansion in peripheral blood and in the pulmonary compartment [145]. The monkeys who received IL-2 treatment showed significantly milder gross TB pathology and reduced bacterial burden in the bronchoalveolar lavage (BAL) fluid compared to the saline-treated group [145]. These findings suggest that simultaneous expansion of Treg and T effector cells allows them to act in concert to attenuate severe lung damage and reduce the bacterial load during pulmonary TB. Taken together, these data suggest that the presence of Treg in the infected organs may be important for balancing protective and damaging immune responses during pulmonary TB.

1.5.2 Cytokine-mediated regulation in TB

Many cytokines from the innate and the adaptive arm of the immune system are induced upon Mtb infection and they are crucial in the control of the infection. However, overexpression of some cytokines may cause excessive inflammation and lead to immunopathology [97, 98, 146-148]. The pro-inflammatory cytokines produced after Mtb infection are IL-2, IFNγ, Type I IFN, IL-6, IL-1α/β, IL-12, TNFα and IL-17 while the anti-inflammatory cytokines, IL-4, IL-6, IL-10 and TGFβ may inhibit the effects of pro-inflammatory cytokines [149]. Actually, the main feature of Mtb is the induction of a Th1 response. Therefore, one could speculate that Th2 response may balance Th1 action and prevent the excessive inflammation mediated by Th1 cytokines. However, the cytokines work in a complex process of regulation and cross-regulation to each other to balance the immune response. Recently, the knowledge of how cytokines interact during chronic infection has contributed to our understanding of cytokine regulation during Mtb infection.

1.5.2.1 Interleukin- 12 (IL-12)

IL-12 is a heterodimeric cytokine composed of two the subunits p35 and p40. When co-expressed in the same cell, these 2 subunits form the biologically active p70 heterodimer [150]. IL-12 is essential to control Mtb infection. Neutralization of IL-12p70 by specific monoclonal antibodies at the initiation of Mtb infection resulted in increased bacterial load and loss of granuloma integrity [151]. The p40 subunit of IL-12, which is mainly secreted by Mtb-activated DCs was found to be required for DC migration and T cell priming during Mtb infection [152]. Mice

lacking IL-12p40 cannot control bacterial growth and rapidly succumb to the infection. This observation was associated with a reduction of IFN γ -producing cells [25, 153]. In addition, when IL-12p70 was given to IL-12p40-deficient mice, the animals were able to limit bacterial growth, maintain the granuloma integrity and prolong survival. After IL-12p70 withdrawal, the IL-12p40-deficient mice exhibited reduced antigen-specific IFN γ -producing cells in lungs, suggesting that IL-12 is not only important during the initiation phase of the immune response against Mtb infection, but is also required throughout chronic infection to maintain immune control over bacterial growth [154].

1.5.2.2 Tumor necrosis factor alpha (TNF α)

The important role of TNF α in host defence against Mtb has been proven both in animal models and in humans. Mice treated with anti-TNF α antibodies displayed increased susceptibility to BCG infection [155]. Anti-TNF α antibody-treated mice and TNF α receptor-deficient mice were highly susceptible to TB and died early after infection with increased bacterial load in the lungs and necrosis within the granulomas [27]. TNF α -deficient mice also showed increased susceptibility to Mtb infection [156]. The critical role of TNF α in human was revealed by the increased rate of reactivation of latent TB in rheumatoid arthritis (RA) patients who received TNF α -blocking medication [28]. TNF α contributes to the control of Mtb infection by the induction of reactive nitrogen and oxygen species by macrophages. TNF α also induces early chemokines, which help activate macrophages and recruit leukocytes during inflammation [157]. Moreover, TNF α plays a role in maintaining the integrity of the granuloma structure as shown by TNF α deficient-mice [156, 158], and in the RA patients treated with Infliximab [28], that exhibit defective granuloma formation. However, TNF α has a paradoxical role in immunity to TB. While it plays a critical role in protection, it may also be a main factor in pathology since TNF α accounts for most of the lung tissue damage caused by the excessive inflammatory response [159]. TB patients treated with thalidomide, a compound that decreases the half-life of TNF α mRNA, showed rapid symptomatic improvement [147]. In mice, local injection of TNF α increased fibrosis [148].

1.5.2.3 Interferon gamma (IFN γ)

It is generally accepted that IFN γ is important to control Mtb infection in mice and humans. IFN γ -deficient mice rapidly succumb to infection with less nitric oxide synthase mRNA in splenic cells, indicating that macrophage activation was impaired leading to shortened life-span of the infected animals [26, 84, 85]. Humans who have a mutation in the IFN γ receptor were found to be more susceptible to mycobacterial infections [160]. In mice, IFN γ controls bacterial growth by the induction of nitric oxide synthesis in macrophages. *NOS2*^{-/-} mice are more susceptible to Mtb infection than WT controls [36]. In human macrophages, IFN γ was found to induce the expression of NOS2 [161], however, the role of nitric oxide in controlling Mtb in human remains unclear [161, 162].

Recent data also support anti-inflammatory functions of IFN γ during TB. For example, IFN γ directly inhibits neutrophil accumulation in the infected lung and impairs neutrophil survival [163]. IFN γ can also act on T cells to promote apoptosis by modulating both T cell susceptibility to apoptosis and altering the level of apoptotic signals [164]. Moreover, IFN γ could regulate the immune pathological response by reducing the level of IL-17 and IL-23 [98].

1.5.2.4 *The interplay between IFN γ , IL-17 and IL-23*

The role of IL-17 and IL-23 was revealed by Cruz A *et al* [97]. In this study, the animals were exposed to BCG several times after Mtb infection. The authors found that repeated exposure to BCG after Mtb infection resulted in dramatic influx of antigen-specific IL-17-producing cells in the animal lungs with severe inflammation. Interestingly, neutralization of IL-17 or the absence of IL-23 improved the pathological reaction with reduced accumulation of granulocytes/neutrophils in the lungs. It is known that IL-23 plays an important role in the maintenance of the IL-17 producing cells and IL-17 is associated with neutrophil recruitment [165]. Neutrophilia is a common phenomenon seen in granulomatous lesion of susceptible mice and associates with severe pathology [24]. It can be concluded that continuous antigen exposure induces the accumulation of IL-23, and consequently enhances ongoing IL-17-mediated responses and finally leads to infiltration of neutrophils and severe pathology.

Interestingly, IFN γ is also able to regulate the induction and expansion of IL-17-producing CD4⁺ T cells [95]. Recently, DesVignes and Ernst showed that IFN γ responsive non-hematopoietic cells, i.e. lung epithelial and endothelial cells, also regulate IL-17-dependent immunopathology. In the absence of IFN γ signalling in non-hematopoietic cells, the animal exhibited higher mortality and increased bacterial burden compared to control mice, the animals overexpressed IL-17 accompanied by massive neutrophil influx and impaired expression of indoleamine-2,3-dioxygenase (IDO) in lung endothelial and epithelial cells. In addition, they also showed that kynurenines, the products of IDO catabolism of tryptophan inhibited the action of IL-23 in maintaining the IL-17-producing Th17 cells *in vitro*, resulting in reduced IL-17 secretion by Th17 cells [98].

Collectively, IFN γ seems to play a central role in preventing mycobacterial associated immune-mediated pathology by directly limiting the differentiation of IL-17-producing cells and indirectly by inducing IDO activation by non-hematopoietic cells.

1.5.2.5 *Interleukin-1 (IL-1)*

Another important cytokine is IL-1. Mtb is a strong inducer of both IL-1 α and IL-1 β at the site of infection [166, 167]. It is clear that mice deficient in IL-1 α , IL-1 β , or IL-1R are highly susceptible to Mtb infection with extensive granuloma necrosis [168, 169]. However, the exact mechanism of how IL-1 controls the bacteria and ensures host survival is still not completely understood. IL-1 activity may regulate

host resistance by modulating cell death [157]. The role of IL-1 signalling in human disease is supported by different studies suggesting associations of polymorphisms in the *Il1* or *Il1r1* genes with susceptibility to TB [170, 171].

1.5.2.6 Type I Interferon

Type I IFNs appears to have a detrimental role during Mtb infection. Type I IFN receptor-deficient mice are more resistant to Mtb infection and display significantly reduced bacterial burdens during the chronic stage of infection when compared to WT animals. Mtb-infected mice treated with the type I IFN-inducer polyinosinicpolycytidylic acid displayed exacerbated lung pathology and bacterial burden [146]. Recently, type I IFNs were shown to be strong inhibitors of IL-1 α , IL-1 β production by macrophages and DCs in the lungs of Mtb-infected mice [166]. Type I IFNs could serve as a negative feedback mediator that prevents over-expression of pro-inflammatory IL-1 α , IL-1 β during chronic infection.

1.5.2.7 Immunosuppressive cytokines

Apart from Th2 cytokines, which are known for their antagonistic effect on Th1 cytokines, the classical regulatory cytokines, such as IL-10 or TGF β also participate in the control of immunopathology during TB. The major mechanisms of IL-10 are to inhibit DC maturation, and IL-12 and TNF α production, thus inhibiting the development of the Th1 response [172, 173]. TGF β is generally known to inhibit T cell proliferation and effector function [65] and is important to maintain Treg cells survival and function [174]. High level of IL-10 and TGF β have been detected in the lungs, BAL, sputum and serum of patients with advance diseases and has been thought that they associated with reactivation TB in humans [175-179].

In mice, IL-10 is induced in the lungs of both resistant and susceptible mice. The mouse strains that express high levels of IL-10 upon infection, such as CBA mice, are naturally more susceptible to TB. When IL-10 activity is neutralized the mice control Mtb infection better. Several data indicated that TGF β can also suppress protective immunity to TB in experimental model such as guinea pigs and BALB/c mice [159, 180]. BALB/c mice treated with TGF β antagonist exhibited enhanced Th1 cytokines, increased the level of iNOS mRNA and displayed decreased bacterial load compared to untreated animals [159]. Interestingly, TGF β antagonist treated mice had more inflamed lesions in the lungs compared to untreated mice [159]. This data indicated that while TGF β plays a role in downmodulation of the Th1 response, it also acts as a suppressor of excessive inflammation to helps maintain lung architecture and functions.

1.5.3 Inhibitory molecule-mediated regulation in TB

Inhibitory molecules such as programmed death-1 (PD-1) and T cell immunoglobulin and mucin domain-3 (Tim-3) have been reported to be involved with negative regulation of immune responses during TB.

PD-1 is expressed on the surface of activated T, B cells, macrophages, monocytes, natural killer (NK) cells, and DCs [181, 182]. PD-1 interacts with its ligands (PD-L1, PD-L2) on APCs [182] resulting in down inhibition of T cell proliferation and cytokine production [183, 184]. PD-1 has been shown to be upregulated on IFN γ -producing T cells and on monocytes from patients with active pulmonary TB [185, 186]. Blockage of the PD-1–PD-L1/L2 pathway enhanced IFN γ production and T cell proliferation [185, 186], suggesting that PD-1–mediated downregulation of the immune response. Interestingly, Mtb infected PD-1 knockout mice showed dramatically reduced survival compared to WT mice [187–189], indicating that PD-1 may play a protective role during Mtb infection. It is worth noting that PD-1 expression was not restricted to the Mtb specific T cells [185].

Tim-3 is another molecule involved in regulating T cell responses and is upregulated on differentiated Th1 and cytotoxic CD8 $^{+}$ T cells [190]. However, expression of Tim-3 can be found on monocytes, macrophages and DCs [191]. Binding of Tim-3 with its ligand Galectin (Gal)-9 leads to T-cell apoptosis [192]. Tim-3 has been suggested as T cell exhaustion marker in tumor immunity and during some virus infections, particularly in HIV-1 infection [193–195]. In the context of TB, upregulation of Tim-3 expression on CD8 $^{+}$ and CD4 $^{+}$ cells has been shown in active TB patients [196, 197] and in Mtb-infected mice [198]. In humans, Tim-3 expression was significantly increased on antigen-specific CD8 $^{+}$ T cells from active pulmonary TB patients compared to tuberculin-positive healthy controls [196]. In Mtb-infected mice, we made a similar observation (study IV). TB10.4-specific CD8 $^{+}$ T cells contained the highest proportion of Tim3 $^{+}$ cells. However, the functional potential of Tim3 $^{+}$ T cells is unclear during Mtb infection. One study on T cells from active TB patients showed that Tim-3 $^{+}$ CD8 $^{+}$ T cells exhibited significantly fewer IFN γ -producing cells than Tim-3 $^{-}$ CD8 $^{+}$ T cells [196]. On the other hand, another study revealed that Tim-3 $^{\text{high}}$ CD4 $^{+}$ and CD8 $^{+}$ T-cell subsets elicited greater IFN γ , TNF α , IL-2 and IL-22 cytokines producing cells than Tim-3 $^{\text{Low}}$ T cells, and that Tim-3-expressing T cells more efficiently limited intracellular Mtb growth [197]. The data suggest that Tim-3 $^{+}$ T cells are capable to mounting a strong response during Mtb infection. Interestingly, in study IV we found that TB10.4-specific CD8 $^{+}$ T cells in Mtb-infected mice were enriched for IFN γ - and TNF α -producing cells. Therefore, Tim-3 may not serve as an exhaustion marker in the context of Mtb infection and its role remains to be fully characterised.

1.6 PULMONARY DCs IN MICE AND THEIR ROLE IN TB

1.6.1 DCs in general

DCs were first described in the mid 1970s by Ralph M. Steinman and Zanvil A. Cohn [199]. DCs are the most potent professional APC. In the presence of danger signals, i.e. pathogen-derived substances, tissue damage, inflammatory cytokines or adjuvants, DCs migrate to secondary lymphoid organs, upregulate high cell surface levels of co-stimulatory molecules and antigen-presenting molecules, and produce cytokines to efficiently interact with naive antigen-specific T cells. Together, these interactions will initiate antigen-specific CD8⁺ and CD4⁺ T cell responses [65]. Conversely, in a tolerogenic setting, DCs can induce anergy in antigen-specific T cells or generate protective Treg cells upon arrival in the LN [200].

1.6.2 Pulmonary DCs in mice

DCs are a heterogeneous group of cells that display differences in anatomic localization, cell surface phenotype, and function. In the mouse lungs, at least four major DC subsets have been identified [201-203]:

- CD11c^{high}CD11b^{low}MHC-II^{high}CD207⁺CD103⁺ migratory DC
- CD11c^{int}CD11b^{high}MHC-II^{high}CD103⁻ migratory DC
- CD103⁻MHC-II^{neg-med}CD11b^{hi} monocytic DCs,
- B220⁺Ly6C⁺MHC-II^{low} plasmacytoid DCs

In mice, the number of pulmonary DCs in the conducting airways, i.e. trachea and major bronchi, is greater than the lung parenchyma [204]. DCs can also be detected in the BAL, especially during inflammatory conditions [60, 201]. DCs present in the lung tissue have an immature phenotype [205]. Circulating monocytes can give rise to lung DCs in steady state and under inflammatory conditions [206]. Monocytes are a population of mononuclear leukocytes that develop in the bone marrow (BM). Monocytes are released into blood circulation and enter tissues where they can differentiate and give rise to macrophages or DCs. During infections, or following inhalation of allergens, epithelial cells in the lungs produce pro-inflammatory chemokines that act on the BM and increase CCR2^{hi} monocytes emigration [207, 208]. When the monocytes reach the airway mucosa, they can up-regulate MHC-II, CD11c and differentiate to DC subtypes which having different functions in the immune responses [42, 201].

In the context of Mtb infection, using a monocyte adoptive transfer model, Sköld and Behar showed that BM-derived monocytes were recruited to the lungs of Mtb-infected mice and gave rise to three different myeloid subsets: CD11b⁺CD11c⁻ (BM-derived monocytes), CD11b⁺CD11c⁺ (resident DCs and iNOS producing cells, i.e. activated macrophages) and CD11b^{low}CD11c⁺ cells [42]. In this thesis (study II), we showed that, by using the same technique, CD11b^{low}CD11c⁺ cells in Mtb-

infected lungs contain a mixture of alveolar macrophages and migratory DC that express alpha E integrin (CD103) on the cell surface [60].

1.6.3 Pulmonary CD103⁺ DCs in mice

Sung and colleagues first identified and characterized mouse pulmonary CD103⁺ DCs [203]. Later, Jakubzick *et al* showed that BM monocytes can serve as progenitors for CD103⁺ DCs during the steady-state. In blood circulation, Ly6C^{high}CCR2^{high} CX3CR1^{low} and Ly6C^{low}CCR2^{high}CX3CR1^{high} monocytes gave rise to CD103⁺ and CD103⁻ DCs in the lungs, respectively [201].

Immunohistochemistry showed that CD103⁺ DCs localise on the basal side of bronchial epithelium and on the parenchymal side of vascular endothelial cells. CD103 and beta 7 (β 7) integrin can interact with E-cadherin that is expressed on the basal side of bronchial epithelial cells [203]. In contrast, fewer CD103⁻ DCs are found in this location and predominantly localize in the peribronchial regions and interstitial space [204]. Interestingly, CD103⁺ DCs express several tight junction proteins including Claudin-1, Claudin-7, and ZO-2. This may allow this DC subset to capture inhaled antigens or pathogens by extending protrusions through the epithelial barrier into the bronchiolar luminal space, [203]. In addition, CD103⁺ DCs have the unique capacity to take up apoptotic bodies and contribute to tolerance to self-antigens during steady-state conditions [209]. In the context of infection or inflammation, CD103⁺ DCs are specialized in cross-presentation of exogenous peptide antigen to CD8⁺ T cells, particularly during viral infections. Animal models of influenza, or respiratory syncytial virus infection [210-213], have shown that CD103⁺ DCs preferentially present viral antigens to naive T cells via cross- presentation, resulting in activation of virus-specific CD8⁺ T cells.

Based on the localization in the lung tissue, it is tempting to speculate that lung CD103⁺ DCs have tolerogenic properties similar to CD103⁺ DCs found in the gut mucosa. CD103⁺ DCs in the gut are able to induce Treg cells via production of TGF β and the vitamin A metabolite, retinoic acid [214]. In favour of this idea, Khare *et al* recently revealed that lung CD103⁺ DCs were capable of inducing Foxp3 expression in CD4⁺ T cells both *in vivo* and *in vitro* [215], and that the induction of Foxp3 expression is dependent on TGF β and retinoic acid, similar to their counterpart in the gut.

We were the first to explore the role of CD103⁺ DCs during pulmonary TB in various inbred mouse strains, i.e. C57BL/6, BALB/c and DBA/2. Still, the exact role of lung CD103⁺ cells in response to Mtb infection remains a puzzle. The results will be discussed in the results and discussion section. Here it is worth noting that the transcription factor Batf3 is required for the development of CD103⁺ DC and that *Batf3*^{-/-} mice lack the lung CD103⁺ DC population [216]. Tussiwand *et al* observed that IL-12p40-serum levels were reduced in Mtb-infected *Batf3*^{-/-} mice, but the markedly reduced number of lung CD103⁺ DC had no effect on the survival in response to the infection [217].

1.6.4 The role of pulmonary DCs in TB

The role of DCs in TB has been addressed using both *in vitro* and *in vivo* models. *In vitro*, Mtb can infect BM-derived DCs [218] and lung DCs [205]. Upon Mtb infection, both DC populations produced TNF and IL-12p70 and were able to stimulate CD4⁺ T cell proliferation [218] and IFN γ production [205]. In addition, Mtb could infect human monocyte-derived immature DC, which induced a mature DC phenotype [219]. *In vivo*, following aerosol infection with Mtb expressing green fluorescent protein (GFP), myeloid DCs (CD11c⁺CD11b⁺ cells) were the major cell population infected with Mtb in the lungs and LNs. [39, 67].

An important role of DCs is to take up antigens and transport them to the draining LN where they prime naïve T cell. This is also true in response to Mtb infection. Wolf AJ *et al* provided data showing that DCs transport live Mtb from the lungs to the draining PLN early after infection [39, 67]. Also, depletion of DCs (CD11c⁺ cells) before intravenous infection with Mtb delayed the development of the antigen-specific CD4⁺ T cell response [72]. In addition, the lung cell population (CD11c⁺CD11b⁺ cells) that were infected with Mtb at high frequency were relatively ineffective in stimulating antigen-specific CD4⁺ T cells compared to other infected myeloid subsets, i.e. alveolar macrophages and recruited interstitial macrophages. Interestingly, CD11c⁺CD11b⁺ DCs in the PLN did not stimulate antigen-specific CD4⁺ T cells better compared to lung CD11c⁺CD11b⁺ DCs [39, 67], suggesting modulation of the antigen presentation and priming process by Mtb. While DCs can be infected directly by Mtb *in vivo*, they are also able to take up apoptotic vesicles from infected macrophages and neutrophils [41, 56] and present peptide antigen via cross-presentation to naïve CD8⁺ T cells [120]. Another important role of DCs during Mtb infection is the production of the Th1-driving cytokine, IL-12.

1.7 HUMAN IMMUNODEFICIENCY VIRUS (HIV) -1

HIV-1 is a lentivirus, member of the retrovirus family. HIV-1 is distributed globally and is the principal causative agent of AIDS [220]. HIV-1 is composed of double stranded RNA encapsulated in the nucleocapsid and matrix made of structural viral proteins. The HIV-1 genome comprises three major structural genes, i.e. group specific antigen (*gag*), polymerase (*pol*) and envelope (*env*), and additional six regulatory and accessory genes (*Tat*, *Rev*, *Nef*, *Vif*, *Vpr*, *Vpu*) [220]. HIV-1 can infect many immune cells such as CD4⁺ T cells, macrophages and DCs [221]. CD4 molecules, which express on T cells and macrophages, is the main receptor for the binding of envelope glycoprotein of the HIV-1 virus, gp120 for virus entry. The gp120 can also bind to C-type lectin DC-SIGN on the surface of DCs [221]. The receptors are essential for virus binding but are not sufficient for virus entry into the cells. Co-receptors are needed for infection. The chemokine receptor CXCR4 and CCR5 are the main co-receptors. Two types of virus-tropisms exist: first, macrophage (M-tropic) viruses can infect macrophages and primary CD4⁺ T cells

and mainly use CCR5. Second, T-cell (T-tropic) viruses can infect CD4⁺ T cells and T-cell lines via the CXCR4 chemokine co-receptor [222]. The R5 virus refers to HIV-1 that uses CCR5 as a co-receptor while X4 viruses specifies HIV-1 that uses CXCR4. Once the virus enters to the target cell, the genome integrates into the host cell genome. Viral genes can be transcribed and translated into viral proteins that are needed for viral replication and dissemination from infected cells to new target cells. HIV-1 can also establish a latent form of infection and residing in the reservoir cells by integration of its genome without replication [222].

Transmission of HIV-1 occurs mostly via sexual intercourse but can also transmit via blood from infected individual, for example during blood transfusion, organ transplantation, or by needle sharing between intravenous drug users [10]. HIV-1 can be transmitted from infected mothers to their children either during pregnancy, during labour, or through breast-feeding [10].

The typical course of HIV infection can be divided into three stages: I) acute stage, II) latent /clinically asymptomatic stage, and III) late/advanced AIDS stage [223]. The acute stage usually last for a few weeks after HIV-1 infection in which the infected individual may experience no symptom or have a “flu-like” illness including headache, sore throat, or fever. The viral load in the blood increase sharply and the number of CD4⁺ T cell drops rapidly [224]. Later, the immune system is able to mount an effective response and neutralizing antibodies are produced. The viral load drops and the number of CD4⁺ T cells increases again, indicating the latent stage. At this stage, the infected individual has no symptom of AIDS but carries HIV-1 and has gradual deterioration of the immune system, which could last for many years [225]. Eventually, the late/AIDS stages develops as CD4⁺ cell count decrease below 350 cells/ μ L, HIV-1-infected individual becomes severe immunosuppression and more prone to various opportunistic infections and usually develop full-blown AIDS after the CD4⁺ cell count below 200 cells/ μ L. Fortunately, the antiviral drug treatment is able to slow down the progression to AIDS due to it reduces the level of HIV particles [12, 13].

1.8 MTB AND HIV-1 CO-INFECTION

The association between HIV-1 and TB has been evident since the start of the HIV-1 epidemic in early 1980s. The risk of acquiring TB depends on many factors. However, a decrease in the number of CD4⁺ T cells in HIV-infected individual compounded by exposure to TB in a TB endemic area is likely the main risk factor [226, 227]. Not only are HIV-1⁺ individuals at greater risk of acquiring Mtb and developing active TB, they are at higher risk of dying of TB. Conversely, not only does HIV-1 affect TB, but TB disease may also accelerate the progression of the HIV-1 infection. Therefore, co-infection with both pathogens accelerates disease progression, worsens the pathogenesis and amplifies the transmission of TB.

The possible ways in which HIV-1-infected individuals acquire active TB may be either due to the rapid progression of new TB infection or re-infection, or due to

reactivation of pre-existing latent TB [228-230]. Differential diagnosis between reactivation of latent TB and newly acquired TB might be important to understand how HIV-1 affects the immune control of TB. Molecular typing (Restriction fragment-length polymorphism (RFLP)) has been used to obtain [229, 230] data from cohorts in Malawi and South Africa, where the TB incidence is high. The results indicated that soon after infection with HIV-1, the increased risk of TB is likely due to new infection rather than reactivation of pre-existing latent TB [229, 230].

1.8.1 How does HIV-1 exacerbate TB?

It is widely accepted that depletion of CD4⁺ T cells is the hallmark of HIV pathogenesis. A decrease in the number and function of CD4⁺ T cells contribute to the increase in susceptibility to new Mtb infection and risk of reactivation of latent TB. This is because the T cell subset and the cytokines produced are crucial for maintaining the granuloma structure that controls TB. However, other mechanisms have been proposed to contribute to this susceptibility including the impairment of Mtb-specific T cells by HIV-1, HIV-1 creates a niche that facilitates entry of Mtb into macrophages [231] and HIV-1 induces dysfunctional macrophages [232]. All in all, HIV-1 affects two principal immune cells needed to control TB: CD4⁺ T cells and macrophages. As a consequence, HIV-1 co-infection will lead to increased bacterial growth and dissemination, and severe pathology.

1.8.1.1 Impact of HIV-1 on the Mtb granuloma and Mtb specific CD4⁺T cells

Autopsy studies conducted in the lungs of co-infected individuals showed poorly formed granulomas with extensive necrosis, and a marked presence of polymorphonuclear cells while the granulomas from HIV-1 negative individuals were composed of macrophages, lymphocytes, epithelioid cells and giant cell with caseous necrosis [233]. The different in pathohistology suggests that HIV-1 may disrupt the normal granuloma structure and leading to exacerbated lung pathology. Depletion of CD4⁺ T cells within the granuloma has been observed in patients with AIDS and tuberculous adenitis [234] as well as in the animal model for TB/SIV co-infection. The co-infected monkeys had significantly fewer CD4⁺ and CD8⁺ T cells within the lung granulomas compared to those with active TB alone [235]. The loss of CD4⁺ T cells in the granuloma may contribute to progressive TB since CD4⁺ T cells are required for control the bacteria and maintenance integrity of granuloma structure.

While it is clear that HIV-1 systematically deplete the number of CD4⁺ T cells and impairs CD4⁺ T cell function [236, 237], it might be difficult to determine whether HIV-1 impairs the function of Mtb-specific T cells within the granuloma. However, several studies have shown that there is an imbalance in cytokines that are involved in controlling Mtb in the granulomas. For example, TNF α production was greatly reduced in autopsy lesions from Mtb/HIV-1-co-infected cases compared to those from the Mtb-infected HIV-1 negative group [233]. In contrast,

another report showed that the expression of TNF α was greater in the co-infected granuloma biopsies [238]. This discrepancy may be due to different stages of the disease. The first observation was done post-mortem and could reflect the immune responses at the end-stage of co-infection. Elevated TNF α levels in the lungs of co-infected patients may stimulate the replication of HIV-1. Nevertheless, there are a number of studies that have assessed Mtb-specific CD4 $^{+}$ T cell function in peripheral blood and pleural fluid from co-infected individuals. The findings showed that HIV-1 decreases Th1 cytokine secretion by Mtb-specific CD4 $^{+}$ T cells isolated from PBMCs, BAL fluid, or pleural fluid [239-243], which suggests that HIV-1 suppresses Mtb-specific immune responses *in vivo*. Moreover, HIV-1 infection decreases CD40 ligand (CD40L) induction on CD4 $^{+}$ cells, leading to diminished activation of macrophages through the CD40 receptor and consequently decreased IL-12 secretion [244], and impaired development of Th1 cells.

1.8.1.2 Impact of HIV-1 on macrophage function

Macrophages are important components of the innate immune response. They are central to the pathogenesis of both TB and HIV-1 infection. They serve as important effector cells against Mtb and as reservoirs for both microorganisms. HIV-1 infects alveolar macrophages both *in vitro* [245] and *in vivo*. In particular, HIV-1 can infect CD36 $^{+}$, CD14 $^{+}$ macrophages from pleural fluid [246]. Unlike CD4 $^{+}$ T cells, HIV-1 infection of macrophages does not result in cell death, but rather persistent HIV-1 infection.

Alveolar macrophage activation and apoptosis are known as a host defence mechanisms against Mtb infection. Therefore, any specific defect in macrophage function and apoptotic pathways could contribute to Mtb persistence and increased pathogenesis. A study by Patel *et al* has shown that HIV-1 reduced Mtb-mediated apoptosis and TNF α production in HIV-1-infected human macrophage cell line as well as alveolar macrophages from HIV-1-infected persons [247]. In addition, HIV-1 infection induced Mtb growth in blood monocyte-derived macrophages [248], and co-infection elevated the level of IL-1 β , IL-6, IL-8, and GM-CSF and correlated with enhanced viral replication [248]. Together, these findings suggest that HIV-1 may impair the ability of macrophages to limit Mtb growth and co-infection with HIV-1 and Mtb seems to facilitate the replication of both pathogens.

In conclusion, not only does HIV-1 infection deplete peripheral CD4 $^{+}$ T cell, the virus reduces the number of CD4 $^{+}$ cells in the granuloma and impairs CD4 $^{+}$ T cell function. HIV-1 also interferes with the macrophage function and apoptosis. This leads to granuloma deformation/disruption, resulting in a worsened pathogenesis and enhance bacterial dissemination and transmission.

1.8.2 How does MTB exacerbate HIV-1 progression?

TB also accelerates the course of HIV-1 disease. A number of studies have indicated that the development of TB is associated with increased HIV-1 replication. Increased viral load was observed in serum samples from HIV-1 infected patients at the time of diagnosis of TB, compared to serum samples obtained before diagnosis [249]. HIV-1 transcriptional activity was also shown to be enhanced in PBMC and serum of HIV-1/TB patients [250]. Interestingly, increased HIV-1 production was clearly shown in BAL fluid from patients co-infected with Mtb [251], indicating that Mtb-infected lungs support extensive viral replication. Pro-inflammatory cytokines that are secreted during Mtb infection, such as $\text{TNF}\alpha$, have been shown to induce viral replication [252] and was elevated in the pleural fluid compared to plasma of co-infected patients [246]. The chemokine MCP-1 was also shown to correlate with HIV-1 replication [253]. Therefore, the levels of $\text{TNF}\alpha$ and MCP-1, induced by TB, may be critical for the increased viral burden in the lungs.

Another interesting aspect of how Mtb modulates HIV-1 is that Mtb infection promotes viral entry by induction the expression of viral co-receptors on the surface of target cells [254]. The co-receptors CCR5 and CXCR4 are required for virus entry [222]. Increased CXCR4 expression was observed on alveolar macrophages isolated from TB patients, and it was confirmed *in vitro* that Mtb increased CXCR4 expression on monocyte-derived macrophage and increased HIV-1 X4 virus type entry [254]. Moreover, Mtb infection of DCs was found to promote HIV-1 virus *trans*-infection (DCs transfer of HIV-1 to CD4^+ T cells) by DCs [255].

In conclusion, co-infection accelerates both TB and HIV-1/AIDS. HIV-1 infection has great impact on the main effector cells for control of Mtb infection. On the other hand, Mtb infection also accelerates the course of HIV-1 infection, which in turn promotes Mtb dissemination and progression of TB (Figure 7).

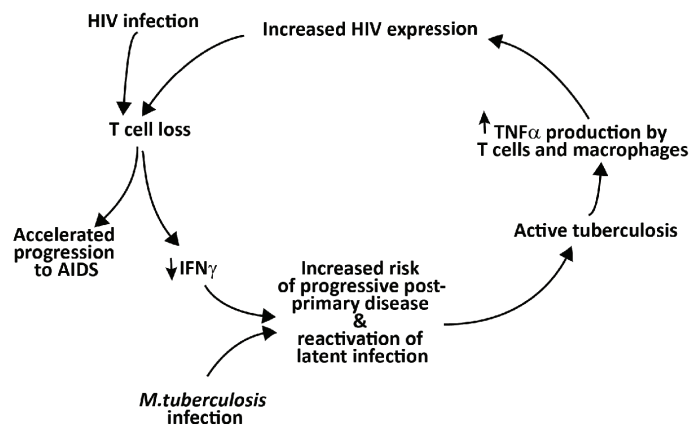


Figure 7. Interaction of Mtb and HIV-1 in co-infection. *redrawn from ref [256].*

2 AIMS OF THE THESIS

The ultimate aim of this thesis was to increase our understanding of the role of immune-regulatory mechanisms in protective immune responses during pulmonary TB and during Mtb/HIV-1 co-infection in the mouse model.

Specific aims were

1. To characterize the role of immuno-regulatory cells in host immunity in Mtb-resistant and susceptible inbred mouse strains (Study I and Study II).
2. To determine the impact of chronic Mtb infection on the immunogenicity of HIV/DNA vaccine (Study III).
3. To establish and characterize a murine model of Mtb/HIV-1 co-infection (Study IV).

3 MATERIALS AND METHODS

Detailed descriptions of the methods and reagents used in this thesis are provided in the respective articles and manuscript. A brief description of materials and methods are present here.

3.1 STUDY I

Mtb resistant (C57BL/6 and BALB/c) and susceptible (DBA/2) inbred mice were infected with a low dose of virulent Mtb (Harlingen strain) via the respiratory route in the Biosafety level (BSL)-3 animal facility at the Astrid Fagraeus Laboratory, Karolinska Institutet (Figure 8). Groups of animals were sacrificed 3-12 weeks after aerosol infection to determine lung pathology and bacterial burden. Investigation of recruitment and function of various myeloid and lymphoid cell subsets in the infected lung tissue and in draining PLN was performed by multicolor flow cytometry.

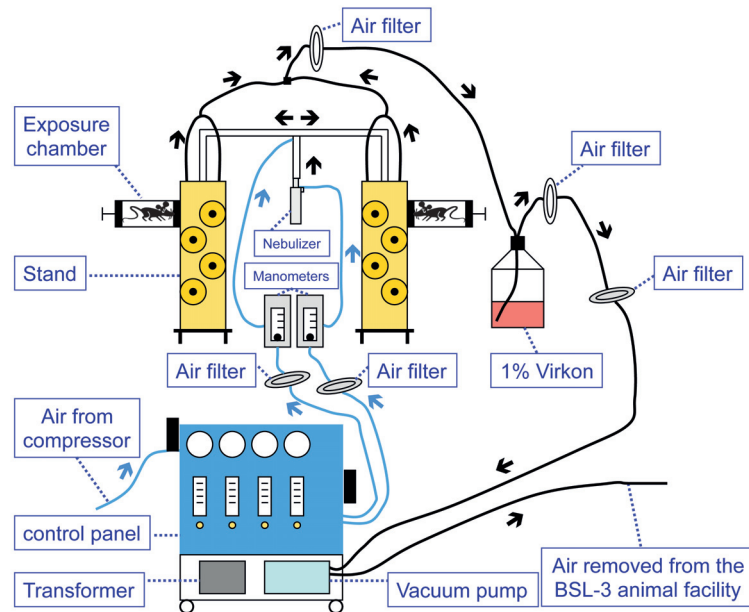


Figure 8. The schematic figure shows the newly established and unique aerosol infection model using a nose-only exposure unit in the BSL-3 animal facility, Karolinska Institutet.

3.2 STUDY II

We co-cultured primary alveolar epithelial cells (AEC) and monocytes from naïve donor mice *in vitro* in order to examine the role of AEC in monocyte biology. We used a primary monocyte adoptive transfer model to delineate the origin of α E-DC during TB, and confocal microscopy on lung tissue sections to determine the localization of α E-DC in infected lungs. By infecting the animals with virulent Mtb (strain H37Rv) expressing GFP, we were able to identify and characterize infected cells *in vivo* using multicolor flow cytometry. Finally, intracellular staining techniques were used to further delineate the cytokine profile of α E-DC during pulmonary TB, and to examine NOS2 production by infected lung cells.

3.3 STUDY III

Mice were infected with Mtb (Harlingen strain) via the respiratory route and vaccinated with the HIV-1 vaccine candidate MultiHIV DNA/protein intraperitoneally, or intramuscularly, seven weeks later. Spleens, lungs, peripheral blood and vaginal secretions were collected for determination of the antibody response, cytokine production and bacterial load (CFU). Serum and vaginal secretions were analysed for IgG and IgA content using an ELISA. The CFU was determined in the lungs. Splenocytes were re-stimulated with antigens *in vitro* and analysed for cytokine production.

3.4 STUDY IV

Co-infection in the murine model was established by combining the murine model of pulmonary TB with the chimeric virus EcoNDK developed by Potash *et al* [257]. Infectious viral particles were produced in the BSL-3 laboratory at the Department of Microbiology, Tumor and Cell Biology, Karolinska Institutet, by transfecting 293T cells with the plasmid encoding the chimeric virus. First, a low dose of virulent Mtb was used to infect WT BALB/c or DBA/2 mice. Three weeks later, purified viral particles were injected intraperitoneally into Mtb-infected, or uninfected animals. After an additional 2-9 weeks, the mice were sacrificed and the lungs and the spleen were aseptically removed. The bacterial load in the lungs was determined by plating lung homogenates on 7H11 agar plates. The viral load in the lung tissue and in the spleen was determined by quantitative PCR (qPCR). For immunological readouts, single-cell suspensions from lungs and spleens were stained for cell surface markers and analysed by flow cytometry. In some experiments, the cells were first re-stimulated *in vitro* before intracellular cytokine staining and FACS analysis. All animal experiments involving Mtb and EcoNDK were performed in the BSL-3 animal facility at the Astrid Fagraeus Laboratory, Karolinska Institutet.

4 RESULTS AND DISCUSSION

4.1 THE ROLE OF α E-DC DURING PULMONARY TB - *PAPER I & II*

While it is clear that immunocompromised individuals are susceptible to TB, the cause of naturally occurring susceptibility in healthy individuals is poorly understood. The mouse model has proven useful for better understanding of how the immune system controls Mtb infections. Various inbred mouse strains exhibit different degrees of susceptibility to Mtb infection [24]. Therefore, we took advantage of WT mice that are either resistant (C57BL/6 or BALB/c) or susceptible (DBA/2) to Mtb infection [258-260] to investigate various cell compartments that may contribute to susceptibility to pulmonary TB, including myeloid cells.

While it is clear that immunocompromised individuals are susceptible to TB, the cause of naturally occurring susceptibility in healthy individuals is poorly understood. The mouse model has proven useful for better understanding of how the immune system controls Mtb infections. Various inbred mouse strains exhibit different degrees of susceptible to Mtb infection [24]. Therefore, we took advantage of WT mice that are either resistant (C57BL/6 or BALB/c) or susceptible (DBA/2) to Mtb infection [258-260] to investigate various cell compartments that may contribute to susceptibility to pulmonary TB, including myeloid cells.

4.1.1 Recruitment of myeloid cells, including inflammatory monocyte, into Mtb infected lungs and macrophage activation are not defective in susceptible mice - *Paper I*

Myeloid cells, such as monocytes, macrophages, DCs and neutrophils have been proven important in controlling Mtb infection [39-42]. Any defect in recruitment of these cells may help explain susceptibility to TB. In this study, we established a murine low dose nose-only aerosol infection model to mimic the natural route of Mtb infection. We utilised this model to dissect various myeloid cell compartments and Treg cells during pulmonary TB. As expected, nine weeks after the infection, susceptible DBA/2 mice displayed more extensive lesions (Figure 9A) and a 10-fold higher bacterial burden in the lung tissue (Figure 9B) compared to resistant C57BL/6 and BALB/c mice. We examined the cellular infiltrate in resistant and susceptible lungs in uninfected mice and at various time points after virulent Mtb aerosol infection. We found that the total number of lung cells increased dramatically in response to Mtb infection and was significantly higher in BALB/c mice than in C57BL/6 mice and DBA/2 mice at weeks three, nine, and 12 pi (Figure 9C). We then further investigated several myeloid cell populations based on the cell surface expression of CD11b, CD11c, Ly6C and Ly6G. In the infected lung tissue of susceptible DBA/2 mice, the number of recruited

neutrophils increased rapidly and continuously during the whole study period (Figure 9D). In comparison, neutrophil infiltration in the lung tissue of resistant C57BL/6 mice remained low. Neutrophil influx has been associated with severe pathology in susceptible mice [24, 97]. However, the number of neutrophils in the lungs of BALB/c and DBA/2 was comparable, indicating that neutrophil infiltration per se does not cause increased susceptibility to Mtb infection, at least in this experimental setting. Inflammatory monocytes recruited to the Mtb-infected lungs rapidly upregulate CD11c [42] and give rise to the CD11b⁺CD11c⁺ subset, which comprises both DCs and activated iNOS-producing macrophages [42]. We found that the number of inflammatory monocytes was comparable in the lungs of all three mouse strains tested (Figure 9E). In addition, the numbers of CD11b⁺CD11c⁺ cells, including iNOS-producing macrophages, was not significantly different between the three mouse strains (Figure 9F,9G). In summary, susceptibility in DBA/2 mice cannot be explained by defective monocyte or neutrophil recruitment, nor in suboptimal macrophage activation based on iNOS expression.

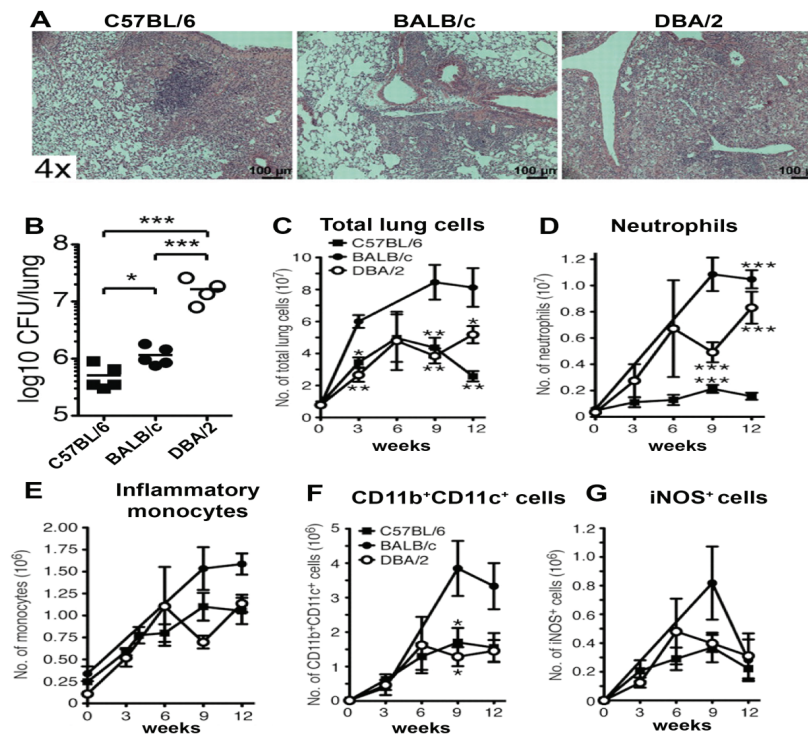


Figure 9. Lung pathology, bacterial load and myeloid cells recruitment in the lungs of Mtb infected mice.

4.1.2 A diminished α E-DC population in the lungs and PLN of susceptible mice during pulmonary TB - *Paper I*

A subset of lung DCs in mice that expresses CD103 (alpha E integrin) and beta 7 integrin was recently identified [203]. α E-DCs are migratory and are able to take up the bacteria and apoptotic vesicles and transport the antigens to the draining LN and present to MHC class I- or class II-restricted T cells [203, 261-264]. α E-DCs in the gut mucosa have tolerogenic properties and are able to induce Treg cells [214]. α E-DCs in the lung mucosa are strategically located and likely to influence the host immune response similar to their counterpart in the gut mucosa. Therefore, we hypothesized that α E-DCs in the lungs are analogous to α E-DC in the gut mucosa and control the inflammatory response during pulmonary TB to help ameliorate disease. As a consequence, defective α E-DC recruitment and function will exacerbate lung inflammation and prevent bacterial clearance.

Therefore, we enumerated and characterized lung and PLN α E-DCs in naïve and Mtb-infected resistant and susceptible mice. We observed that the number of α E-DC was comparable in the naïve lungs of all mouse strains analysed. In response to Mtb infection the number of lung α E-DCs increased dramatically in resistant animals (Figure 10A). In contrast, highly susceptible mice failed to recruit α E-DCs even during chronic infection. A similar pattern was observed in the PLN (Figure 10B). Mtb-infected resistant mouse strains recruited a higher number of α E-DCs to the site of infection than susceptible mice, suggesting that α E-DCs have a protective role in host immunity during pulmonary TB. In addition, the lower number of α E-DCs in the draining PLN may reflect reduced α E-DC migration from the Mtb-infected lungs in susceptible mice.

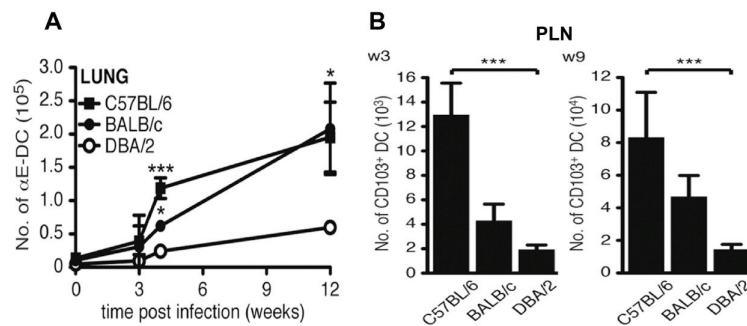


Figure 10. Number of α E-DCs recruited to the lungs and PLN during Mtb infection.

Previous data have shown that during steady-state conditions, BM inflammatory monocytes gives rise to lung α E-DC [262]. We extended these observations and showed that recruited monocytes can differentiate into α E-DC in Mtb-infected

mice (paper II, see below). Since recruitment of inflammatory monocytes is not defective in the susceptible mice, it seems likely that monocyte differentiation into α E-DCs is altered in susceptible animals during TB.

4.1.3 α E-DCs have a skewed cytokine profile during pulmonary TB -*Paper I & II*

Paper I we showed that lung α E-DC was the only myeloid cell population that did not produce TNF α during pulmonary TB. Instead, α E-DC contained the highest percentage of TGF β -producing cells after *in vitro* stimulation (Paper I). TNF α is a pro-inflammatory cytokine required for control of Mtb in both humans and mice [27, 28, 155, 156], while TGF β is known for immune suppressive function and induction of Treg cells [214, 265, 266]. In addition, in Paper II, we showed that the α E-DC population contained the highest proportion of IL-12p40 producing cells. IL-12 is known to drive Th1 response and it is critical for control Mtb [25, 152, 154]. However, IL-12 together with TGF β are also able to promote conversion of Treg cells into IFN γ -expressing cells in a colitis experimental model [267]. Interestingly, the Foxp3⁺IFN γ ⁺ T cells maintained their regulatory functions and suppressed colitis development [267]. Similarly, after infection with a virulent clinical Mtb isolate, Foxp3⁺ Treg cells produced IFN γ during pulmonary TB (Paper I). IL-12 and TGF β production by α E-DCs may promote the induction of Foxp3⁺ IFN γ ⁺ Treg cells that could help ameliorate the disease during the chronic state.

In conclusion, during the chronic phase of TB, a balance between pro-inflammatory and anti-inflammatory reactions is needed in order to prevent excessive inflammation that may cause tissue damage. α E-DCs may play role in balancing inflammatory reactions by producing anti-inflammatory cytokines and inducing, or maintaining, Treg cells in infected lungs.

4.1.4 A diminished Foxp3⁺ Treg cell population in Mtb-infected lungs of susceptible mice – *Paper I*

When we developed the hypothesis regarding the role of lung α E-DC in host immunity during pulmonary TB, there was only evidence from the gut mucosa showing that α E-DCs are able to induce Treg cells [214]. Still, we determined if the failure to recruit α E-DCs in Mtb-infected susceptible mice correlated with a reduced number of Treg cells in the infected lung tissue. Interestingly, we found that the CD4⁺ T cell population in the lungs of resistant mice contained a significant proportion of Treg cells. In contrast, the frequency of Treg cells was dramatically reduced in the CD4⁺ T cell population at the peak of the immune response (three weeks pi), and they were essentially absent from the lungs of chronically infected susceptible mice (12 weeks pi). Surprisingly, despite the difference in the lung Treg cell compartment, no difference in the percentages or absolute numbers of Treg cells was found in the draining PLN three or 12 weeks pi in all three mouse strains tested. Furthermore, we observed that these Treg

cells isolated from Mtb-infected mice, but not from naïve mice, produced IFN γ after *in vitro* polyclonal activation.

The ability of α E-DCs to induce Treg cells in the lungs was not observed until recently. α E-DCs in the lungs are indeed able to induce Treg cells via a TGF β - and retinoic acid-dependent mechanism [215]. In addition, Batf3^{-/-} mice, that lack the α E-DC population, failed to induce tolerance to inhaled ovalbumin [215], implying a tolerogenic function for lung α E-DC. Moreover, IL-12 together with TGF β are able to promote conversion of Treg cells into IFN γ -expressing cells that maintain their regulatory property [267]. In summary, our results showed that the reduced number of α E-DCs in Mtb-infected susceptible mice and that α E-DCs produced TGF β and IL-12 coincided with a diminished pool of lung Treg cells and increased lung inflammation, suggesting that α E-DCs play a role in regulating the immune response via TGF β and IL-12 production.

In conclusion, our results identify differences among α E-DCs and Treg cells in Mtb-resistant and susceptible inbred mice that may increase our understanding of immune regulation during pulmonary TB.

4.1.5 Recruited monocytes differentiate into lung and PLN α E-DC during pulmonary TB – paper II

Inflammatory monocytes give rise to the lung α E-DCs during steady state and under inflammatory conditions [201]. However, data supporting inflammatory monocyte differentiation into α E-DCs during pulmonary TB was missing. To determine whether recruited monocytes are precursor cells to α E-DCs in the lung and PLN during pulmonary TB and contribute to the increase in cell numbers in response to infection, we took advantage of a monocyte adoptive transfer model using enriched primary BM monocytes from naïve donor mice [42]. Enriched BM monocytes from naïve CD45.2⁺ C57BL/6 mice were adoptively transferred into Mtb-infected CD45.1⁺ congenic recipient mice. Endogenous and transferred cells in the lung tissue were identified and analysed 10 days later. Our results showed for the first time that recruited inflammatory monocytes differentiated into CD11b⁺CD11c⁺Ly6C⁺CD103⁺MHC-II⁺ cells in the infected lungs and PLN. This cell surface phenotype is identical to endogenous α E-DC and we conclude that recruited inflammatory monocytes give rise to α E-DC in both the lungs and in the PLN during pulmonary TB (Figure 11).

4.1.6 α E-DCs localize beneath the bronchial epithelial cell layer and near the vascular wall in Mtb-infected lungs – paper II

Sung *et al* first identified murine α E-DC in the lung tissue, and showed that α E-DC localize near the basal surface of bronchial epithelial cells and in close proximity to vascular endothelial cells [203]. To confirm the tissue localization of α E-DC in naïve mice, we used the co-expression of CD103 and MHC-II as a criterion to distinguish α E-DC from other lymphoid and myeloid cell subsets in lung tissue sections.

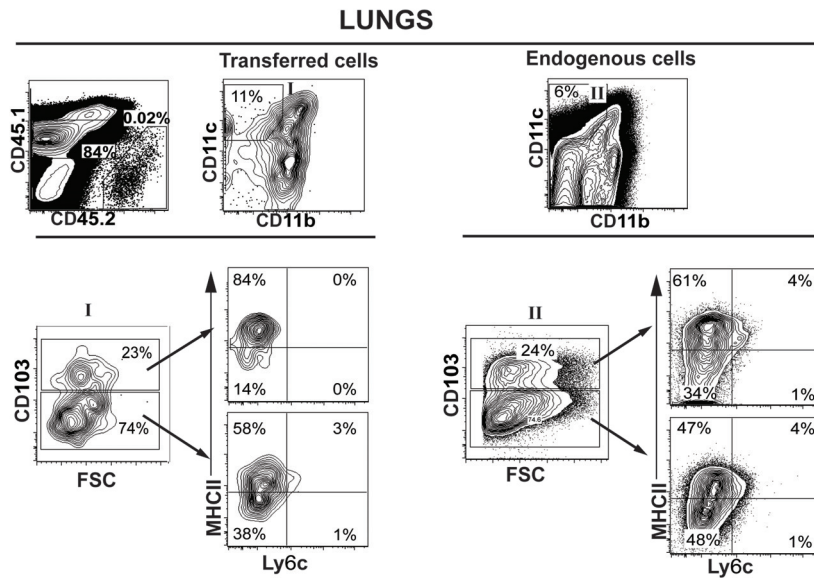


Figure 11. Recruited inflammatory monocytes differentiate into lung α E-DCs during pulmonary TB.

As expected CD103⁺MHC-II⁺ α E-DC localize in close proximity to the basolateral side of the bronchial epithelial cell layer in naïve mouse lungs. Also, CD103⁺MHC-II⁺ α E-DC were identified close to the arterial wall (Figure 12A).

We have shown that the functional potential of α E-DCs was preserved during early and chronic Mtb infection (Paper I) [43]. Since the localization near the bronchial epithelium may contribute to α E-DC function during TB, we determined if α E-DC tissue localization change in response to Mtb infection. Similar to naïve mice, α E-DC localized near the basolateral side of the bronchial epithelium and close to the arterial vasculature in Mtb-infected mice (Figure 12B).

In conclusion, while Mtb infection increases the absolute number of lung α E-DCs, it does not influence α E-DC tissue localization in the infected lungs. The constant localization next to the bronchial epithelium in naïve and infected mice may help explain the conserved functional potential of α E-DCs during TB.

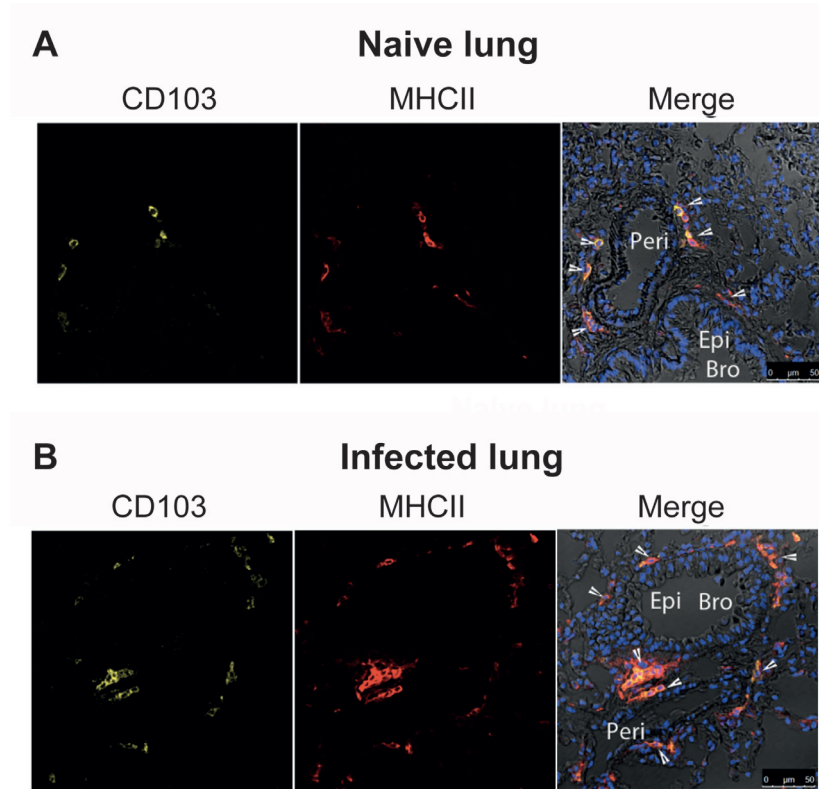


Figure 12. Tissue localization of lung α E-DCs in uninfected mice and during pulmonary TB. *Peri* = Perivascular wall, *Epi* = Epithelium, *Bro* = Bronchus.

4.1.7 α E-DC is not a main target for *Mtb* *in vivo* – paper II

α E-DCs line the conducting airways and express tight junction proteins [203]. This may allow them to readily capture inert antigens, or infectious microorganisms by extending their dendrites through the epithelial barrier into the airway lumen. We therefore used GFP-expressing *Mtb* to investigate if α E-DC is targeted by the bacterium *in vivo*. We found that only a minor fraction of α E-DC in the lungs was infected (Figure 13B). Enumeration of infected α E-DC confirmed that α E-DC population is not a main target for the bacterium at this stage of the disease (three weeks pi). For comparison, we included the percentage and total number of infected cells in each myeloid cell subsets in the bar graph (Figure 13A). α E-DCs were identified in the CD11b⁺CD11c⁺ cell subsets and were found to contain the lowest proportion and number of infected cells at three weeks pi despite the localization near the airways. We also observed that CD11b⁺CD11c⁺

cells were infected in the PLN. Compared to the lung tissue, the frequency and absolute number of infected cells was approximately 10-fold lower in the PLN. In addition, we also show that virulent Mtb did not significantly alter cell surface expression levels of MHC-II on infected cells, which is in agreement with the literatures [39, 268].

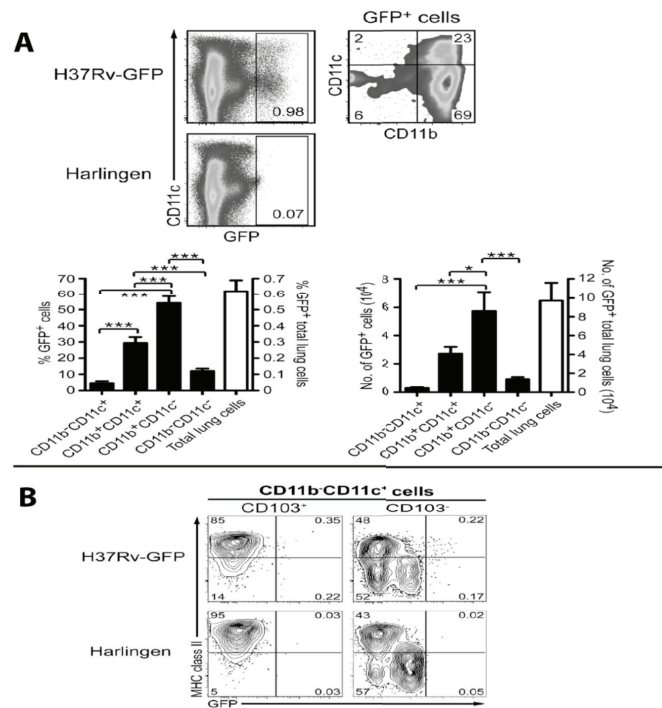


Figure 13. Few lung α E-DCs are Mtb-infected *in vivo*.

Our results clearly showed that only a minor fraction of α E-DCs was Mb-infected at this early time point. Thus DC subset is therefore less likely to transport the pathogen to the PLN. However, α E-DC might play role in T cell priming since this DC subset is able to take up apoptotic cells in the lungs and transfer the antigens to the PLN to prime antigen specific T cells [264].

Summary - Paper I & II

Our results suggest a role for α E-DCs during pulmonary TB (Figure 14), in which inflammatory monocytes are recruited into the Mtb-infected lung tissue and, depending on which non-hematopoietic cells they interact with, differentiate along different paths to give rise to multiple monocyte-derived cells, including DC with a distinctive α E-DCs phenotype. The interaction of monocytes and airway epithelial cells may support differentiation into α E-DC that express CD103 integrin that interacts with E-cadherin at the basolateral side of lung epithelial cells. During the initial phase of Mtb infection, α E-DC can be, albeit not the main target, infected by Mtb and may potentially take up apoptotic vesicles that contain Mtb-derived antigens and migrate to the draining PLN where they can prime naïve T cells, including CD8⁺ T cells. Based on the cytokine production and data from other investigators, α E-DCs may induce, or maintain, Treg cells during Mtb infection and have an immunosuppressive role. If so, α E-DCs can play role in balancing excessive inflammation during chronic infection. The defect in formation of α E-DCs and their functions may contribute to susceptibility in TB

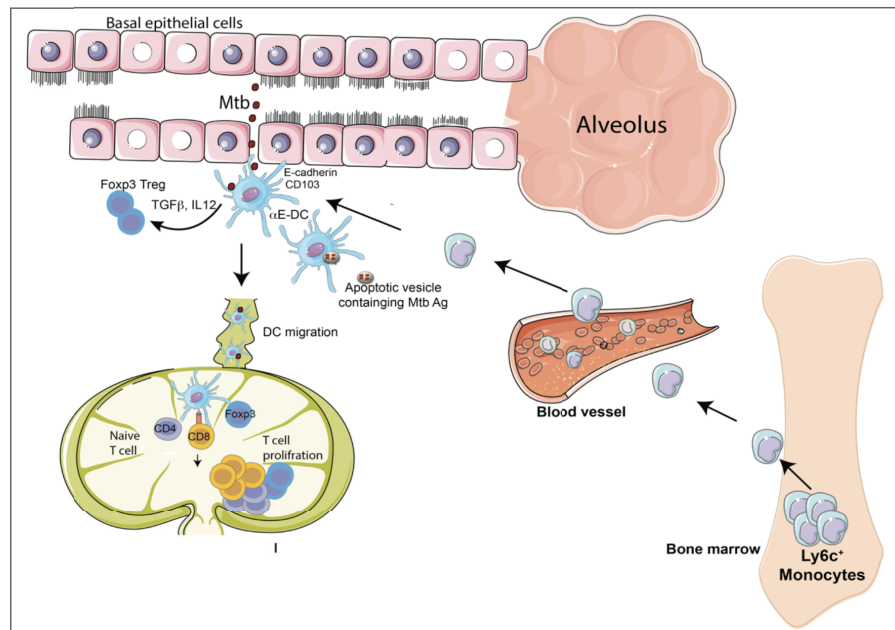


Figure 14. A proposed role for α E-DCs during pulmonary TB.

4.2 ONGOING MTB INFECTION INTERFERES WITH THE HIV VACCINE RESPONSE IN MICE - PAPER III

Due to the facts that an estimated one-third of the world's population have been infected by Mtb [1] and the areas of the highest prevalence of HIV are geographically the same as the Mtb endemic region [10], the effectiveness of current HIV vaccine development might be affected by pre-existing immune responses against the bacterium. Therefore, in this study we aimed to investigate the impact of ongoing Mtb infection on the immunogenicity of a HIV DNA/protein vaccine candidate in a mouse model. We used the MultiHIV DNA (DNA plasmids encoding gp160 of HIV-1 subtype B; p37Gag, Nef, Tat, and Rev) vaccine candidate [269, 270] with double recombinant HIV viral protein boosts (gp160Env, p24Gag, Tat and Nef) [271, 272]. Mtb-resistant female C57BL/6 mice were aerosol infected seven weeks prior to the start of the HIV vaccination regimen. We investigated the local immune response at the vaginal mucosal surface, and systemic cellular and humoral immune responses to the vaccine.

4.2.1 Ongoing Mtb infection impairs humoral immune response induced by HIV vaccination

After acquiring HIV, neutralizing and non-neutralizing antibodies develop in response to HIV antigens [273-276]. Most cases of HIV transmission occur at the mucosal surface of the genital organs [277] where IgA is an important class of immunoglobulin. High level of anti-HIV Env IgA in cervicovaginal washes of highly HIV-exposed persistently seronegative women indicates an important role of mucosal IgA in HIV protection [278, 279]. Also, anti-HIV IgA has recently been found to protect monkeys from SIV after viral challenge via the rectal route [280].

In this study, we tested if ongoing Mtb infection affects the antibody response elicited by the HIV vaccine. We determined specific IgA and IgG antibodies to HIV proteins, i.e. p24Gag and gp160Env, both in vaginal discharge and in serum. We found that Mtb-infected mice that were vaccinated intranasally exhibited lower levels of p24Gag-specific, but not gp160Env-specific, vaginal IgA four weeks post-vaccination compared to uninfected mice (Figure 15A-B). Intranasal vaccination induced higher level of p24Gag-specific IgA in vaginal secretions while intramuscular vaccination elicited higher serum levels of IgA specific for both p24Gag and gp160Env (Figure 15C,15D). Interestingly, the specific IgA levels were suppressed in Mtb-infected mice that were vaccinated via the intranasal, but not via the intramuscular route.

Two weeks after second proteins boost, p24Gag- and gp160Env-specific serum IgGs were also suppressed in intranasally HIV vaccinated Mtb-infected mice (Figure 15E,15F). Although at four weeks after the second proteins boost there was a slight decrease in the level of IgGs in the Mtb-infected mice, but the difference did not reach statistical significance.

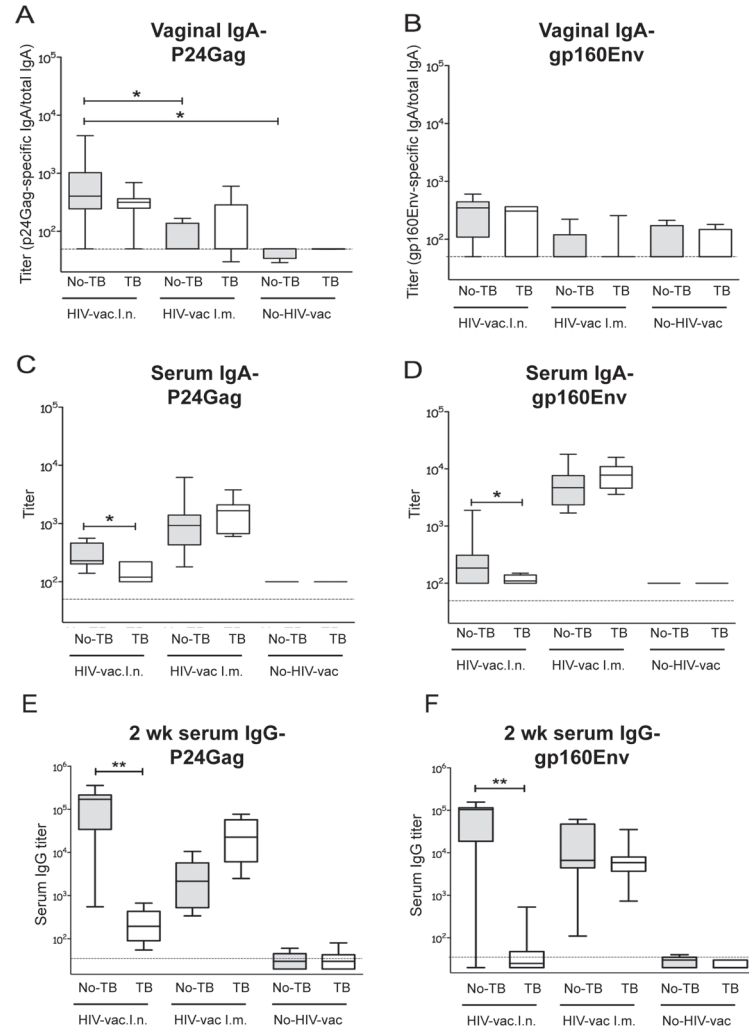


Figure 15. Effect of Mtb infection on HIV-specific serum IgG titers induced by MultiHIV DNA vaccination followed by protein boost.

Next, we determined the neutralization capability of the serum antibodies by using the 50% HIV neutralization assay. We found that intramuscular vaccination elicited three-fold higher HIV-neutralizing activity than that after intranasal vaccination. Interestingly, while Mtb infection had no effect on the neutralizing activity in sera of intranasally vaccinated mice, it was reduced more than three-fold in animals that were vaccinated via the intramuscular route.

In conclusion, our results showed for the first time that chronic Mtb infection had negative effects on the development of specific antibodies to the vaccine components, i.e. low level of mucosal IgA and serum IgGs and reduced serum neutralizing capability. However, the observed effects depended on the vaccination route.

4.2.2 Ongoing Mtb Infection suppressed the T cell response induced by the HIV vaccine

CD4⁺ and CD8⁺ T cells that are capable of producing both IFN γ and IL-2 were suggested to play role in the control of HIV infection [281-283]. We next sought to determine whether Mtb infection affects vaccine-induced IFN γ , IL-2 and/or TNF α producing CD8⁺ or CD4⁺ T cells. Splenocytes were re-stimulated with HIV p24Gag peptide pools *ex vivo* and cytokines expression were determined by intracellular cytokine staining. We found that uninfected mice induced high numbers of p24Gag-specific CD4⁺ and CD8⁺ T cells expressing only one of the cytokines IFN γ or TNF α , and low to moderate numbers of IL-2 producing cells as compared to Mtb-infected and vaccinated mice regardless of vaccination route (Figure 16B,16C). Importantly, both the number and the proportion of multifunctional CD4⁺ T cells were significantly decreased in spleens of Mtb-infected/intramuscular HIV-vaccinated mice compared to uninfected/HIV-vaccinated animals; six-fold reduction of triple cytokine-producing CD4⁺ T cells, and nine-fold reduction of IFN γ /TNF α producing CD4⁺ T cells were observed (Figure 16A). A similar trend was also found in animals vaccinated via the intranasal route. In conclusion, our data show that Mtb infection had an adverse effect on multiple effector functions of the adaptive immune response believed to be important for efficient control of HIV infection.

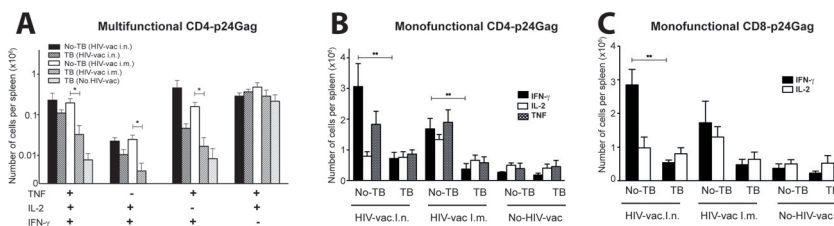


Figure 16. HIV p24Gag-specific T cell cytokine responses in spleens of uninfected or Mtb-infected mice vaccinated with MultiHIV DNA/protein.

Summary Paper III

Mtb infection interferes with both humoral and cellular immune responses to a HIV DNA/protein vaccine candidate. The impairment of HIV-specific immune responses in Mtb-infected mice can be identified as:

- Low level of IgA in vaginal discharges and low level of IgGs in serum following intranasal HIV vaccination
- Reduced serum neutralizing capability after intramuscular HIV vaccination
- Decrease in number of either IFN γ or TNF α producing CD4 $^{+}$ and CD8 $^{+}$ T cells regardless of vaccination route
- A diminished vaccine-specific multifunctional CD4 $^{+}$ T cell response after intramuscular HIV vaccination

4.3 A MURINE MODEL OF MTB/HIV-1 CO-INFECTION FOR STUDIES ON PATHOGEN-SPECIFIC T CELL RESPONSES *IN VIVO* -PAPER IV

Mtb/HIV-1 co-infection causes a major global health problem. Preventive vaccines are not yet available for any of the two pathogens. A challenge for vaccine development is to understand the components of protective immunity for each pathogen as well as during co-infection. Animal models can be important for studying immune responses during co-infection. However, finding a suitable animal model is problematic since HIV does not cause disease in conventional WT mice, or in NHPs. Despite the limitation, co-infection in NHP can be performed using simian immunodeficiency virus (SIV) and Mtb [284, 285]. However, the NHP model faces the problem of high cost, to genetically manipulate the host and ethical issues. Thus, there is an urgent need for a small-animal model that is robust, easy to manipulate, has low cost and a large availability of reagents for Mtb/HIV-1 co-infection investigations. In this study we exploited the chimeric virus EcoNDK, which is able to infect immune-competent WT mice [257], in combination with our murine TB model to establish a mouse model of Mtb/HIV-1 co-infection.

4.3.1 Mtb/EcoNDK co-infected mice displayed a significantly higher viral load, but co-infection had no impact on disease progression

We first infected mice with a low dose of virulent Mtb via the respiratory route. Three weeks post infection the animals were injected with a single dose of the virus intraperitoneally to establish Mtb/EcoNDK co-infection. After an additional two weeks, we examined viral replication in lung cells and splenocytes and found a significantly higher viral load in Mtb/EcoNDK co-infected mice compared to

EcoNDK-infected animals (Figure 17). In addition, we determined the bacterial load in the lungs and we monitored the change in weight of the animals over time. We observed no significant difference in bacterial burden, or difference in weight between Mtb/EcoNDK co-infected animal and animals infected with Mtb alone.

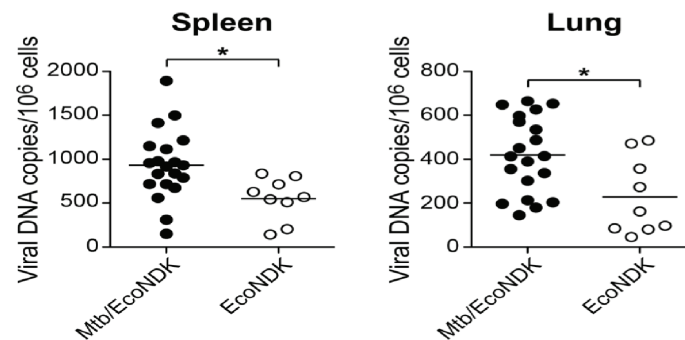


Figure 17. Increased viral load in Mtb/EcoNDK co-infected mice.

4.3.2 Characterization of the Mtb-specific CD8⁺ T cell response during the early stage of Mtb/EcoNDK infection

We enumerated the number of CD4⁺ T cells and CD8⁺ T cell in the lungs and spleen of infected animal. We found no significant difference in the number of CD4⁺ T cells and CD8⁺ T cells in Mtb/EcoNDK co-infected mice compared to animals infected with Mtb alone. In a time-course experiment we used tetramer technology to characterize the Mtb-specific CD8⁺ T cell response. We found that following Mtb infection the number of TB10.4-specific CD8⁺ T cells was significantly higher in the lungs of resistant BALB/c mice compared to susceptible DBA/2 mice. We extended these observations to our co-infection model. Interestingly, the number and proportion of Mtb-specific CD8⁺ T cells in the spleen of co-infection mice were significantly higher than in Mtb-infected mice (Figure 18). However, the difference in the generation of Mtb-specific CD8⁺ T cells in the lungs of two groups of mice did not reach statistical significance. We did observe that lung Mtb-specific CD8⁺ T cells in co-infected animals expressed significantly higher level of the $\alpha\beta$ T-cell receptor. Overall, EcoNDK influence the adaptive T cell response directed towards the bacterium.

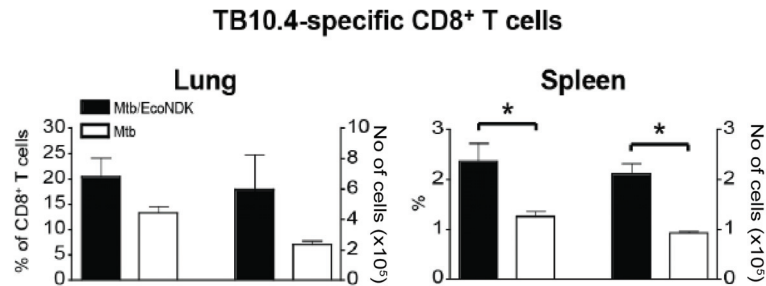


Figure 18. Mtb-specific CD8⁺ T cells in the lungs and in the spleen of Mtb/EcoNDK co-infected mice.

One of the characteristics of HIV pathogenesis is chronic immune activation, which include hyperactivation of immune cells [286], high turn-over of lymphocytes [287], increased levels of inflammatory cytokines [288] and the expression of activation or exhaustion makers on both CD4⁺ and CD8⁺ T cells [289, 290]. Tim-3 and PD-1 have been implicated as T cell exhaustion markers and associated with disease progression in HIV infection [193-195, 291]. Increased Tim-3 expression on CD8⁺ T cells has been shown to correlate with severity of pulmonary TB in humans [196]. The interaction of exhaustion molecules and their ligands may play role in regulating host immune responses to both HIV and Mtb infection. Therefore, we characterised the expression of Tim-3 and PD-1 on total CD4⁺ and CD8⁺ T cells, and Mtb-specific CD8⁺ T cells. In addition, we determined the cytokine profile of the T cell subsets in Mtb-infected and Mtb/EcoNDK co-infected mice, respectively. Even though we did not observe any significant difference in the expression of Tim-3 and PD-1 between Mtb infected- and co-infected mice, we found that Tim-3 and PD-1 are utilized differently by CD4⁺ T cells, TB10.420–28 peptide. The number and proportion of Tim-3 expression CD8⁺ T cells was higher than among CD4⁺ T cells. Furthermore, Tim-3 expression was even more pronounced on TB10.4-specific CD8⁺ T cells while PD-1 was preferentially expressed on CD4⁺ T cell (Figure 19). Finally, we showed that TB10.4-specific CD8⁺Tim3⁺ T cells were enriched for TNFα- and IFNγ-producing cells during the early stage of co-infection.

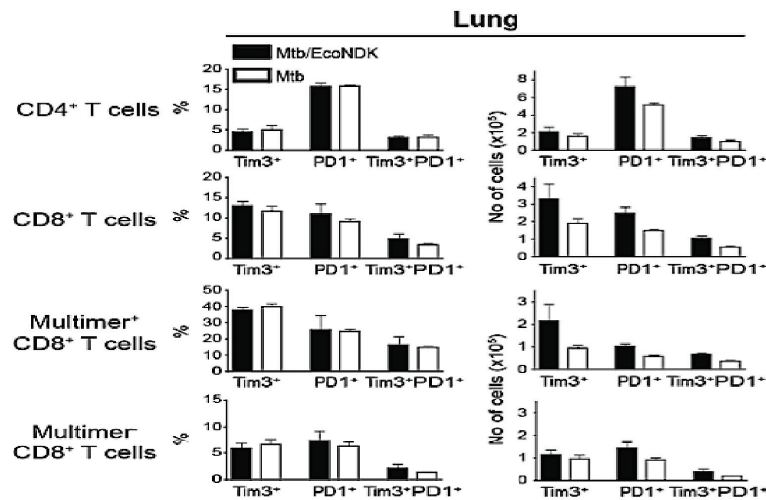


Figure 19. Different Tim-3 and PD-1 expression profiles on CD4⁺ and CD8⁺ T cell subsets in infected mice.

In conclusion, we have shown that we were able to successfully establish a small animal model for Mtb/HIV-1 co-infection. Our murine co-infection model may be a useful tool to elucidate immune responses directed against both pathogens.

Summary Paper IV

We established a mouse model of Mtb/HIV-1 co-infection using the chimeric EcoNDK virus and virulent Mtb. The characteristics of the co-infected mice are

- Higher virus burden in the lungs and spleen of co-infected mice
- No sign of increased pathology, i.e. no change in bacterial burden or weight loss
- Significantly increased number and proportion of Mtb-specific CD8⁺ T cells in the spleen
- Mtb-specific CD8⁺ T cells expressed high levels of Tim-3
- Mtb-specific CD8⁺Tim-3⁺ T-cells produced both IFN γ and TNF α

5 ACKNOWLEDGEMENTS

I gratefully acknowledge the support from the Royal Thai Government, Thailand for my PhD scholarship and deeply appreciate the additional support from Stiftelsen Sigurd och Elsa Goljes Minne.

Every journey has an end. Finally, my PhD degree is just around the corner. I would like to take this opportunity to express my sincere gratitude and thank many people who have walked along with me on this path.

Markus Sköld, my main supervisor, for your great courage to accept me as your first PhD student. You are an excellent supervisor. I deeply appreciate your enthusiasm in helping to train me how to perform animal experiments and developing my scientific and critical thinking. You make me feel so privileged to work with animals and virulent *Mycobacterium tuberculosis*. You always have time for me, are patient with me and never get tired to discuss with me. I learned so much from you. I feel that I have got all your support all the time. I think I am very lucky to have had the opportunity to work with you. Without you, I would not have succeeded in completing my PhD studies. Thank you so much.

Prof. Markus Maeurer, my co supervisor, for taking me in your group and guiding me to my main supervisor. Thank you for your kindness and all support.

Prof. Hans Wigzell: for accepting to be my co supervisor.

To all other current and previous Maeurer's lab members: I feel so grateful to know all of you, first at SMI, then at MTC and now at HS. **Isabelle Magalhaes**: for your friendship and encouragement over the years. **Lalit Rene**: I am seeing the change in your life, from a brilliant Indian boy, and now you are a father!! Of course the brilliant is still with you©. Thanks for being you and rescuing my soul in the darkness of life. **Rebecca Axelsson Robertson**: for your friendship and organizing great activities for us. **Nancy Alvarez de Andara**: a star from Honduras, for our happy time and great talk. Thanks **Aditya Sai**: the metro boy who has never called me by my name. **Lena Pelez-Bercoff**: for your friendship and coffee time. **Antonio Rothfuchs**: thanks for making such a nice environment in the lab and office at MTC; I will miss the nice coffee smell. **Vishnu Priya**: for your company and great office mate at MTC!! **Davide Valentini**: for fun, laugh and cheer. **Marlene Quesada-Rolander**: for your help in administrative issues and nice discussion. **Shreemanta K Parida**, a new member but we have known you for a long time, thanks for your kind heart and great indian food.

Collective thanks to **Thomas Poirer, Liu Zhenjiang, Qingda Meng** and former members **Nalini Kumar Vadu, Simanni Gaseitsiwe, Giovanni Ferrara, Muhammad Rashid**. Special thanks to **Raija Ahmed**: a kind lady on earth, for always taking care of me and cheering me up. **Shahnaz Madhavifar**: lively and happy señorita, you always brought care, laugh and fun to our group. I still remember the sweet lunch with teardrops!! thank you.

Lech Ignatowicz: my partner in crime. It is hard to forget the great offers, 'I can kill for you' or 'I kill, you take organs'. Thanks for all the time that we worked and had fun together, and your trust in me☺.

Jolanta Mazurek: for nice discussion and all the bacteria ☺

Marian Jansson and Andrezj Pawlowski: for our nice regular lab meeting.

Staff at the Astrid Fagraeus Laboratory, Karolinska Institutet, and MTC animal facilities, especially **Christel Werner** for taking care of the animals.

Prof. Cecilia Naucner Söderberg and her lab's member at CMM: **Chato, Maral, Koon Chu Yaiw** and **Aleem**: for supporting the confocal microscopy work.

Prof. Carmen Fernández, and **Olga Chuquimi**, Stockholm University: for training AEC isolation.

Pontus Jureen: for your great help in bacteria.

Sherwin Chan: for your kindly help in molecular technique.

Thanks to my students **Solomon** and **Aline**.

Prof. Martin Rottenberg's group. Thanks for treating the neighbours so nicely. **Martin**: you are a special and down to earth professor. Thanks for your kindness. The big **Berit**: for your kind heart and Fikas. Small Berit, **Berit Carow**: the TB queen, we had so many discussions on scientific topics and many more. Thanks for reading the Immunobiology textbooks together, and our travel time. Not only my scientific partner, you are a smart scientist, sporty girl, and a great baker, all in one. The first cake that I baked in my life was taught by you and it was delicious. **Suman Kumar**: you rock!!, kake, I am missing your greetings every morning. **Carina Olivera** : my ice skate trainer, thanks for fun time after work, ice-creams in the summer, chika!!. Also thanks **Gao** and **Pouria**.

MTC pub crew: **Mario Codemo, Anuj Patak, Katja Obieglo, Miriam Klien** and again Carina and Suman. We rock and are incredible!! Thank you for supporting my dream job☺.

Thanks to former and present SMI, MTC and KI friends: **Lena Wehlin, Emma, Senia, Rozina, Lotta, Sunitha, Sadia, Pradeep, Himjo, Ajay, Sridharen, Rajender, Essam, Sree Harsha, Frank and Guido.**

Special thanks to **Suhas Darekar, Harsha Shekar, Shahul Hameed, Anuj Patak, Romanico Arrighi** and **Ajay Kale** for being consistent & persistent for badminton games every week (we did not care if it was raining or snowing) for over 2 years, amazing!! Thanks for bringing me a lot of fun not only in the games but also life. I cannot say how much joy that we had together from all those countless fun activities. My life in Stockholm would have been so boring without you guys.

I would also like to thank Lalit and Suhas's wife: **Dipti** and **Ashwini**, respectively for your kindness to prepare great Indian food and have activities with me.

Ranjana Sarma: a unique and special Indian girl, for your great company during the last year here.

Patricia Munzeri: a kind and calm doctor from Tanzania, I am glad that I know you and you and I become best friends. Thanks for all your support.

Srisuda Panusorn: my Thai friend at MTC for your friendship.

Nong Joe and Nong B: for your great company, taking good care of me, laugh and fun during the first 2 years in Stockholm.

I would like to thank **Jae and JJ:** **Jae**, you are the first friends in Stockholm. The way I met you was amazing and the scenes on that day are still very clear in my mind. Thanks for your great company and friendship for all the time here. You mean a lot to me, little girl. **JJ:** for your gentleman, love and take good care of Jae.

Special thanks to **Chato Taher:** a smart doctor from Erbil, for being you as you are and your great support over the years. Also thanks for bringing the wonderful Kurdish people to my life; **Dr. Luqman:** a talented and humble man, I am glad that we met and become close friend. Thanks for your encouragement and support. I own you and your lovely wife: **Shaween** many many things. To **Dr. Hogir, Dr. Hozan & Dalia, Dr. Hazhar, Dr. Aram,** and **Dr. Dashti & Dr. Resheen** and **Dr. Zagros & Dr. Vian.** Thank you guys for delicious kurdish food & BBQ, great talks and many activities together. Zor supas!

To my family: my mom, my dear brothers and their families and relatives in Thailand for your endless love. In memory of my dad, who I love and miss dearly.

To all the animals in the experiments: thank you for your sacrifice for the sake of science.

6 REFERENCES

1. WHO. Global Tuberculosis Report. In; 2012.
2. Vitoria M, Granich R, Gilks CF, Gunneberg C, Hosseini M, Were W, *et al.* The global fight against HIV/AIDS, tuberculosis, and malaria: current status and future perspectives. *Am J Clin Pathol* 2009,**131**:844-848.
3. Lienhardt C, Glaziou P, Uplekar M, Lönnroth K, Getahun H, Raviglione M. Global tuberculosis control: lessons learnt and future prospects. *Nature Reviews Microbiology* 2012.
4. Glaziou P, Falzon D, Floyd K, Raviglione M. Global epidemiology of tuberculosis. *Semin Respir Crit Care Med* 2013,**34**:3-16.
5. Bloom BR. Tuberculosis. Back to a frightening future. *Nature* 1992,**358**:538-539.
6. Raviglione MC, Snider DE, Jr., Kochi A. Global epidemiology of tuberculosis. Morbidity and mortality of a worldwide epidemic. *JAMA* 1995,**273**:220-226.
7. Trunz BB, Fine P, Dye C. Effect of BCG vaccination on childhood tuberculous meningitis and miliary tuberculosis worldwide: a meta-analysis and assessment of cost-effectiveness. *Lancet* 2006,**367**:1173-1180.
8. Brennan MJ, Stone MR, Evans T. A rational vaccine pipeline for tuberculosis. *Int J Tuberc Lung Dis* 2012,**16**:1566-1573.
9. Moss JA. HIV/AIDS Review. *Radiol Technol* 2013,**84**:247-267; quiz p 268-270.
10. UNAIDS. Global Report UNAIDS Report on the global AIDS epidemic | 2012. In; 2012.
11. Bertozzi S, Padian NS, Wegbreit J, DeMaria LM, Feldman B, Gayle H, *et al.* HIV/AIDS Prevention and Treatment. 2006.
12. Fischl MA, Richman DD, Grieco MH, Gottlieb MS, Volberding PA, Laskin OL, *et al.* The efficacy of zidovudine (AZT) in the treatment of patients with AIDS and AIDS-related complex. A double-blind, placebo-controlled trial. *The New England journal of medicine* 1987,**317**:185-191.
13. Hammer SM, Katzenstein DA, Hughes MD, Gundacker H, Schooley RT, Haubrich RH, *et al.* A trial comparing nucleoside monotherapy with combination therapy in HIV-infected adults with CD4 cell counts from 200 to 500 per cubic millimeter. AIDS Clinical Trials Group Study 175 Study Team. *N Engl J Med* 1996,**335**:1081-1090.
14. Sharma SK, Mohanan S, Sharma A. Relevance of latent TB infection in areas of high TB prevalence. *Chest* 2012,**142**:761-773.
15. Manabe YC, Bishai WR. Latent Mycobacterium tuberculosis-persistence, patience, and winning by waiting. *Nat Med* 2000,**6**:1327-1329.
16. Poulsen A. Some clinical features of tuberculosis. 1. Incubation period. *Acta Tuberc Scand* 1950,**24**:311-346.
17. O'Garra A, Redford PS, McNab FW, Bloom CI, Wilkinson RJ, Berry MP. The immune response in tuberculosis. *Annu Rev Immunol* 2013,**31**:475-527.
18. Richeldi L. An update on the diagnosis of tuberculosis infection. *Am J Respir Crit Care Med* 2006,**174**:736-742.
19. Harboe M, Oettinger T, Wiker HG, Rosenkrands I, Andersen P. Evidence for occurrence of the ESAT-6 protein in Mycobacterium tuberculosis and virulent Mycobacterium bovis and for its absence in Mycobacterium bovis BCG. *Infect Immun* 1996,**64**:16-22.
20. Lazarevic V, Pawar S, Flynn J. Measuring T-cell function in animal models of tuberculosis by ELISPOT. *Methods Mol Biol* 2005,**302**:179-190.
21. Chackerian AA, Alt JM, Perera TV, Dascher CC, Behar SM. Dissemination of Mycobacterium tuberculosis is influenced by host factors and precedes the initiation of T-cell immunity. *Infect Immun* 2002,**70**:4501-4509.

22. McElvania Tekippe E, Allen IC, Hulseberg PD, Sullivan JT, McCann JR, Sandor M, *et al.* Granuloma formation and host defense in chronic Mycobacterium tuberculosis infection requires PYCARD/ASC but not NLRP3 or caspase-1. *PLoS One* 2010,**5**:e12320.
23. Rhoades ER, Frank AA, Orme IM. Progression of chronic pulmonary tuberculosis in mice aerogenically infected with virulent Mycobacterium tuberculosis. *Tuber Lung Dis* 1997,**78**:57-66.
24. Chackerian AA, Behar SM. Susceptibility to Mycobacterium tuberculosis: lessons from inbred strains of mice. *Tuberculosis (Edinb)* 2003,**83**:279-285.
25. Cooper AM, Magram J, Ferrante J, Orme IM. Interleukin 12 (IL-12) is crucial to the development of protective immunity in mice intravenously infected with mycobacterium tuberculosis. *J Exp Med* 1997,**186**:39-45.
26. Flynn JL, Chan J, Triebold KJ, Dalton DK, Stewart TA, Bloom BR. An essential role for interferon gamma in resistance to Mycobacterium tuberculosis infection. *J Exp Med* 1993,**178**:2249-2254.
27. Flynn JL, Goldstein MM, Chan J, Triebold KJ, Pfeffer K, Lowenstein CJ, *et al.* Tumor necrosis factor-alpha is required in the protective immune response against Mycobacterium tuberculosis in mice. *Immunity* 1995,**2**:561-572.
28. Keane J, Gershon S, Wise RP, Mirabile-Levens E, Kasznica J, Schwieterman WD, *et al.* Tuberculosis associated with infliximab, a tumor necrosis factor alpha-neutralizing agent. *N Engl J Med* 2001,**345**:1098-1104.
29. McCune RM, Jr., McDermott W, Tompsett R. The fate of Mycobacterium tuberculosis in mouse tissues as determined by the microbial enumeration technique. II. The conversion of tuberculous infection to the latent state by the administration of pyrazinamide and a companion drug. *J Exp Med* 1956,**104**:763-802.
30. McCune RM, Feldmann FM, McDermott W. Microbial persistence. II. Characteristics of the sterile state of tubercle bacilli. *J Exp Med* 1966,**123**:469-486.
31. McCune RM, Feldmann FM, Lambert HP, McDermott W. Microbial persistence. I. The capacity of tubercle bacilli to survive sterilization in mouse tissues. *J Exp Med* 1966,**123**:445-468.
32. Scanga CA, Mohan VP, Joseph H, Yu K, Chan J, Flynn JL. Reactivation of latent tuberculosis: variations on the Cornell murine model. *Infect Immun* 1999,**67**:4531-4538.
33. Kramnik I, Demant P, Bloom BB. Susceptibility to tuberculosis as a complex genetic trait: analysis using recombinant congenic strains of mice. *Novartis Found Symp* 1998,**217**:120-131; discussion 132-127.
34. Harper J, Skerry C, Davis SL, Tasneen R, Weir M, Kramnik I, *et al.* Mouse model of necrotic tuberculosis granulomas develops hypoxic lesions. *J Infect Dis* 2012,**205**:595-602.
35. Driver ER, Ryan GJ, Hoff DR, Irwin SM, Basaraba RJ, Kramnik I, *et al.* Evaluation of a mouse model of necrotic granuloma formation using C3HeB/FeJ mice for testing of drugs against Mycobacterium tuberculosis. *Antimicrob Agents Chemother* 2012,**56**:3181-3195.
36. Reece ST, Loddenkemper C, Askew DJ, Zedler U, Schommer-Leitner S, Stein M, *et al.* Serine protease activity contributes to control of Mycobacterium tuberculosis in hypoxic lung granulomas in mice. *J Clin Invest* 2010,**120**:3365-3376.
37. Zuniga J, Torres-Garcia D, Santos-Mendoza T, Rodriguez-Reyna TS, Granados J, Yunis EJ. Cellular and humoral mechanisms involved in the control of tuberculosis. *Clin Dev Immunol* 2012,**2012**:193923.
38. van Crevel R, Ottenhoff TH, van der Meer JW. Innate immunity to Mycobacterium tuberculosis. *Clin Microbiol Rev* 2002,**15**:294-309.

39. Wolf AJ, Linas B, Trevejo-Nunez GJ, Kincaid E, Tamura T, Takatsu K, *et al.* Mycobacterium tuberculosis infects dendritic cells with high frequency and impairs their function in vivo. *J Immunol* 2007;**179**:2509-2519.
40. Urdahl KB, Shafiani S, Ernst JD. Initiation and regulation of T-cell responses in tuberculosis. *Mucosal Immunol* 2011;**4**:288-293.
41. Blomgran R, Ernst JD. Lung neutrophils facilitate activation of naive antigen-specific CD4+ T cells during Mycobacterium tuberculosis infection. *J Immunol* 2011;**186**:7110-7119.
42. Skold M, Behar SM. Tuberculosis triggers a tissue-dependent program of differentiation and acquisition of effector functions by circulating monocytes. *J Immunol* 2008;**181**:6349-6360.
43. Leepiyasakulchai C, Ignatowicz L, Pawlowski A, Kallenius G, Skold M. Failure to recruit anti-inflammatory CD103+ dendritic cells and a diminished CD4+ Foxp3+ regulatory T cell pool in mice that display excessive lung inflammation and increased susceptibility to Mycobacterium tuberculosis. *Infect Immun* 2012;**80**:1128-1139.
44. Bermudez LE, Goodman J. Mycobacterium tuberculosis invades and replicates within type II alveolar cells. *Infect Immun* 1996;**64**:1400-1406.
45. Das B, Kashino SS, Pulu I, Kalita D, Swami V, Yeager H, *et al.* CD271(+) bone marrow mesenchymal stem cells may provide a niche for dormant Mycobacterium tuberculosis. *Sci Transl Med* 2013;**5**:170ra113.
46. Philips JA, Ernst JD. Tuberculosis pathogenesis and immunity. *Annu Rev Pathol* 2012;**7**:353-384.
47. Ehlers S. DC-SIGN and mannosylated surface structures of Mycobacterium tuberculosis: a deceptive liaison. *Eur J Cell Biol* 2010;**89**:95-101.
48. Zimmerli S, Edwards S, Ernst JD. Selective receptor blockade during phagocytosis does not alter the survival and growth of Mycobacterium tuberculosis in human macrophages. *Am J Respir Cell Mol Biol* 1996;**15**:760-770.
49. Lee BY, Clemens DL, Horwitz MA. The metabolic activity of Mycobacterium tuberculosis, assessed by use of a novel inducible GFP expression system, correlates with its capacity to inhibit phagosomal maturation and acidification in human macrophages. *Mol Microbiol* 2008;**68**:1047-1060.
50. van der Wel N, Hava D, Houben D, Fluitsma D, van Zon M, Pierson J, *et al.* M. tuberculosis and M. leprae translocate from the phagolysosome to the cytosol in myeloid cells. *Cell* 2007;**129**:1287-1298.
51. Hagedorn M, Rohde KH, Russell DG, Soldati T. Infection by tubercular mycobacteria is spread by nonlytic ejection from their amoeba hosts. *Science* 2009;**323**:1729-1733.
52. Houben D, Demangel C, van Ingen J, Perez J, Baldeon L, Abdallah AM, *et al.* ESX-1-mediated translocation to the cytosol controls virulence of mycobacteria. *Cell Microbiol* 2012;**14**:1287-1298.
53. Ernst JD, Trevejo-Nunez G, Banaiee N. Genomics and the evolution, pathogenesis, and diagnosis of tuberculosis. *J Clin Invest* 2007;**117**:1738-1745.
54. Chen M, Gan H, Remold HG. A mechanism of virulence: virulent Mycobacterium tuberculosis strain H37Rv, but not attenuated H37Ra, causes significant mitochondrial inner membrane disruption in macrophages leading to necrosis. *J Immunol* 2006;**176**:3707-3716.
55. Divangahi M, Behar SM, Remold H. Dying to live: how the death modality of the infected macrophage affects immunity to tuberculosis. *Adv Exp Med Biol* 2013;**783**:103-120.
56. Blomgran R, Desvignes L, Briken V, Ernst JD. Mycobacterium tuberculosis inhibits neutrophil apoptosis, leading to delayed activation of naive CD4 T cells. *Cell Host Microbe* 2012;**11**:81-90.

57. Behar SM, Divangahi M, Remold HG. Evasion of innate immunity by Mycobacterium tuberculosis: is death an exit strategy? *Nat Rev Microbiol* 2010;**8**:668-674.
58. Behar SM, Martin CJ, Booty MG, Nishimura T, Zhao X, Gan HX, *et al*. Apoptosis is an innate defense function of macrophages against Mycobacterium tuberculosis. *Mucosal Immunol* 2011;**4**:279-287.
59. Gill WP, Harik NS, Whiddon MR, Liao RP, Mittler JE, Sherman DR. A replication clock for Mycobacterium tuberculosis. *Nat Med* 2009;**15**:211-214.
60. Leepiyasakulchai C, Taher C, Chuquimia OD, Mazurek J, Soderberg-Naucler C, Fernandez C, *et al*. Infection Rate and Tissue Localization of Murine IL-12p40-Producing Monocyte-Derived CD103(+) Lung Dendritic Cells during Pulmonary Tuberculosis. *PLoS One* 2013;**8**:e69287.
61. Zhang Y, Broser M, Cohen H, Bodkin M, Law K, Reibman J, *et al*. Enhanced interleukin-8 release and gene expression in macrophages after exposure to Mycobacterium tuberculosis and its components. *The Journal of clinical investigation* 1995;**95**:586-592.
62. Lu B, Rutledge BJ, Gu L, Fiorillo J, Lukacs NW, Kunkel SL, *et al*. Abnormalities in monocyte recruitment and cytokine expression in monocyte chemoattractant protein 1-deficient mice. *The Journal of experimental medicine* 1998;**187**:601-608.
63. Davis JM, Ramakrishnan L. The role of the granuloma in expansion and dissemination of early tuberculous infection. *Cell* 2009;**136**:37-49.
64. Davis JM, Clay H, Lewis JL, Ghorri N, Herbolme P, Ramakrishnan L. Real-time visualization of mycobacterium-macrophage interactions leading to initiation of granuloma formation in zebrafish embryos. *Immunity* 2002;**17**:693-702.
65. Murphy K, Travers P, Walport M. *Immunobiology*. 7 ed. New York: Garland Science, Taylor & Francis Group, LLC; 2008.
66. Kleinnijenhuis J, Oosting M, Joosten LA, Netea MG, Van Crevel R. Innate immune recognition of Mycobacterium tuberculosis. *Clin Dev Immunol* 2011;**2011**:405310.
67. Wolf AJ, Desvignes L, Linas B, Banaiee N, Tamura T, Takatsu K, *et al*. Initiation of the adaptive immune response to Mycobacterium tuberculosis depends on antigen production in the local lymph node, not the lungs. *J Exp Med* 2008;**205**:105-115.
68. Reiley WW, Calayag MD, Wittmer ST, Huntington JL, Pearl JE, Fountain JJ, *et al*. ESAT-6-specific CD4 T cell responses to aerosol Mycobacterium tuberculosis infection are initiated in the mediastinal lymph nodes. *Proc Natl Acad Sci U S A* 2008;**105**:10961-10966.
69. Beckman EM, Porcelli SA, Morita CT, Behar SM, Furlong ST, Brenner MB. Recognition of a lipid antigen by CD1-restricted alpha beta+ T cells. *Nature* 1994;**372**:691-694.
70. Porcelli S, Morita CT, Brenner MB. CD1b restricts the response of human CD4-8- T lymphocytes to a microbial antigen. *Nature* 1992;**360**:593-597.
71. Cohen NR, Garg S, Brenner MB. Antigen Presentation by CD1 Lipids, T Cells, and NKT Cells in Microbial Immunity. *Adv Immunol* 2009;**102**:1-94.
72. Tian T, Woodworth J, Skold M, Behar SM. In vivo depletion of CD11c+ cells delays the CD4+ T cell response to Mycobacterium tuberculosis and exacerbates the outcome of infection. *J Immunol* 2005;**175**:3268-3272.
73. Miller JD, van der Most RG, Akondy RS, Glidewell JT, Albott S, Masopust D, *et al*. Human effector and memory CD8+ T cell responses to smallpox and yellow fever vaccines. *Immunity* 2008;**28**:710-722.
74. Wallgren A. The time-table of tuberculosis. *Tubercle* 1948;**29**:245-251.
75. Hamilton-Easton A, Eichelberger M. Virus-specific antigen presentation by different subsets of cells from lung and mediastinal lymph node tissues of influenza virus-infected mice. *J Virol* 1995;**69**:6359-6366.

76. Bonato VL, Medeiros AI, Lima VM, Dias AR, Faccioliti LH, Silva CL. Downmodulation of CD18 and CD86 on macrophages and VLA-4 on lymphocytes in experimental tuberculosis. *Scandinavian journal of immunology* 2001,**54**:564-573.
77. Kan-Sutton C, Jagannath C, Hunter RL, Jr. Trehalose 6,6'-dimycolate on the surface of Mycobacterium tuberculosis modulates surface marker expression for antigen presentation and costimulation in murine macrophages. *Microbes and infection / Institut Pasteur* 2009,**11**:40-48.
78. Shafiani S, Tucker-Heard G, Kariyone A, Takatsu K, Urdahl KB. Pathogen-specific regulatory T cells delay the arrival of effector T cells in the lung during early tuberculosis. *J Exp Med* 2010,**207**:1409-1420.
79. Scott-Browne JP, Shafiani S, Tucker-Heard G, Ishida-Tsubota K, Fontenot JD, Rudensky AY, et al. Expansion and function of Foxp3-expressing T regulatory cells during tuberculosis. *J Exp Med* 2007,**204**:2159-2169.
80. Demangel C, Bertolino P, Britton WJ. Autocrine IL-10 impairs dendritic cell (DC)-derived immune responses to mycobacterial infection by suppressing DC trafficking to draining lymph nodes and local IL-12 production. *European journal of immunology* 2002,**32**:994-1002.
81. Lazarevic V, Nolt D, Flynn JL. Long-term control of Mycobacterium tuberculosis infection is mediated by dynamic immune responses. *J Immunol* 2005,**175**:1107-1117.
82. Flynn JL, Chan J. Immunology of tuberculosis. *Annu Rev Immunol* 2001,**19**:93-129.
83. Green AM, Difazio R, Flynn JL. IFN-gamma from CD4 T cells is essential for host survival and enhances CD8 T cell function during Mycobacterium tuberculosis infection. *J Immunol* 2013,**190**:270-277.
84. Caruso AM, Serbina N, Klein E, Triebold K, Bloom BR, Flynn JL. Mice deficient in CD4 T cells have only transiently diminished levels of IFN-gamma, yet succumb to tuberculosis. *J Immunol* 1999,**162**:5407-5416.
85. Cooper AM, Dalton DK, Stewart TA, Griffin JP, Russell DG, Orme IM. Disseminated tuberculosis in interferon gamma gene-disrupted mice. *J Exp Med* 1993,**178**:2243-2247.
86. Muller I, Cobbold SP, Waldmann H, Kaufmann SH. Impaired resistance to Mycobacterium tuberculosis infection after selective in vivo depletion of L3T4+ and Lyt-2+ T cells. *Infect Immun* 1987,**55**:2037-2041.
87. Pearl JE, Saunders B, Ehlers S, Orme IM, Cooper AM. Inflammation and lymphocyte activation during mycobacterial infection in the interferon-gamma-deficient mouse. *Cell Immunol* 2001,**211**:43-50.
88. Kannanganat S, Ibegbu C, Chennareddi L, Robinson HL, Amara RR. Multiple-cytokine-producing antiviral CD4 T cells are functionally superior to single-cytokine-producing cells. *Journal of virology* 2007,**81**:8468-8476.
89. Day CL, Abrahams DA, Lerumo L, Janse van Rensburg E, Stone L, O'Rie T, et al. Functional capacity of Mycobacterium tuberculosis-specific T cell responses in humans is associated with mycobacterial load. *J Immunol* 2011,**187**:2222-2232.
90. Sutherland JS, Adetifa IM, Hill PC, Adegbola RA, Ota MO. Pattern and diversity of cytokine production differentiates between Mycobacterium tuberculosis infection and disease. *European journal of immunology* 2009,**39**:723-729.
91. Caccamo N, Guggino G, Joosten SA, Gelsomino G, Di Carlo P, Titone L, et al. Multifunctional CD4(+) T cells correlate with active Mycobacterium tuberculosis infection. *European journal of immunology* 2010,**40**:2211-2220.
92. Aagaard C, Hoang T, Dietrich J, Cardona PJ, Izzo A, Dolganov G, et al. A multistage tuberculosis vaccine that confers efficient protection before and after exposure. *Nature medicine* 2011,**17**:189-194.

93. Mueller H, Fae KC, Magdorf K, Ganoza CA, Wahn U, Guehlich U, *et al.* Granulysin-expressing CD4⁺ T cells as candidate immune marker for tuberculosis during childhood and adolescence. *PLoS One* 2011,**6**:e29367.
94. Serbina NV, Lazarevic V, Flynn JL. CD4⁺ T cells are required for the development of cytotoxic CD8⁺ T cells during Mycobacterium tuberculosis infection. *J Immunol* 2001,**167**:6991-7000.
95. Cruz A, Khader SA, Torrado E, Fraga A, Pearl JE, Pedrosa J, *et al.* Cutting edge: IFN-gamma regulates the induction and expansion of IL-17-producing CD4⁺ T cells during mycobacterial infection. *J Immunol* 2006,**177**:1416-1420.
96. Lockhart E, Green AM, Flynn JL. IL-17 production is dominated by gamma delta T cells rather than CD4⁺ T cells during Mycobacterium tuberculosis infection. *J Immunol* 2006,**177**:4662-4669.
97. Cruz A, Fraga AG, Fountain JJ, Rangel-Moreno J, Torrado E, Saraiva M, *et al.* Pathological role of interleukin 17 in mice subjected to repeated BCG vaccination after infection with Mycobacterium tuberculosis. *J Exp Med* 2010,**207**:1609-1616.
98. Desvignes L, Ernst JD. Interferon-gamma-responsive nonhematopoietic cells regulate the immune response to Mycobacterium tuberculosis. *Immunity* 2009,**31**:974-985.
99. Moguees T, Goodrich ME, Ryan L, LaCourse R, North RJ. The relative importance of T cell subsets in immunity and immunopathology of airborne Mycobacterium tuberculosis infection in mice. *J Exp Med* 2001,**193**:271-280.
100. Flynn JL, Goldstein MM, Triebold KJ, Koller B, Bloom BR. Major histocompatibility complex class I-restricted T cells are required for resistance to Mycobacterium tuberculosis infection. *Proc Natl Acad Sci U S A* 1992,**89**:12013-12017.
101. Sousa AO, Mazzaccaro RJ, Russell RG, Lee FK, Turner OC, Hong S, *et al.* Relative contributions of distinct MHC class I-dependent cell populations in protection to tuberculosis infection in mice. *Proc Natl Acad Sci U S A* 2000,**97**:4204-4208.
102. Chen CY, Huang D, Wang RC, Shen L, Zeng G, Yao S, *et al.* A critical role for CD8⁺ T cells in a nonhuman primate model of tuberculosis. *PLoS Pathog* 2009,**5**:e1000392.
103. Lewinsohn DA, Heinzel AS, Gardner JM, Zhu L, Alderson MR, Lewinsohn DM. Mycobacterium tuberculosis-specific CD8⁺ T cells preferentially recognize heavily infected cells. *Am J Respir Crit Care Med* 2003,**168**:1346-1352.
104. Lewinsohn DA, Winata E, Swarbrick GM, Tanner KE, Cook MS, Null MD, *et al.* Immunodominant tuberculosis CD8 antigens preferentially restricted by HLA-B. *PLoS Pathog* 2007,**3**:1240-1249.
105. Axelsson-Robertson R, Loxton AG, Walzl G, Ehlers MM, Kock MM, Zumla A, *et al.* A broad profile of co-dominant epitopes shapes the peripheral Mycobacterium tuberculosis specific CD8⁺ T-cell immune response in South African patients with active tuberculosis. *PLoS One* 2013,**8**:e58309.
106. Canaday DH, Wilkinson RJ, Li Q, Harding CV, Silver RF, Boom WH. CD4⁺ and CD8⁺ T cells kill intracellular Mycobacterium tuberculosis by a perforin and Fas/Fas ligand-independent mechanism. *J Immunol* 2001,**167**:2734-2742.
107. Hsu T, Hingley-Wilson SM, Chen B, Chen M, Dai AZ, Morin PM, *et al.* The primary mechanism of attenuation of bacillus Calmette-Guerin is a loss of secreted lytic function required for invasion of lung interstitial tissue. *Proceedings of the National Academy of Sciences of the United States of America* 2003,**100**:12420-12425.
108. Mazzaccaro RJ, Gedde M, Jensen ER, van Santen HM, Ploegh HL, Rock KL, *et al.* Major histocompatibility class I presentation of soluble antigen facilitated by Mycobacterium tuberculosis infection. *Proceedings of the National Academy of Sciences of the United States of America* 1996,**93**:11786-11791.

109. Baena A, Porcelli SA. Evasion and subversion of antigen presentation by *Mycobacterium tuberculosis*. *Tissue Antigens* 2009;**74**:189-204.
110. Winau F, Weber S, Sad S, de Diego J, Hoops SL, Breiden B, *et al.* Apoptotic vesicles crossprime CD8 T cells and protect against tuberculosis. *Immunity* 2006;**24**:105-117.
111. Schaible UE, Winau F, Sieling PA, Fischer K, Collins HL, Hagens K, *et al.* Apoptosis facilitates antigen presentation to T lymphocytes through MHC-I and CD1 in tuberculosis. *Nat Med* 2003;**9**:1039-1046.
112. Behar SM. Antigen-specific CD8(+) T cells and protective immunity to tuberculosis. *Adv Exp Med Biol* 2013;**783**:141-163.
113. Axelsson-Robertson R, Ahmed RK, Weichold FF, Ehlers MM, Kock MM, Sizemore D, *et al.* Human leukocyte antigens A*3001 and A*3002 show distinct peptide-binding patterns of the *Mycobacterium tuberculosis* protein TB10.4: consequences for immune recognition. *Clin Vaccine Immunol* 2011;**18**:125-134.
114. Chan J, Xing Y, Magliozzo RS, Bloom BR. Killing of virulent *Mycobacterium tuberculosis* by reactive nitrogen intermediates produced by activated murine macrophages. *J Exp Med* 1992;**175**:1111-1122.
115. Stenger S, Hanson DA, Teitelbaum R, Dewan P, Niazi KR, Froelich CJ, *et al.* An antimicrobial activity of cytolytic T cells mediated by granulysin. *Science* 1998;**282**:121-125.
116. Lewinsohn DM, Alderson MR, Briden AL, Riddell SR, Reed SG, Grabstein KH. Characterization of human CD8+ T cells reactive with *Mycobacterium tuberculosis*-infected antigen-presenting cells. *J Exp Med* 1998;**187**:1633-1640.
117. Kamath AB, Woodworth J, Xiong X, Taylor C, Weng Y, Behar SM. Cytolytic CD8+ T cells recognizing CFP10 are recruited to the lung after *Mycobacterium tuberculosis* infection. *J Exp Med* 2004;**200**:1479-1489.
118. Flynn JL. Lessons from experimental *Mycobacterium tuberculosis* infections. *Microbes Infect* 2006;**8**:1179-1188.
119. Lazarevic V, Flynn J. CD8+ T cells in tuberculosis. *Am J Respir Crit Care Med* 2002;**166**:1116-1121.
120. Behar SM, Woodworth JS, Wu Y. Next generation: tuberculosis vaccines that elicit protective CD8+ T cells. *Expert Rev Vaccines* 2007;**6**:441-456.
121. Glatman-Freedman A, Casadevall A. Serum therapy for tuberculosis revisited: reappraisal of the role of antibody-mediated immunity against *Mycobacterium tuberculosis*. *Clin Microbiol Rev* 1998;**11**:514-532.
122. Rawool DB, Bitsaktsis C, Li Y, Gosselin DR, Lin Y, Kurkure NV, *et al.* Utilization of Fc receptors as a mucosal vaccine strategy against an intracellular bacterium, *Francisella tularensis*. *J Immunol* 2008;**180**:5548-5557.
123. Ulrichs T, Kosmiadi GA, Trusov V, Jorg S, Pradl L, Titukhina M, *et al.* Human tuberculous granulomas induce peripheral lymphoid follicle-like structures to orchestrate local host defence in the lung. *J Pathol* 2004;**204**:217-228.
124. Tsai MC, Chakravarty S, Zhu G, Xu J, Tanaka K, Koch C, *et al.* Characterization of the tuberculous granuloma in murine and human lungs: cellular composition and relative tissue oxygen tension. *Cell Microbiol* 2006;**8**:218-232.
125. Maglione PJ, Xu J, Chan J. B cells moderate inflammatory progression and enhance bacterial containment upon pulmonary challenge with *Mycobacterium tuberculosis*. *J Immunol* 2007;**178**:7222-7234.
126. Vordermeier HM, Venkataprasad N, Harris DP, Ivanyi J. Increase of tuberculous infection in the organs of B cell-deficient mice. *Clin Exp Immunol* 1996;**106**:312-316.
127. Bosio CM, Gardner D, Elkins KL. Infection of B cell-deficient mice with CDC 1551, a clinical isolate of *Mycobacterium tuberculosis*: delay in dissemination and development of lung pathology. *J Immunol* 2000;**164**:6417-6425.

128. Ramakrishnan L. Revisiting the role of the granuloma in tuberculosis. *Nat Rev Immunol* 2012,**12**:352-366.
129. Salgame P. MMPs in tuberculosis: granuloma creators and tissue destroyers. *The Journal of clinical investigation* 2011,**121**:1686-1688.
130. Hunter RL. Pathology of post primary tuberculosis of the lung: an illustrated critical review. *Tuberculosis (Edinb)* 2011,**91**:497-509.
131. Lin PL, Rodgers M, Smith L, Bigbee M, Myers A, Bigbee C, *et al.* Quantitative comparison of active and latent tuberculosis in the cynomolgus macaque model. *Infect Immun* 2009,**77**:4631-4642.
132. Lin PL, Pawar S, Myers A, Pegu A, Fuhrman C, Reinhart TA, *et al.* Early events in Mycobacterium tuberculosis infection in cynomolgus macaques. *Infect Immun* 2006,**74**:3790-3803.
133. Lin PL, Myers A, Smith L, Bigbee C, Bigbee M, Fuhrman C, *et al.* Tumor necrosis factor neutralization results in disseminated disease in acute and latent Mycobacterium tuberculosis infection with normal granuloma structure in a cynomolgus macaque model. *Arthritis Rheum* 2010,**62**:340-350.
134. Capuano SV, 3rd, Croix DA, Pawar S, Zinovik A, Myers A, Lin PL, *et al.* Experimental Mycobacterium tuberculosis infection of cynomolgus macaques closely resembles the various manifestations of human M. tuberculosis infection. *Infect Immun* 2003,**71**:5831-5844.
135. Sakaguchi S, Sakaguchi N, Shimizu J, Yamazaki S, Sakihama T, Itoh M, *et al.* Immunologic tolerance maintained by CD25+ CD4+ regulatory T cells: their common role in controlling autoimmunity, tumor immunity, and transplantation tolerance. *Immunological reviews* 2001,**182**:18-32.
136. Belkaid Y, Tarbell K. Regulatory T cells in the control of host-microorganism interactions (*). *Annual review of immunology* 2009,**27**:551-589.
137. Chen X, Zhou B, Li M, Deng Q, Wu X, Le X, *et al.* CD4(+)CD25(+)FoxP3(+) regulatory T cells suppress Mycobacterium tuberculosis immunity in patients with active disease. *Clin Immunol* 2007,**123**:50-59.
138. He XY, Xiao L, Chen HB, Hao J, Li J, Wang YJ, *et al.* T regulatory cells and Th1/Th2 cytokines in peripheral blood from tuberculosis patients. *Eur J Clin Microbiol Infect Dis* 2010,**29**:643-650.
139. Rahman S, Gudetta B, Fink J, Granath A, Ashenafi S, Aseffa A, *et al.* Compartmentalization of immune responses in human tuberculosis: few CD8+ effector T cells but elevated levels of FoxP3+ regulatory t cells in the granulomatous lesions. *Am J Pathol* 2009,**174**:2211-2224.
140. Shang S, Harton M, Tamayo MH, Shanley C, Palanisamy GS, Caraway M, *et al.* Increased Foxp3 expression in guinea pigs infected with W-Beijing strains of M. tuberculosis. *Tuberculosis (Edinb)* 2011,**91**:378-385.
141. Green AM, Mattila JT, Bigbee CL, Bongers KS, Lin PL, Flynn JL. CD4(+) regulatory T cells in a cynomolgus macaque model of Mycobacterium tuberculosis infection. *J Infect Dis* 2010,**202**:533-541.
142. Shafiani S, Dinh C, Ertelt JM, Moguche AO, Siddiqui I, Smigielski KS, *et al.* Pathogen-Specific Treg Cells Expand Early during Mycobacterium tuberculosis Infection but Are Later Eliminated in Response to Interleukin-12. *Immunity* 2013.
143. Quinn KM, McHugh RS, Rich FJ, Goldsack LM, de Lisle GW, Buddle BM, *et al.* Inactivation of CD4+ CD25+ regulatory T cells during early mycobacterial infection increases cytokine production but does not affect pathogen load. *Immunology and cell biology* 2006,**84**:467-474.
144. Ozeki Y, Sugawara I, Udagawa T, Aoki T, Osada-Oka M, Tateishi Y, *et al.* Transient role of CD4+CD25+ regulatory T cells in mycobacterial infection in mice. *International immunology* 2010,**22**:179-189.

145. Chen CY, Huang D, Yao S, Halliday L, Zeng G, Wang RC, *et al.* IL-2 simultaneously expands Foxp3⁺ T regulatory and T effector cells and confers resistance to severe tuberculosis (TB): implicative Treg-T effector cooperation in immunity to TB. *J Immunol* 2012,**188**:4278-4288.
146. Antonelli LR, Gigliotti Rothfuchs A, Goncalves R, Roffe E, Cheever AW, Bafica A, *et al.* Intranasal Poly-IC treatment exacerbates tuberculosis in mice through the pulmonary recruitment of a pathogen-permissive monocyte/macrophage population. *J Clin Invest* 2010,**120**:1674-1682.
147. Kaplan G. Cytokine regulation of disease progression in leprosy and tuberculosis. *Immunobiology* 1994,**191**:564-568.
148. Hernandez-Pando R, Aguilar D, Hernandez ML, Orozco H, Rook G. Pulmonary tuberculosis in BALB/c mice with non-functional IL-4 genes: changes in the inflammatory effects of TNF-alpha and in the regulation of fibrosis. *Eur J Immunol* 2004,**34**:174-183.
149. Cooper AM, Khader SA. The role of cytokines in the initiation, expansion, and control of cellular immunity to tuberculosis. *Immunol Rev* 2008,**226**:191-204.
150. Gubler U, Chua AO, Schoenhaut DS, Dwyer CM, McComas W, Motyka R, *et al.* Coexpression of two distinct genes is required to generate secreted bioactive cytotoxic lymphocyte maturation factor. *Proceedings of the National Academy of Sciences of the United States of America* 1991,**88**:4143-4147.
151. Cooper AM, Roberts AD, Rhoades ER, Callahan JE, Getzy DM, Orme IM. The role of interleukin-12 in acquired immunity to Mycobacterium tuberculosis infection. *Immunology* 1995,**84**:423-432.
152. Khader SA, Partida-Sanchez S, Bell G, Jelley-Gibbs DM, Swain S, Pearl JE, *et al.* Interleukin 12p40 is required for dendritic cell migration and T cell priming after Mycobacterium tuberculosis infection. *J Exp Med* 2006,**203**:1805-1815.
153. Cooper AM, Kipnis A, Turner J, Magram J, Ferrante J, Orme IM. Mice lacking bioactive IL-12 can generate protective, antigen-specific cellular responses to mycobacterial infection only if the IL-12 p40 subunit is present. *J Immunol* 2002,**168**:1322-1327.
154. Feng CG, Jankovic D, Kullberg M, Cheever A, Scanga CA, Hieny S, *et al.* Maintenance of pulmonary Th1 effector function in chronic tuberculosis requires persistent IL-12 production. *J Immunol* 2005,**174**:4185-4192.
155. Kindler V, Sappino AP, Grau GE, Piguet PF, Vassalli P. The inducing role of tumor necrosis factor in the development of bactericidal granulomas during BCG infection. *Cell* 1989,**56**:731-740.
156. Bean AG, Roach DR, Briscoe H, France MP, Korner H, Sedgwick JD, *et al.* Structural deficiencies in granuloma formation in TNF gene-targeted mice underlie the heightened susceptibility to aerosol Mycobacterium tuberculosis infection, which is not compensated for by lymphotoxin. *J Immunol* 1999,**162**:3504-3511.
157. Torrado E, Cooper AM. Cytokines in the balance of protection and pathology during mycobacterial infections. *Adv Exp Med Biol* 2013,**783**:121-140.
158. Roach DR, Bean AG, Demangel C, France MP, Briscoe H, Britton WJ. TNF regulates chemokine induction essential for cell recruitment, granuloma formation, and clearance of mycobacterial infection. *J Immunol* 2002,**168**:4620-4627.
159. Hernandez-Pando R, Orozco-Esteves H, Maldonado HA, Aguilar-Leon D, Vilchis-Landeros MM, Mata-Espinosa DA, *et al.* A combination of a transforming growth factor-beta antagonist and an inhibitor of cyclooxygenase is an effective treatment for murine pulmonary tuberculosis. *Clin Exp Immunol* 2006,**144**:264-272.
160. Jouanguy E, Doffinger R, Dupuis S, Pallier A, Altare F, Casanova JL. IL-12 and IFN-gamma in host defense against mycobacteria and salmonella in mice and men. *Curr Opin Immunol* 1999,**11**:346-351.

161. Jung JY, Madan-Lala R, Georgieva M, Rengarajan J, Sohaskey CD, Bange FC, *et al.* The intracellular environment of human macrophages that produce nitric oxide promotes growth of mycobacteria. *Infection and immunity* 2013;**81**:3198-3209.
162. Rich EA, Torres M, Sada E, Finegan CK, Hamilton BD, Toossi Z. Mycobacterium tuberculosis (MTB)-stimulated production of nitric oxide by human alveolar macrophages and relationship of nitric oxide production to growth inhibition of MTB. *Tubercle and lung disease : the official journal of the International Union against Tuberculosis and Lung Disease* 1997;**78**:247-255.
163. Nandi B, Behar SM. Regulation of neutrophils by interferon-gamma limits lung inflammation during tuberculosis infection. *J Exp Med* 2011;**208**:2251-2262.
164. Li X, McKinstry KK, Swain SL, Dalton DK. IFN-gamma acts directly on activated CD4+ T cells during mycobacterial infection to promote apoptosis by inducing components of the intracellular apoptosis machinery and by inducing extracellular proapoptotic signals. *J Immunol* 2007;**179**:939-949.
165. Stark MA, Huo Y, Burcin TL, Morris MA, Olson TS, Ley K. Phagocytosis of apoptotic neutrophils regulates granulopoiesis via IL-23 and IL-17. *Immunity* 2005;**22**:285-294.
166. Mayer-Barber KD, Andrade BB, Barber DL, Hieny S, Feng CG, Caspar P, *et al.* Innate and adaptive interferons suppress IL-1alpha and IL-1beta production by distinct pulmonary myeloid subsets during Mycobacterium tuberculosis infection. *Immunity* 2011;**35**:1023-1034.
167. Mayer-Barber KD, Barber DL, Shenderov K, White SD, Wilson MS, Cheever A, *et al.* Caspase-1 independent IL-1beta production is critical for host resistance to mycobacterium tuberculosis and does not require TLR signaling in vivo. *J Immunol* 2010;**184**:3326-3330.
168. Sugawara I, Yamada H, Hua S, Mizuno S. Role of interleukin (IL)-1 type 1 receptor in mycobacterial infection. *Microbiol Immunol* 2001;**45**:743-750.
169. Yamada H, Mizuno S, Horai R, Iwakura Y, Sugawara I. Protective role of interleukin-1 in mycobacterial infection in IL-1 alpha/beta double-knockout mice. *Lab Invest* 2000;**80**:759-767.
170. Wilkinson RJ, Patel P, Llewelyn M, Hirsch CS, Pasvol G, Snounou G, *et al.* Influence of polymorphism in the genes for the interleukin (IL)-1 receptor antagonist and IL-1beta on tuberculosis. *J Exp Med* 1999;**189**:1863-1874.
171. Bellamy R, Ruwende C, Corrah T, McAdam KP, Whittle HC, Hill AV. Assessment of the interleukin 1 gene cluster and other candidate gene polymorphisms in host susceptibility to tuberculosis. *Tuber Lung Dis* 1998;**79**:83-89.
172. Beamer GL, Flaherty DK, Assogba BD, Stromberg P, Gonzalez-Juarrero M, de Waal Malefyt R, *et al.* Interleukin-10 promotes Mycobacterium tuberculosis disease progression in CBA/J mice. *J Immunol* 2008;**181**:5545-5550.
173. Turner J, Gonzalez-Juarrero M, Ellis DL, Basaraba RJ, Kipnis A, Orme IM, *et al.* In vivo IL-10 production reactivates chronic pulmonary tuberculosis in C57BL/6 mice. *J Immunol* 2002;**169**:6343-6351.
174. Tran DQ. TGF-beta: the sword, the wand, and the shield of FOXP3(+) regulatory T cells. *Journal of molecular cell biology* 2012;**4**:29-37.
175. Fiorenza G, Ratani L, Farroni MA, Bogue C, Dlugovitzky DG. TNF-alpha, TGF-beta and NO relationship in sera from tuberculosis (TB) patients of different severity. *Immunol Lett* 2005;**98**:45-48.
176. Bonecini-Almeida MG, Ho JL, Boechat N, Huard RC, Chitale S, Doo H, *et al.* Down-modulation of lung immune responses by interleukin-10 and transforming growth factor beta (TGF-beta) and analysis of TGF-beta receptors I and II in active tuberculosis. *Infect Immun* 2004;**72**:2628-2634.

177. Verbon A, Juffermans N, Van Deventer SJ, Speelman P, Van Deutekom H, Van Der Poll T. Serum concentrations of cytokines in patients with active tuberculosis (TB) and after treatment. *Clin Exp Immunol* 1999;**115**:110-113.
178. Olobo JO, Geletu M, Demissie A, Eguale T, Hiwot K, Aderaye G, *et al.* Circulating TNF-alpha, TGF-beta, and IL-10 in tuberculosis patients and healthy contacts. *Scand J Immunol* 2001;**53**:85-91.
179. Toossi Z, Gogate P, Shiratsuchi H, Young T, Ellner JJ. Enhanced production of TGF-beta by blood monocytes from patients with active tuberculosis and presence of TGF-beta in tuberculous granulomatous lung lesions. *J Immunol* 1995;**154**:465-473.
180. Dai G, McMurray DN. Effects of modulating TGF-beta 1 on immune responses to mycobacterial infection in guinea pigs. *Tuber Lung Dis* 1999;**79**:207-214.
181. Agata Y, Kawasaki A, Nishimura H, Ishida Y, Tsubata T, Yagita H, *et al.* Expression of the PD-1 antigen on the surface of stimulated mouse T and B lymphocytes. *International immunology* 1996;**8**:765-772.
182. Jin HT, Ahmed R, Okazaki T. Role of PD-1 in regulating T-cell immunity. *Current topics in microbiology and immunology* 2011;**350**:17-37.
183. Freeman GJ, Long AJ, Iwai Y, Bourque K, Chernova T, Nishimura H, *et al.* Engagement of the PD-1 immunoinhibitory receptor by a novel B7 family member leads to negative regulation of lymphocyte activation. *The Journal of experimental medicine* 2000;**192**:1027-1034.
184. Latchman Y, Wood CR, Chernova T, Chaudhary D, Borde M, Chernova I, *et al.* PD-L2 is a second ligand for PD-1 and inhibits T cell activation. *Nature immunology* 2001;**2**:261-268.
185. Singh A, Mohan A, Dey AB, Mitra DK. Inhibiting the Programmed Death 1 Pathway Rescues Mycobacterium tuberculosis-Specific Interferon gamma-Producing T Cells From Apoptosis in Patients With Pulmonary Tuberculosis. *The Journal of infectious diseases* 2013;**208**:603-615.
186. Jurado JO, Alvarez IB, Pasquinelli V, Martinez GJ, Quiroga MF, Abbate E, *et al.* Programmed death (PD)-1:PD-ligand 1/PD-ligand 2 pathway inhibits T cell effector functions during human tuberculosis. *Journal of immunology* 2008;**181**:116-125.
187. Barber DL, Mayer-Barber KD, Feng CG, Sharpe AH, Sher A. CD4 T cells promote rather than control tuberculosis in the absence of PD-1-mediated inhibition. *Journal of immunology* 2011;**186**:1598-1607.
188. Lazar-Molnar E, Chen B, Sweeney KA, Wang EJ, Liu W, Lin J, *et al.* Programmed death-1 (PD-1)-deficient mice are extraordinarily sensitive to tuberculosis. *Proceedings of the National Academy of Sciences of the United States of America* 2010;**107**:13402-13407.
189. Tousif S, Singh Y, Prasad DV, Sharma P, Van Kaer L, Das G. T cells from Programmed Death-1 deficient mice respond poorly to Mycobacterium tuberculosis infection. *PLoS One* 2011;**6**:e19864.
190. Monney L, Sabatos CA, Gaglia JL, Ryu A, Waldner H, Chernova T, *et al.* Th1-specific cell surface protein Tim-3 regulates macrophage activation and severity of an autoimmune disease. *Nature* 2002;**415**:536-541.
191. Anderson AC, Anderson DE, Bregoli L, Hastings WD, Kassam N, Lei C, *et al.* Promotion of tissue inflammation by the immune receptor Tim-3 expressed on innate immune cells. *Science* 2007;**318**:1141-1143.
192. Zhu C, Anderson AC, Schubart A, Xiong H, Imitola J, Khoury SJ, *et al.* The Tim-3 ligand galectin-9 negatively regulates T helper type 1 immunity. *Nature immunology* 2005;**6**:1245-1252.
193. Jones RB, Ndhlovu LC, Barbour JD, Sheth PM, Jha AR, Long BR, *et al.* Tim-3 expression defines a novel population of dysfunctional T cells with highly elevated frequencies in progressive HIV-1 infection. *J Exp Med* 2008;**205**:2763-2779.

194. Day CL, Kaufmann DE, Kiepiela P, Brown JA, Moodley ES, Reddy S, *et al.* PD-1 expression on HIV-specific T cells is associated with T-cell exhaustion and disease progression. *Nature* 2006,**443**:350-354.
195. D'Souza M, Fontenot AP, Mack DG, Lozupone C, Dillon S, Meditz A, *et al.* Programmed death 1 expression on HIV-specific CD4+ T cells is driven by viral replication and associated with T cell dysfunction. *J Immunol* 2007,**179**:1979-1987.
196. Wang X, Cao Z, Jiang J, Li Y, Dong M, Ostrowski M, *et al.* Elevated expression of Tim-3 on CD8 T cells correlates with disease severity of pulmonary tuberculosis. *J Infect* 2011,**62**:292-300.
197. Qiu Y, Chen J, Liao H, Zhang Y, Wang H, Li S, *et al.* Tim-3-expressing CD4+ and CD8+ T cells in human tuberculosis (TB) exhibit polarized effector memory phenotypes and stronger anti-TB effector functions. *PLoS pathogens* 2012,**8**:e1002984.
198. Henao-Tamayo M, Irwin SM, Shang S, Ordway D, Orme IM. T lymphocyte surface expression of exhaustion markers as biomarkers of the efficacy of chemotherapy for tuberculosis. *Tuberculosis* 2011,**91**:308-313.
199. Steinman RM, Cohn ZA. Pillars Article: Identification of a novel cell type in peripheral lymphoid organs of mice. I. Morphology, quantitation, tissue distribution. *J. Exp. Med.* 1973. 137: 1142-1162. *J Immunol* 2007,**178**:5-25.
200. Yamazaki S, Morita A. Dendritic cells in the periphery control antigen-specific natural and induced regulatory T cells. *Front Immunol* 2013,**4**:151.
201. Jakubzick C, Tacke F, Ginhoux F, Wagers AJ, van Rooijen N, Mack M, *et al.* Blood monocyte subsets differentially give rise to CD103+ and CD103- pulmonary dendritic cell populations. *J Immunol* 2008,**180**:3019-3027.
202. de Heer HJ, Hammad H, Soullie T, Hijdra D, Vos N, Willart MA, *et al.* Essential role of lung plasmacytoid dendritic cells in preventing asthmatic reactions to harmless inhaled antigen. *The Journal of experimental medicine* 2004,**200**:89-98.
203. Sung SS, Fu SM, Rose CE, Jr., Gaskin F, Ju ST, Beaty SR. A major lung CD103 (alphaE)-beta7 integrin-positive epithelial dendritic cell population expressing Langerin and tight junction proteins. *J Immunol* 2006,**176**:2161-2172.
204. Desch AN, Henson PM, Jakubzick CV. Pulmonary dendritic cell development and antigen acquisition. *Immunol Res* 2013,**55**:178-186.
205. Gonzalez-Juarrero M, Orme IM. Characterization of murine lung dendritic cells infected with Mycobacterium tuberculosis. *Infect Immun* 2001,**69**:1127-1133.
206. Geissmann F, Jung S, Littman DR. Blood monocytes consist of two principal subsets with distinct migratory properties. *Immunity* 2003,**19**:71-82.
207. Serbina NV, Pamer EG. Monocyte emigration from bone marrow during bacterial infection requires signals mediated by chemokine receptor CCR2. *Nat Immunol* 2006,**7**:311-317.
208. Plantinga M, Guillems M, Vanheerswynghe M, Deswarte K, Branco-Madeira F, Toussaint W, *et al.* Conventional and monocyte-derived CD11b(+) dendritic cells initiate and maintain T helper 2 cell-mediated immunity to house dust mite allergen. *Immunity* 2013,**38**:322-335.
209. del Rio ML, Bernhardt G, Rodriguez-Barbosa JI, Forster R. Development and functional specialization of CD103+ dendritic cells. *Immunol Rev* 2010,**234**:268-281.
210. Ho AW, Prabhu N, Betts RJ, Ge MQ, Dai X, Hutchinson PE, *et al.* Lung CD103+ dendritic cells efficiently transport influenza virus to the lymph node and load viral antigen onto MHC class I for presentation to CD8 T cells. *J Immunol* 2011,**187**:6011-6021.
211. Helft J, Manicassamy B, Guernonprez P, Hashimoto D, Silvén A, Agudo J, *et al.* Cross-presenting CD103+ dendritic cells are protected from influenza virus infection. *J Clin Invest* 2012,**122**:4037-4047.

212. Kim TS, Braciale TJ. Respiratory dendritic cell subsets differ in their capacity to support the induction of virus-specific cytotoxic CD8+ T cell responses. *PLoS One* 2009;**4**:e4204.
213. Lukens MV, Kruijsen D, Coenjaerts FE, Kimpfen JL, van Bleek GM. Respiratory syncytial virus-induced activation and migration of respiratory dendritic cells and subsequent antigen presentation in the lung-draining lymph node. *J Virol* 2009;**83**:7235-7243.
214. Coombes JL, Siddiqui KR, Arancibia-Carcamo CV, Hall J, Sun CM, Belkaid Y, *et al.* A functionally specialized population of mucosal CD103+ DCs induces Foxp3+ regulatory T cells via a TGF-beta and retinoic acid-dependent mechanism. *J Exp Med* 2007;**204**:1757-1764.
215. Khare A, Krishnamoorthy N, Oriss TB, Fei M, Ray P, Ray A. Cutting Edge: Inhaled Antigen Upregulates Retinaldehyde Dehydrogenase in Lung CD103+ but Not Plasmacytoid Dendritic Cells To Induce Foxp3 De Novo in CD4+ T Cells and Promote Airway Tolerance. *J Immunol* 2013;**191**:25-29.
216. Edelson BT, Kc W, Juang R, Kohyama M, Benoit LA, Klekotka PA, *et al.* Peripheral CD103+ dendritic cells form a unified subset developmentally related to CD8alpha+ conventional dendritic cells. *The Journal of experimental medicine* 2010;**207**:823-836.
217. Tussiwand R, Lee WL, Murphy TL, Mashayekhi M, Wumesh KC, Albring JC, *et al.* Compensatory dendritic cell development mediated by BATF-IRF interactions. *Nature* 2012;**490**:502-507.
218. Bodnar KA, Serbina NV, Flynn JL. Fate of Mycobacterium tuberculosis within murine dendritic cells. *Infect Immun* 2001;**69**:800-809.
219. Mihret A, Mamo G, Tafesse M, Hailu A, Parida S. Dendritic Cells Activate and Mature after Infection with Mycobacterium tuberculosis. *BMC Res Notes* 2011;**4**:247.
220. Turner BG, Summers MF. Structural biology of HIV. *Journal of molecular biology* 1999;**285**:1-32.
221. Geijtenbeek TB, Kwon DS, Torensma R, van Vliet SJ, van Duijnhoven GC, Middel J, *et al.* DC-SIGN, a dendritic cell-specific HIV-1-binding protein that enhances trans-infection of T cells. *Cell* 2000;**100**:587-597.
222. Gorry PR, Ancuta P. Coreceptors and HIV-1 pathogenesis. *Current HIV/AIDS reports* 2011;**8**:45-53.
223. Pantaleo G, Graziosi C, Fauci AS. New concepts in the immunopathogenesis of human immunodeficiency virus infection. *The New England journal of medicine* 1993;**328**:327-335.
224. Daar ES, Moudgil T, Meyer RD, Ho DD. Transient high levels of viremia in patients with primary human immunodeficiency virus type 1 infection. *The New England journal of medicine* 1991;**324**:961-964.
225. Fauci AS, Schnittman SM, Poli G, Koenig S, Pantaleo G. NIH conference. Immunopathogenic mechanisms in human immunodeficiency virus (HIV) infection. *Annals of internal medicine* 1991;**114**:678-693.
226. Tuberculosis outbreak among persons in a residential facility for HIV-infected persons--San Francisco. *MMWR Morb Mortal Wkly Rep* 1991;**40**:649-652.
227. Di Perri G, Cruciani M, Danzi MC, Luzzati R, De Checchi G, Malena M, *et al.* Nosocomial epidemic of active tuberculosis among HIV-infected patients. *Lancet* 1989;**2**:1502-1504.
228. Daley CL, Small PM, Schecter GF, Schoolnik GK, McAdam RA, Jacobs WR, Jr., *et al.* An outbreak of tuberculosis with accelerated progression among persons infected with the human immunodeficiency virus. An analysis using restriction-fragment-length polymorphisms. *N Engl J Med* 1992;**326**:231-235.

229. Crampin AC, Mwaungulu JN, Mwaungulu FD, Mwafulirwa DT, Munthali K, Floyd S, *et al.* Recurrent TB: relapse or reinfection? The effect of HIV in a general population cohort in Malawi. *AIDS* 2010,**24**:417-426.
230. Sonnenberg P, Murray J, Glynn JR, Shearer S, Kambashi B, Godfrey-Faussett P. HIV-1 and recurrence, relapse, and reinfection of tuberculosis after cure: a cohort study in South African mineworkers. *Lancet* 2001,**358**:1687-1693.
231. Rosas-Taraco AG, Arce-Mendoza AY, Caballero-Olin G, Salinas-Carmona MC. Mycobacterium tuberculosis upregulates coreceptors CCR5 and CXCR4 while HIV modulates CD14 favoring concurrent infection. *AIDS Res Hum Retroviruses* 2006,**22**:45-51.
232. Diedrich CR, Flynn JL. HIV-1/mycobacterium tuberculosis coinfection immunology: how does HIV-1 exacerbate tuberculosis? *Infect Immun* 2011,**79**:1407-1417.
233. de Noronha AL, Bafica A, Nogueira L, Barral A, Barral-Netto M. Lung granulomas from Mycobacterium tuberculosis/HIV-1 co-infected patients display decreased in situ TNF production. *Pathol Res Pract* 2008,**204**:155-161.
234. Shen JY, Barnes PF, Rea TH, Meyer PR. Immunohistology of tuberculous adenitis in symptomatic HIV infection. *Clin Exp Immunol* 1988,**72**:186-189.
235. Diedrich CR, Mattila JT, Klein E, Janssen C, Phuah J, Sturgeon TJ, *et al.* Reactivation of latent tuberculosis in cynomolgus macaques infected with SIV is associated with early peripheral T cell depletion and not virus load. *PLoS One* 2010,**5**:e9611.
236. Lane HC, Depper JM, Greene WC, Whalen G, Waldmann TA, Fauci AS. Qualitative analysis of immune function in patients with the acquired immunodeficiency syndrome. Evidence for a selective defect in soluble antigen recognition. *N Engl J Med* 1985,**313**:79-84.
237. Clerici M, Stocks NI, Zajac RA, Boswell RN, Lucey DR, Via CS, *et al.* Detection of three distinct patterns of T helper cell dysfunction in asymptomatic, human immunodeficiency virus-seropositive patients. Independence of CD4+ cell numbers and clinical staging. *J Clin Invest* 1989,**84**:1892-1899.
238. Bezuidenhout J, Roberts T, Muller L, van Helden P, Walzl G. Pleural tuberculosis in patients with early HIV infection is associated with increased TNF-alpha expression and necrosis in granulomas. *PLoS One* 2009,**4**:e4228.
239. Geldmacher C, Ngwenyama N, Schuetz A, Petrovas C, Reither K, Heeregrave EJ, *et al.* Preferential infection and depletion of Mycobacterium tuberculosis-specific CD4 T cells after HIV-1 infection. *J Exp Med* 2010,**207**:2869-2881.
240. Geldmacher C, Schuetz A, Ngwenyama N, Casazza JP, Sanga E, Saathoff E, *et al.* Early depletion of Mycobacterium tuberculosis-specific T helper 1 cell responses after HIV-1 infection. *J Infect Dis* 2008,**198**:1590-1598.
241. Hertoghe T, Wajja A, Ntambi L, Okwera A, Aziz MA, Hirsch C, *et al.* T cell activation, apoptosis and cytokine dysregulation in the (co)pathogenesis of HIV and pulmonary tuberculosis (TB). *Clin Exp Immunol* 2000,**122**:350-357.
242. Mendonca M, Tanji MM, Silva LC, Silveira GG, Oliveira SC, Duarte AJ, *et al.* Deficient in vitro anti-mycobacterial immunity despite successful long-term highly active antiretroviral therapy in HIV-infected patients with past history of tuberculosis infection or disease. *Clin Immunol* 2007,**125**:60-66.
243. Zhang M, Gong J, Iyer DV, Jones BE, Modlin RL, Barnes PF. T cell cytokine responses in persons with tuberculosis and human immunodeficiency virus infection. *J Clin Invest* 1994,**94**:2435-2442.
244. Vanham G, Penne L, Devalck J, Kestens L, Colebunders R, Bosmans E, *et al.* Decreased CD40 ligand induction in CD4 T cells and dysregulated IL-12 production during HIV infection. *Clin Exp Immunol* 1999,**117**:335-342.

245. Park IW, Koziel H, Hatch W, Li X, Du B, Groopman JE. CD4 receptor-dependent entry of human immunodeficiency virus type-1 env-pseudotypes into CCR5-, CCR3-, and CXCR4-expressing human alveolar macrophages is preferentially mediated by the CCR5 coreceptor. *Am J Respir Cell Mol Biol* 1999;**20**:864-871.
246. Lawn SD, Pisell TL, Hirsch CS, Wu M, Butera ST, Toossi Z. Anatomically compartmentalized human immunodeficiency virus replication in HLA-DR+ cells and CD14+ macrophages at the site of pleural tuberculosis coinfection. *J Infect Dis* 2001;**184**:1127-1133.
247. Patel NR, Zhu J, Tachado SD, Zhang J, Wan Z, Saukkonen J, *et al.* HIV impairs TNF-alpha mediated macrophage apoptotic response to Mycobacterium tuberculosis. *J Immunol* 2007;**179**:6973-6980.
248. Pathak S, Wentzel-Larsen T, Asjo B. Effects of in vitro HIV-1 infection on mycobacterial growth in peripheral blood monocyte-derived macrophages. *Infect Immun* 2010;**78**:4022-4032.
249. Goletti D, Weissman D, Jackson RW, Graham NM, Vlahov D, Klein RS, *et al.* Effect of Mycobacterium tuberculosis on HIV replication. Role of immune activation. *J Immunol* 1996;**157**:1271-1278.
250. Toossi Z, Mayanja-Kizza H, Hirsch CS, Edmonds KL, Spahlinger T, Hom DL, *et al.* Impact of tuberculosis (TB) on HIV-1 activity in dually infected patients. *Clin Exp Immunol* 2001;**123**:233-238.
251. Nakata K, Rom WN, Honda Y, Condos R, Kanegasaki S, Cao Y, *et al.* Mycobacterium tuberculosis enhances human immunodeficiency virus-1 replication in the lung. *Am J Respir Crit Care Med* 1997;**155**:996-1003.
252. Schutze S, Machleidt T, Kronke M. Mechanisms of tumor necrosis factor action. *Semin Oncol* 1992;**19**:16-24.
253. Lim SP, Garzino-Demo A. The human immunodeficiency virus type 1 Tat protein up-regulates the promoter activity of the beta-chemokine monocyte chemoattractant protein 1 in the human astrocytoma cell line U-87 MG: role of SP-1, AP-1, and NF-kappaB consensus sites. *J Virol* 2000;**74**:1632-1640.
254. Hoshino Y, Tse DB, Rochford G, Prabhakar S, Hoshino S, Chitkara N, *et al.* Mycobacterium tuberculosis-induced CXCR4 and chemokine expression leads to preferential X4 HIV-1 replication in human macrophages. *J Immunol* 2004;**172**:6251-6258.
255. Reuter MA, Pecora ND, Harding CV, Canaday DH, McDonald D. Mycobacterium tuberculosis promotes HIV trans-infection and suppresses major histocompatibility complex class II antigen processing by dendritic cells. *Journal of virology* 2010;**84**:8549-8560.
256. Wallis RS, Ellner JJ. Cytokines and tuberculosis. *J Leukoc Biol* 1994;**55**:676-681.
257. Potash MJ, Chao W, Bentsman G, Paris N, Saini M, Nitkiewicz J, *et al.* A mouse model for study of systemic HIV-1 infection, antiviral immune responses, and neuroinvasiveness. *Proc Natl Acad Sci U S A* 2005;**102**:3760-3765.
258. Jung YJ, Ryan L, LaCourse R, North RJ. Differences in the ability to generate type 1 T helper cells need not determine differences in the ability to resist Mycobacterium tuberculosis infection among mouse strains. *J Infect Dis* 2009;**199**:1790-1796.
259. Medina E, North RJ. Evidence inconsistent with a role for the Bcg gene (Nramp1) in resistance of mice to infection with virulent Mycobacterium tuberculosis. *J Exp Med* 1996;**183**:1045-1051.
260. Medina E, North RJ. Resistance ranking of some common inbred mouse strains to Mycobacterium tuberculosis and relationship to major histocompatibility complex haplotype and Nramp1 genotype. *Immunology* 1998;**93**:270-274.
261. Nakano H, Free ME, Whitehead GS, Maruoka S, Wilson RH, Nakano K, *et al.* Pulmonary CD103(+) dendritic cells prime Th2 responses to inhaled allergens. *Mucosal Immunol* 2012;**5**:53-65.

262. del Rio ML, Rodriguez-Barbosa JI, Bolter J, Ballmaier M, Dittrich-Breiholz O, Kracht M, *et al.* CX3CR1+ c-kit+ bone marrow cells give rise to CD103+ and CD103-dendritic cells with distinct functional properties. *J Immunol* 2008;**181**:6178-6188.
263. Beaty SR, Rose CE, Jr., Sung SS. Diverse and potent chemokine production by lung CD11bhigh dendritic cells in homeostasis and in allergic lung inflammation. *J Immunol* 2007;**178**:1882-1895.
264. Desch AN, Randolph GJ, Murphy K, Gautier EL, Kedl RM, Lahoud MH, *et al.* CD103+ pulmonary dendritic cells preferentially acquire and present apoptotic cell-associated antigen. *J Exp Med* 2011;**208**:1789-1797.
265. Vignali DA, Collison LW, Workman CJ. How regulatory T cells work. *Nat Rev Immunol* 2008;**8**:523-532.
266. Josefowicz SZ, Lu LF, Rudensky AY. Regulatory T cells: mechanisms of differentiation and function. *Annu Rev Immunol* 2012;**30**:531-564.
267. Feng T, Cao AT, Weaver CT, Elson CO, Cong Y. Interleukin-12 converts Foxp3+ regulatory T cells to interferon-gamma-producing Foxp3+ T cells that inhibit colitis. *Gastroenterology* 2011;**140**:2031-2043.
268. Kincaid EZ, Wolf AJ, Desvignes L, Mahapatra S, Crick DC, Brennan PJ, *et al.* Codominance of TLR2-dependent and TLR2-independent modulation of MHC class II in Mycobacterium tuberculosis infection in vivo. *Journal of immunology* 2007;**179**:3187-3195.
269. Sandstrom E, Nilsson C, Hejdeman B, Brave A, Bratt G, Robb M, *et al.* Broad immunogenicity of a multigene, multiclade HIV-1 DNA vaccine boosted with heterologous HIV-1 recombinant modified vaccinia virus Ankara. *J Infect Dis* 2008;**198**:1482-1490.
270. Brave A, Boberg A, Gudmundsdottir L, Rollman E, Hallermalm K, Ljungberg K, *et al.* A new multi-clade DNA prime/recombinant MVA boost vaccine induces broad and high levels of HIV-1-specific CD8(+) T-cell and humoral responses in mice. *Mol Ther* 2007;**15**:1724-1733.
271. Brave A, Johansen K, Palma P, Benthin R, Hinkula J. Maternal immune status influences HIV-specific immune responses in pups after DNA prime protein boost using mucosal adjuvant. *Vaccine* 2008;**26**:5957-5966.
272. Hinkula J, Devito C, Zuber B, Benthin R, Ferreira D, Wahren B, *et al.* A novel DNA adjuvant, N3, enhances mucosal and systemic immune responses induced by HIV-1 DNA and peptide immunizations. *Vaccine* 2006;**24**:4494-4497.
273. Gray ES, Madiga MC, Moore PL, Mlisana K, Abdool Karim SS, Binley JM, *et al.* Broad neutralization of human immunodeficiency virus type 1 mediated by plasma antibodies against the gp41 membrane proximal external region. *J Virol* 2009;**83**:11265-11274.
274. Stamatatos L, Morris L, Burton DR, Mascola JR. Neutralizing antibodies generated during natural HIV-1 infection: good news for an HIV-1 vaccine? *Nat Med* 2009;**15**:866-870.
275. Gray ES, Moore PL, Choge IA, Decker JM, Bibollet-Ruche F, Li H, *et al.* Neutralizing antibody responses in acute human immunodeficiency virus type 1 subtype C infection. *J Virol* 2007;**81**:6187-6196.
276. Richman DD, Wrin T, Little SJ, Petropoulos CJ. Rapid evolution of the neutralizing antibody response to HIV type 1 infection. *Proc Natl Acad Sci U S A* 2003;**100**:4144-4149.
277. von Bubnoff A. The great barrier. Newspaper Article. *IAVI Rep* 2008;**12**:10-14.
278. Devito C, Hinkula J, Kaul R, Lopalco L, Bwayo JJ, Plummer F, *et al.* Mucosal and plasma IgA from HIV-exposed seronegative individuals neutralize a primary HIV-1 isolate. *AIDS* 2000;**14**:1917-1920.

279. Choi RY, Levinson P, Guthrie BL, Lohman-Payne B, Bosire R, Liu AY, *et al.* Cervicovaginal HIV-1-neutralizing immunoglobulin A detected among HIV-1-exposed seronegative female partners in HIV-1-discordant couples. *AIDS* 2012;**26**:2155-2163.
280. Watkins JD, Sholukh AM, Mukhtar MM, Siddappa NB, Lakhashe SK, Kim M, *et al.* Anti-HIV IgA isotypes: differential virion capture and inhibition of transcytosis are linked to prevention of mucosal R5 SHIV transmission. *AIDS* 2013;**27**:F13-F20.
281. Pereyra F, Addo MM, Kaufmann DE, Liu Y, Miura T, Rathod A, *et al.* Genetic and immunologic heterogeneity among persons who control HIV infection in the absence of therapy. *J Infect Dis* 2008;**197**:563-571.
282. Owen RE, Heitman JW, Hirschhorn DF, Lanteri MC, Biswas HH, Martin JN, *et al.* HIV+ elite controllers have low HIV-specific T-cell activation yet maintain strong, polyfunctional T-cell responses. *AIDS* 2010;**24**:1095-1105.
283. Betts MR, Nason MC, West SM, De Rosa SC, Migueles SA, Abraham J, *et al.* HIV nonprogressors preferentially maintain highly functional HIV-specific CD8+ T cells. *Blood* 2006;**107**:4781-4789.
284. Mattila JT, Diedrich CR, Lin PL, Phuah J, Flynn JL. Simian immunodeficiency virus-induced changes in T cell cytokine responses in cynomolgus macaques with latent *Mycobacterium tuberculosis* infection are associated with timing of reactivation. *J Immunol* 2011;**186**:3527-3537.
285. Mehra S, Golden NA, Dutta NK, Midkiff CC, Alvarez X, Doyle LA, *et al.* Reactivation of latent tuberculosis in rhesus macaques by coinfection with simian immunodeficiency virus. *J Med Primatol* 2011;**40**:233-243.
286. Lane HC, Masur H, Edgar LC, Whalen G, Rook AH, Fauci AS. Abnormalities of B-cell activation and immunoregulation in patients with the acquired immunodeficiency syndrome. *N Engl J Med* 1983;**309**:453-458.
287. Hellerstein M, Hanley MB, Cesar D, Siler S, Papageorgopoulos C, Wieder E, *et al.* Directly measured kinetics of circulating T lymphocytes in normal and HIV-1-infected humans. *Nat Med* 1999;**5**:83-89.
288. Valdez H, Lederman MM. Cytokines and cytokine therapies in HIV infection. *AIDS Clin Rev* 1997:187-228.
289. Khaitan A, Unutmaz D. Revisiting immune exhaustion during HIV infection. *Curr HIV/AIDS Rep* 2011;**8**:4-11.
290. Hazenberg MD, Stuart JW, Otto SA, Borleffs JC, Boucher CA, de Boer RJ, *et al.* T-cell division in human immunodeficiency virus (HIV)-1 infection is mainly due to immune activation: a longitudinal analysis in patients before and during highly active antiretroviral therapy (HAART). *Blood* 2000;**95**:249-255.
291. Trautmann L, Janbazian L, Chomont N, Said EA, Gimmig S, Bessette B, *et al.* Upregulation of PD-1 expression on HIV-specific CD8+ T cells leads to reversible immune dysfunction. *Nat Med* 2006;**12**:1198-1202.

I



Failure To Recruit Anti-Inflammatory CD103⁺ Dendritic Cells and a Diminished CD4⁺ Foxp3⁺ Regulatory T Cell Pool in Mice That Display Excessive Lung Inflammation and Increased Susceptibility to *Mycobacterium tuberculosis*

Chaniya Leepiyasakulchai,^a Lech Ignatowicz,^a Andrzej Pawlowski,^b Gunilla Källénius,^b and Markus Sköld^a

Department of Microbiology, Tumor and Cell Biology, Karolinska Institutet, Stockholm, Sweden,^a and Department of Clinical Science and Education, Karolinska Institutet, Stockholm, Sweden^b

Susceptibility to *Mycobacterium tuberculosis* is characterized by excessive lung inflammation, tissue damage, and failure to control bacterial growth. To increase our understanding of mechanisms that may regulate the host immune response in the lungs, we characterized dendritic cells expressing CD103 (α_E integrin) (α E-DCs) and CD4⁺ Foxp3⁺ regulatory T (T_{reg}) cells during *M. tuberculosis* infection. In resistant C57BL/6 and BALB/c mice, the number of lung α E-DCs increased dramatically during *M. tuberculosis* infection. In contrast, highly susceptible DBA/2 mice failed to recruit α E-DCs even during chronic infection. Even though tumor necrosis factor alpha (TNF- α) is produced by multiple DCs and macrophage subsets and is required for control of bacterial growth, α E-DCs remained TNF- α negative. Instead, α E-DCs contained a high number of transforming growth factor beta-producing cells in infected mice. Further, we show that T_{reg} cells in C57BL/6 and DBA/2 mice induce gamma interferon during pulmonary tuberculosis. In contrast to resistant mice, the T_{reg} cell population was diminished in the lungs, but not in the draining pulmonary lymph nodes (PLN), of highly susceptible mice during chronic infection. T_{reg} cells have been reported to inhibit *M. tuberculosis*-specific T cell immunity, leading to increased bacterial growth. Still, despite the reduced number of lung T_{reg} cells in DBA/2 mice, the bacterial load in the lungs was increased compared to resistant animals. Our results show that α E-DCs and T_{reg} cells that may regulate the host immune response are increased in *M. tuberculosis*-infected lungs of resistant mice but diminished in infected lungs of susceptible mice.

Mycobacterium tuberculosis, the causative agent of pulmonary tuberculosis (TB), remains a threat to global health and is a leading cause of death from infectious disease in the world (60). The murine model of pulmonary TB has demonstrated the critical role of proinflammatory effector functions mediated by activated macrophages (M ϕ) and major histocompatibility complex (MHC)-restricted T cell responses to control the infection and ameliorate disease (10, 42). Following *M. tuberculosis* aerosol infection, the differences in the ability to control bacterial growth, lung lesions, and survival between various inbred mouse strains are dramatic (2, 7, 27, 33, 44, 45, 59). It is interesting that *M. tuberculosis*-susceptible mice can display lesions similar to those in humans with active TB, including severe inflammation in infected lungs and extensive tissue damage (2, 27). Many of the observations made to explain susceptibility to *M. tuberculosis* infection using animal models have translated into human pulmonary TB, and susceptibility to mycobacterial infection is dramatically increased in, for example, immunocompromised patients (11, 19, 20, 34, 35, 41, 47). Still, the cause of naturally occurring susceptibility to *M. tuberculosis* in seemingly healthy individuals is poorly understood. Since the nature of the inflammatory response to *M. tuberculosis* in mice correlates with lung damage and inability to control the infection (reviewed in reference 7), we took advantage of wild-type (WT) mice that are either resistant (C57BL/6 and BALB/c) or susceptible (DBA/2) to *M. tuberculosis* infection (33, 44, 45). The mouse model allowed us to investigate immunoregulatory mechanisms in the lung tissue during pulmonary TB that may balance proinflammatory reactions and that control the in-

fection and tolerogenic mechanisms induced to prevent tissue damage and loss of function.

The CD103 (integrin α_E) cell surface marker can be used to identify a unique CD11b⁺ CD11c⁺ CD103⁺ dendritic cell (α E-DC) population located in the skin and at mucosal sites in the intestine and lungs (reviewed in reference 13). The role of lung α E-DCs in host immunity is not well characterized, especially during bacterial infections. Still, α E-DCs seem to have a distinct role in host immunity compared to proinflammatory CD103⁺ DCs in the lung tissue (3, 30, 58). Lung α E-DCs have migratory properties and are able to take up antigens, including apoptotic cells, that are transported to draining lymph nodes (LN) and presented to MHC class I- or class II-restricted T cells (15, 16, 22, 46). Thus, α E-DCs in the lung mucosa are strategically located and likely to influence the host immune response during pulmonary TB.

In the present study, we show that *M. tuberculosis*-susceptible mice display worse lung lesions and reduced ability to control *M. tuberculosis* growth. We show that the number of lung α E-DCs

Received 22 June 2011 Returned for modification 28 July 2011

Accepted 19 December 2011

Published ahead of print 3 January 2012

Editor: J. L. Flynn

Address correspondence to Markus Sköld, markus.skold@ki.se.

Copyright © 2012, American Society for Microbiology. All Rights Reserved.

doi:10.1128/IAI.05552-11

increases dramatically in *M. tuberculosis*-infected resistant mouse strains, while susceptible mice display a reduced number of α E-DCs, but not other myeloid cell subsets, in response to *M. tuberculosis* infection. During early and chronic stages of *M. tuberculosis* infection, lung α E-DCs have an anti-inflammatory cytokine profile compared to other monocyte, DC, M ϕ , and neutrophil subsets in the infected lungs. We also report that *M. tuberculosis* changes the functional potential of CD4⁺ Foxp3⁺ regulatory T (T_{reg}) cells, which induce gamma interferon (IFN- γ) 6 to 10 weeks postinfection (p.i.). The change in functional potential precedes a diminished pool of T_{reg} cells in the lungs, but not in the draining pulmonary lymph nodes (PLN), of susceptible mice at week 12 p.i.

MATERIALS AND METHODS

Mice. Female C57BL/6NCrI, BALB/cNCrI, and DBA/2NCrI mice (6 to 9 weeks old) were purchased from Charles River (Germany). The animals used in this study were housed under specific-pathogen-free conditions in a biosafety level 3 animal facility at the Astrid Fagraeus Laboratory, Swedish Institute for Communicable Disease Control. All animal experiments were conducted in accordance with the Swedish Animal Welfare Act and approved by the Swedish Institute for Communicable Disease Control and by the Stockholm North Ethical Committee, Swedish Board of Agriculture (permit numbers N343/7 and N369/10). The health status of the mice was monitored daily by animal care technicians or veterinarians to ensure humane treatment.

***M. tuberculosis* aerosol infection.** The clinical *M. tuberculosis* isolate, strain Harlingen, used for the *M. tuberculosis* aerosol infections was kindly provided by J. van Embden, National Institute of Public Health and the Environment, The Netherlands, and originally characterized by Kiers et al. (36). The bacteria were grown to mid-log phase in Sauton medium supplemented with 8 μ g/ml polymyxin B and 5 μ g/ml amphotericin B at 37°C, aliquoted, and stored in medium containing 10% glycerol at -80°C.

For aerosol infections, an *M. tuberculosis* aliquot was thawed at room temperature, spun at 10,000 rpm for 5 min, and triturated through a 25-gauge needle to disperse bacterial clumps. The bacterial suspension was diluted to 1×10^6 CFU/ml in sterile phosphate-buffered saline (PBS), 0.02% Tween 80, and placed in a nebulizer (MiniHeart Lo-Flo Nebulizer; Westmed, Tucson, AZ). The animals were infected with a low dose of *M. tuberculosis* via the respiratory route using a nose-only exposure system (In-Tox Products, Moriarty, NM) calibrated to deliver 20 to 200 CFU into the lungs. The animals were exposed to the *M. tuberculosis*-containing aerosol for 20 min. In some experiments, the number of viable bacteria that reached the lungs was determined on day 1 p.i. The aerosol infections were performed in the biosafety level 3 animal facility at the Astrid Fagraeus Laboratory, Swedish Institute for Communicable Disease Control.

CFU determination. The mice were anesthetized by exposure to isoflurane and euthanized by cervical dislocation. Both lungs were used for day 1 CFU determinations. For week 9 CFU determinations, only the right lung was used. For the later time point, blood was removed from the lung tissue by perfusing the heart with PBS, the tissue was aseptically removed, and the lungs were mechanically homogenized in PBS by passing the tissue through a steel mesh. Viable mycobacteria were quantified by plating the lung homogenates onto Middlebrook 7H11 agar plates. Colonies were counted after 2 to 3 weeks of incubation at 37°C.

Histology. Lung tissue from naïve or *M. tuberculosis*-infected mice was fixed in 4% paraformaldehyde and then embedded in paraffin. Five-micrometer tissue sections were stained with hematoxylin and eosin using a Shandon Varistain Gemini instrument or with Ziehl-Neelsen stain with the Putt modification to visualize acid-fast bacilli. Lung sections from 3 to 5 individual mice per group in two separate experiments were picked randomly and evaluated, blinded, for the relative size of the lung lesions, cellular infiltration, and the presence of acid-fast bacilli in infected mice.

***M. tuberculosis* cell wall extract.** The bacteria (H37Rv reference strain) were grown in Middlebrook medium at 37°C. The bacteria were centrifuged and heat killed at 70°C. The pellet was sonicated and freeze-dried on acetone with cotton.

Preparation of single-cell suspensions. At the indicated time points, single-cell suspensions were prepared from lungs and PLN. The mice were euthanized, and blood was removed from the lung tissue by perfusing the heart with PBS. The lungs and PLN were aseptically removed and placed in RPMI 1640 medium. The lungs were cut into small pieces and incubated in complete RPMI 1640 medium (supplemented with 10% fetal calf serum, penicillin-streptomycin, L-glutamine, sodium-pyruvate, and HEPES buffer, all from Sigma-Aldrich) containing 140 U/ml collagenase type IV (Sigma-Aldrich) for 90 min at 37°C, 5% CO₂. DNase I (Sigma-Aldrich) was added to the cell suspensions at a final concentration of 200 U/ml during the last 10 min of the incubation. The digested lung tissue was then passed through a steel mesh cup sieve (Sigma-Aldrich). Any remaining erythrocytes were lysed using lysis buffer (H₂O, 0.15 M NH₄Cl, 1 mM KHCO₃, 0.1 mM NaEDTA, pH 7.2 to 7.4), washed, and resuspended in RPMI 1640 medium. The cell suspension was passed through a 70- μ m cell strainer (BD Falcon), washed, and resuspended in complete RPMI 1640 medium.

Single-cell suspensions were obtained from PLN using collagenase type IV and DNase I as described above. The PLN were then disaggregated using the frosted ends of two glass slides, washed, and resuspended in complete RPMI 1640 medium.

Total viable cells were enumerated using a hemocytometer and trypan blue exclusion of dead cells. Lung cells and PLN cells from infected mice were analyzed individually. PLN cells from naïve mice were pooled in each experiment.

Flow cytometry. Staining for surface markers was done by resuspending 2×10^6 cells in fluorescence-activated cell sorter (FACS) buffer (PBS with 1% [wt/vol] bovine serum albumin [BSA] and 2 mM NaN₃). The cells were incubated with purified anti-mouse CD16/CD32 (2.4G2; BD Pharmingen) at 20 μ g/ml for 15 min at 4°C to block nonspecific binding. The cells were washed and incubated for 15 min at 4°C with primary antibodies specific for surface markers, or appropriate isotype controls, diluted in FACS buffer. The following allophycocyanin (APC)-, phycoerythrin (PE)-, PE-Cy7-, or peridinin chlorophyll protein (PerCP)-conjugated or biotinylated anti-mouse monoclonal antibodies (MAbs) were obtained from BD Pharmingen: anti-CD103 (M290), anti-CD11b (M1/70), anti-CD19 (1D3), anti-Ly6G (1A8), anti-Ly6C (AL-21), anti-CD3 ϵ (145-2C11), and anti-CD4 (RM4-5). Streptavidin-Pacific orange was purchased from Invitrogen. The following fluorescein isothiocyanate (FITC)-, PE-, PE-Cy5.5-, APC-, Alexa Fluor 700-, or APC-Alexa Fluor 750-conjugated or biotinylated anti-mouse MAbs were purchased from eBioscience: anti-CD45.2 (104), anti-CD11c (N418), anti-CD11b (M1/70), anti-CD19 (1D3), anti-CD8 α (53-6.7), anti-CD8 β (H35-17.2), and anti-B220 (RA3-6B2). Anti-MHC class II (I-A/I-E)-PerCP (M5/114.15.2) was purchased from Biolegend. The stained cells were washed and fixed in freshly prepared 2% paraformaldehyde in PBS for 2 h at 4°C. Fixed cells were washed and resuspended in FACS buffer before analysis by flow cytometry.

For detection of inducible nitric oxide synthase (iNOS)-producing cells, the fixed cells were permeabilized for 20 min at room temperature using a Cytofix/Cytoperm kit from BD Biosciences. Intracellular iNOS was detected using an anti-iNOS-FITC MAb (clone 6; BD Transduction Laboratories) and compared to cells stained with a relevant isotype control MAb. The stained cells were washed and analyzed immediately by flow cytometry.

The cells were passed through a 70- μ m nylon mesh before they were collected using a BD FACSAria (BD Biosciences) and analyzed using FlowJo software (version 8.8.6; Tree Star). All electronic gates and quadrants were set after relevant isotype control MAbs.

Foxp3⁺ T_{reg} cells were identified at various time points after *M. tuberculosis* aerosol infection. After surface staining, the cells were washed,

fixed, permeabilized, and stained for intracellular Foxp3 by using an anti-mouse Foxp3-PE (MF23) MAb and mouse Foxp3 buffer set according to the manufacturer's instructions (BD Pharmingen).

In vitro stimulation of lung and PLN cells and intracellular-cytokine staining. To examine the cytokine profile of myeloid cells, single-cell suspensions were prepared from *M. tuberculosis*-infected mice and kept in complete RPMI 1640 medium or stimulated with 100 ng/ml *Escherichia coli* lipopolysaccharide (LPS) (Sigma-Aldrich) or 10 µg/ml *M. tuberculosis* cell wall extract in the presence of 10 µg/ml brefeldin A (Sigma-Aldrich) for 5 h at 37°C, 5% CO₂.

Adherent cells were detached by incubating the cells in PBS, 2 mM EDTA, for 10 min at 37°C, 5% CO₂. The cells were stained for the indicated cell surface markers, fixed in 2% paraformaldehyde, permeabilized, and stained for intracellular cytokines: anti-tumor necrosis factor alpha (TNF-α)-FITC (MP6-XT22) (eBioscience) and anti-transforming growth factor beta (TGF-β)-APC (1D11) (R&D Systems) or relevant isotype controls. Stained cells were washed twice in permeabilization buffer and once with FACS buffer and analyzed immediately.

For determination of cytokine production by CD4⁺ Foxp3⁺ T cells and T_{reg} cells, single-cell suspensions from total lungs and PLN were kept in complete RPMI 1640 medium or stimulated with 50 ng/ml phorbol 12-myristate 13-acetate (PMA) (Sigma-Aldrich) and 10 µg/ml ionomycin (Sigma-Aldrich) in the presence of 10 µg/ml brefeldin A for 4 h at 37°C, 5% CO₂. The cells were then stained for the indicated lymphocyte surface markers, fixed using 2% paraformaldehyde, permeabilized, and stained for Foxp3 and IFN-γ (XMG1.2 conjugated to PE-Cy7; eBioscience) or relevant isotype controls.

RESULTS

Exacerbated lung lesions and higher bacterial burden in *M. tuberculosis*-infected lungs of susceptible mice. At mucosal surfaces, the immune system has to balance inflammatory reactions induced to eradicate potential harmful pathogens, such as *M. tuberculosis*, and at the same time avoid tissue damage and potential loss of function of the affected organ. During active pulmonary TB, the *M. tuberculosis*-induced lesions may erode the tissue as the disease progresses, leading to destruction of the lung architecture and scarring (12, 27).

We infected three groups of mice with a low dose (159 ± 46 CFU [mean ± standard deviation {SD}]; *n* = 4) of virulent *M. tuberculosis* (Harlingen strain) via the respiratory route and confirmed the striking differences in lung lesions and ability to control bacterial replication between resistant (C57BL/6 and BALB/c) and susceptible (DBA/2) inbred mice 9 weeks p.i. during chronic *M. tuberculosis* infection (Fig. 1) (33, 44). Hematoxylin and eosin staining showed that susceptible DBA/2 mice displayed larger lesions and more extensive loss of alveolar architecture (Fig. 1A) (4). Intracellular acid-fast bacilli were clearly detectable in infected lungs of all three mouse strains analyzed (Fig. 1B) (44). The ability to control bacterial replication 9 weeks p.i. was investigated by plating lung homogenates onto Middlebrook 7H11 agar plates (Fig. 1B). A significantly higher bacterial burden was observed in the lungs of BALB/c mice than in C57BL/6 mice (51). The bacterial burden in highly susceptible DBA/2 mice was approximately 10-fold higher in the lung tissue than in C57BL/6 and BALB/c mice (33, 44, 59).

By comparing WT inbred mouse strains that are either resistant or highly sensitive to low-dose virulent *M. tuberculosis* aerosol infection, we confirmed that susceptible mice have a more severe inflammatory reaction in the lungs and reduced ability to control bacterial growth (Fig. 1). Next, we asked how host immunity differs in animals that are resistant to *M. tuberculosis* infection com-

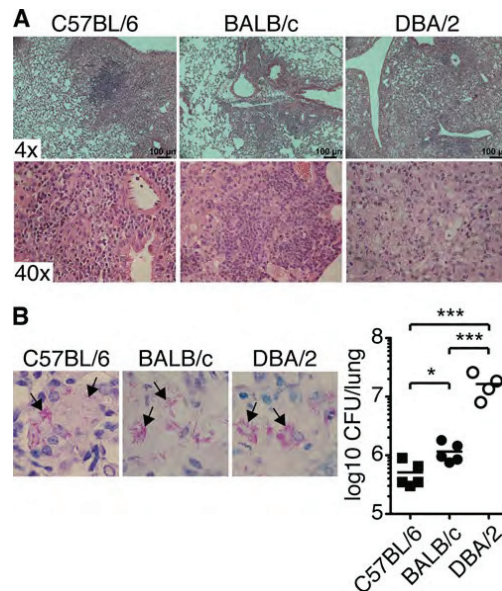


FIG 1 Lung lesions and bacterial burden in *M. tuberculosis*-infected mice. The photomicrographs show representative sections of formalin-fixed paraffin-embedded lung tissue stained with hematoxylin and eosin to determine lung pathology (A) or with Putt's stain to visualize acid-fast bacilli (B) from C57BL/6 (left), BALB/c (middle), and DBA/2 (right) mice infected with aerosolized virulent *M. tuberculosis* (9 weeks p.i.). (B, left) The arrows indicate examples of rod-shaped bacteria or clusters of bacteria. Magnification, ×100. (Right) CFU in the lungs 9 weeks p.i. Lung lesions and the ability to control *M. tuberculosis* growth were determined in two separate experiments, with 3 to 5 mice per group in each experiment. The graph shows means ± SEM from one representative experiment. *, *P* < 0.05; ***, *P* < 0.001 by one-way ANOVA with Bonferroni posttest.

pared to naturally susceptible WT mice. Therefore, we investigated the cellular infiltration in infected organs and the pro- and anti-inflammatory properties of the host immune response during pulmonary TB.

Inflammatory monocyte recruitment into *M. tuberculosis*-infected lungs and Mφ activation are not defective in susceptible mice. Using a monocyte adoptive-transfer model, we have directly shown that many of the Mφ and DC subsets that appear in *M. tuberculosis*-infected lung tissue and draining PLN at the peak of the host immune response are monocyte derived (56). To determine if diminished monocyte recruitment may help explain naturally occurring susceptibility to *M. tuberculosis*, we examined the cellular infiltrate in resistant and susceptible lung tissue in uninfected mice and at various time points after virulent *M. tuberculosis* aerosol infection (Fig. 2). The CD11b/CD11c expression profile was determined on gated CD45.2⁺ CD19⁺ cells from naïve and *M. tuberculosis*-infected mice (Fig. 2A and data not shown). CD11b⁺ CD11c⁺ myeloid cells were then analyzed further. Recruited neutrophils were defined as Ly6C^{int} (intermediate level of Ly6C) Ly6G⁺ cells and inflammatory monocytes as Ly6C⁺ Ly6G⁺ cells (18, 56, 57). We found that the total number of lung cells increased dramatically in response to *M. tuberculosis* infection and

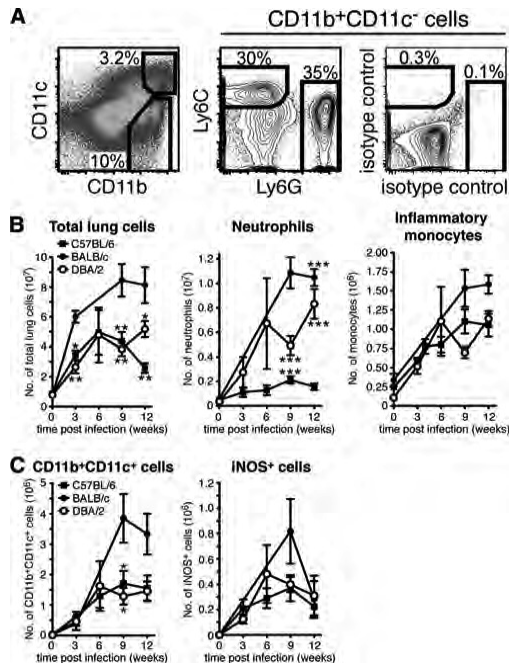


FIG 2 Neutrophil, inflammatory monocyte, DC, and M ϕ populations in the lungs of naive and *M. tuberculosis*-infected mice. (A) Single-cell suspensions were prepared from the uninfected or *M. tuberculosis*-infected lung tissues of individual mice and stained for cell surface expression of CD11b and CD11c (left), Ly6C and Ly6G (middle), or isotype control MAb (right). Ly6C⁺Ly6G⁻ inflammatory monocytes and Ly6C⁺Ly6G⁺ neutrophils were identified within the CD11b⁺CD11c⁻ gate (pregated on CD45.2⁺CD19⁻ cells [data not shown]). The plots show lung cells analyzed 12 weeks p.i. from one representative experiment. (B) Graphs displaying the absolute numbers of total lung cells (left), neutrophils (middle), and inflammatory monocytes (right) in uninfected lungs and at various time points after *M. tuberculosis* infection. (C) Graphs displaying the absolute numbers of CD11b⁺CD11c⁺ cells (left) in uninfected lungs and at various time points after *M. tuberculosis* infection. iNOS-producing cells were identified in the CD11b⁺CD11c⁺ subset (right). The absolute number of myeloid cells was determined in 3 to 11 separate experiments with 2 or 3 mice per group in each experiment. The results were pooled from all replicate experiments. The graphs show means \pm standard errors of the mean (SEM). Statistically significant differences between the mouse strains are denoted as follows: *, $P < 0.05$; **, $P < 0.01$; ***, $P < 0.001$ by one-way ANOVA with Bonferroni posttest.

was significantly higher in BALB/c mice than in C57BL/6 mice and DBA/2 mice at weeks 3, 9, and 12 p.i. (Fig. 2B) (33, 56). In the infected lung tissue of susceptible DBA/2 mice, the number of recruited neutrophils increased rapidly and continuously during the whole study period until 12 weeks p.i. (Fig. 2B). In comparison, neutrophil infiltration into the lung tissue of resistant C57BL/6 mice remained low. Still, levels of neutrophil recruitment into BALB/c and DBA/2 lungs were comparable, showing that neutrophil infiltration *per se* does not cause increased susceptibility to *M. tuberculosis* infection.

Following *M. tuberculosis* infection, Ly6C⁺ inflammatory monocytes are recruited to the lung tissue (23, 56). Our results

showed that there was no difference in the number of inflammatory monocytes recruited to *M. tuberculosis*-infected C57BL/6 and DBA/2 lungs (Fig. 2B). We also found that infected BALB/c lungs contained the highest number of recruited monocytes of the tested mouse strains 9 to 12 weeks p.i. (Fig. 2B). Our results suggest that defective monocyte recruitment into infected lungs does not explain increased susceptibility to *M. tuberculosis* in the mouse model.

Inflammatory monocytes recruited to the *M. tuberculosis*-infected lungs rapidly upregulate CD11c (56). The CD11b⁺CD11c⁺ subset in inflamed or *M. tuberculosis*-infected lung tissue is a heterogeneous population, comprising both DCs and activated iNOS-producing M ϕ (23, 32, 39, 56). We enumerated CD11b⁺CD11c⁺ myeloid cells in infected lung tissue to determine if susceptibility to *M. tuberculosis* can be explained by a reduced number of CD11b⁺CD11c⁺ cells (Fig. 2C). In addition, because CD11b⁺CD11c⁺ cells are the main producers of iNOS, an enzyme required for control of *M. tuberculosis* growth (42), we determined the number of activated iNOS-producing M ϕ in resistant and susceptible lungs (Fig. 2C). Upon *M. tuberculosis* aerosol infection of C57BL/6, BALB/c, and DBA/2 mice, the number of both CD11b⁺CD11c⁺ cells and iNOS⁺ M ϕ increased during the first 6 to 9 weeks p.i. before it reached a plateau and remained relatively constant, or even declined in BALB/c mice, until week 12 p.i. We did not detect a significant difference in the number of CD11b⁺CD11c⁺ cells or iNOS⁺ M ϕ between the three mouse strains tested. In conclusion, neither defective monocyte or neutrophil recruitment nor M ϕ activation seems to explain the increased susceptibility to *M. tuberculosis* in DBA/2 mice.

Diminished α E-DC population in the lungs of susceptible mice during pulmonary TB. α E-DCs have a distinct role in host immunity compared to proinflammatory CD103⁻ lung DCs, including the cytokine and chemokine profile and the ability to migrate to the draining PLN for T helper cell activation or to cross-present antigens to MHC class I-restricted CD8⁺ T cells (3, 14, 16, 46, 58). We characterized and enumerated lung α E-DCs to delineate their role in host immunity during pulmonary TB.

The α E-DC population in resistant and susceptible lung tissue was examined by flow cytometry in uninfected mice and at various time points after *M. tuberculosis* aerosol infection (Fig. 3). First, the CD11b/CD11c expression profile was determined on gated CD45.2⁺CD19⁻ cells (Fig. 3A and data not shown). α E-DCs were identified in the CD11b⁺CD11c⁺ myeloid cell subset in C57BL/6, BALB/c, and DBA/2 *M. tuberculosis*-infected lungs (Fig. 3A and data not shown). In all three mouse strains analyzed, α E-DCs expressed high levels of MHC class II and lacked expression of Ly6C, a marker for less differentiated cells, such as inflammatory monocytes, recruited to the *M. tuberculosis*-infected lung tissue (Fig. 3A) (56, 57).

Following *M. tuberculosis* infection, the number of α E-DCs increased early after infection (3 weeks p.i.) and remained high during chronic infection (weeks 9 to 12 p.i.) in resistant C57BL/6 and BALB/c mice (Fig. 3B). In comparison, accumulation of α E-DCs in susceptible mice was significantly reduced (Fig. 3B).

The increased number of α E-DCs in infected resistant mouse strains and the low numbers of α E-DCs in susceptible mice suggest that α E-DCs have a protective role in host immunity during pulmonary *M. tuberculosis*.

Susceptible mice display reduced numbers of α E-DCs in the draining PLN in response to *M. tuberculosis* infection. While

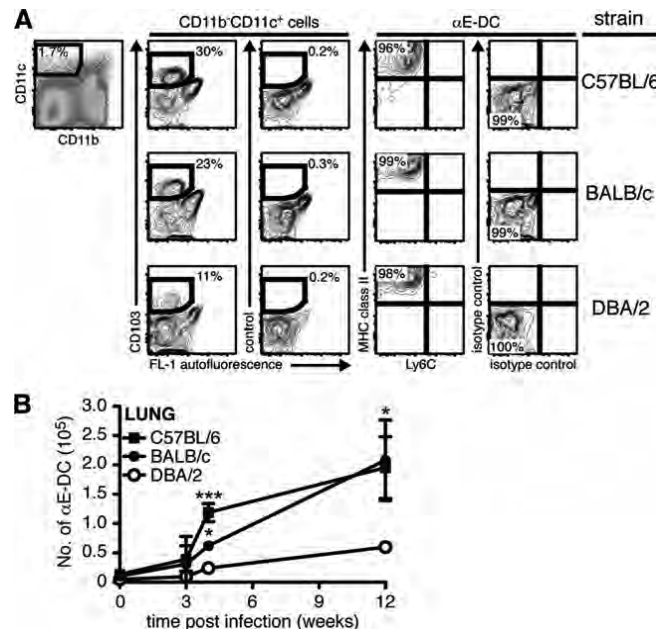


FIG 3 αE-DC populations in the lungs of naïve and *M. tuberculosis*-infected mice. (A) Groups of C57BL/6, BALB/c, and DBA/2 mice were infected with a low dose of virulent *M. tuberculosis* via the respiratory route. Single-cell suspensions were prepared from infected lungs 12 weeks p.i. and stained for CD45.2, CD19, CD11b, and CD11c (left and data not shown). αE-DCs were identified in the CD11b⁺CD11c⁺ gate (pregated on CD45.2⁺CD19⁺ cells [data not shown]) compared to an isotype control MAb (middle). The gated αE-DCs were examined for cell surface expression of Ly6C and MHC class II compared to isotype controls (right). The plots show lung cells from one representative experiment. (B) Graph showing the absolute numbers of αE-DCs in uninfected and *M. tuberculosis*-infected C57BL/6, BALB/c, and DBA/2 mice. Statistically significant differences between C57BL/6 and DBA/2 mice, or between BALB/c and DBA/2 mice, are indicated. At week 4 p.i., we also detected a statistically significant difference between C57BL/6 and BALB/c mice (**). The cell surface phenotype and the absolute number of αE-DCs were determined in nine separate experiments with 2 or 3 mice per group in each experiment. The results were pooled from all replicate experiments. The graphs show means ± SD. *, $P < 0.05$; **, $P < 0.01$; ***, $P < 0.001$ by one-way ANOVA with Bonferroni posttest.

alveolar Mφ are considered to be the main target, DCs are infected by the bacterium and have been suggested to disseminate live *M. tuberculosis* via the lymphatics to the draining PLN, where the MHC-restricted T cell response is initiated (6, 61, 62). A more detailed analysis of the DCs that help spread *M. tuberculosis* *in vivo* is currently lacking. Considering the tissue localization of αE-DCs beneath the bronchial epithelial cell layer, their migratory potential and spreading of *M. tuberculosis* by infected DCs suggest that αE-DCs are involved in bacterial dissemination and priming of *M. tuberculosis*-specific CD8⁺ T cells in the PLN (16, 46, 58, 62). Therefore, we determined if αE-DCs are present in the PLN of naïve mice after *M. tuberculosis* aerosol infection at the peak of the immune response and during chronic infection (Fig. 4). MHC class II^{hi} αE-DCs were identified in the CD11b⁺CD11c⁺ gate in naïve C57BL/6 mice and in C57BL/6, BALB/c, and DBA/2 mice 3 weeks p.i. (Fig. 4A and B) (46). After *M. tuberculosis* infection, the total number of PLN cells seemed lower in DBA/2 mice, but due to the high variability between experiments, we did not detect a statistically significant difference (by one-way analysis of variance [ANOVA] with Bonferroni posttest) between the three mouse strains analyzed. Enumeration of PLN αE-DCs showed that the absolute number was significantly reduced in DBA/2 mice com-

pared to C57BL/6 mice at both 3 and 9 weeks p.i. (Fig. 4C). The difference between C57BL/6 mice and BALB/c mice, and the difference between BALB/c mice and DBA/2 mice, was not statistically significant. Still, the trend was the same, with a higher number of αE-DCs in the more resistant BALB/c mice than in the DBA/2 mice. The reduced number of αE-DCs in the draining PLN may reflect reduced αE-DC migration from the *M. tuberculosis*-infected lungs in susceptible mice.

αE-DCs have a skewed cytokine profile during pulmonary TB. Sterile models of inflammation and *in vitro* studies have shown that αE-DCs are functionally different from other DC subsets found in the lung tissue, including the cytokine and chemokine profiles and different responses in T cell activation (3, 14, 16, 46, 58).

To determine the functional potential of αE-DCs and other myeloid cell subsets, including inflammatory monocytes, neutrophils, Mφ, and DCs, we investigated the cytokine profiles during pulmonary TB (Fig. 5). Single-cell suspensions were prepared from total lung tissue of C57BL/6, BALB/c, and DBA/2 mice 3 or 12 weeks p.i. with a low dose of aerosolized *M. tuberculosis*. CD11b/CD11c profiling (gated on CD45.2⁺CD19⁺ cells) (data not shown) was used to identify the main myeloid cell subsets in

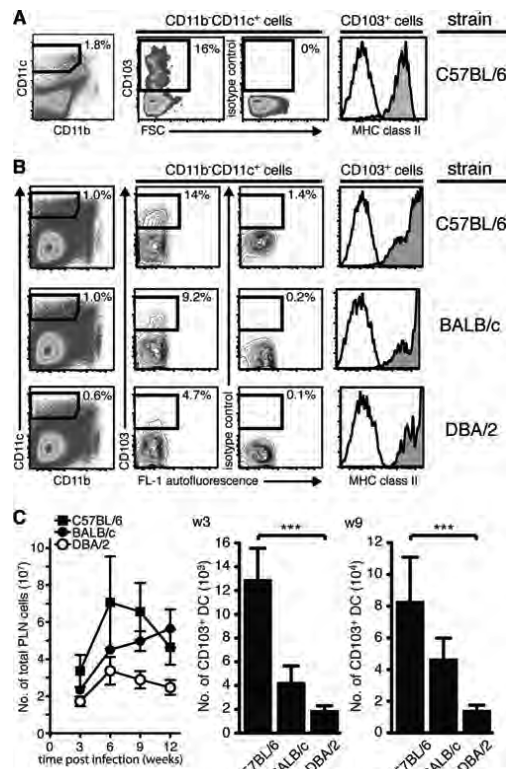


FIG 4 αE-DC populations in the PLN of naïve and *M. tuberculosis*-infected mice. (A) Single-cell suspensions were prepared from pooled PLN from five naïve C57BL/6 mice and stained for CD45.2, CD19, CD11b, and CD11c (left and data not shown) and for CD103 and MHC class II (right). αE-DCs were identified in the CD11b⁺CD11c⁺ gate (pregated on CD45.2⁺CD19⁺ cells [data not shown]) compared to an isotype control MAb. Gated αE-DCs were examined for cell surface expression of MHC class II (filled histograms) compared to an isotype control MAb (open histograms). (B) Groups of C57BL/6, BALB/c, and DBA/2 mice were infected with a low dose of virulent *M. tuberculosis* via the respiratory route. αE-DCs in the PLN were identified and analyzed as described for panel A. The plots show PLN cells analyzed 3 weeks p.i. from one representative experiment. (C) Graph showing the absolute number of PLN cells 3 to 12 weeks p.i. (left). The bar graphs show the absolute number of αE-DCs in *M. tuberculosis*-infected PLN 3 weeks (w3) or 9 weeks (w9) p.i. The cell surface phenotype and the absolute number of αE-DCs in the PLN were determined in three separate experiments with 2 or 3 mice per group in each experiment. The results were pooled from all replicate experiments. The graphs show means and SEM. ***, $P < 0.001$ by one-way ANOVA with Bonferroni posttest.

the infected lung tissue after *in vitro* stimulation (Fig. 5A). The percentage and absolute number of TNF- α - and TGF- β -producing cells, as well as the mean fluorescence intensity of the cytokine staining in positive cells, were compared in four myeloid cell subsets (Fig. 5A and B). The CD11b⁺CD11c⁺ population was divided into αE-DCs and CD103⁺ cells, which may contain alveolar M ϕ ; CD11b⁺CD11c⁺ cells (activated M ϕ and DCs); and CD11b⁺CD11c⁺ cells (inflammatory monocytes and granulocytes) (23, 56).

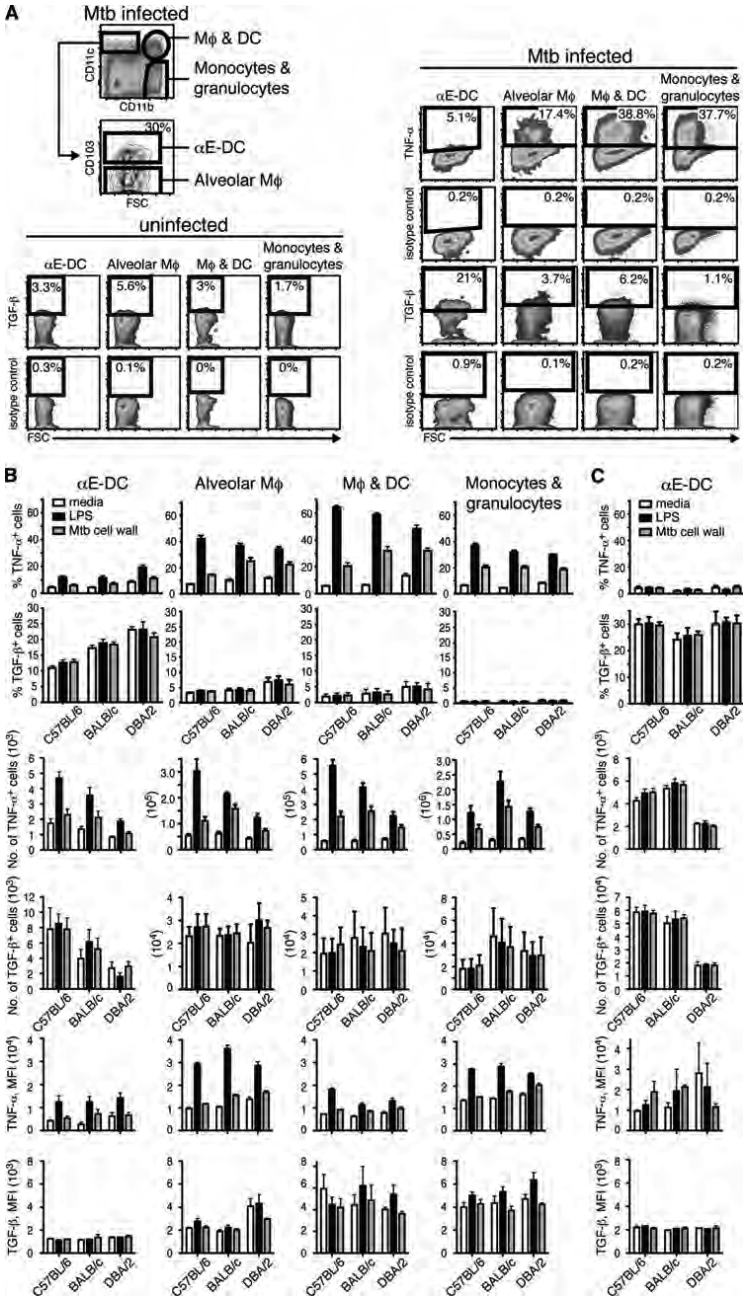
TNF- α is a proinflammatory cytokine required for control of *M. tuberculosis* growth in both humans and mice (20, 35). In response to *M. tuberculosis* cell wall extract or LPS stimulation, several of the myeloid cell subsets (alveolar M ϕ , activated M ϕ and DCs, and inflammatory monocytes and granulocytes) contained a high proportion of TNF- α -producing cells. In contrast, in response to the same stimulation, αE-DCs remained essentially TNF- α negative (Fig. 5A and B). Here, we show that of all the myeloid cell subsets analyzed, αE-DCs in infected mice contained the highest percentage of TGF- β -producing cells (Fig. 5B). Interestingly, even though the absolute number of TGF- β -producing αE-DCs was clearly reduced in *M. tuberculosis*-susceptible DBA/2 mice, αE-DCs in *M. tuberculosis*-infected DBA/2 mice contained a significantly higher ($P < 0.01$ by one-way ANOVA with Bonferroni posttest) frequency of TGF- β -producing cells 3 weeks p.i.

To determine if the functional potential of αE-DC changes during the course of *M. tuberculosis* infection, we investigated the cytokine profile of αE-DCs in chronically infected mice (Fig. 5C). Similar to week 3 p.i., αE-DCs in C57BL/6, BALB/c, and DBA/2 mice remained TNF- α negative 12 weeks p.i. Also, even though the total number of TGF- β ⁺ αE-DCs was significantly reduced ($P < 0.001$ by one-way ANOVA with Bonferroni posttest) in DBA/2 mice, the αE-DC subsets in all three mouse strains tested contained similar high frequencies of TGF- β -producing cells in chronically infected mice. Accordingly, αE-DCs display an anti-inflammatory cytokine profile in *M. tuberculosis*-infected lungs compared to other myeloid cell subsets, a phenotype that was conserved between resistant and susceptible mouse strains and that was maintained during the course of the infection.

These results support an anti-inflammatory role for αE-DCs in host immunity during pulmonary TB.

Diminished Foxp3⁺ T_{reg} cell population in *M. tuberculosis*-infected lungs of susceptible mice. Excessive inflammatory reactions, including T cell activity, at mucosal surfaces can be detrimental to the host, resulting in tissue damage and loss of function of the affected organ. We determined if failure to recruit αE-DCs in *M. tuberculosis*-infected susceptible mice correlated with a reduced number of T_{reg} cells in the infected lung tissue. Single-cell suspensions were prepared from *M. tuberculosis*-infected (3 or 12 weeks p.i.) C57BL/6, BALB/c, and DBA/2 lungs (Fig. 6A) and PLN (Fig. 6B). The cells were stained for cell surface expression of CD19, CD4, and CD8 β (Fig. 6 and data not shown). After fixation, the cells were permeabilized and stained for intracellular expression of the transcription factor Foxp3. Foxp3 was not detected in CD8⁺ T cells in the infected lungs or PLN (Fig. 6). Foxp3 expression is unique to T_{reg} cells, and Foxp3 mRNA levels are the same in uninfected lungs of C57BL/6 and DBA/2 mice (21, 40). Also, we observed the same number of T_{reg} cells in naïve C57BL/6 and DBA/2 lung tissue (data not shown). In agreement with previous findings, the CD4⁺ T cell population in the lungs of C57BL/6 mice, and in BALB/c mice, contained a significant proportion of T_{reg} cells that increased as the infection progressed (54). In contrast, the frequency of T_{reg} cells was dramatically reduced in the CD4⁺ T cell population early after *M. tuberculosis* infection at the peak of the immune response (3 weeks p.i.), and they were essentially absent from the chronically infected DBA/2 lungs (12 weeks p.i.).

Surprisingly, despite the difference in the CD4⁺ T_{reg} cell compartment in the *M. tuberculosis*-infected lungs of resistant and susceptible mice, no difference in the percentages or abso-



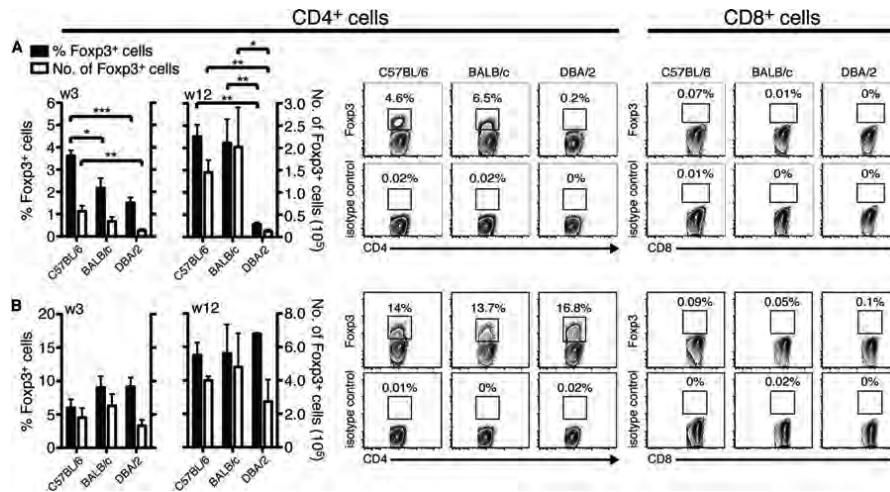


FIG 6 T_{reg} cell populations in the lungs and PLN of *M. tuberculosis*-infected mice. C57BL/6, BALB/c, and DBA/2 mice were infected with a low dose of aerosolized virulent *M. tuberculosis*, and the presence of T_{reg} cells in the infected lungs (A) and PLN (B) was analyzed three (w3), or 12 weeks (w12) p.i. The bar graphs show the percentages of T_{reg} cells among CD4⁺ cells and the absolute numbers of T_{reg} cells in infected lungs (A) and PLN (B) of C57BL/6, BALB/c, and DBA/2 mice at the indicated time points after infection. The contour plots display Foxp3 expression in gated CD4⁺ cells (left) and in gated CD8⁺ cells (right) (week 12 p.i.; both T cell subsets were pregated on CD19[−] cells [data not shown]) compared to an isotype control. The Foxp3⁺ T_{reg} population was analyzed in three separate experiments with five mice per group in each experiment. The plots show lung cells and PLN cells analyzed 12 weeks p.i. from one representative experiment. The results were pooled from all replicate experiments. The graphs display means and SEM. *, $P < 0.05$; **, $P < 0.01$; ***, $P < 0.001$ by one-way ANOVA with Bonferroni posttest.

lute numbers of Foxp3⁺ T_{reg} cells was found in the draining PLN 3 or 12 weeks p.i. In all three mouse strains tested, the frequency and absolute numbers of PLN T_{reg} cells increased over time (Fig. 6B).

In summary, our results show that the reduced number of TGF- β -producing α E-DCs in *M. tuberculosis*-susceptible mice correlates with the diminished pool of Foxp3⁺ T_{reg} cells during the peak of the immune response (week 3 p.i.) and in chronically infected lung tissue.

Increased IFN- γ production by T_{reg} cells in resistant and susceptible mice in response to *M. tuberculosis* infection. The absence of T_{reg} cells in chronically *M. tuberculosis*-infected susceptible lung tissue is reminiscent of the dramatically reduced number of T_{reg} cells found in the gut following lethal oral infection with *Toxoplasma gondii*, which is another T helper 1-inducing pathogen (48). The reduction in T_{reg} cell numbers in *T. gondii*-infected mice was accompanied by the induction of IFN- γ in the remaining T_{reg} cells (48). We therefore investigated if the functional potential of lung T_{reg} cells changed in response to *M. tuberculosis*

infection (54). The data presented in Fig. 7 show that *M. tuberculosis* infection influenced the cytokine profile of T_{reg} cells in C57BL/6 and DBA/2 mice 6 to 10 weeks p.i. CD4⁺ Foxp3[−] T cells and T_{reg} cells in naïve and *M. tuberculosis*-infected lungs were stimulated polyclonally and analyzed for IFN- γ production. T cells from naïve mice kept in medium alone or stimulated with PMA and ionomycin contained few IFN- γ -producing cells (Fig. 7 and data not shown) (48). Similar to CD4⁺ Foxp3[−] T cells, a large fraction of the stimulated T_{reg} cells in the lungs and PLN produced IFN- γ at 6 to 10 weeks p.i. We did not find any significant differences in the percentages of IFN- γ -producing CD4⁺ Foxp3[−] T cells or T_{reg} cells between C57BL/6 and DBA/2 mice (Fig. 7B and C). After determining the absolute number of IFN- γ -producing T_{reg} cells in the lungs, we observed a statistically significantly higher number in C57BL/6 mice at weeks 6 and 10 p.i. (Fig. 7C). In the PLN, the absolute number of IFN- γ -producing T_{reg} cells was significantly higher in C57BL/6 mice only at week 6 p.i. Among CD4⁺ Foxp3[−] T cells, we did not observe any significant differences in the PLN but did find a

FIG 5 α E-DC cytokine profile in *M. tuberculosis* (Mtb)-infected mice. Three mouse strains (C57BL/6, BALB/c, and DBA/2) were infected with a low dose of aerosolized virulent *M. tuberculosis*. Three or 12 weeks p.i., total lung cells were kept in medium or stimulated with LPS or *M. tuberculosis* cell wall extract. (A) The cell surface was stained for CD45.2 and CD19 (data not shown) and for CD11b, CD11c, and CD103 (top left). TNF- α and TGF- β production was compared between α E-DCs; CD11b⁺ CD11c⁺ CD103[−] cells, which may contain alveolar M ϕ ; CD11b⁺ CD11c⁺ CD103⁺ cells, which contain both activated M ϕ and DCs; and CD11b⁺ CD11c[−] cells, which are monocytes and granulocytes right and bottom (left). The plots show *M. tuberculosis* cell wall extract-stimulated lung cells from uninfected mice or lung cells analyzed 3 weeks p.i. from one representative experiment. FSC, forward light scatter. (B) Bar graphs showing the percentages (top two rows), absolute numbers (middle two rows), and mean fluorescence intensity (MFI) (bottom two rows) of TNF- α or TGF- β -producing α E-DCs in week 3 p.i. compared to the myeloid cell subsets shown in panel A. (C) Lung cells from C57BL/6, BALB/c, and DBA/2 mice were prepared 12 weeks p.i. as described above and analyzed for TNF- α and TGF- β production. The functional potential of α E-DCs was determined in four separate experiments with 2 or 3 mice per group in each experiment. The results were pooled from all replicate experiments. The graphs display means and SEM.

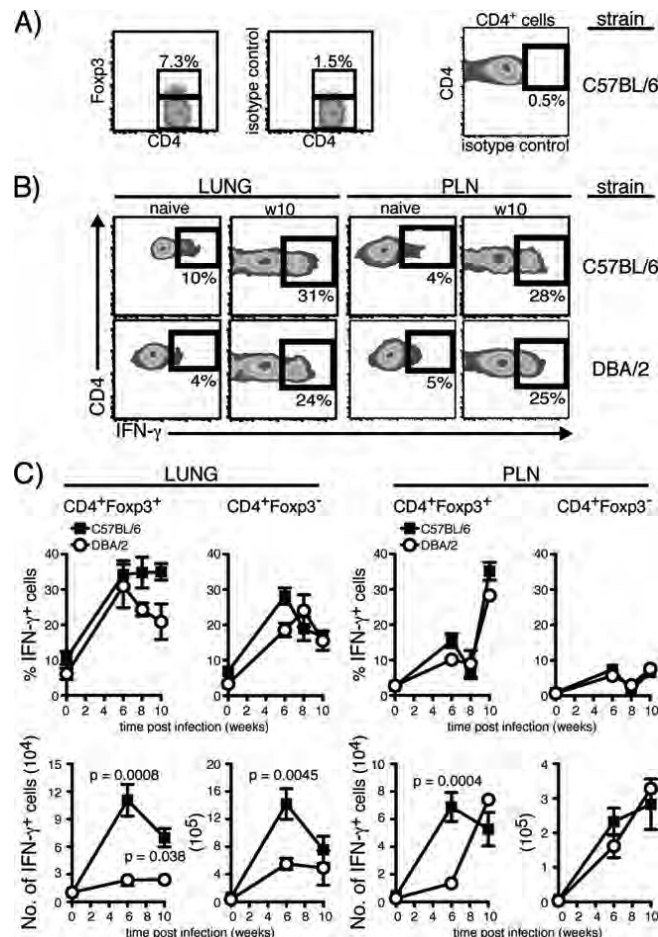


FIG 7 Cytokine production by T_{reg} cells during *M. tuberculosis* infection. Total lung cells and PLN cells were isolated from naive or *M. tuberculosis*-infected C57BL/6 and DBA/2 mice and stimulated polyclonally *in vitro*. (A) Plots showing identification of lung $CD4^{+} Foxp3^{-}$ T cells and T_{reg} cells (left) (pregated on $CD4^{+} CD19^{-}$ cells [data not shown]). The gated cells were analyzed for intracellular cytokines using the gate set after the isotype control (right). The plots show stimulated lung cells analyzed 10 weeks p.i. from one representative experiment. (B) Plots showing stimulated lung T_{reg} cells (left) and PLN T_{reg} cells (right) from naive mice or cells analyzed 10 weeks (w10) p.i. from one representative experiment. (C) Graphs showing the percentages (top) and absolute numbers (bottom) of IFN- γ -producing T_{reg} cells and $Foxp3^{-} CD4^{+}$ T cells in uninfected and infected lung tissue (left) or in the PLN (right). The functional potential of T_{reg} cells was determined in two separate experiments with 2 or 3 mice per group in each experiment. The results were pooled from all replicate experiments. The graphs display means \pm SEM, and a *t* test was used to determine statistical differences between C57BL/6 and DBA/2 mice at the various time points.

significantly higher number of IFN- γ producers in the lungs of C57BL/6 mice at week 6 p.i. (Fig. 7C).

In summary, our results show that T_{reg} cells in resistant and susceptible mice acquire the ability to produce IFN- γ in response to *M. tuberculosis* infection.

DISCUSSION

During pulmonary TB, disease progression in mice infected via the respiratory route is in many respects similar to human disease,

including gradual progression of lung pathology, while other organs are less affected even though the bacteria can disseminate there from the lung tissue (2, 27). Animal models have proven useful in identifying factors important for control of mycobacterial growth, including proinflammatory mediators, like TNF- α or IFN- γ and the IFN- γ receptor (11, 19, 20, 34). Many of these findings have translated into human disease, and there are several studies demonstrating the importance of TNF- α , IFN- γ , and the IFN- γ receptor in the human immune response against mycobac-

terial infections, including *M. tuberculosis* (35, 41, 47). Still, susceptibility to *M. tuberculosis* in otherwise seemingly healthy individuals is poorly understood. In the present study, we took advantage of WT inbred mouse strains to increase our understanding of naturally occurring susceptibility to low-dose aerosol infection with virulent *M. tuberculosis*. Comparisons between different inbred WT mouse strains have identified numerous features of the host immune response that may help explain increased susceptibility to *M. tuberculosis* infection (2, 4, 6, 7, 27, 33, 44, 45, 59). For example, even though increased *M. tuberculosis* dissemination in the lung tissue has been shown to characterize susceptible mice (4), early *M. tuberculosis* dissemination from the lungs to the PLN may support a more robust *M. tuberculosis*-specific T cell response in resistant animals (6), and these T cells may localize more efficiently within the resistant lung tissue to help control the infection (59). The lungs pose a particular problem for the immune system trying to eradicate invading microorganisms, such as *M. tuberculosis*. While innate and adaptive immune effector functions are required for control of *M. tuberculosis* growth, excessive immune activation can lead to tissue damage and loss of function. Hence, a balance between inflammatory and tolerogenic immune reactions must be maintained at mucosal surfaces. This is illustrated by the extensive infiltration of lymphocytes and mononuclear cells into the lungs of Foxp3-deficient mice that lack T_{reg} cells (37). Here, we show that lung cells with anti-inflammatory effector functions are significantly reduced during chronic infection in *M. tuberculosis*-susceptible mice.

Recent studies using the mouse model have shown that T_{reg} cells are able to inhibit the antigen-specific T cell response during pulmonary TB and reduce the ability of the immune system to control bacterial growth (38, 54, 55). Also, in TB patients, the number of T_{reg} cells increases in infected tissues and isolated T_{reg} cells are able to suppress antigen-specific T cell responses *in vitro* (8, 24, 25, 53). However, the exact role of T_{reg} cells during pulmonary TB is not fully characterized. For example, while Scott-Browne reported that T_{reg} cell depletion reduces bacterial growth early after *M. tuberculosis* infection (54), Quinn et al. found that inhibition of T_{reg} cell activity *in vivo* prior to *M. tuberculosis* infection increased the frequency of IFN- γ - and IL-2-producing cells but had no effect on bacterial growth or lung lesions early after infection (52). Similarly, Ozeki et al. demonstrated that depletion of T_{reg} cells early after *M. tuberculosis* infection increased IFN- γ production by CD4⁺ T cells and reduced the bacterial load. Interestingly, this effect was not observed if the T_{reg} cells were depleted at later stages of the infection, suggesting different roles for T_{reg} cells at early and later stages of pulmonary TB (50). Shafiani et al. used a different approach to investigate how T_{reg} cells influence *M. tuberculosis*-specific T cell immunity and bacterial growth early after *M. tuberculosis* infection (55). While the authors observed an increase in the lung CFU and a reduced number of *M. tuberculosis*-specific T cells in animals receiving adoptively transferred T_{reg} cells, the effects on the *M. tuberculosis*-specific T cell response was transient, and the effects on bacterial growth after day 35 p.i. were not determined (55). Our data show that *M. tuberculosis* infection induces IFN- γ production by T_{reg} cells by weeks 6 to 10 p.i. (Fig. 7). Even though we did not examine T_{reg} cell function at earlier time points, a possible explanation for the temporary effects observed by Shafiani et al. could be a change in the functional potential of the transferred cells in *M. tuberculosis*-infected recipients over time. The cytokine profile of T_{reg} cells in the lungs of *M.*

tuberculosis-infected mice has been addressed by others (54). Scott-Browne et al. did not observe IFN- γ production by T_{reg} cells in response to *M. tuberculosis* infection. An explanation for the different findings may be found in how the cells were stimulated prior to intracellular-cytokine staining. We based our protocol on the work published by Oldenhove et al. and used PMA and ionomycin, while Scott-Browne et al. used anti-CD3 plus anti-CD28 stimulation (48, 54). Another explanation could be the use of different strains of *M. tuberculosis*, which can affect T cell function and lung pathology, depending on bacterial virulence (17, 49). We used the clinical *M. tuberculosis* isolate strain Harlingen, which, at least in *in vitro*-infected M ϕ , seems to be more virulent than the laboratory strain H37Rv used by Scott-Browne et al. and Carow et al. (5, 54).

M. tuberculosis-specific T cells are first detected in the PLN, but only after live bacteria have disseminated there from the lungs (6, 61). Even though the exact phenotype of the DCs that transport the bacteria to the PLN is not known, the majority of the infected cells in the PLN are CD11b⁺ CD11c⁺ at days 14 to 28 p.i. (62). Interestingly, *Mycobacterium bovis* BCG has also been suggested to disseminate in infected DCs (26). In the PLN, some of the BCG-infected DCs were reported to be CD11b negative, similar to α E-DCs (26). Since lung α E-DCs are migratory and are able to prime T cells in the PLN, perhaps *M. tuberculosis*-infected α E-DCs, or α E-DCs that have taken up infected cells undergoing apoptosis, are involved in initiating the adaptive T cell response during pulmonary TB (16).

Instead of observing an increased percentage of T_{reg} cells in infected susceptible lung tissue, which could help explain the increase in the bacterial burden, we found that the frequency of T_{reg} cells was significantly reduced 3 weeks p.i., and they were almost completely absent in chronically infected mice (Fig. 6). Thus, Foxp3⁺ T_{reg} cell activity is less likely to explain the failure of the immune system in DBA/2 mice to control bacterial growth in the lungs at later stages of the infection. Despite the differences in the infected lungs, the frequency of Foxp3⁺ T_{reg} cells in the CD4⁺ T cell compartment in the PLN was not significantly different between the three mouse strains tested (Fig. 6). Therefore, the absence of T_{reg} cells in the chronically infected DBA/2 lungs was not due to systemic failure to generate T_{reg} cells in this susceptible mouse strain during chronic TB.

Why do T_{reg} cells not localize in the infected susceptible lungs? Because α E-DCs in the gut-associated lymphoid tissue are able to influence both priming and homing of MHC-restricted T cells and to induce T_{reg} cells to dampen overly aggressive immune responses (1, 9, 29, 31), we speculate that α E-DCs are analogues of their gut counterparts and play a role in host immunity during pulmonary TB by influencing T_{reg} cell biology in the lungs. α E-DCs have been shown to produce the chemokine CCL22 under steady-state conditions and during allergic airway inflammation (3). CCR4, the receptor for CCL22, is expressed on T_{reg} cells and induces T_{reg} cell migration (28). Moreover, a large fraction of lung α E-DCs are TGF- β ⁺ during TB (Fig. 5), and TGF- β is important for peripheral T_{reg} cell function and homeostasis (43). The reduced number of α E-DCs in *M. tuberculosis*-infected DBA/2 mice may therefore negatively affect T_{reg} recruitment or maintenance in the lungs.

α E-DCs have been shown to be Ly6C⁺ monocyte derived under steady-state conditions (30). Our data show that monocyte recruitment is not defective in susceptible mice (Fig. 2B). Instead,

our results suggest that monocyte differentiation is altered in the *M. tuberculosis*-infected DBA/2 lung tissue. While the number of α E-DCs was reduced in infected susceptible mice, the number of CD11b⁺ CD11c⁺ cells and the number of iNOS-producing M ϕ were not (Fig. 2C) (33). In summary, changes in monocyte differentiation in *M. tuberculosis*-infected lung tissue likely explain the reduced number of α E-DCs in susceptible mice during pulmonary TB.

In conclusion, our results identify differences among α E-DCs and T_{reg} cells in *M. tuberculosis*-resistant and -susceptible inbred mice that may increase our understanding of immune regulation during pulmonary TB.

ACKNOWLEDGMENTS

This work was supported by grants from the Swedish Research Council (grant no. K2007-57X-20360-01-4), The Swedish Heart-Lung Foundation, Stiftelsen Clas Groschinskys Minnesfond, and Karolinska Institutet to M.S.C.L. was supported by a scholarship from the Royal Thai Government, and L.I. was the recipient of a Marie-Curie Host Fellowship for Early Stage Researchers Training grant and was supported by a grant from Stiftelsen Sigurd och Elsa Goljes Minne.

We acknowledge Markus Maeurer, Karolinska Institutet; Mats Spångberg and Helene Fredlund; and the staff of the biosafety level 3 animal facility, Astrid Fagraeus Laboratory, Swedish Institute for Communicable Disease Control, for their help in facilitating these experiments. We are grateful to Samuel Behar, Brigham and Women's Hospital and Harvard Medical School, for his help in establishing the aerosol infection model and for critically reading the manuscript and to Gunilla Högberg, Karolinska University Hospital, for her help with the lung histology.

REFERENCES

- Annacker O, et al. 2005. Essential role for CD103 in the T cell-mediated regulation of experimental colitis. *J. Exp. Med.* 202:1051–1061.
- Basaraba RJ. 2008. Experimental tuberculosis: the role of comparative pathology in the discovery of improved tuberculosis treatment strategies. *Tuberculosis* 88(Suppl. 1):S35–S47.
- Beatty SR, Rose CE Jr, Sung SS. 2007. Diverse and potent chemokine production by lung CD11b^{high} dendritic cells in homeostasis and in allergic lung inflammation. *J. Immunol.* 178:1882–1895.
- Cardona PJ, et al. 2003. Widespread bronchogenic dissemination makes DBA/2 mice more susceptible than C57BL/6 mice to experimental aerosol infection with *Mycobacterium tuberculosis*. *Infect. Immun.* 71:5845–5854.
- Carow B, et al. 2011. Silencing suppressor of cytokine signaling-1 (SOCS1) in macrophages improves *Mycobacterium tuberculosis* control in an interferon-gamma (IFN- γ)-dependent manner. *J. Biol. Chem.* 286:26873–26887.
- Chackerian AA, Alt JM, Perera TV, Dascher CC, Behar SM. 2002. Dissemination of *Mycobacterium tuberculosis* is influenced by host factors and precedes the initiation of T-cell immunity. *Infect. Immun.* 70:4501–4509.
- Chackerian AA, Behar SM. 2003. Susceptibility to *Mycobacterium tuberculosis*: lessons from inbred strains of mice. *Tuberculosis* 83:279–285.
- Chen X, et al. 2007. CD4(+)CD25(+)FoxP3(+) regulatory T cells suppress *Mycobacterium tuberculosis* immunity in patients with active disease. *Clin. Immunol.* 123:50–59.
- Coombes JL, et al. 2007. A functionally specialized population of mucosal CD103⁺ DCs induces Foxp3⁺ regulatory T cells via a TGF- β and retinoic acid-dependent mechanism. *J. Exp. Med.* 204:1757–1764.
- Cooper AM. 2009. Cell-mediated immune responses in tuberculosis. *Annu. Rev. Immunol.* 27:393–422.
- Cooper AM, et al. 1993. Disseminated tuberculosis in interferon gamma gene-disrupted mice. *J. Exp. Med.* 178:2243–2247.
- Dannenberger Jr, AM. 2006. Pathogenesis of human pulmonary tuberculosis: insights from the rabbit model. ASM Press, Washington, DC.
- del Rio ML, Bernhardt G, Rodriguez-Barbosa JJ, Forster R. 2010. Development and functional specialization of CD103⁺ dendritic cells. *Immunol. Rev.* 234:268–281.
- del Rio ML, et al. 2008. CX3CR1⁺ c-kit⁺ bone marrow cells give rise to CD103⁺ and CD103[−] dendritic cells with distinct functional properties. *J. Immunol.* 181:6178–6188.
- del Rio ML, Rodriguez-Barbosa JJ, Kremmer E, Forster R. 2007. CD103[−] and CD103⁺ bronchial lymph node dendritic cells are specialized in presenting and cross-presenting innocuous antigen to CD4⁺ and CD8⁺ T cells. *J. Immunol.* 178:6861–6866.
- Desch AN, et al. 2011. CD103⁺ pulmonary dendritic cells preferentially acquire and present apoptotic cell-associated antigen. *J. Exp. Med.* 208:1789–1797.
- Dunn PL, North RJ. 1995. Virulence ranking of some *Mycobacterium tuberculosis* and *Mycobacterium bovis* strains according to their ability to multiply in the lungs, induce lung pathology, and cause mortality in mice. *Infect. Immun.* 63:3428–3437.
- Fleming TJ, Fleming ML, Malek TR. 1993. Selective expression of Ly-6G on myeloid lineage cells in mouse bone marrow. RB6-8C5 mAb to granulocyte-differentiation antigen (Gr-1) detects members of the Ly-6 family. *J. Immunol.* 151:2399–2408.
- Flynn JL, et al. 1993. An essential role for interferon gamma in resistance to *Mycobacterium tuberculosis* infection. *J. Exp. Med.* 178:2249–2254.
- Flynn JL, et al. 1995. Tumor necrosis factor- α is required in the protective immune response against *Mycobacterium tuberculosis* in mice. *Immunity* 2:561–572.
- Fontenot JD, Gavin MA, Rudensky AY. 2003. Foxp3 programs the development and function of CD4⁺CD25⁺ regulatory T cells. *Nat. Immunol.* 4:330–336.
- GeurtsvanKessel CH, et al. 2008. Clearance of influenza virus from the lung depends on migratory langerin⁺CD11b[−] but not plasmacytoid dendritic cells. *J. Exp. Med.* 205:1621–1634.
- Gonzalez-Juarrero M, Shim TS, Kipnis A, Junqueira-Kipnis AP, Orme IM. 2003. Dynamics of macrophage cell populations during murine pulmonary tuberculosis. *J. Immunol.* 171:3128–3135.
- Guyot-Revol V, Innes JA, Hackforth S, Hinks T, Lalvani A. 2006. Regulatory T cells are expanded in blood and disease sites in patients with tuberculosis. *Am. J. Respir. Crit. Care Med.* 173:803–810.
- Hougardy JM, et al. 2007. Regulatory T cells depress immune responses to protective antigens in active tuberculosis. *Am. J. Respir. Crit. Care Med.* 176:409–416.
- Humphreys IR, et al. 2006. A role for dendritic cells in the dissemination of mycobacterial infection. *Microbes Infect.* 8:1339–1346.
- Hunter RL, Jagannath C, Actor JK. 2007. Pathology of postprimary tuberculosis in humans and mice: contradiction of long-held beliefs. *Tuberculosis* 87:267–278.
- Iellem A, et al. 2001. Unique chemotactic response profile and specific expression of chemokine receptors CCR4 and CCR8 by CD4(+)CD25(+) regulatory T cells. *J. Exp. Med.* 194:847–853.
- Jaensson E, et al. 2008. Small intestinal CD103⁺ dendritic cells display unique functional properties that are conserved between mice and humans. *J. Exp. Med.* 205:2139–2149.
- Jakubzik C, et al. 2008. Blood monocyte subsets differentially give rise to CD103⁺ and CD103[−] pulmonary dendritic cell populations. *J. Immunol.* 180:3019–3027.
- Johansson-Lindbom B, et al. 2005. Functional specialization of gut CD103⁺ dendritic cells in the regulation of tissue-selective T cell homing. *J. Exp. Med.* 202:1063–1073.
- Julia V, et al. 2002. A restricted subset of dendritic cells captures airborne antigens and remains able to activate specific T cells long after antigen exposure. *Immunity* 16:271–283.
- Jung YJ, Ryan L, LaCourse R, North RJ. 2009. Differences in the ability to generate type 1 T helper cells need not determine differences in the ability to resist *Mycobacterium tuberculosis* infection among mouse strains. *J. Infect. Dis.* 199:1790–1796.
- Kamijo R, et al. 1993. Mice that lack the interferon-gamma receptor have profoundly altered responses to infection with *Bacillus Calmette-Guérin* and subsequent challenge with lipopolysaccharide. *J. Exp. Med.* 178:1435–1440.
- Keane J, et al. 2001. Tuberculosis associated with infliximab, a tumor necrosis factor- α -neutralizing agent. *N. Engl. J. Med.* 345:1098–1104.
- Kiers A, Drost AP, van Soolingen D, Veen J. 1997. Use of DNA fingerprinting in international source case finding during a large outbreak of tuberculosis in The Netherlands. *Int. J. Tuberc. Lung Dis.* 1:239–245.
- Kim JM, Rasmussen JP, Rudensky AY. 2007. Regulatory T cells prevent

- catastrophic autoimmunity throughout the lifespan of mice. *Nat. Immunol.* 8:191–197.
38. Kursar M, et al. 2007. Cutting edge: regulatory T cells prevent efficient clearance of *Mycobacterium tuberculosis*. *J. Immunol.* 178:2661–2665.
 39. Landsman L, Varol C, Jung S. 2007. Distinct differentiation potential of blood monocyte subsets in the lung. *J. Immunol.* 178:2000–2007.
 40. Lo Re S, et al. 25 August 2011, posting date. PDGF-producing CD4⁺ Foxp3⁺ regulatory T lymphocytes promote lung fibrosis. *Am. J. Respir. Crit. Care Med.* doi:10.1164/rccm.201103-0516OC.
 41. Lopez-Maderuelo D, et al. 2003. Interferon-gamma and interleukin-10 gene polymorphisms in pulmonary tuberculosis. *Am. J. Respir. Crit. Care Med.* 167:970–975.
 42. MacMicking JD, et al. 1997. Identification of nitric oxide synthase as a protective locus against tuberculosis. *Proc. Natl. Acad. Sci. U. S. A.* 94:5243–5248.
 43. Marie JC, Letterio JJ, Gavin M, Rudensky AY. 2005. TGF-beta1 maintains suppressor function and Foxp3 expression in CD4⁺CD25⁺ regulatory T cells. *J. Exp. Med.* 201:1061–1067.
 44. Medina E, North RJ. 1996. Evidence inconsistent with a role for the Bcg gene (Nramp1) in resistance of mice to infection with virulent *Mycobacterium tuberculosis*. *J. Exp. Med.* 183:1045–1051.
 45. Medina E, North RJ. 1998. Resistance ranking of some common inbred mouse strains to *Mycobacterium tuberculosis* and relationship to major histocompatibility complex haplotype and Nramp1 genotype. *Immunology* 93:270–274.
 46. Nakano H, et al. 2012. Pulmonary CD103(+) dendritic cells prime Th2 responses to inhaled allergens. *Mucosal Immunol.* 5:53–65.
 47. Newport MJ, et al. 1996. A mutation in the interferon-gamma-receptor gene and susceptibility to mycobacterial infection. *N. Engl. J. Med.* 335:1941–1949.
 48. Oldenhove G, et al. 2009. Decrease of Foxp3⁺ Treg cell number and acquisition of effector cell phenotype during lethal infection. *Immunity* 31:772–786.
 49. Ordway D, et al. 2007. The hypervirulent *Mycobacterium tuberculosis* strain HN878 induces a potent TH1 response followed by rapid down-regulation. *J. Immunol.* 179:522–531.
 50. Ozeki Y, et al. 2010. Transient role of CD4⁺CD25⁺ regulatory T cells in mycobacterial infection in mice. *Int. Immunol.* 22:179–189.
 51. Paula MO, et al. 2011. Host genetic background affects regulatory T-cell activity that influences the magnitude of cellular immune response against *Mycobacterium tuberculosis*. *Immunol. Cell Biol.* 89:526–534.
 52. Quinn KM, et al. 2006. Inactivation of CD4⁺CD25⁺ regulatory T cells during early mycobacterial infection increases cytokine production but does not affect pathogen load. *Immunol. Cell Biol.* 84:467–474.
 53. Ribeiro-Rodrigues R, et al. 2006. A role for CD4⁺CD25⁺ T cells in regulation of the immune response during human tuberculosis. *Clin. Exp. Immunol.* 144:25–34.
 54. Scott-Browne JP, et al. 2007. Expansion and function of Foxp3-expressing T regulatory cells during tuberculosis. *J. Exp. Med.* 204:2159–2169.
 55. Shafiani S, Tucker-Heard G, Kariyone A, Takatsu K, Urdahl KB. 2010. Pathogen-specific regulatory T cells delay the arrival of effector T cells in the lung during early tuberculosis. *J. Exp. Med.* 207:1409–1420.
 56. Skold M, Behar SM. 2008. Tuberculosis triggers a tissue-dependent program of differentiation and acquisition of effector functions by circulating monocytes. *J. Immunol.* 181:6349–6360.
 57. Sunderkotter C, et al. 2004. Subpopulations of mouse blood monocytes differ in maturation stage and inflammatory response. *J. Immunol.* 172:4410–4417.
 58. Sung SS, et al. 2006. A major lung CD103 (alphaE)-beta7 integrin-positive epithelial dendritic cell population expressing Langerin and tight junction proteins. *J. Immunol.* 176:2161–2172.
 59. Turner J, et al. 2001. Immunological basis for reactivation of tuberculosis in mice. *Infect. Immun.* 69:3264–3270.
 60. WHO. 2010. Global tuberculosis control: WHO report 2010. WHO/HTM/TB/2010.7. World Health Organization, Geneva, Switzerland.
 61. Wolf AJ, et al. 2008. Initiation of the adaptive immune response to *Mycobacterium tuberculosis* depends on antigen production in the local lymph node, not the lungs. *J. Exp. Med.* 205:105–115.
 62. Wolf AJ, et al. 2007. *Mycobacterium tuberculosis* infects dendritic cells with high frequency and impairs their function in vivo. *J. Immunol.* 179:2509–2519.

II

Infection Rate and Tissue Localization of Murine IL-12p40-Producing Monocyte-Derived CD103⁺ Lung Dendritic Cells during Pulmonary Tuberculosis

Chaniya Leepiyasakulchai¹, Chato Taher², Olga D. Chuquimia³, Jolanta Mazurek¹, Cecilia Söderberg-Naucler², Carmen Fernández³, Markus Sköld^{1*}

¹ Department of Microbiology, Tumor and Cell Biology, Karolinska Institutet, Stockholm, Sweden, ² Department of Medicine, Solna, Center for Molecular Medicine, Karolinska Institutet, Stockholm, Sweden, ³ Department of Immunology, Wenner-Gren Institute, Stockholm University, Stockholm, Sweden

Abstract

Non-hematopoietic cells, including lung epithelial cells, influence host immune responses. By co-culturing primary alveolar epithelial cells and monocytes from naïve donor mice, we show that alveolar epithelial cells support monocyte survival and differentiation in vitro, suggesting a role for non-hematopoietic cells in monocyte differentiation during the steady state in vivo. CD103⁺ dendritic cells (αE-DC) are present at mucosal surfaces. Using a murine primary monocyte adoptive transfer model, we demonstrate that αE-DC in the lungs and pulmonary lymph nodes are monocyte-derived during pulmonary tuberculosis. The tissue localization may influence the functional potential of αE-DC that accumulate in *Mycobacterium tuberculosis*-infected lungs. Here, we confirm the localization of αE-DC in uninfected mice beneath the bronchial epithelial cell layer and near the vascular wall, and show that αE-DC have a similar distribution in the lungs during pulmonary tuberculosis and are detected in the bronchoalveolar lavage fluid from infected mice. Lung DC can be targeted by *M. tuberculosis* in vivo and play a role in bacterial dissemination to the draining lymph node. In contrast to other DC subsets, only a fraction of lung αE-DC are infected with the bacterium. We also show that virulent *M. tuberculosis* does not significantly alter cell surface expression levels of MHC class II on infected cells in vivo and that αE-DC contain the highest frequency of IL-12p40⁺ cells among the myeloid cell subsets in infected lungs. Our results support a model in which inflammatory monocytes are recruited into the *M. tuberculosis*-infected lung tissue and, depending on which non-hematopoietic cells they interact with, differentiate along different paths to give rise to multiple monocyte-derived cells, including DC with a distinctive αE-DC phenotype.

Citation: Leepiyasakulchai C, Taher C, Chuquimia OD, Mazurek J, Söderberg-Naucler C, et al. (2013) Infection Rate and Tissue Localization of Murine IL-12p40-Producing Monocyte-Derived CD103⁺ Lung Dendritic Cells during Pulmonary Tuberculosis. PLoS ONE 8(7): e69287. doi:10.1371/journal.pone.0069287

Editor: Pere-Joan Cardona, Fundació Institut d'Investigació en Ciències de la Salut Germans Trias i Pujol, Universitat Autònoma de Barcelona, CIBERES, Spain

Received: February 20, 2013; **Accepted:** June 07, 2013; **Published:** July 8, 2013

Copyright: © 2013 Leepiyasakulchai et al. This is an open-access article distributed under the terms of the Creative Commons Attribution License, which permits unrestricted use, distribution, and reproduction in any medium, provided the original author and source are credited.

Funding: This work was supported by grants from The Swedish Research Council (grant no. K2007-57X-20360-01-4, www.vr.se), The Swedish Heart-Lung Foundation and Konung Oscar II:s jubileumsfond (www.hjart-lungfonden.se), Stiftelsen Clas Groschinskys Minnesfond (www.groschinsky.org) and Karolinska Institutet (ki.se) to MS. CL was supported by a scholarship from the Royal Thai Government and a grant from Stiftelsen Sigurd och Elsa Goljes Minne. The funders had no role in study design, data collection and analysis, decision to publish, or preparation of the manuscript.

Competing interests: The authors have declared that no competing interests exist.

* E-mail: markus.skold@ki.se

Introduction

Pulmonary tuberculosis (TB) is a leading cause of death from infectious disease in the world and remains a global threat to public health [1]. Alveolar macrophages (Mφ) are initial targets for *Mycobacterium tuberculosis*, which later spreads to other myeloid cell subsets in the infected lung tissue, many of which originate from recruited Ly6C⁺ inflammatory monocytes [2-5]. Ly6C⁺ monocyte formation in the bone marrow [6,7], followed by release into circulation and subsequent recruitment and differentiation into various dendritic cell (DC) and Mφ subsets in mycobacterial-infected tissues is important for anti-bacterial

effector functions mediated by innate and adaptive immune cells, and for disease outcome in mice and in humans [3-5,8-14]. Reduced number of monocytes in peripheral blood correlates with increased susceptibility to *M. tuberculosis* and to the live vaccine strain Bacille Calmette–Guérin (BCG) [10,11,13]. A likely explanation for this is the numerous functions monocyte-derived cells have in host immunity in response to mycobacterial infections [3]. Infected monocyte-derived Mφ have direct bactericidal effector functions mediated by for example inducible nitric oxide synthase (iNOS) [3,8,14]. In addition, DC can be divided into several functionally distinct subsets, including CD103⁺ DC (αE-DC) in the lungs that have a

skewed cytokine profile during pulmonary TB [15,16]. α E-DC development depends on the transcription factors IRF8 and Batf3 [17]. In support of an important role for DC in controlling mycobacterial infections, IRF8-deficiency increase susceptibility in humans and in animal models [10,12].

Moreover, DC can activate *M. tuberculosis*-specific T cells in secondary lymphoid organs [9]. Differentiation of IFN- γ -producing *M. tuberculosis*-specific T helper 1 (Th1) cells is dependent on IL-12p40 secreted by DC, and both Th1 cells and IL-12p40 is required for control of bacterial growth [18–21]. In the present study we show that primary alveolar epithelial cells (AEC) from naive donor mice support monocyte survival and differentiation in vitro, and that recruited monocytes can differentiate into α E-DC in *M. tuberculosis*-infected lungs and in the draining pulmonary lymph node (PLN). Once recruited into infected lungs, α E-DC localize near the bronchial epithelial cell layer and in close proximity to the vascular wall. A small number of α E-DC are also found in the bronchoalveolar lavage (BAL) fluid from *M. tuberculosis*-infected mice. We also confirm that several myeloid cell subsets are targeted by *M. tuberculosis* during the peak of the immune response, and despite localizing in close proximity to the airways only a small fraction of lung α E-DC is infected with *M. tuberculosis* in vivo [2]. As expected, *M. tuberculosis*-infected myeloid cells that localized in the lungs did not downregulate cell surface expression of MHC class II during the first month of infection [2,22]. Finally, we extend our previous findings on the cytokine profile of lung α E-DC during TB and show that α E-DC contain a high percentage of IL-12p40-producing cells suggesting a role for α E-DC in Th1 cell priming [16].

Materials and Methods

Ethics Statement

All animal experiments were conducted in accordance with the Swedish Animal Welfare Act. Karolinska Institutet and the Stockholm North Ethical Committee, the Swedish Board of Agriculture approved all animal experiments involving *M. tuberculosis* (permit number N369/10). In some experiments, uninfected animals were housed under pathogen-free conditions at the Animal Department of the Arrhenius Laboratories, Stockholm University, Sweden. The experiments were performed in accordance with the guidelines of the Animal Research Ethics Board at Stockholm University (permit number N27/10).

In all animal experiments, the health status of the mice was monitored daily by animal care technicians or veterinarians to ensure humane treatment.

Mice

Female C57BL/6 and BALB/c mice (6–9 weeks old) were purchased from Charles River (Germany). C57BL/6 mice expressing the CD45.1 allele of the CD45 molecule were obtained from the animal facility at the Department of Microbiology, Tumor and Cell Biology, Karolinska Institutet.

For experiments involving primary AEC, 8–12-week old female C57BL/6 mice were purchased from NOVA-SCB, Sweden, and TLR4^{-/-} mice were obtained from Karolinska

Institutet with the permission of S. Akira (Osaka University, Japan) [23].

M. tuberculosis aerosol infection

The clinical *M. tuberculosis* isolate, strain Harlingen, used for the *M. tuberculosis* aerosol infections was kindly provided by Dr. J. van Embden, National Institute of Public Health and the Environment, The Netherlands [24]. GFP-expressing *M. tuberculosis*, strain H37Rv, was kindly provided by Dr. M. Lerm, Linköping University [25,26]. *M. tuberculosis* aerosol infection were performed as previously described [16]. In brief, frozen aliquots were thawed and bacterial clumps were dispersed. The bacteria were diluted to 1×10^6 CFU/ml in sterile PBS, 0.02% Tween 80, and placed in a nebulizer (MiniHeart Lo-Flo Nebulizer, Westmed, Tucson, AZ). The animals were infected with a low-dose of *M. tuberculosis* via the respiratory route using a nose-only exposure system (In-Tox Products, Moriarty, NM) calibrated to deliver 20–200 colony-forming units (CFU) into the lungs. The animals used in this study were infected and housed under specific pathogen-free conditions in a biosafety level-3 animal facility at the Astrid Fagraeus Laboratory, Karolinska Institutet.

CFU determination

The mice were anesthetized by exposure to isoflurane and euthanized by cervical dislocation. Both lungs were used for day one CFU determinations. Viable mycobacteria were quantified by plating the lung homogenates onto Middlebrook 7H11 agar plates. Colonies were counted after 2–3 weeks of incubation at 37°C.

Monocyte adoptive transfer into *M. tuberculosis*-infected recipient mice

1×10^6 primary monocytes were enriched from bone marrow of naive donor C57BL/6 mice and adoptively transferred into *M. tuberculosis*-infected (Harlingen strain) C57BL/6.CD45.1 recipient mice as previously described [3]. Adoptive transfers were performed three weeks post infection (p.i.). Single cell suspensions were prepared from total lung tissue and PLN at day 10 after cell transfer. The cell surface phenotype of CD45.2⁺ transferred cells was analyzed using flow cytometry as described below. All recipient mice were analyzed individually.

Immunohistochemistry

Lung tissue from naive or *M. tuberculosis*-infected mice were perfused with PBS and cut into smaller pieces. The tissue samples were fixed in 4% paraformaldehyde for 2h and dehydrated in 30% sucrose at 4°C overnight before embedding in OCT freezing media (Thermo Scientific). 5- μ m sections were cut using a cryostat (Microm HM550, Thermo Scientific) and adhered to Superfrost Plus slides (Thermo Scientific). Sections were kept at -20°C until use.

The sections were dried for 20 minutes at room temperature (RT) before blocking with 2% normal mouse serum in common Ab diluent (BioGenex) and Tris buffer containing 0.01% Triton X-100 (Sigma Aldrich) for 30 minutes at RT before washing and subsequent blocking using Dako protein block (Dako) for

30 minutes at RT. An unconjugated primary rat anti-mouse MHC class II (M5/114.15.2) mAb, or an isotype control mAb (BD bioscience), was added and incubated for 1h at RT. 2% goat serum was then used for blocking (30 minutes at RT), followed by staining with a secondary goat anti-rat IgG (H+L)-Alexa Fluor 633 mAb (Invitrogen) for 1 hour at RT. Next, the sections were then blocked with 2% normal rat serum prior to staining with anti-mouse CD103-PE (M290), or an isotype control mAb (BD Biosciences) for 2h at RT. Nuclei were detected with 4',6-diamidino-2-phenylindole (DAPI) (Invitrogen). Stained slides were mounted with fluorescence mounting medium (Dako) and images were acquired using a Leica TCS SP5 II confocal microscope (Leica).

Preparation of single-cell suspensions

At the indicated timepoints, single-cell suspensions were prepared from lungs and PLN. The mice were euthanized and blood removed from the lung tissue by perfusing the heart with PBS. Lungs and PLN were aseptically removed and placed in RPMI 1640 medium. The lungs were cut into small pieces and incubated in complete RPMI 1640 medium (supplemented with 10% fetal calf serum, penicillin/streptomycin, L-glutamine, sodium-pyruvate and HEPES buffer, all from Sigma-Aldrich) containing 140 U/ml collagenase type IV (Sigma-Aldrich) for 90 minutes at 37°C, 5% CO₂. DNase I (Sigma-Aldrich) was added to the cell suspensions, at a final concentration of 200 U/ml, during the last 10 minutes of the incubation. The digested lung tissue was then passed through steel mesh cup sieve (Sigma-Aldrich). Any remaining erythrocytes were lysed using a lysis buffer (H₂O, 0.15 M NH₄Cl, 1 mM KHCO₃, 0.1 mM NaEDTA, pH 7.2-7.4), washed and resuspended in RPMI 1640 medium. The cell suspension was passed through a 70-µm cell strainer (BD Falcon), washed and resuspended in complete RPMI 1640 medium.

BAL was collected from euthanized BALB/c mice by delivering 1.5 ml of PBS through the tracheal tube using a 18 gauge needle. The fluid was gently drawn back immediately after delivery. The cells in 0.75-1.2 ml of BAL were collected by centrifugation, counted and analyzed by flow cytometry.

Single-cell suspensions were obtained from PLN using collagenase type IV and DNase I as described above. The PLN were then disaggregated using the frosted ends of two glass slides, washed and resuspended in complete RPMI 1640 medium.

Total viable cells were enumerated using a hemocytometer and trypan blue exclusion of dead cells.

Primary AEC and monocyte in vitro co-culture

Primary AEC, containing both type I and type II AEC, were enriched from naive donor mice as described by Chuquimia et al [27]. First, the lungs were perfused with RPMI medium to remove red blood cells, followed by installation of dispase (Gibco-Invitrogen) into the lungs via the trachea. The lungs were then removed and digested using dispase for 45 minutes at RT. The single-cell suspension that was obtained by loosening the parenchymal tissue was treated with DNase I (Sigma) for 30 minutes at RT, and passed through 70 µm and 40 µm cell strainers. Remaining RBC were lysed as described

above. To obtain AEC, the cell suspension was then depleted of CD45⁺ and CD146⁺ cells using magnetic cell sorting with LD separation columns (Miltenyi Biotec). Enriched AEC (5×10⁴ cells/well) were cultured in complete RPMI 1640 medium at 37°C, 5% CO₂ for two days. Non-adherent cells were removed before primary bone marrow monocytes were added in complete RPMI 1640 medium at a monocyte/AEC-ratio of 5:1. In some experiments, primary WT or TLR4^{-/-} monocytes were cultured with AEC-derived media (1/2 final dilution) obtained from untreated, or LPS-stimulated AEC as described previously [28]. Monocyte differentiation was examined after 3-10 days as indicated.

A commercially available ELISA kit (R&D Systems) was used according to the manufacturer's instructions to determine the GM-CSF-levels in unstimulated AEC culture supernatants.

Flow cytometry

Staining for surface markers was done by resuspending 2×10⁶ cells in FACS buffer (PBS with 1% (w/v) BSA and 2 mM NaN₃). The cells were incubated with purified anti-mouse CD16/CD32 (2.4G2, BD Pharmingen) at 10 µg/ml for 15 min at 4°C to block nonspecific binding. The cells were washed and incubated for 15 minutes at 4°C with primary mAbs, or appropriate isotype control mAbs, diluted in FACS buffer. The anti-CD103 (M290)-PE and anti-CD45.1 (A20)-FITC mAbs were purchased from BD Biosciences. Streptavidin-Pacific Orange was purchased from Invitrogen. The following PE-, PE-Cy5.5-, PE-Cy7, APC-, AlexaFluor 700-conjugated or biotinylated anti-mouse mAbs were purchased from eBioscience: anti-CD45.2 (104), anti-CD11c (N418), anti-CD11b (M1/70), anti-CD19 (1D3). Anti-I-A/I-E-PerCP (M5/114.15.2) was purchased from Biolegend. Stained cells were washed and fixed in freshly prepared 2% paraformaldehyde in PBS for 2h at 4°C. Fixed cells were washed and resuspended in FACS buffer before analysis.

For detection of iNOS-producing cells, the fixed cells were permeabilized for 30 minutes at RT using a Cytofix/Cytoperm™ kit from BD Biosciences. Intracellular iNOS was detected using an unconjugated anti-iNOS-mAb (clone 6, BD Transduction Laboratories) coupled to the Zenon complex-Alexa Fluoro 647 (Invitrogen) according to the manufacturer's instructions, and incubated for 30 minutes at RT. Specific iNOS-staining was compared to a relevant isotype control mAb (BD Transduction Laboratories). Stained cells were washed and analyzed immediately by flow cytometry.

The cells were collected using a BD LSR II or a BD FACSCanto (BD Biosciences) and analyzed using FlowJo software (version 8.8.6, Tree Star). All gates and quadrants were set after relevant isotype control mAbs.

In vitro stimulation of lung cells and intracellular cytokine staining

Single cell suspensions were prepared from *M. tuberculosis*-infected mice and kept in complete RPMI 1640 medium, or stimulated with 100 ng/ml *E. coli* LPS (Sigma-Aldrich) or 10 µg/ml *M. tuberculosis* cell wall extract (prepared as previously described [16]) in the presence of 10 µg/ml Brefeldin A (Sigma-Aldrich) for 5h at 37°C, 5% CO₂.

Adherent cells were detached by incubating the cells in PBS, 2 mM EDTA, for 10 minutes at 37°C, 5% CO₂. The cells were stained for the indicated cell surface markers, fixed in 2% paraformaldehyde, permeabilized and stained for the intracellular cytokines IL-10-FITC (JES5-16E3, eBioscience) and IL-12-APC (C15.6, BD Bioscience) or relevant isotype control mAbs. Stained cells were washed twice in permeabilization buffer and once with FACS buffer and analyzed immediately.

Results

Primary AEC support monocyte survival and differentiation in vitro

Because myeloid cells reside in close proximity to AEC we investigated if AEC, or AEC-derived soluble factors, support monocyte differentiation in vitro. Primary monocytes and AEC were purified as previously described and co-cultured in vitro for three, six or ten days as outlined in Materials and Methods (figure 1) [3,27]. Alternatively, primary WT or TLR4^{-/-} monocytes were cultured alone in AEC-conditioned media from untreated AEC, or from LPS-stimulated AEC, respectively (data not shown). The supernatant from untreated AEC contain detectable amounts of several cytokines and chemokines, for example GM-CSF and MCP-1 [27]. After 24 h, we detected 464 pg/ml of GM-CSF in the supernatants from unstimulated AEC used in this study. The range and the amounts of the various soluble factors produced by AEC is markedly increased after LPS stimulation. For example, LPS increases GM-CSF production twofold [27]. In contrast, the M-CSF levels were undetectable by ELISA in the supernatants from unstimulated and from LPS-stimulated AEC [27].

Ly6C⁺ bone marrow monocytes have the same cell surface phenotype as inflammatory monocytes in circulation and were used in the in vitro co-culture experiments, and in the adoptive transfer experiments described below, as a substitute for Ly6C⁺ inflammatory monocytes in peripheral blood [3,5]. Primary monocytes enriched from the bone marrow also express CD11b, but lack expression of CD11c, MHC class II and CD103 (Figure 1A and data not shown) [3]. Monocytes cultured in media alone did not survive, and preliminary data suggests that monocytes cultured in media supplemented with either AEC supernatant did not change CD11c, MHC class II or CD103 cell surface expression (data not shown). In contrast, monocytes cultured in contact with primary AEC upregulated low levels of CD11c within three days (Figure 1B). The percentage of CD11c⁺ cells and the CD11c surface expression levels remained constant during the whole experiment. We also investigated CD11b⁺CD11c⁺ and CD11b⁺CD11c⁻ monocyte-derived cells for MHC class II and Ly6C cell surface expression (Figure 1B). While CD11b⁺CD11c⁻ cells remained MHC class II⁻, CD11b⁺CD11c⁺ cells expressed low levels of MHC class II. We also observed that CD11b⁺CD11c⁺ cells expressed lower levels of Ly6C than CD11b⁺CD11c⁻ cells. Even though the latter population did not upregulate CD11c or MHC class II, the fraction of Ly6C-expressing cells decreased from around 50% to approximately 20% by day 10, suggesting a more differentiated phenotype. Finally, we did not detect CD103

expression by any myeloid cell subset in the in vitro co-cultures (data not shown).

To the best of our knowledge it has not previously been shown that primary AEC interaction with primary monocytes in vitro support monocyte survival and differentiation without the addition of exogenous factors.

Recruited monocytes differentiate into lung αE-DC during pulmonary TB

Several lung Mφ and DC subsets originate from monocytes recruited into the inflamed lung tissue from peripheral blood [3]. To determine whether recruited monocytes are precursor cells to lung αE-DC during pulmonary TB and contribute to the increase in cell numbers in response to infection we took advantage of a monocyte adoptive transfer model using enriched primary bone marrow monocytes from naïve donor mice [3,16].

We have previously observed that a monocyte-derived CD11b⁺CD11c⁺ population expressing high levels of MHC class II start to appear in *M. tuberculosis* infected lungs around day six after monocyte adoptive transfer. This myeloid cell subset lacked cell surface expression of typical Mφ markers [3]. We therefore waited 10 days before we analyzed the recipient mice for monocyte-derived cells (Figure 2). Recipient cells were identified based on CD45.1 cell surface expression. The CD45.1^{high} lung cells are mostly autofluorescent alveolar Mφ and were excluded in the analysis to enable easy identification of αE-DC. Donor cells were identified based on CD45.2 cell surface expression compared to an isotype control mAb (Figure 2A). The CD11b/CD11c cell surface expression profile of endogenous and monocyte-derived cells enabled us to identify several myeloid cell subsets [3,29]. The various subsets were then analyzed further based on Ly6C, MHC class II and CD103 expression. The CD11b⁺CD11c⁻ subset contains a significant proportion of Ly6C⁺ cells expressing low levels of MHC class II and few CD103⁺ cells, and is a mixture of monocytes and small Mφ [3,29]. In addition, the endogenous CD11b⁺CD11c⁻ cell population also contained granulocytes [3,29]. Recruited monocytes rapidly upregulate CD11c in *M. tuberculosis*-infected lung tissue [3]. The CD11b⁺CD11c^{intermediate} population contains few Ly6C⁺ cells, but a higher percentage of MHC class II⁺ cells compared to the CD11b⁺CD11c⁻ subset. CD11b⁺CD11c^{intermediate} cells do not express CD103 and are monocytes and small Mφ [3,29]. In contrast to monocytes differentiating in uninfected lung tissue, monocytes in *M. tuberculosis*-infected lungs form a large fraction of CD11b⁺CD11c⁺ cells. This subset has downregulated Ly6C, contain a high percentage of MHC class II⁺ cells, but no CD103⁺ cells. The CD11b⁺CD11c⁺ subset contain both activated iNOS⁺ Mφ, and DC [3,29]. Finally, endogenous CD11b⁺CD11c⁺ cells contain a fraction of autofluorescent alveolar Mφ and CD103⁺ αE-DC [15,29]. Both subsets lack expression of Ly6C, but αE-DC express higher cell surface levels of MHC class II. Recruited monocytes also give rise to CD11b⁺CD11c⁺ cells that are Ly6C⁻, CD103⁺ and express high levels of MHC class II, i.e. αE-DC (Figure 2). It is noteworthy that CD11b⁺CD11c⁺ cells are the only myeloid subset containing a significant proportion of CD103⁺ cells. At present, it is not known if the monocyte-

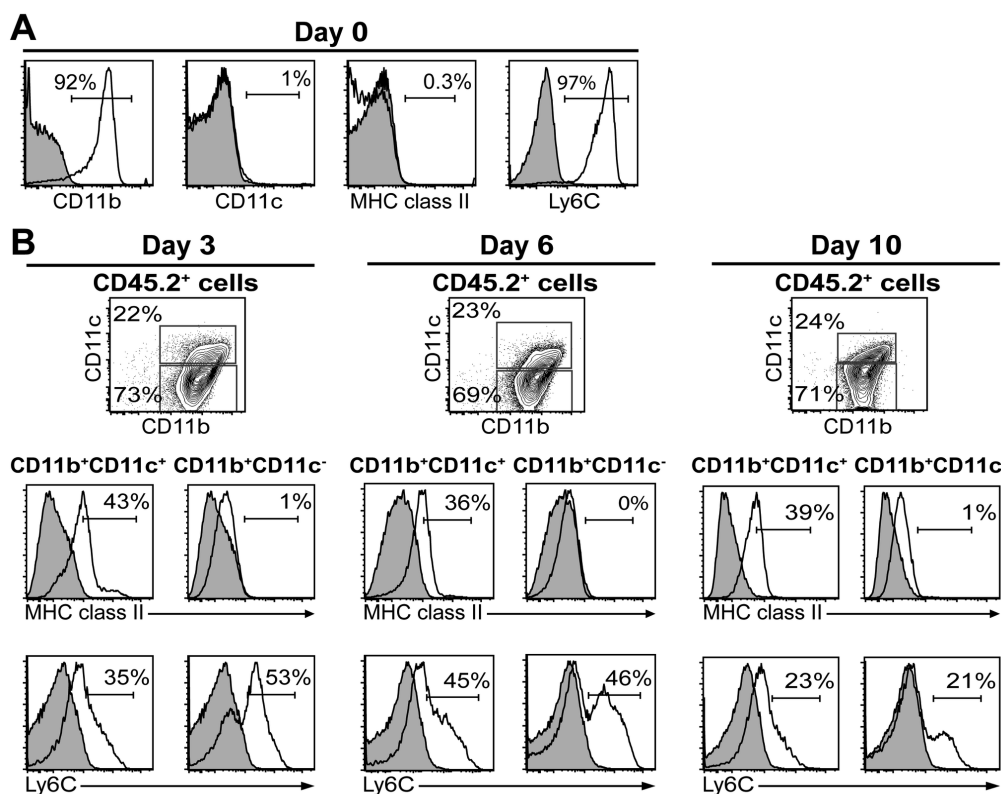


Figure 1. Primary monocytes survive and differentiate when cultured with AEC in vitro. Primary monocytes and AEC were enriched from naive donor mice and co-cultured for three, six or ten days. (A) The histograms show the phenotype of the enriched monocytes used in the co-culture experiments. (B) The cells were harvested at the indicated timepoints and stained for cell surface markers. Cultured myeloid cells were identified based on CD45.2 cell surface expression (data not shown) and analyzed for CD11b and CD11c expression (upper panels). The lower panels display MHC class II and Ly6C cell surface expression (open histograms) on gated CD11b⁺CD11c⁺ and CD11b⁺CD11c⁻ monocyte-derived cells. Filled histograms show isotype control stainings. One representative experiment out of three separate experiments is shown.

doi: 10.1371/journal.pone.0069287.g001

derived CD11b⁺CD11c⁺CD103⁺ population contains alveolar Mφ in the *M. tuberculosis*-infected lungs.

Our results show for the first time that recruited inflammatory monocytes can differentiate into CD11b⁺CD11c⁺Ly6C⁺CD103⁺MHC class II⁺ αE-DC in the lung tissue during pulmonary TB.

Recruited monocytes give rise to αE-DC in lymph nodes draining the lung tissue during TB

Similar to the lungs, inflammatory monocytes contribute to several myeloid cell subsets in the PLN following *M. tuberculosis* infection [3]. We used our monocyte adoptive transfer model to determine if αE-DC in the PLN are monocyte-

derived during pulmonary TB (Figure 3). Similar to the lung tissue, the CD11b/CD11c expression profile was used to divide the myeloid cell compartment into three subsets (Figure 3A). We then compared CD45.1⁺ endogenous cells and CD45.2⁺ transferred cells in infected recipient mice. The only endogenous myeloid cell subset that contained a significant proportion of CD103⁺ cells did not express CD11b but was CD11c⁺. The CD11b⁺CD11c⁺CD103⁺ cells were Ly6C⁺ and MHC class II^{high} (Figure 3B).

Approximately one third of the recruited monocytes were CD11b⁺CD11c⁺ on day 10 after adoptive transfer (Figure 3A). This subset was CD103⁺; most cells expressed Ly6C⁺ and low cell surface levels of MHC class II compared to isotype control

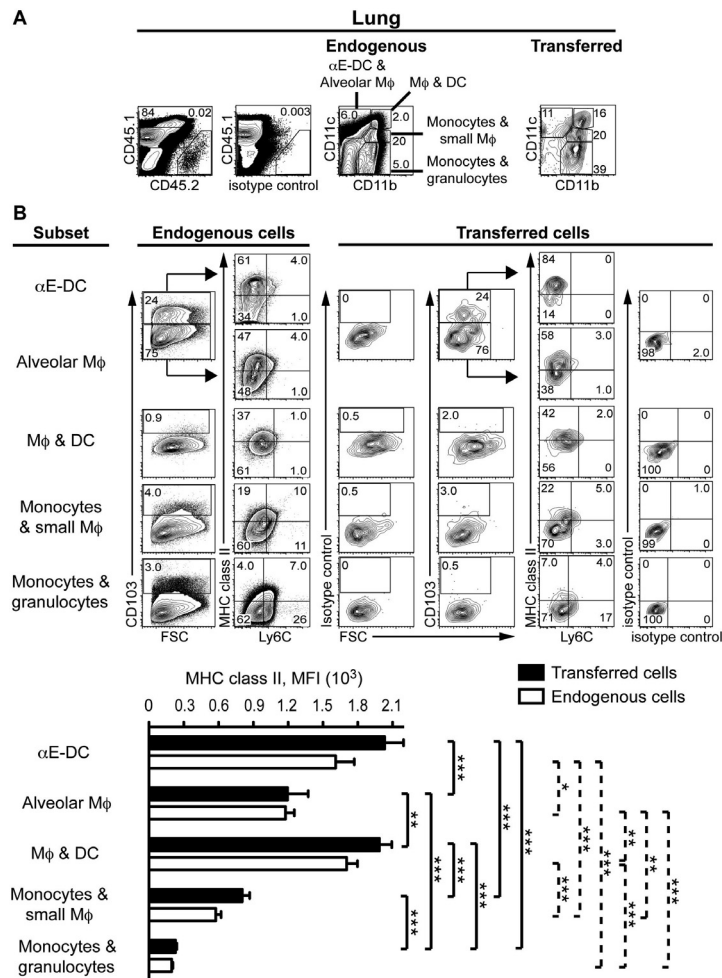


Figure 2. Recruited inflammatory monocytes differentiate into lung α E-DC during pulmonary TB. Monocytes enriched from naive CD45.2⁺ C57BL/6 mice were adoptively transferred into *M. tuberculosis*-infected CD45.1⁺ congenic recipient mice (three weeks p.i.). Endogenous and transferred cells in lung tissue were identified and analyzed 10 days later. (A) Donor cells were identified based on CD45.2 expression compared to an isotype control mAb (left panels). Several myeloid cell subsets were then identified in gated CD45.1⁺ endogenous and CD45.2⁺ transferred cells based on the CD11b and CD11c expression profile (right panels). Endogenous α E-DC and alveolar M ϕ were identified among CD11b⁺CD11c⁺ cells, while CD11b⁺CD11c⁺ cells contain M ϕ and DC. Endogenous CD11b^{intermediate}CD11c^{intermediate} cells are monocytes and small M ϕ , and endogenous CD11b⁺CD11c⁺ cells contain monocytes and granulocytes. The corresponding myeloid subsets were identified among transferred cells. (B) Each myeloid subset was analyzed for CD103, Ly6C and MHC class II cell surface expression. CD103-expressing Ly6C⁺MHC class II⁺ α E-DC were identified in the CD11b⁺CD11c⁺ gate among both endogenous and transferred cells (upper panels). The graph displays MHC class II cell surface expression levels (mean \pm SEM) on gated transferred and endogenous cells. *, $p < 0.05$; **, $p < 0.01$; ***, $p < 0.001$ by one-way ANOVA with Bonferroni posttest. Solid lines denote comparisons between transferred cells and dotted lines denote comparisons between endogenous cells. Monocyte differentiation in *M. tuberculosis*-infected recipient mice was analyzed in two separate experiments with five recipient mice in each experiment.

doi: 10.1371/journal.pone.0069287.g002

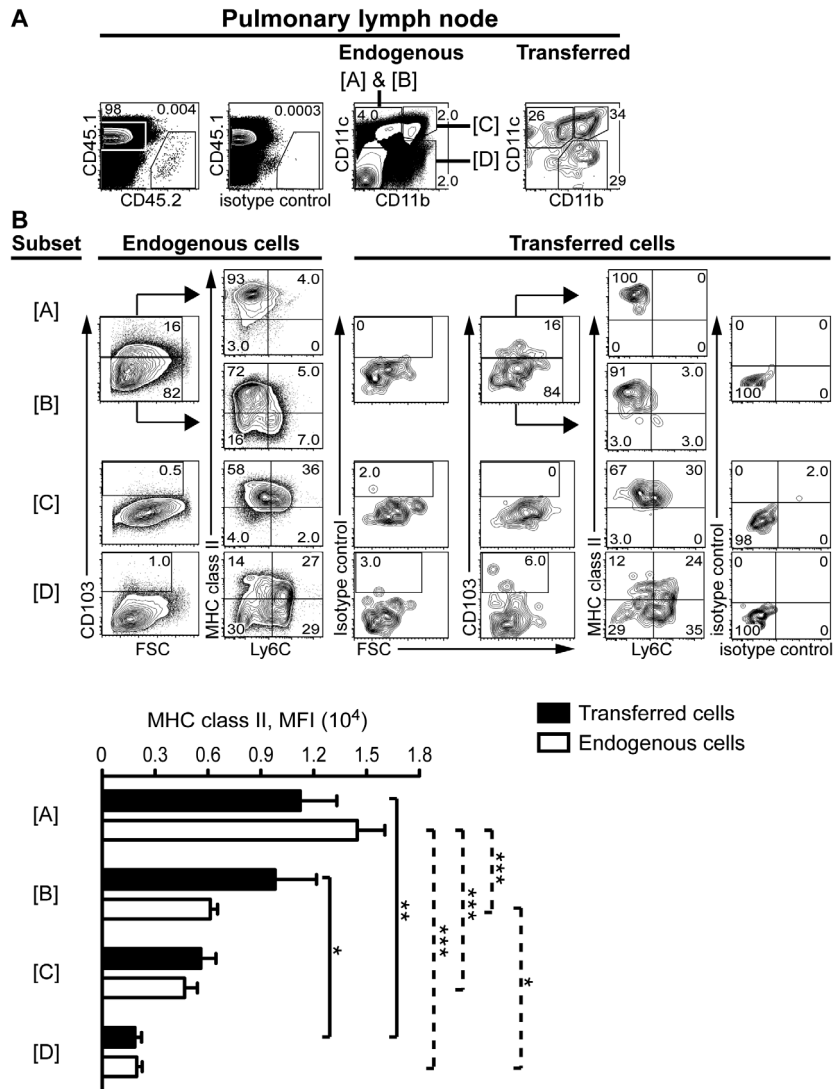


Figure 3. Recruited inflammatory monocytes give rise to α E-DC in the draining PLN during TB. (A) Primary monocytes were adoptively transferred and identified in infected recipient mice as described in Figure 1 (upper left panels). The myeloid cell subsets were identified based on CD11b and CD11c expression profile (labeled [A]-[D], upper right panels). (B) The myeloid cell subsets were analyzed further for CD103, Ly6C and MHC class II cell surface expression. CD103-expressing Ly6C-MHC class II⁺ α E-DC were found within the CD11b⁺CD11c⁺ population (upper panels). The graph shows MHC class II cell surface expression levels (mean \pm SEM) on gated transferred and endogenous cells. The graph shows MHC class II cell surface expression levels (mean \pm SEM) on gated transferred and endogenous cells. *, $p < 0.05$; **, $p < 0.01$; ***, $p < 0.001$ by one-way ANOVA with Bonferroni posttest. Solid lines denote comparisons between transferred cells and dotted lines denote comparisons between endogenous cells. Monocyte differentiation in *M. tuberculosis*-infected recipient mice was analyzed in two separate experiments with five recipient mice in each experiment.

doi: 10.1371/journal.pone.0069287.g003

mAbs (Figure 3B). One third of the monocyte-derived cells were CD11b⁺CD11c⁺ that did not express CD103, expressed low levels of Ly6C and were MHC class II⁺ (Figure 3). This subset contains myeloid DC and MAC-3⁺ iNOS-producing cells [2,3]. Finally, one third of the monocyte-derived cells expressed CD11c, but not CD11b (Figure 3A). CD103⁺ cells were identified in this CD11b⁺CD11c⁺ subset that were Ly6C⁺ and expressed high cell surface levels of MHC class II (Figure 3B).

Our original finding shows that inflammatory monocytes can give rise to α E-DC that appear in the PLN draining the lung tissue during pulmonary TB.

α E-DC localize beneath the bronchial epithelial cell layer and near the vascular wall in *M. tuberculosis*-infected lungs

Sung et al first identified murine α E-DC in the lung tissue, and showed that α E-DC localize near the basal surface of bronchial epithelial cells and in close proximity to vascular endothelial cells [15]. To confirm the tissue localization of α E-DC in naïve mice, we used the co-expression pattern of CD103 and MHC class II as a criterion to distinguish α E-DC from other lymphoid and myeloid cell subsets in lung tissue sections (Figure 4). As expected CD103⁺MHC class II⁺ α E-DC localize in close proximity to the basolateral side of the bronchial epithelial cell layer in naïve mouse lungs. Also, CD103⁺MHC class II⁺ α E-DC were identified close to the arterial wall (Figure 4A).

We have shown that the functional potential of α E-DC was preserved during early and chronic *M. tuberculosis* infection [16]. Since the localization near the bronchial epithelium may contribute to α E-DC function during TB, we determined if α E-DC tissue localization change in response to *M. tuberculosis* infection. Figure 4B identifies CD103⁺ MHC class II⁺ α E-DC in *M. tuberculosis*-infected lungs three weeks p.i. At this timepoint, the absolute number of lung α E-DC increases almost 15-fold in resistant C57BL/6 and BALB/c mice in response to *M. tuberculosis* infection compared to naïve animals [16]. Similar to naïve mice, α E-DC localize near the basolateral side of the bronchial epithelium and close to the arterial vasculature in *M. tuberculosis*-infected mice.

α E-DC localization near the airways during TB prompted us to investigate if α E-DC were detected in BAL fluid collected from naïve or *M. tuberculosis*-infected BALB/c mice (Figure 4C). Most cells in the BAL from naïve mice were CD11b⁺CD11c⁺CD103⁺ alveolar M ϕ while α E-DC were essentially undetectable. While the absolute number of total BAL cells increased 17-fold by week 18 p.i., the absolute number of alveolar M ϕ remained unchanged. We also observed that most alveolar M ϕ upregulated MHC class II during TB. In response to *M. tuberculosis* infection α E-DC were detectable in the BAL, but remained a minor cell subset in the BAL fluid (Figure 4C).

In conclusion, while *M. tuberculosis* infection increases the absolute number of lung α E-DC, it does not influence α E-DC tissue localization in the infected lungs with the exception of the BAL fluid, in which the absolute number of α E-DC increased in response to infection. The constant localization next to the bronchial epithelium in naïve and infected mice may help explain the conserved functional potential of α E-DC during TB.

A minor fraction of α E-DC is infected with *M. tuberculosis* in vivo

Multiple myeloid cell subsets are infected with *M. tuberculosis* following aerosol infection [2]. Since DC have been implicated in mycobacterial dissemination from the lungs to the draining PLN, we investigated if α E-DC are targeted by *M. tuberculosis* in vivo [2,30]. Three weeks p.i. at the peak of the immune response, CD11b⁺CD11c⁺ cells have been shown to be the main target of *M. tuberculosis* in the infected lungs [2]. We used GFP-expressing virulent *M. tuberculosis* strain H37Rv to identify infected myeloid cells, and cells isolated from animals infected with the GFP⁺ *M. tuberculosis* strain Harlingen as a negative control for the gating strategy (figures 5–7). We confirmed that a large fraction of the CD11b⁺CD11c⁺ lung cells are *M. tuberculosis*-infected (Figure 5A). However, the CD11b⁺CD11c⁺ population contained the highest frequency of infected cells. This population of infected cells was MHC class II negative (see Figure 7), but with the current cell surface staining strategy we cannot determine if the cells are infected monocytes or neutrophils [2,3]. Finally, around two percent of infected myeloid lung cells were CD11b⁺CD11c⁺, which include both alveolar M ϕ and α E-DC (Figure 5A).

In agreement with previous observations made three weeks p.i., we found that CD11b⁺CD11c⁺ myeloid DC contain the highest frequency of *M. tuberculosis*-infected cells in the draining PLN (Figure 5A) [2]. We also observed that $12.1 \pm 1.7\%$, $n = 9$ [mean \pm SD] of CD11b⁺CD11c⁺ cells are infected in the PLN. Compared to the lung tissue, the frequency and absolute number of infected cells was approximately 10-fold lower in the PLN (Figure 5A).

Based on morphology, cell surface phenotype and functional potential, CD11b⁺CD11c⁺ cells in *M. tuberculosis*-infected lungs contain both DC and activated M ϕ [3,29]. Also, infected lung cells have been shown to express iNOS, even though the majority of infected cells remained iNOS negative [31]. Using GFP-expressing *M. tuberculosis*, we were able to further delineate the functional potential of infected CD11b⁺CD11c⁺ lung cells (Figure 5B). On average, 20.1% of infected CD11b⁺CD11c⁺ lung cells co-expressed iNOS, supporting the idea that this myeloid cell subset contain infected and activated M ϕ [3]. Our results also show that most iNOS-producing CD11b⁺CD11c⁺ lung cells are not infected with *M. tuberculosis* (Figure 5B).

In figure 6 we investigate if α E-DC are infected with *M. tuberculosis* at week three p.i. Only $0.15 \pm 0.088\%$, $n = 16$ [mean \pm SD] appeared to be infected. As in Figure 5, we compared mice infected with GFP-expressing H37Rv with the GFP-negative strain Harlingen. In comparison $0.54 \pm 0.30\%$, $n = 16$ [mean \pm SD] of CD103⁺CD11b⁺CD11c⁺ cells that contain alveolar M ϕ were infected. Enumeration of infected α E-DC confirms that this DC population is not a major target for the bacterium at this stage of the disease. For comparison, we included the total number of infected iNOS⁺ and iNOS⁺ CD11b⁺CD11c⁺ myeloid cells in the bar graph in Figure 6B. Both CD11b⁺CD11c⁺ cell subsets are to a larger extent than α E-DC infected with *M. tuberculosis* three weeks p.i.

Our results clearly show that virulent *M. tuberculosis* preferentially infects certain myeloid cell subsets that localize in the lungs or in the PLN, while other myeloid cells, including α E-

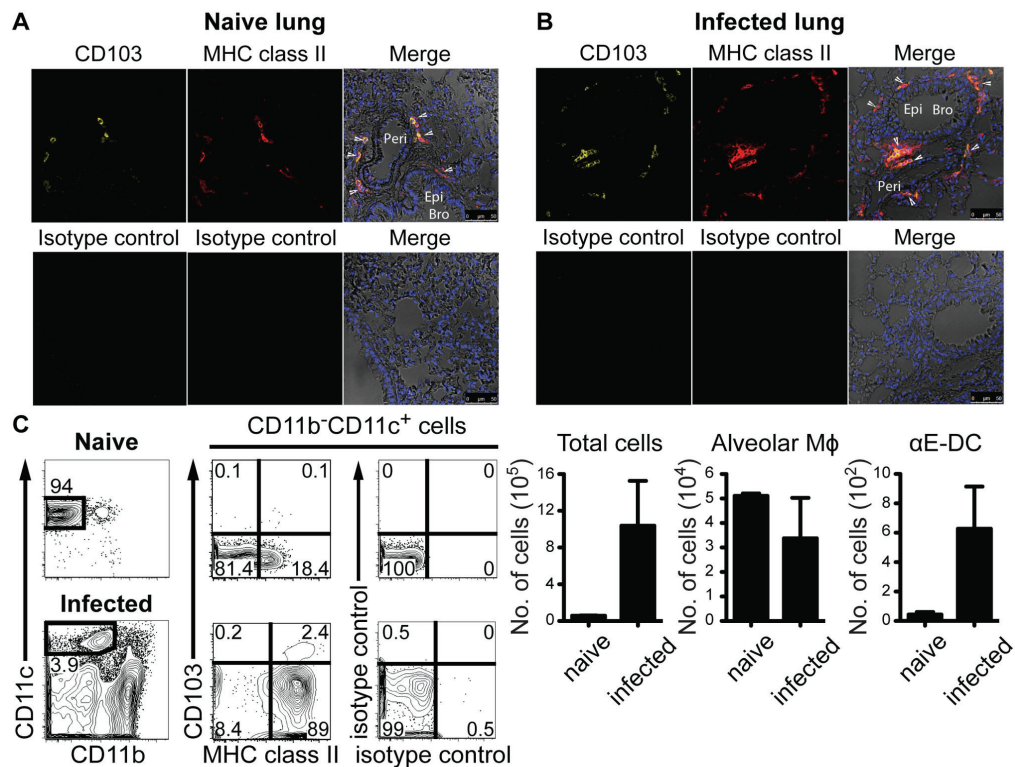


Figure 4. Tissue localization of lung αE-DC in uninfected mice and during pulmonary TB. Fixed lung tissue sections from C57BL/6 mice were stained with DAPI, and with CD103 and MHC class II mAbs, or isotype controls, to identify DAPI⁺ CD103⁺ MHC class II⁺ αE-DC in uninfected (A) or *M. tuberculosis*-infected (three weeks p.i.) (B) lungs. Arrowheads indicate the localization of some lung αE-DC. αE-DC localization in the lungs was determined in five separate experiments. Peri = Perivascular wall, Epi = Epithelium, Bro = Bronchus. (C) The contour-plots show identification of CD11b⁺ CD11c⁺ cells (pre-gated on CD45.2⁺ CD19⁻ cells, data not shown) in BAL collected from 10 pooled uninfected (upper panels) BALB/c mice, or a *M. tuberculosis*-infected (18 weeks p.i., lower panels) BALB/c mouse. Gated CD11b⁺ CD11c⁺ cells were analyzed further for CD103 and MHC class II cell surface expression. The graphs display the absolute number of cells (mean ± SD) in BAL fluid from uninfected and infected animals. Alveolar Mφ and αE-DC in BAL were examined in two separate experiments.

doi: 10.1371/journal.pone.0069287.g004

DC, remain essentially uninfected despite the localization near the airways.

***M. tuberculosis*-infected myeloid cells in the lungs do not down-regulate MHC class II cell surface expression**

We took advantage of the GFP-expressing *M. tuberculosis* to determine if infected myeloid cells in the lungs expressed lower cell surface levels of MHC class II. Using the same gating strategy as in Figure 2, we identified myeloid cell subsets containing αE-DC/alveolar Mφ, DC/Mφ, monocytes/small Mφ, and monocytes/granulocytes (Figure 7). Within each subset we distinguished between GFP⁻ uninfected cells and GFP⁺ infected

cells and determined the mean fluorescence intensity (MFI) of the MHC class II cell surface expression. We did not detect any significant difference in MHC class II expression levels between uninfected and *M. tuberculosis*-infected cells three weeks post aerosol infection with virulent mycobacteria (Figure 7).

Lung αE-DC contain the highest frequency of IL-12p40-producing cells in response to *M. tuberculosis* infection

Since protective immunity against *M. tuberculosis* is dependent on IL-12p40 production [20], we wanted to

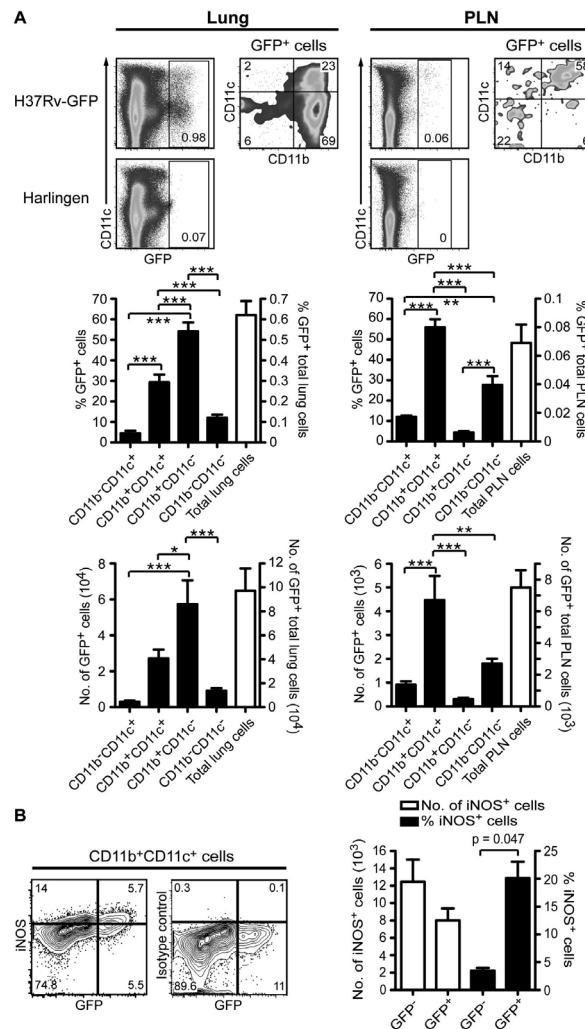


Figure 5. Infected myeloid cells during pulmonary TB. C57BL/6 mice were infected with *M. tuberculosis* (strain H37Rv-GFP, or strain Harlingen) via the respiratory route. Three weeks p.i., total lung and PLN cell suspensions were stained for cell surface markers and infected cells were identified based on GFP expression (pre-gated on CD45.2⁺ CD19⁻ cells, data not shown). (A) The contour plots show identification of H37Rv-GFP-infected cells in the lungs (left panels) and in the PLN (right panels). For comparison, the lower plots display lung- and PLN cells infected with *M. tuberculosis* strain Harlingen. The bar graphs display the percentage and absolute number of infected total cells and defined cell subsets in the lungs (left panels) and in the PLN (right panels). The graphs display mean \pm SEM. *, $p < 0.05$; **, $p < 0.01$; ***, $p < 0.001$ by one-way ANOVA with Bonferroni posttest. (B) The contour plot shows iNOS- and GFP-expression in gated CD11b⁺CD11c⁺ lung cells (left panel). The iNOS staining was compared to an isotype control mAb (right panel) and GFP-expression was compared to Harlingen-infected lung cells (data not shown). The bar graph displays the absolute number and the percentage of iNOS⁺ CD11b⁺CD11c⁺ cells (mean \pm SEM). iNOS-expression is compared in uninfected (GFP⁻) and infected (GFP⁺) cells. A *t* test was used to determine statistical difference between uninfected and infected cells. Infected cells were analyzed in four separate experiments.

doi: 10.1371/journal.pone.0069287.g005

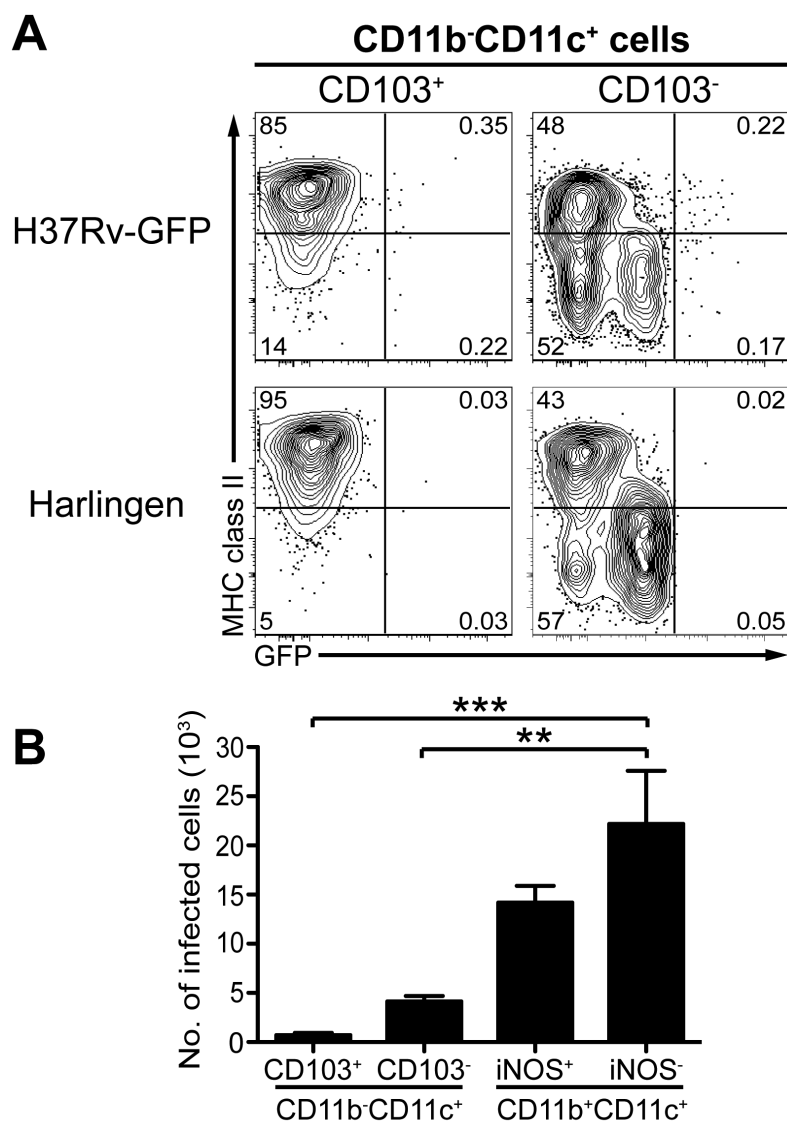


Figure 6. Few *M. tuberculosis*-infected lung αE-DC in vivo. C57BL/6 mice were infected with *M. tuberculosis* strain H37Rv-GFP, or strain Harlingen. αE-DC and alveolar Mφ were identified in infected lungs three weeks p.i. in the CD11b⁺CD11c⁺ gate as described in Figure 2. (A) The contour plots show GFP- and MHC class II expression by lung αE-DC and alveolar Mφ from mice infected with H37Rv-GFP (upper panels) or Harlingen (lower panels). The quadrants were set after a relevant isotype control mAb (not shown) and after the GFP⁺ mycobacteria. (B) The graph shows the absolute number of infected αE-DC and alveolar Mφ three weeks p.i., as well as the absolute number of infected cells among iNOS⁺ and iNOS⁻ CD11b⁺CD11c⁺ cells. The graphs display mean ± SEM. **, p<0.01; ***, p<0.001 by one-way ANOVA with Bonferroni posttest. *M. tuberculosis* infection of lung αE-DC was determined in four independent experiments.

doi: 10.1371/journal.pone.0069287.g006

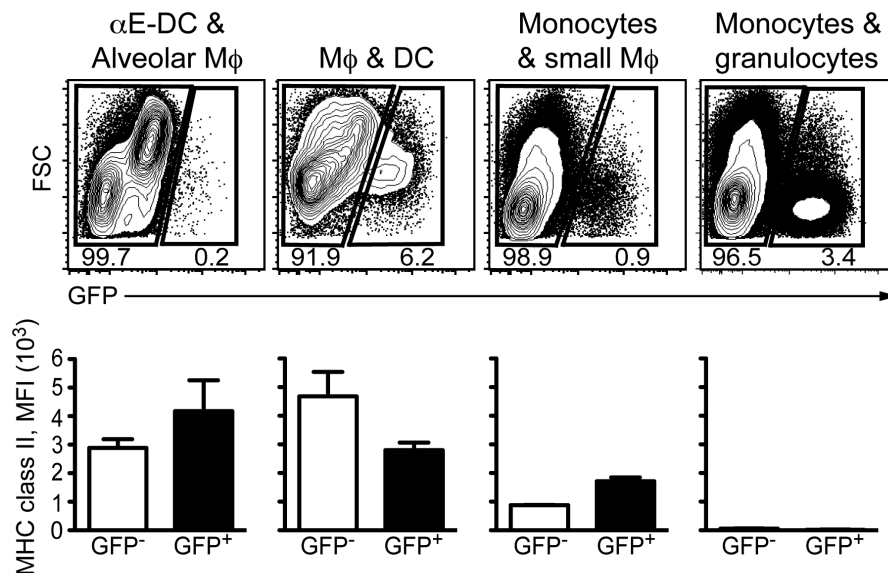


Figure 7. MHC class II expression levels on *M. tuberculosis*-infected myeloid cells. C57BL/6 mice were infected with *M. tuberculosis* H37Rv-GFP via the respiratory route and the indicated myeloid cell subsets were identified in infected lungs as described in Figure 1. Based on GFP expression, uninfected (GFP⁻) and infected (GFP⁺) cells were further analyzed for MHC class II cell surface expression levels. A *t* test was used to determine statistical difference between uninfected and infected cells. One representative experiment out of four separate experiments is shown.

doi: 10.1371/journal.pone.0069287.g007

determine the main source of IL-12p40 in the *M. tuberculosis*-infected lungs three to six weeks p.i. (Figure 8). The single cell suspensions prepared from total lung tissue were kept in media alone, or stimulated with LPS or *M. tuberculosis* cell wall extract. The main myeloid cell subsets were then identified as described in Figure 2 and we determined the frequency and the absolute number of IL-10 and IL-12p40-producing cells (Figure 8).

αE-DC, alveolar Mφ and CD11b⁺CD11c⁻ monocytes/granulocytes were essentially negative for IL-10. In contrast, CD11b⁺CD11c⁺ Mφ/DC and CD11b^{intermediate}CD11c^{intermediate} monocytes/small Mφ did contain detectable IL-10-producing cells, especially after LPS stimulation (Figure 8B).

Strikingly, αE-DC contained a significantly higher percentage of IL-12p40-producing cells compared to all other myeloid cell subsets, irrespective if the cells were kept in media alone, stimulated with LPS or the *M. tuberculosis* cell wall extract ($p < 0.001$ by one-way ANOVA with Bonferroni posttest) (Figure 8B). *M. tuberculosis* cell wall extract stimulation did not significantly increase the frequency of IL-12p40 producing αE-DC, alveolar Mφ or Mφ/DC. By comparison, LPS stimulation lead to an increased percentage of IL-12p40⁺ cells in all three subsets. After αE-DC, CD11b⁺CD11c⁺ Mφ/DC contained the highest percentage of IL-12p40⁺ cells. We also found that IL-10

and IL-12p40 were mainly produced by separate CD11b⁺CD11c⁺ cell subsets (Figure 8A).

In summary, we extend our previous findings on the cytokine profile of αE-DC during pulmonary TB and show that αE-DC are potent IL-12p40-producing, but not IL-10-producing cells in the *M. tuberculosis*-infected lungs [16].

Discussion

Non-hematopoietic cells are posed to influence the outcome of *M. tuberculosis* infection [32]. Given that stromal cells, including lung epithelial cells, shape the DC phenotype [33–35], and considering the unique functional potential of αE-DC in *M. tuberculosis*-infected lungs [16], we determined the tissue localization of lung αE-DC in infected mice to be in close proximity to the bronchial epithelial cell layer and vascular wall, similar to lung αE-DC localization in uninfected lungs (Figure 4) [15]. We also detected an increased number of αE-DC in the BAL fluid from *M. tuberculosis*-infected mice similar to what has been described in the BAL from mice exposed to cigarette smoke [36]. Our original observation was that monocytes recruited into *M. tuberculosis*-infected lungs differentiate into CD11b⁺CD11c⁺ cells 6–10 days after cell transfer [3]. The differentiated cells lacked expression of typical Mφ cell surface markers and in the present study we have shown that this

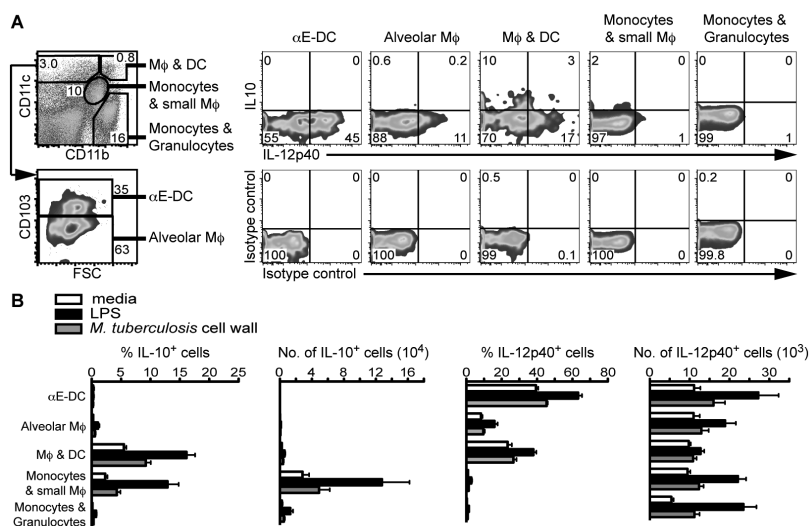


Figure 8. Lung αE-DC produce IL-12p40 during pulmonary TB. C57BL/6 mice were infected with a low dose of *M. tuberculosis* via the respiratory route. Three p.i., total lung cells were kept in media, or stimulated with LPS or *M. tuberculosis* cell wall extract and analyzed for intracellular IL-10 and IL-12p40. (A) The cell surface was stained for CD45.2 and CD19 (data not shown), and CD11b, CD11c and CD103. IL-10 and IL-12p40 production was compared between αE-DC, alveolar Mφ, the subset containing both activated Mφ and DC, and monocytes and granulocytes. The plots show *M. tuberculosis* cell wall extract-stimulated infected lung cells from one representative experiment. (B) The bar graphs show the percentage and absolute number of IL-10 and IL-12p40-producing myeloid cells three to six weeks p.i. IL-10 and IL-12p40 production by αE-DC was determined in two separate experiments with 2–3 mice per group in each experiment. The results have been pooled from all replicate experiments. The graphs display mean ± SEM.

doi: 10.1371/journal.pone.0069287.g008

population contain monocyte-derived αE-DC (Figure 2). The late appearance of monocyte-derived αE-DC compared to other DC and Mφ subsets was a puzzling observation, but may reflect the need for the recruited monocytes to localize in close proximity to, and interacting with, bronchial epithelial cells expressing E-cadherin on the basolateral side [37,38]. The airway epithelium can produce soluble factors that influence DC recruitment. For example, CCL2 and CCL20 production by airway epithelial cells may help specify the tissue localization of CCR2⁺ monocytes, or immature DC during inflammatory conditions [39,40]. Lung epithelial cells may also provide imprinting signals and contribute to the functional potential of DC in the inflamed lungs, including GM-CSF and thymic stromal-derived lymphopoietin [34,41]. Soluble GM-CSF can also differentiate CX₃CR1⁺ c-kit⁺ bone marrow cells into CD11b⁺CD103⁺ DC in vitro [42]. Thus, the bronchial epithelium may provide imprinting signals for αE-DC differentiation in the lungs just as epithelial cells in the gut-associated lymphoid tissue support tolerogenic DC formation in the gut mucosa [43].

The role of GM-CSF in αE-DC differentiation and function is not fully delineated. While an important role for GM-CSF was described by Greter et al [44], and by Unkel et al using a murine model of influenza infection [35], Edelson and

colleagues presented data arguing against an essential role for GM-CSF in lung αE-DC development, even though αE-DC unable to respond to GM-CSF did express reduced cell surface levels of CD103 [45].

Jakubzick et al has shown that CCR2⁺ inflammatory monocytes give rise to lung αE-DC during steady state conditions [46]. In figure 2 we show that monocyte-derived CD11b⁺CD11c⁺ cells appearing in *M. tuberculosis*-infected lungs 10 days after cell transfer also contain αE-DC. Similar to the infected lungs, recruited monocytes upregulate high cell surface levels of CD11c within four days in infected PLN. By day 10, the cells have given rise to a monocyte-derived CD11b⁺CD11c⁺ DC subset that express CD83 and high levels of CD86, indicative of a mature DC phenotype [3]. In the present study we show that the monocyte-derived CD11b⁺CD11c⁺ DC subset in the infected PLN contain αE-DC expressing high cell surface levels of MHC class II (Figure 3).

The exact phenotype of the DC that have been implicated in disseminating live mycobacteria to the draining PLN to initiate the adaptive T cell response has not been fully defined, but the CD11b⁺CD11c⁺ DC subset is a potential candidate [2,30,47]. As αE-DC can localize beneath the bronchial epithelial cell layer and express tight junction proteins that allow αE-DC to

sample the airways for inert antigens, or infectious microorganisms [15], we used GFP-expressing *M. tuberculosis* to investigate if α E-DC are targeted by the bacterium in vivo, and therefore likely candidates for mediating bacterial spread and T cell priming. Because we used a low dose aerosol infection model, we were not able to detect cells containing mycobacteria within the first week of infection. Instead, we settled for week three p.i. to examine which myeloid cells were infected in the lungs and PLN (Figure 5). Our results clearly show that only a minor fraction of α E-DC is *M. tuberculosis*-infected at this early timepoint and these cells are therefore less likely to transport the pathogen to the PLN (Figure 6).

Still, a role for α E-DC in T cell priming after *M. tuberculosis* infection cannot be fully ruled out since this DC subset is able to take up apoptotic cells in the lungs and transfer the antigens to the PLN to prime specific T cells [48]. Mutations in transcription factors required for proper DC development and function can provide further clues to the role of these cells during mycobacterial infections. The basic leucine zipper transcription factor Batf3 is required for the development of migratory α E-DC [17]. Tussiwand et al recently described reduced serum levels of IL-12p40 in *M. tuberculosis*-infected Batf3^{-/-} mice [49]. Activation of *M. tuberculosis*-specific T cells was not addressed in the absence of Batf3, but animal survival was not negatively affected [49]. Considering the importance of the MHC class II-restricted T cell response to control *M. tuberculosis* growth [31], it seems likely that CD4⁺ T cell priming is sufficient in Batf3^{-/-} mice during TB, similar to what has been described in animal models of West Nile virus infection and experimental autoimmune encephalitis [45,50]. Following low dose *M. tuberculosis* aerosol infection, the absence of CD8⁺ T cell is less dramatic [31]. Impaired, or delayed, activation of the MHC class I-restricted *M. tuberculosis*-specific CD8⁺ T cell response cannot be ruled out in Batf3^{-/-} mice.

The GFP-expressing mycobacteria also enabled us to investigate if MHC class II cell surface expression is downregulated on infected cells compared to uninfected cells in vivo. Three weeks p.i. we did not detect any significant difference in MHC class II expression levels between infected and uninfected lung cells (Figure 7). Other investigators used a similar approach to examine if live virulent *M. tuberculosis* modulates MHC class II expression on myeloid cells in infected lungs [2,22]. Kincaid et al reported no difference in MHC class II cell surface expression levels between infected and uninfected CD11b^{medium}CD11c^{low} cells, which they referred to as recruited M ϕ , 21, 28 and 35 days p.i. The authors also showed that on day 21 p.i., infected CD11b^{high}CD11c^{high} cells, referred to as myeloid DC, expressed significantly higher levels of MHC class II. However, no difference in MHC class II cell surface expression was observed on infected and uninfected CD11b^{high}CD11c^{high} cells 28 and 35 days p.i [22]. When Wolf et

al compared MHC class II cell surface expression on infected myeloid cell subsets in the lungs over time (14–28 days p.i.), the results showed that the expression levels were not reduced, and could even increase on infected neutrophils [2]. There is also in vivo data on MHC class II expression after BCG-GFP infection. Pecora et al infected mice with 2000–4000 CFU and by day 28 p.i. the authors observed approximately 40% reduction in MHC class II expression levels on lung CD11b^{high}CD11c^{negative-intermediate} M ϕ and CD11b^{high}CD11c^{high} DC [51]. We speculate that the difference in mycobacterial strains used, or in the number of bacteria seeded into the lungs, may explain the different results regarding MHC class II expression levels on myeloid cell subsets in infected lungs. We therefore conclude that our results on the MHC class II expression levels on infected and uninfected myeloid cells in the lungs are comparable to previously published results using virulent *M. tuberculosis*. In vitro experiments have demonstrated that *M. tuberculosis* can interfere with several aspects of MHC class II-mediated antigen processing (reviewed in 52). Even though infected myeloid cells in vivo do not dramatically change MHC class II cell surface expression levels within the first weeks of infection, virulent mycobacteria may still inhibit activation of MHC class II-restricted CD4⁺ T cells [2].

One drawback with our experimental approach was that we were unable to investigate MHC class II cell surface expression levels on infected cells during chronic TB. At this later stage of the disease, MHC class II levels in infected lungs have been reported to be downregulated, even though no distinction was made between uninfected and *M. tuberculosis*-infected cells [29]. Taken together, monocytes recruited into the uninfected, or *M. tuberculosis*-infected lung tissue, are able to interact with multiple non-hematopoietic cells that can influence myeloid cell differentiation. Interaction with lung epithelial cells may help explain the formation of monocyte-derived α E-DC with a unique functional potential during TB.

Acknowledgements

We acknowledge Markus Maeurer, Mats Spångberg and Helene Fredlund, and the staff of the biosafety level-3 animal facility, the Astrid Fagraeus Laboratory, Karolinska Institutet, for their help and support. We are grateful to Maria Lerm, Linköping University, for providing the GFP-expressing mycobacteria.

Author Contributions

Conceived and designed the experiments: CL CT ODC JM CSN CF MS. Performed the experiments: CL CT ODC JM MS. Analyzed the data: CL CT ODC JM CSN CF MS. Contributed reagents/materials/analysis tools: CL CT ODC JM CSN CF MS. Wrote the manuscript: CL CT ODC JM CSN CF MS.

References

1. WHO (2010) Global tuberculosis control: Who. WHO/HTM/TB Report 2010/2010.7 Geneva, Switzerland: World Health Organization.
2. Wolf AJ, Linas B, Trevejo-Nuñez GJ, Kincaid E, Tamura T et al. (2007) Mycobacterium tuberculosis infects dendritic cells with high frequency and impairs their function in vivo. J Immunol 179: 2509–2519. PubMed: 17675513.
3. Sköld M, Behar SM (2008) Tuberculosis triggers a tissue-dependent program of differentiation and acquisition of effector functions by circulating monocytes. J Immunol 181: 6349–6360. PubMed: 18941226.

4. Geissmann F, Jung S, Littman DR (2003) Blood monocytes consist of two principal subsets with distinct migratory properties. *Immunity* 19: 71–82. doi:10.1016/S1074-7613(03)00174-2. PubMed: 12871640.
5. Sunderkötter C, Nikolic T, Dillon MJ, Van Rooijen N, Stehling M et al. (2004) Subpopulations of mouse blood monocytes differ in maturation stage and inflammatory response. *J Immunol* 172: 4410–4417. PubMed: 15034056.
6. de Bruijn MF, Sliker WA, van der Loo JC, Voerman JS, van Ewijk W et al. (1994) Distinct mouse bone marrow macrophage precursors identified by differential expression of ER-MP12 and ER-MP20 antigens. *Eur J Immunol* 24: 2279–2284. doi:10.1002/eji.1830241003. PubMed: 7925556.
7. Nikolic T, de Bruijn MF, Lutz MB, Leenen PJ (2003) Developmental stages of myeloid dendritic cells in mouse bone marrow. *Int Immunol* 15: 515–524. doi:10.1093/intimm/dxg050. PubMed: 12663681.
8. Walker L, Lowrie DB (1981) Killing of *Mycobacterium microti* by immunologically activated macrophages. *Nature* 293: 69–71. doi:10.1038/293069a0. PubMed: 7266662.
9. Tian T, Woodworth J, Sköld M, Behar SM (2005) In vivo depletion of CD11c+ cells delays the CD4+ T cell response to *Mycobacterium tuberculosis* and exacerbates the outcome of infection. *J Immunol* 175: 3268–3272. PubMed: 16116218.
10. Hambleton S, Salem S, Bustamante J, Bigley V, Boisson-Dupuis S et al. (2011) IRF8 mutations and human dendritic-cell immunodeficiency. *N Engl J Med* 365: 127–138. doi:10.1056/NEJMoa1100066. PubMed: 21524210.
11. Teitelbaum R, Schubert W, Gunther L, Kress Y, Macaluso F et al. (1999) The M cell as a portal of entry to the lung for the bacterial pathogen *Mycobacterium tuberculosis*. *Immunity* 10: 641–650. doi:10.1016/S1074-7613(00)80063-1. PubMed: 10403639.
12. Marquis JF, LaCourse R, Ryan L, North RJ, Gros P (2009) Disseminated and rapidly fatal tuberculosis in mice bearing a defective allele at IFN regulatory factor 8. *J Immunol* 182: 3008–3015. doi:10.4049/jimmunol.0800680. PubMed: 19234196.
13. Peters W, Scott HM, Chambers HF, Flynn JL, Charo IF et al. (2001) Chemokine receptor 2 serves an early and essential role in resistance to *Mycobacterium tuberculosis*. *Proc Natl Acad Sci U S A* 98: 7958–7963. doi:10.1073/pnas.131207398. PubMed: 11438742.
14. MacMicking JD, North RJ, LaCourse R, Mudgett JS, Shah SK et al. (1997) Identification of nitric oxide synthase as a protective locus against tuberculosis. *Proc Natl Acad Sci U S A* 94: 5243–5248. doi:10.1073/pnas.94.10.5243. PubMed: 9144222.
15. Sung SS, Fu SM, Rose CE Jr., Gaskin F, Ju ST et al. (2006) A major lung CD103 (alphaE)-beta7 integrin-positive epithelial dendritic cell population expressing Langerin and tight junction proteins. *J Immunol* 176: 2161–2172. PubMed: 16455972.
16. Leepiyasakulchai C, Ignatowicz L, Pawlowski A, Källénius G, Sköld M (2012) Failure To Recruit Anti-Inflammatory CD103+ Dendritic Cells and a Diminished CD4+ Foxp3+ Regulatory T Cell Pool in Mice That Display Excessive Lung Inflammation and Increased Susceptibility to *Mycobacterium tuberculosis*. *Infect Immun* 80: 1128–1139. doi:10.1128/IAI.05552-11. PubMed: 22215739.
17. Edelson BT, Kc W, Juang R, Kohyama M, Benoit LA, et al. (2010) Peripheral CD103+ dendritic cells form a unified subset developmentally related to CD8alpha+ conventional dendritic cells. *J Exp Med* 207: 823–836.
18. Khader SA, Partida-Sanchez S, Bell G, Jelley-Gibbs DM, Swain S et al. (2006) Interleukin 12p40 is required for dendritic cell migration and T cell priming after *Mycobacterium tuberculosis* infection. *J Exp Med* 203: 1805–1815. doi:10.1084/jem.20052545. PubMed: 16818672.
19. Cooper AM, Dalton DK, Stewart TA, Griffin JP, Russell DG et al. (1993) Disseminated tuberculosis in interferon gamma gene-disrupted mice. *J Exp Med* 178: 2243–2247. doi:10.1084/jem.178.6.2243. PubMed: 8245795.
20. Cooper AM, Magram J, Ferrante J, Orme IM (1997) Interleukin 12 (IL-12) is crucial to the development of protective immunity in mice intravenously infected with *Mycobacterium tuberculosis*. *J Exp Med* 186: 39–45. doi:10.1084/jem.186.1.39. PubMed: 9206995.
21. Flynn JL, Chan J, Triebold KJ, Dalton DK, Stewart TA et al. (1993) An essential role for interferon gamma in resistance to *Mycobacterium tuberculosis* infection. *J Exp Med* 178: 2249–2254. doi:10.1084/jem.178.6.2249.
22. Kincaid EZ, Wolf AJ, Desvignes L, Mahapatra S, Crick DC et al. (2007) Codominance of TLR2-dependent and TLR2-independent modulation of MHC class II in *Mycobacterium tuberculosis* infection in vivo. *J Immunol* 179: 3187–3195. PubMed: 17709534.
23. Hoshino K, Takeuchi O, Kawai T, Sanjo H, Ogawa T et al. (1999). Cutting Edge Toll-Like Recept 4 (TLR4)-deficient mice are hyporesponsive to lipopolysaccharide: evidence for TLR4 as the Lps gene product. *J Immunol* 162: 3749–3752.
24. Kiers A, Drost AP, van Soolingen D, Veen J (1997) Use of DNA fingerprinting in international source case finding during a large outbreak of tuberculosis in The Netherlands. *Int J Tuberc Lung Dis* 1: 239–245. PubMed: 9432370.
25. Welin A, Raffetseder J, Eklund D, Stendahl O, Lerm M (2011) Importance of phagosomal functionality for growth restriction of *Mycobacterium tuberculosis* in primary human macrophages. *J Innate Immun* 3: 508–518. doi:10.1159/000325297. PubMed: 21576918.
26. Valdivia RH, Hromockyj AE, Monack D, Ramakrishnan L, Falkow S (1996) Applications for green fluorescent protein (GFP) in the study of host-pathogen interactions. *Gene* 173: 47–52. doi:10.1016/0378-1119(95)00706-7. PubMed: 8707055.
27. Chuquimia OD, Petrusdottir DH, Rahman MJ, Hartl K, Singh M et al. (2012) The role of alveolar epithelial cells in initiating and shaping pulmonary immune responses: communication between innate and adaptive immune systems. *PLOS ONE* 7: e32125. doi:10.1371/journal.pone.0032125. PubMed: 22393384.
28. Chuquimia OD, Petrusdottir DH, Periolo N, Fernández C (2013) Alveolar epithelial cells are critical in protection of the respiratory tract by secretion of factors able to modulate the activity of pulmonary macrophages and directly control bacterial growth. *Infect Immun* 81: 381–389. doi:10.1128/IAI.00950-12. PubMed: 23147039.
29. Gonzalez-Juarrero M, Shim TS, Kipnis A, Junqueira-Kipnis AP, Orme IM (2003) Dynamics of macrophage cell populations during murine pulmonary tuberculosis. *J Immunol* 171: 3128–3135. PubMed: 12960339.
30. Humphreys IR, Stewart GR, Turner DJ, Patel J, Karamanou D et al. (2006) A role for dendritic cells in the dissemination of mycobacterial infection. *Microbes Infect* 8: 1339–1346. doi:10.1016/j.micinf.2005.12.023. PubMed: 16697232.
31. Mogues T, Goodrich ME, Ryan L, LaCourse R, North RJ (2001) The relative importance of T cell subsets in immunity and immunopathology of airborne *Mycobacterium tuberculosis* infection in mice. *J Exp Med* 193: 271–280. doi:10.1084/jem.193.3.271. PubMed: 11157048.
32. Desvignes L, Ernst JD (2009) Interferon-gamma-responsive nonhematopoietic cells regulate the immune response to *Mycobacterium tuberculosis*. *Immunity* 31: 974–985. doi:10.1016/j.immuni.2009.10.007. PubMed: 20064452.
33. Svensson M, Maroof A, Ato M, Kaye PM (2004) Stromal cells direct local differentiation of regulatory dendritic cells. *Immunity* 21: 805–816. doi:10.1016/j.immuni.2004.10.012. PubMed: 15589169.
34. Hammad H, Chieppa M, Perros F, Willart MA, Germain RN et al. (2009) House dust mite allergen induces asthma via Toll-like receptor 4 triggering of airway structural cells. *Nat Med* 15: 410–416. doi:10.1038/nm.1946. PubMed: 19330007.
35. Unkel B, Hoegner K, Clausen BE, Lewe-Schlosser P, Bodner J et al. (2012) Alveolar epithelial cells orchestrate DC function in murine viral pneumonia. *J Clin Invest* 122: 3652–3664. doi:10.1172/JCI62139. PubMed: 22996662.
36. Demoor T, Bracke KR, Dupont LL, Plantinga M, Bondue B et al. (2011) The role of ChemR23 in the induction and resolution of cigarette smoke-induced inflammation. *J Immunol* 186: 5457–5467. doi:10.4049/jimmunol.1003862. PubMed: 21430224.
37. Cepek KL, Shaw SK, Parker CM, Russell GJ, Morrow JS et al. (1994) Adhesion between epithelial cells and T lymphocytes mediated by E-cadherin and the alpha E beta 7 integrin. *Nature* 372: 190–193. doi:10.1038/372190a0. PubMed: 7969453.
38. del Rio ML, Bernhardt G, Rodriguez-Barbosa JI, Förster R (2010) Development and functional specialization of CD103+ dendritic cells. *Immunol Rev* 234: 268–281. doi:10.1111/j.10105-2896.2009.00874.x. PubMed: 20193025.
39. Pichavant M, Charbonnier AS, Taront S, Brichet A, Wallaert B et al. (2005) Asthmatic bronchial epithelium activated by the proteolytic allergen Der p 1 increases selective dendritic cell recruitment. *J Allergy Clin Immunol* 115: 771–778. doi:10.1016/j.jaci.2004.11.043. PubMed: 15805997.
40. Nathan AT, Peterson EA, Chakir J, Wills-Karp M (2009) Innate immune responses of airway epithelium to house dust mite are mediated through beta-glucan-dependent pathways. *J Allergy Clin Immunol* 123: 612–618. doi:10.1016/j.jaci.2008.12.006. PubMed: 19178937.
41. Osterlund C, Grönlund H, Polovic N, Sundström S, Gafvelin G et al. (2009) The non-proteolytic house dust mite allergen Der p 2 induce NF-kappaB and MAPK dependent activation of bronchial epithelial cells. *Clin Exp Allergy* 39: 1199–1208. doi:10.1111/j.1365-2222.2009.03264.x. PubMed: 19486032.
42. del Rio ML, Rodriguez-Barbosa JI, Bötter J, Ballmaier M, Dittrich-Breiholz O et al. (2008) CX3CR1+ c-kit+ bone marrow cells give rise to

- CD103+ and CD103- dendritic cells with distinct functional properties. *J Immunol* 181: 6178-6188. PubMed: 18941208.
43. Iliev ID, Spadoni I, Mileti E, Matteoli G, Sonzogni A et al. (2009) Human intestinal epithelial cells promote the differentiation of tolerogenic dendritic cells. *Gut* 58: 1481-1489. doi:10.1136/gut.2008.175166. PubMed: 19570762.
 44. Greter M, Helft J, Chow A, Hashimoto D, Mortha A et al. (2012) GM-CSF controls nonlymphoid tissue dendritic cell homeostasis but is dispensable for the differentiation of inflammatory dendritic cells. *Immunity* 36: 1031-1046. doi:10.1016/j.immuni.2012.03.027. PubMed: 22749353.
 45. Edelson BT, Bradstreet TR, Kc W, Hildner K, Herzog JW, et al. (2011) Batf3-dependent CD11b(low/-) peripheral dendritic cells are GM-CSF-independent and are not required for Th cell priming after subcutaneous immunization. *PLoS One* 6: e25660.
 46. Jakubzick C, Tacke F, Ginhoux F, Wagers AJ, van Rooijen N et al. (2008) Blood monocyte subsets differentially give rise to CD103+ and CD103- pulmonary dendritic cell populations. *J Immunol* 180: 3019-3027. PubMed: 18292524.
 47. Chackerian AA, Alt JM, Perera TV, Dascher CC, Behar SM (2002) Dissemination of *Mycobacterium tuberculosis* is influenced by host factors and precedes the initiation of T-cell immunity. *Infect Immun* 70: 4501-4509. doi:10.1128/IAI.70.8.4501-4509.2002. PubMed: 12117962.
 48. Desch AN, Randolph GJ, Murphy K, Gautier EL, Kedl RM et al. (2011) CD103+ pulmonary dendritic cells preferentially acquire and present apoptotic cell-associated antigen. *J Exp Med* 208: 1789-1797. doi: 10.1084/jem.20110538. PubMed: 21859845.
 49. Tussiwand R, Lee WL, Murphy TL, Mashayekhi M, Wumesh KC et al. (2012) Compensatory dendritic cell development mediated by BATF-IRF interactions. *Nature* 490: 502-507. doi:10.1038/nature11531. PubMed: 22992524.
 50. Hildner K, Edelson BT, Purtha WE, Diamond M, Matsushita H et al. (2008) Batf3 deficiency reveals a critical role for CD8alpha+ dendritic cells in cytotoxic T cell immunity. *Science* 322: 1097-1100. doi:10.1126/science.1164206. PubMed: 19008445.
 51. Pecora ND, Fulton SA, Reba SM, Drage MG, Simmons DP et al. (2009) *Mycobacterium bovis* BCG decreases MHC-II expression in vivo on murine lung macrophages and dendritic cells during aerosol infection. *Cell Immunol* 254: 94-104. doi:10.1016/j.cellimm.2008.07.002. PubMed: 18762288.
 52. Harding CV, Boom WH (2010) Regulation of antigen presentation by *Mycobacterium tuberculosis*: a role for Toll-like receptors. *Nat Rev Microbiol* 8: 296-307. doi:10.1038/nrmicro2321. PubMed: 20234378.

III

Mycobacterium tuberculosis Infection Interferes with HIV Vaccination in Mice

Lech Ignatowicz¹, Jolanta Mazurek¹, Chaniya Leepiyasakulchai¹, Markus Sköld¹, Jorma Hinkula², Gunilla Källénius³, Andrzej Pawlowski^{3*}

1 Department of Microbiology, Tumor and Cell Biology, Karolinska Institutet, Stockholm, Sweden, **2** Department of Clinical and Experimental Medicine, Linköping University, Linköping, Sweden, **3** Department of Clinical Science and Education, Karolinska Institutet, Stockholm, Sweden

Abstract

Tuberculosis (TB) has emerged as the most prominent bacterial disease found in human immunodeficiency virus (HIV)-positive individuals worldwide. Due to high prevalence of asymptomatic *Mycobacterium tuberculosis* (*Mtb*) infections, the future HIV vaccine in areas highly endemic for TB will often be administered to individuals with an ongoing *Mtb* infection. The impact of concurrent *Mtb* infection on the immunogenicity of a HIV vaccine candidate, MultiHIV DNA/protein, was investigated in mice. We found that, depending on the vaccination route, mice infected with *Mtb* before the administration of the HIV vaccine showed impairment in both the magnitude and the quality of antibody and T cell responses to the vaccine components p24Gag and gp160Env. Mice infected with *Mtb* prior to intranasal HIV vaccination exhibited reduced p24Gag-specific serum IgG and IgA, and suppressed gp160Env-specific serum IgG as compared to respective titers in uninfected HIV-vaccinated controls. Importantly, in *Mtb*-infected mice that were HIV-vaccinated by the intramuscular route the virus neutralizing activity in serum was significantly decreased, relative to uninfected counterparts. In addition mice concurrently infected with *Mtb* had fewer p24Gag-specific IFN- γ -expressing T cells and multifunctional T cells in their spleens. These results suggest that *Mtb* infection might interfere with the outcome of prospective HIV vaccination in humans.

Citation: Ignatowicz L, Mazurek J, Leepiyasakulchai C, Sköld M, Hinkula J, et al. (2012) *Mycobacterium tuberculosis* Infection Interferes with HIV Vaccination in Mice. PLoS ONE 7(7): e41205. doi:10.1371/journal.pone.0041205

Editor: Thomas Jens Scriba, University of Cape Town, South Africa

Received: March 12, 2012; **Accepted:** June 18, 2012; **Published:** July 23, 2012

Copyright: © 2012 Ignatowicz et al. This is an open-access article distributed under the terms of the Creative Commons Attribution License, which permits unrestricted use, distribution, and reproduction in any medium, provided the original author and source are credited.

Funding: This work was supported by the European Commission grant MEST-CT-2005-020872 (<http://ec.europa.eu/research/mariecurieactions/>) to JM, LI and AP, the Swedish Research Council grant No. K2007-58X-13027 (<http://www.vr.se/>) to GK, the Swedish International Development Agency (SIDA/Sarec; <http://www.sida.se/>) grant to JH, a scholarship from the Royal Thai Government to CL and by the Swedish Research Council grant No. K2007-57X-20360-01-4 (<http://www.vr.se/>) to MS. The funders had no role in study design, data collection and analysis, decision to publish, or preparation of the manuscript.

Competing Interests: The authors have declared that no competing interests exist.

* E-mail: andrzej.pawlowski@ki.se

Introduction

Despite recent advances in highly active anti-retroviral therapy, human immunodeficiency virus (HIV) infections and the resulting acquired immunodeficiency syndrome (AIDS) remain an important cause of morbidity and mortality worldwide with 2.6 million new cases and 1.8 million deaths reported in 2009 [1]. Therefore, it is widely acknowledged that a safe and effective HIV prophylactic vaccine would be the best long-term measure to bring the HIV/AIDS epidemics under control.

It has been suggested that the effectiveness of vaccines in the population is affected by several factors such as age [2], malnutrition [3], and concurrent infections [4–9]. One of the factors that could potentially affect HIV vaccination efficacy is high prevalence of tuberculosis (TB) in HIV endemic regions. Over 90% of the world's HIV/AIDS cases are in Africa where TB is the leading cause of HIV-related mortality [10]. The HIV and TB epidemics fuel each other [11] and the relationship between HIV and *Mycobacterium tuberculosis* (*Mtb*) infection in co-infected individuals has been shown to be synergistic; latent *Mtb* infection is activated by HIV-induced immunodeficiency and latent HIV in proviral form is triggered by TB-induced immune activation [12,13]. In addition, TB impairs recovery of immune system in HIV-infected patients undergoing anti-retroviral therapy [14].

Studies of long-term non-progressors, a small subset of HIV-1 infected individuals who have stable CD4 T cell counts for more than 5 years without retroviral therapy [15], firmly suggest that an effective immune response helps control the infection and disease. These studies imply that, by analogy to natural HIV infection in long-term non-progressors, an efficient HIV vaccine should elicit cytotoxic T cell responses [16], and multifunctional T cells that produce multiple cytokines in response to HIV antigens [17]. In addition to cell-mediated immunity, the HIV vaccine should evoke early and robust broadly virus-neutralizing antibodies [18] similar to those identified in a subset of HIV-1 infected subjects [19]. It is also considered important that, in order to prevent the infection or reduce the infectious inoculum, the HIV vaccine should induce immune responses at mucosal surfaces, which represent sites of HIV entry [20,21].

An extensive search for a HIV vaccine has resulted in a large number of vaccine candidates that in laboratory animals elicited immune responses against HIV antigens [22]. Based on results of immunogenicity and protection studies in non-human primates several promising HIV vaccine candidates were taken to clinical trials. To date, out of several vaccine candidates investigated in clinical phase II/III trials, only one showed moderate level of protective efficacy. Thus, although level of protection afforded by this vaccine was unsatisfactory, the trial demonstrated that

construction of an effective HIV vaccine is possible [23]. Nevertheless, future HIV vaccine studies should, in addition to defining protective immune responses, also focus on factors that could interfere with vaccine-induced protection.

One of the overlooked issues that have potential impact on HIV vaccine development stems from the fact that geographical areas with the highest prevalence of HIV and *Mtb* infections overlap. Consequently, future HIV vaccine will often be administered to individuals harboring latent or undiagnosed active TB. Several acute or chronic infections, such as measles, malaria, and helminthes have previously been found to interfere with efficacy of vaccination against unrelated pathogens [4–9]. In contrast, the impact of TB on HIV vaccine efficacy has not yet been addressed in preclinical studies, despite the high prevalence of TB in HIV vaccine target populations.

In this study we investigated the effect of concurrent chronic *Mtb* infection on immunogenicity of a HIV DNA/protein vaccine candidate that has generated promising results in a mouse model [24]. We found that both the magnitude and the quality of antibody and T cell responses to such vaccine were impaired by *Mtb* infection.

Results

Concurrent *Mtb* Infection Impairs IgA Levels Induced by the HIV Vaccination

The humoral response mediated by IgA at mucosal surfaces may help prevent HIV infection or reduce the viral load [20]. We therefore assessed the impact of ongoing *Mtb* infection on IgA responses to HIV vaccination by examining the relative levels of p24Gag and gp160Env-specific IgA in vaginal secretions and sera from *Mtb*-infected and MultiHIV DNA/protein-vaccinated mice, as compared to uninfected vaccinated animals.

Importantly, HIV vaccination of mice via the intranasal (i.n.) route resulted in moderately high levels of p24Gag- and gp160Env-specific vaginal IgA 4 weeks (wk) post-vaccination (Fig. 1A and B). Compared to uninfected mice, the titers seemed lower in *Mtb*-infected animals, although the difference did not reach statistical significance. As expected, intramuscular (i.m.) vaccination did not induce any detectable IgA in vaginal secretions. The HIV vaccine-induced serum IgA levels were higher following i.m. vaccination when compared to i.n. vaccination (Figure 1C and D). While the anti-p24Gag and anti-gp160Env serum IgA levels elicited by i.m. vaccination were not modified by prior *Mtb* infection, those induced by i.n. vaccination were significantly suppressed in *Mtb*-infected mice ($P < 0.05$).

Thus, *Mtb* infection was shown to diminish HIV-specific IgA responses at mucosal surfaces.

Concurrent *Mtb* Infection Reduces Serum Antibody Responses to the MultiHIV DNA/Protein Vaccine Administered I.N

To determine whether concurrent *Mtb* infection affects IgG responses to HIV vaccination, we investigated serum p24Gag- and gp160Env-specific IgG in *Mtb*-infected and uninfected mice after MultiHIV DNA/protein immunization.

Two wk post-vaccination (after the second protein boost) uninfected mice had high serum levels of anti-p24Gag IgG (Figure 2A) and anti-gp160Env IgG (Figure 2B). The IgG titers in mice vaccinated by the i.n. route were over 1 log higher than those in mice vaccinated by the i.m. route, but the difference did not reach statistical significance. Strikingly, in *Mtb*-infected and i.n. vaccinated mice, anti-p24Gag serum IgG were reduced by almost 3 logs (Figure 2A; $P < 0.01$) and anti-gp160Env serum IgG were

virtually absent (Figure 2B; $P < 0.01$), as compared to the serum IgG levels in uninfected mice. Unlike serum IgG responses elicited by i.n. vaccination, those induced by i.m. vaccination were not impaired by the concurrent *Mtb* infection.

Both p24Gag- and gp160Env-specific serum IgG elicited by i.n. vaccination decreased significantly 4 wk post-infection (Figure 2C and D; $P < 0.05$). Despite this reduction the trend for compromised HIV antibody responses in *Mtb*-infected relative to uninfected animals could still be observed. Conversely, at 4 wk, p24Gag- and gp160Env-specific serum IgG levels induced by the i.m. vaccination remained as high as at 2 wk and were not affected by pre-existing *Mtb* infection.

Of note, MultiHIV DNA/protein elicited moderately high anti-Nef and anti-Tat serum IgG that were not altered by a concurrent *Mtb* infection, irrespective of the vaccination route (Figure S1).

Our results show that, in addition to affecting the specific mucosal IgA response, *Mtb* infection can, depending on the vaccination route, significantly reduce the serum IgG titers induced by a HIV vaccine.

Concurrent *Mtb* Infection Reduces HIV Vaccine-induced Virus Neutralizing Activity in Sera of Mice Vaccinated by the I.M. Route

Studies of long-term non-progressors indicate that more important than the amount of HIV-specific antibodies is their ability to neutralize the virus [15,19]. In order to assess the impact of prior *Mtb* infection on the quality of antibody responses to subsequent HIV vaccination, we investigated heterologous HIV neutralizing activity in 4 wk post-vaccination sera from uninfected or *Mtb*-infected and MultiHIV DNA/protein-vaccinated mice.

Using the 50% HIV neutralization assay we found, that i.n. vaccination of mice with MultiHIV DNA/protein elicited moderate neutralizing serum antibody responses whereas i.m. vaccination resulted in 3-fold higher HIV neutralizing activity (Figure 3; $P < 0.05$). However, while concurrent *Mtb* infection had no effect on neutralizing activity in sera of i.n. vaccinated mice, it reduced over 3-fold the neutralizing response in mice that received the HIV vaccine through the i.m. route ($P < 0.001$).

In conclusion, *Mtb* infection not only reduces the amount of antibodies induced by the HIV vaccine, but also impairs the quality of the antibody response to vaccination.

Concurrent *Mtb* Infection Amplifies the Th1 Bias of Immune Responses elicited by HIV Vaccine

Assessment of vaccine elicited production of IgG1 versus IgG2a indirectly measures differential Th2-Th1 immune responses and may provide clues that could explain the reduced virus-neutralizing activity in *Mtb*-infected mice. In order to investigate in more detail the impact of concurrent *Mtb* infection on Th2-Th1 responses elicited by the HIV vaccine, p24Gag-specific serum IgG1 and IgG2a were determined 4 wk post-vaccination. Uninfected mice inoculated with the HIV vaccine through either the i.n. or the i.m. route had high p24Gag-specific serum IgG1:IgG2a ratios, indicative of immune response with a prevalent Th2 component (Figure 4). Importantly, *Mtb* infection prior to HIV vaccination resulted in 5-fold reduced IgG1:IgG2a ratios regardless of the vaccination route ($P < 0.001$).

Here we show that the host immune response initiated by *Mtb* infection adversely affects the IgG1 : IgG2a ratio elicited by the HIV vaccine. This may explain the reduced neutralizing activity in sera that we observed in *Mtb*-infected HIV vaccinated animals.

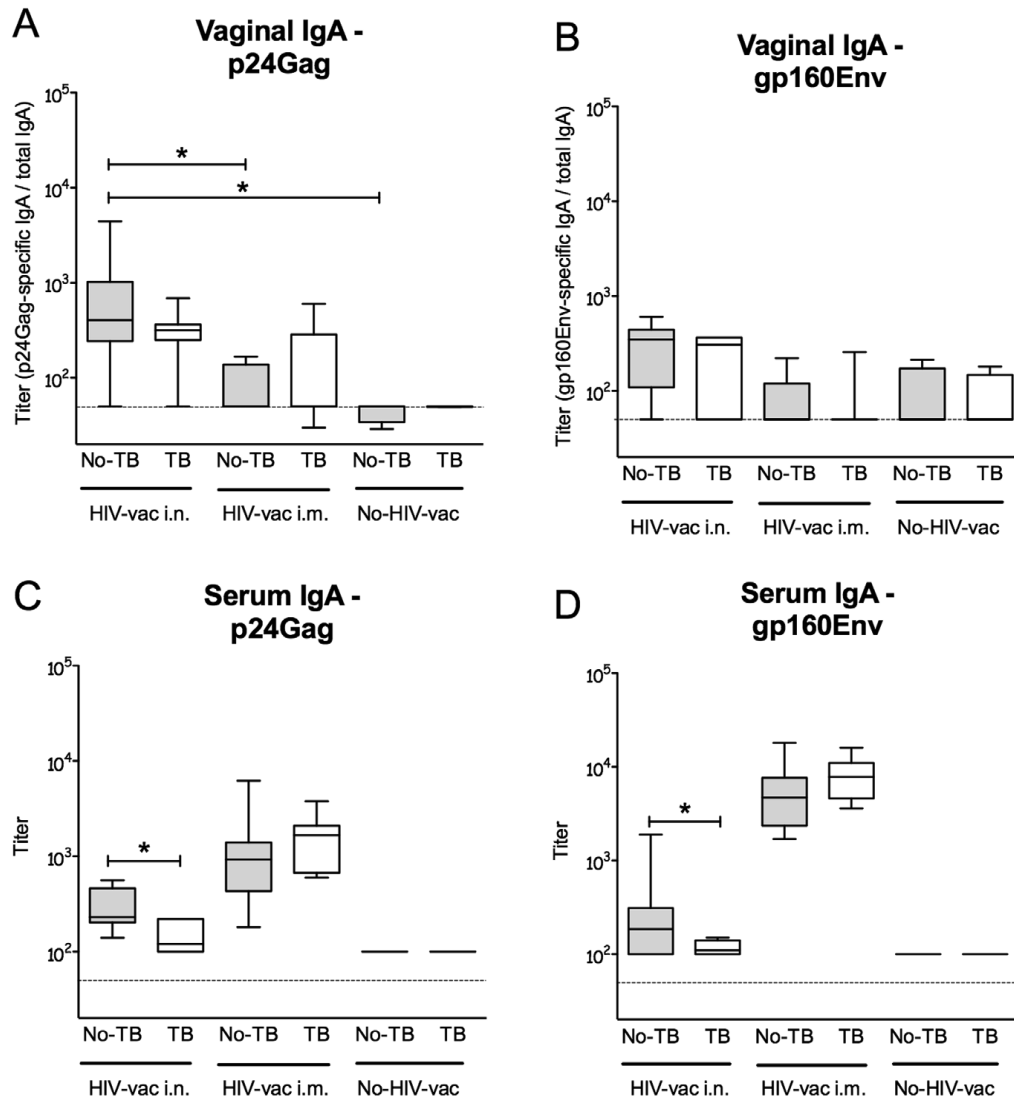


Figure 1. HIV-specific vaginal secretory and serum IgA in uninfected and *Mtb*-infected C57BL/6 mice post-vaccination with MultiHIV DNA/protein. Uninfected C57BL/6 mice, or *Mtb* aerosol-infected mice, were immunized and boosted with MultiHIV DNA/protein as described in Materials and Methods. Vaginal secretions were collected 4 wk post-vaccination and HIV p24Gag-specific and gp160Env-specific IgA were determined in vaginal washings (A, B) and serum (C, D) as described in Materials and Methods. The median endpoint titer of 6–8 mice/group from one individual experiment is shown as a solid line. The box defines the 75th and 25th percentiles and the whiskers define the maximum and minimum values. Dashed line indicates the ELISA sensitivity threshold. (*: $P < 0.05$). HIV-specific IgA levels were examined in two separate experiments.
doi:10.1371/journal.pone.0041205.g001

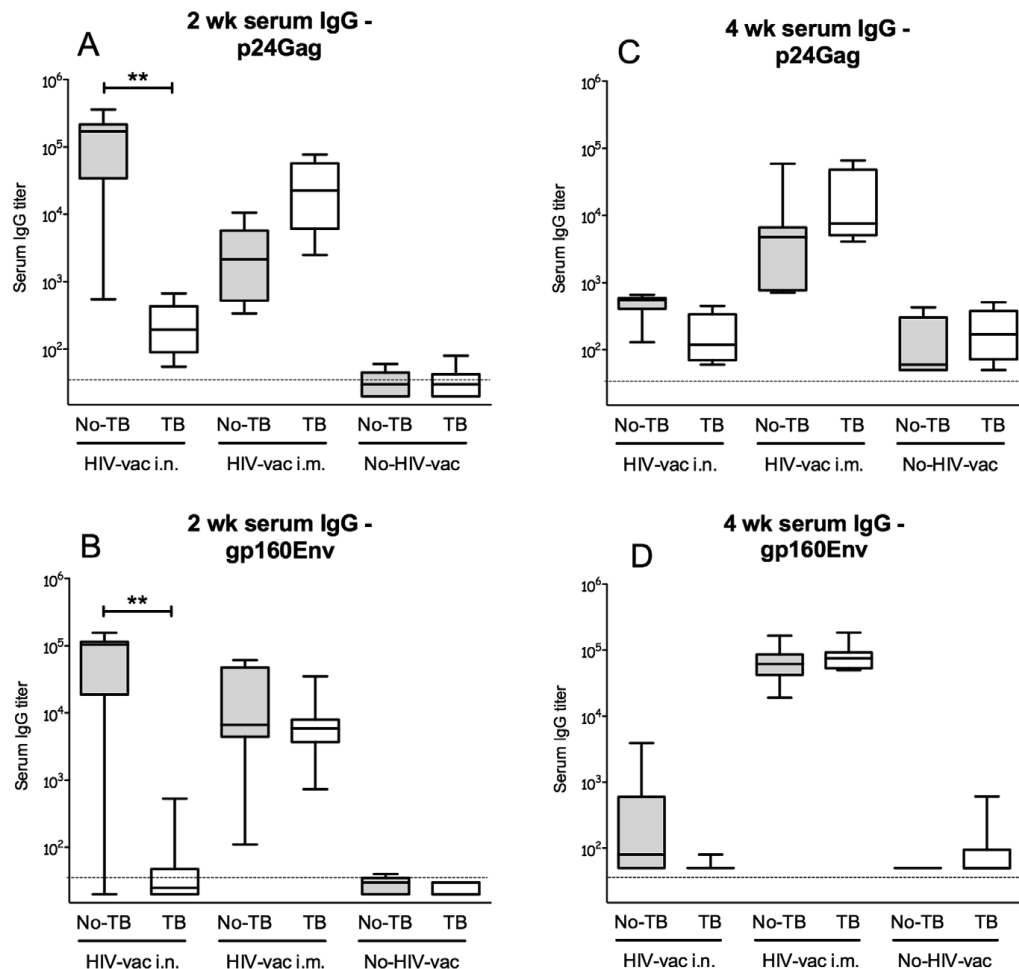


Figure 2. Effect of *Mtb* infection on HIV-specific serum IgG titers induced by MultiHIV DNA vaccination followed by protein boost. Uninfected or low-dose *Mtb* aerosol-infected (7 wk post infection) C57BL/6 mice were vaccinated i.n. or i.m. with MultiHIV DNA encoding HIV-1 subtype B gp160Env, p37Gag, Nef, Tat, and Rev in N3 adjuvant followed by two booster inoculations of recombinant HIV proteins (gp160Env, p24Gag, Tat, and Nef) in L3 adjuvant. HIV-specific serum IgG levels were measured 2 (A, B) and 4 wk (C, D) post-vaccination with HIV antigen-ELISA using p24Gag (A, C) and gp160Env (B, D) as coating antigens, as described in Materials and Methods. Median endpoint titer of 6–8 mice/group from one individual experiment is shown as a solid line. The box defines the 75th and 25th percentiles and the whiskers define the maximum and minimum values. Dashed line indicates the ELISA sensitivity threshold. (*: $P < 0.05$; **: $P < 0.01$). The IgG titers were examined in two separate experiments.

doi:10.1371/journal.pone.0041205.g002

T Cell Responses to MultiHIV DNA/Protein Are Suppressed in Mice Infected with *Mtb* Prior to Vaccination

Induction of T cells expressing Th1 cytokines: IFN- γ , IL-2, or TNF is necessary for efficient protection against intracellular pathogens such as HIV [25]. HIV-specific multifunctional T cells that simultaneously produce more than one cytokine were recently suggested to play an important role in the control of HIV infection [17]. We studied the magnitude and the quality of T cell responses

in splenocytes of MultiHIV DNA/protein-immunized mice 4 wk post-vaccination. We analyzed the numbers and frequencies of CD4 and CD8 T cells that expressed intracellular IFN- γ , IL-2, or TNF, upon restimulation with HIV p24Gag peptide pools *ex vivo*. We found that i.n. vaccination of uninfected mice induced high numbers of p24Gag-specific CD4 (Figure 5A and C) and CD8 (Figure 5B and D) T cells expressing IFN- γ or TNF and low to moderate numbers of IL-2 producing cells as compared to the non-vaccinated controls. The numbers of p24Gag-specific single

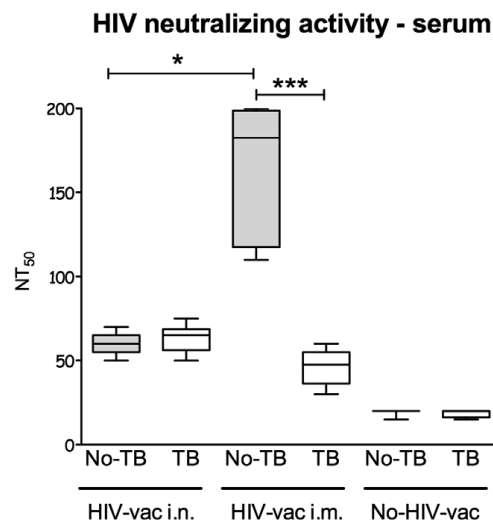


Figure 3. Effect of *Mtb* infection on MultiHIV DNA/protein-induced HIV neutralizing activity in mouse sera. Sera from uninfected and *Mtb*-infected C57BL/6 mice subsequently vaccinated i.n. or i.m. with MultiHIV DNA/protein were collected 4 wk post-vaccination. *Ex vivo* HIV-1 neutralization assay was performed on PHA-stimulated PBMCs using two heterologous HIV-1 strains and serially diluted immune mouse sera as described in Materials and Methods. Neutralization titer is defined as reciprocal dilution of serum resulting in 50% inhibition of viral infectivity estimated on the basis of HIV p24 antigen production in PBMCs (NT₅₀). Median NT₅₀ of 6–8 mice/group from one individual experiment is shown as a solid line. The box defines the 75th and 25th percentiles and the whiskers define the maximum and minimum values (*: $P < 0.05$; ***: $P < 0.001$). The HIV neutralizing activity in mouse sera was investigated in two separate experiments. doi:10.1371/journal.pone.0041205.g003

cytokine producing T cells in i.m. vaccinated mice did not significantly differ from those in mice vaccinated by the i.n. route.

In contrast to non-*Mtb* infected HIV-vaccinated mice, *Mtb*-infected mice had significantly fewer cytokine producing splenic T cells (Figure 5A and B), regardless of the vaccination route. In *Mtb*-infected animals vaccinated i.n., p24Gag-specific IFN- γ -producing CD4 T cells were reduced 4-fold ($P < 0.01$) and TNF-producing CD4 T cells were reduced 2-fold compared to uninfected controls. Similarly, in *Mtb*-infected animals vaccinated i.m., p24Gag-specific IFN- γ -producing CD4 T cells were reduced 4.5-fold ($P < 0.01$) and TNF-producing CD4 T cells were reduced 3-fold compared to uninfected control mice (Figure 5A). A similar decrease of IFN- γ -producing T cells in *Mtb*-infected mice was found in the CD8 T cell subset (5-fold for i.n. route; $P < 0.01$, and 3.5-fold for the i.m. route; Figure 5B). Even though the difference did not reach statistical significance, *Mtb*-infection seemed to negatively influence IL-2 production by antigen-specific CD4 and CD8 T cells following i.m., but not i.n., vaccination (Figure 5).

In addition to CD4 and CD8 T cells producing single cytokines, spleens of uninfected HIV-vaccinated mice contained measurable levels of p24Gag-specific multifunctional CD4 T cells which simultaneously expressed IFN- γ /IL-2, IFN- γ /TNF, IL-2/TNF, or IFN- γ /TNF/IL-2 and were similar in mice vaccinated through the i.n. and the i.m. route (Figure 6A). Importantly, both numbers (Figure 6A) and proportions (Figure 6B) of CD4 multifunctional T

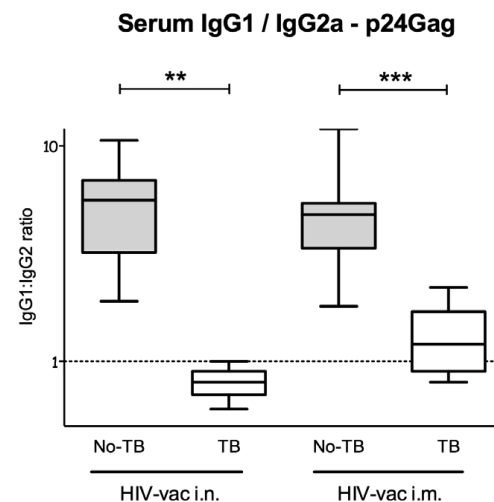


Figure 4. IgG1:IgG2a ratios of HIV p24Gag-specific antibodies in sera of uninfected and *Mtb*-infected mice vaccinated with MultiHIV DNA/protein. Uninfected C57BL/6 mice, or mice infected with *Mtb* via the respiratory route, were immunized and boosted with MultiHIV DNA/protein, as described in Materials and Methods. IgG1:IgG2a ratios were calculated using p24Gag-specific antibody titers determined with ELISA in sera 4 wk post-vaccination. Median IgG1:IgG2a ratio of 6–8 mice/group from one individual experiment is shown as a solid line. The box defines the 75th and 25th percentiles and the whiskers define the maximum and minimum values (**: $P < 0.01$; ***: $P < 0.001$). The IgG1:IgG2a ratios were determined in two separate experiments. doi:10.1371/journal.pone.0041205.g004

cells were significantly decreased in spleens of mice that harbored *Mtb* infection at the time of HIV vaccination through the i.m. route, compared to uninfected HIV-vaccinated animals; 6-fold reduction of IFN- γ /IL-2/TNF, and 9-fold reduction of IFN- γ /TNF expressing CD4 T cells were found. A similar trend of diminished levels of IFN- γ /IL-2/TNF and IFN- γ /TNF cells was noted in spleens of i.n. vaccinated mice that were *Mtb*-infected prior to HIV-vaccination. In contrast, *Mtb* infection prior to HIV vaccination did not affect levels of IL-2/TNF expressing p24Gag-specific CD4 T cells (Figure 6). Similarly to the virus-specific humoral response induced by the HIV vaccine, *Mtb* infection has an adverse effect on HIV-specific T cell immunity.

In conclusion, our data show that *Mtb* negatively influences multiple effector functions believed to be important for efficient control of HIV infection.

Mice Aerosol-Infected with a Low *Mtb* Dose Develop Chronic TB Infection Unaffected by Subsequent HIV Vaccination

In order to evaluate if HIV vaccine may interfere with the course of *Mtb* infection we infected resistant C57BL/6 mice with a low dose of aerosolized *Mtb* via the respiratory route (50–100 bacteria/lung) followed by vaccination with MultiHIV DNA by the i.n. or the i.m. route. Throughout the entire experimental period *Mtb*-infected mice remained in good physical condition and did not show any symptoms of disease. As expected, at the end of the experiment (17 wk post-infection) lungs of all infected mice contained between 4.8–6.0 logs bacteria (Figure S2). Lung

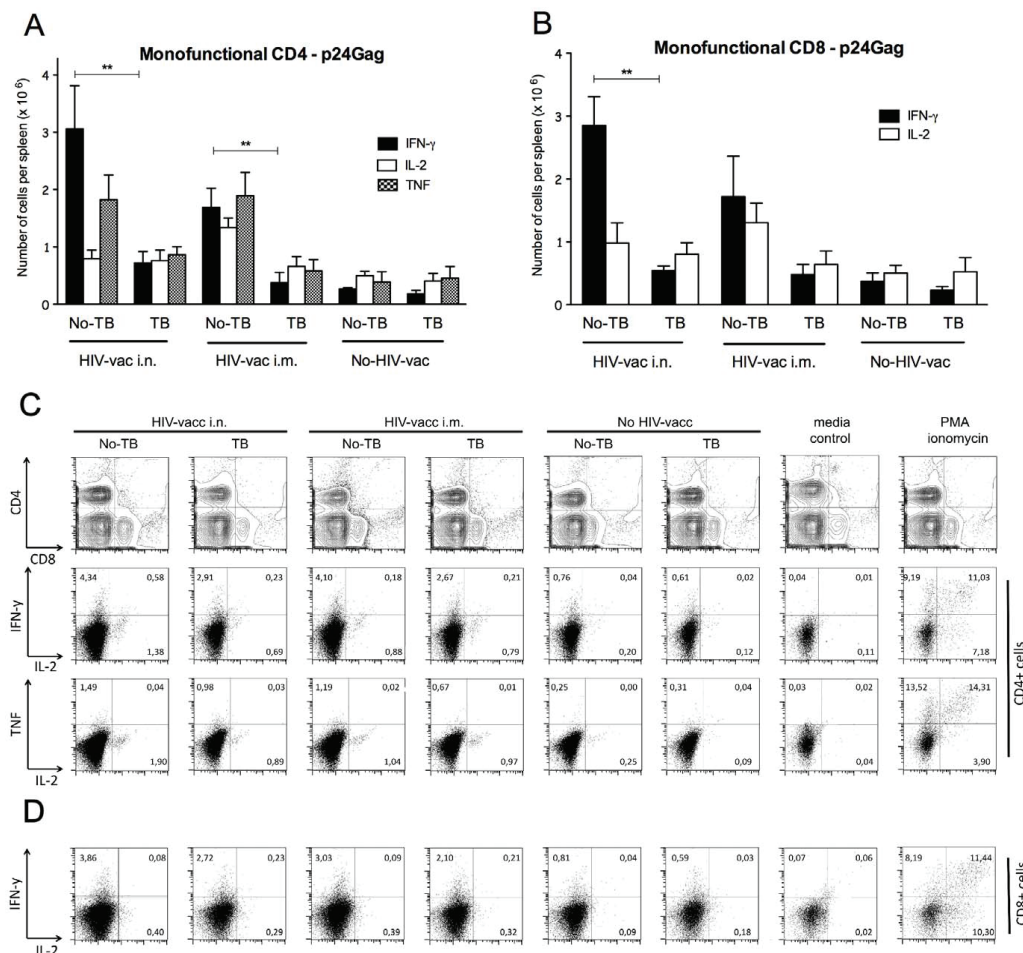


Figure 5. HIV p24Gag-specific T cell cytokine responses in spleens of uninfected or *Mtb*-infected mice vaccinated with MultiHIV DNA/protein. Splenocytes from *Mtb*-infected or uninfected mice, which were immunized and boosted with MultiHIV DNA/protein, were isolated 4 wk post-vaccination, restimulated *ex vivo* with p24Gag antigen, and stained for CD4 and CD8 markers and for intracellular IFN- γ , TNF, and IL-2 (details in Materials and Methods). Numbers of p24Gag-specific CD4+ (A) and CD8+ (B) T cells producing one of three cytokines were determined by flow cytometry. Mean number of single cytokine-producing T cells \pm SEM are shown (6–8 animals/group from one individual experiment; **, $P < 0.01$). Flow cytometry plots depict representative intracellular cytokine staining of CD4+ (C) and CD8+ (D) T cells. The cytokine profile of p24Gag-specific T cells was determined in two separate experiments.
doi:10.1371/journal.pone.0041205.g005

bacterial burdens of mice that post-infection received MultiHIV DNA/protein vaccine did not significantly differ from those of non-vaccinated mice irrespective of vaccination route.

Discussion

It has become increasingly clear that for an effective HIV-1 vaccine to materialize two issues will be critical: a durable antibody response with broad-neutralizing capacity to block the virus transmission [22] and a robust cellular response to limit virus replication in those who already are infected [26]. Using two

vaccination routes we investigated the impact of concurrent *Mtb* infection on the immunogenicity of a HIV DNA/protein vaccine candidate in *Mtb* resistant C57BL/6 mice. Remarkably, we found that this subclinical chronic *Mtb* infection impaired both the magnitude and the quality of antibody and T cell responses to the vaccine components p24Gag and gp160Env. Thus, *Mtb*-infected mice showed significant albeit transient decrease of p24Gag-specific serum IgG titers elicited by i.n. vaccination and sustained reduction of both p24Gag- and gp160Env-specific serum IgA induced by i.m. vaccination. Importantly, although concurrent

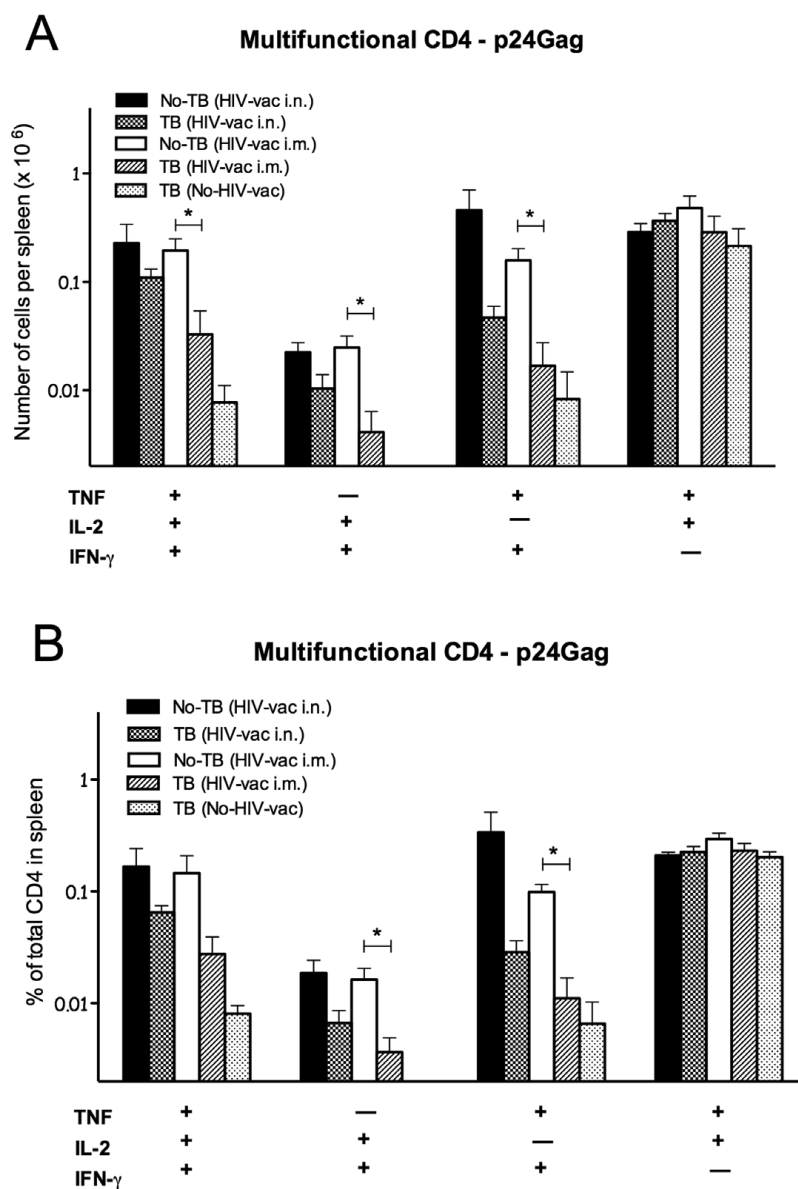


Figure 6. Multifunctional HIV p24 antigen-specific T cells in spleens of uninfected or *Mtb*-infected mice vaccinated with MultiHIV DNA/protein. Splenocytes from *Mtb*-infected or uninfected mice, subsequently immunized and boosted with MultiHIV DNA/protein, were isolated 4 wk post-vaccination, restimulated *ex vivo* with HIV p24 antigen, and stained for CD4 markers and for intracellular IFN- γ , TNF, and IL-2 (details in Materials and Methods). Frequencies of HIV p24 antigen-specific multifunctional CD4 T cells simultaneously producing IFN- γ , IL-2 and TNF were determined by flow cytometry. Mean numbers (A) and frequencies (B) \pm SEM of multifunctional T cells are shown (6–8 animals/group from one individual experiment; *: $P < 0.05$). The presence of multifunctional T cells was examined in two separate experiments. doi:10.1371/journal.pone.0041205.g006

Mtb infection in i.m. vaccinated mice did not affect HIV-specific serum IgG levels, it resulted in a significant decrease in serum neutralizing activity towards heterologous HIV clades. Also, *Mtb*-infected mice had, irrespective of the HIV vaccination route, fewer p24Gag-specific IFN- γ - or TNF-producing splenic T cells, and, importantly, reduced levels of p24Gag-specific multifunctional T cells simultaneously expressing IFN- γ , TNF, and IL-2.

Thus, in our study, pre-existing subclinical chronic *Mtb* infection in mice interfered with many types of immune responses to HIV antigens which are considered important for both natural and vaccine-induced immunity, such as mucosal and serum antibodies, including neutralizing antibodies [27,16], robust CD4 and CD8 T cell responses [17,20], and multifunctional T cells [28]. This is, to our knowledge, the first report on detrimental effect of *Mtb* infection on development of post-vaccination HIV immunity. Furthermore, this is also the first report on impairment by mycobacteria of immune responses to any type of heterologous antigens, with the exception of an early study by Dubos et al who showed, that infection of mice with BCG or administration of mycobacterial lipids could, depending on the administration route, either protect from or enhance concurrent infection with *Staphylococcus aureus* [29,30].

It has previously been reported that some chronic and acute infections other than TB, including those with intracellular pathogens, may modify immune responses to and efficacy of heterologous vaccines. Helminth infections have been implicated in a compromised protective efficacy of tetanus [31] and BCG vaccinations [32]. Malaria has been suggested to suppress antibody responses to meningococcal C [33] and *Salmonella typhi* O [34] polysaccharide vaccines and tetanus vaccine [35]. Immunosuppressive effects of malaria have also been associated with increased risk of bacterial infections [36] and increased HIV loads [37]. Similarly, certain viral infections, have been found to interfere with immune responses to unrelated vaccines and concurrent infections; attenuated polio virus administered with oral polio vaccine has been associated with reduced efficacy of BCG vaccination [38], measles was found to non-specifically suppress immune responses to secondary bacterial infections for instance *Listeria monocytogenes* [39] and HIV infection has been shown to increase the risk of mycobacterial diseases including TB [12].

The mechanisms underlying the ability of certain pathogens to impair immune responses to heterologous vaccines or concurrent infections, including detrimental effect of *Mtb* infection on HIV vaccination described here, remain as yet unclear. In this study we found that chronic *Mtb* infection impairs both humoral and cellular immune responses elicited by HIV vaccination; therefore we expect that more than one mechanism is involved. One of the better-explored mechanisms of pathogen-related immune subversion is exerted by helminths and protozoa and relies on an induction of a highly Th2 cell-polarized environment. Because of the crossregulation between Th1 and Th2 responses, the helminth-induced pertinent Th2 bias may result in the increased susceptibility to Th1-controlled infections [40,41] and decreased responses to vaccinations [31,32,42]. However, this mechanism does not account for the *Mtb*-mediated suppression of HIV vaccine-induced responses reported here because, instead of increased Th2 polarization, we observed augmented Th1 bias in mice infected with *Mtb* prior to HIV vaccination.

Studies of HIV positive subjects reveal the presence of both neutralizing antibodies and serum antibodies that will enhance HIV infection, the latter with opsonizing activity allowing the virus to enter and multiply inside host cells [43]. The balance between two types of antibodies changes as the disease progresses and during advanced stages the proportion of infection-enhancing

opsonizing antibodies are generally higher than neutralizing antibodies. It could be hypothesized that *Mtb* infection drives mainly production of opsonizing IgG antibodies. This could be the reason why despite high serum levels of IgG elicited by i.m. HIV vaccination in both *Mtb*-infected and non-infected mice, serum antibodies of infected animals had much lower neutralizing ability than in non *Mtb*-infected counterparts.

Since *Mtb* and HIV do not share antigenic epitopes, it is unlikely that the observed inhibition by concurrent TB of immune responses to the HIV vaccine candidate is antigen-specific. Instead, it could be envisaged that non-antigen specific “bystander” suppressive mechanisms are involved in such inhibition. Indeed, evidence supports the idea that infection-induced specific regulatory T cells, in addition to suppression of specific immune responses, can also suppress unrelated immune responses in a non-antigen specific manner, either through direct cellular contact or via the regulatory cytokines they produce [44–46]. Regulatory T cells have been shown to be induced both in active and latent TB [47] and have been implicated in the downregulation of immune control of *Mtb* infection and progression to active disease [48,49]. Additionally, the impairment of humoral and T cell responses to intranasal HIV vaccination which we found in *Mtb*-infected mice could also result from a competitive presentation of *Mtb* antigens and HIV vaccine antigens co-localizing in respiratory tract-associated lymph nodes [50].

In summary, we report for the first time that chronic *Mtb* infection of mice prior to inoculation with an experimental HIV vaccine has detrimental effect on vaccine-specific antibody and T cell responses. These results suggest that asymptomatic *Mtb* infection could also interfere with prospective HIV vaccination in humans. Therefore, we firmly believe that our findings have important implications for the development of potential HIV candidates. When ultimately a HIV vaccine is available, the need for such a vaccine will be greatest where TB is endemic. As estimated by the WHO currently one third of the world’s population is latently infected with *Mtb* [51]. This vast number of latently infected constitutes the main reservoir for adult pulmonary TB; in about 5–10% of such individuals the infection becomes reactivated mainly when the immune system is compromised [52]. Recent studies on mutation rates of *Mtb* bacilli suggest that during the latent stage of infection, the bacteria are able to slowly replicate [53–54]. This may lead to low level engagement of the immune system [55]. Studies of low dose *Mtb* aerosol infections in macaques, resulting in approximately half of the monkeys being classified as latently infected that may naturally reactivate, and observations from epidemiological studies strongly suggest that the transition from latent to active TB is a multistage and gradual process [56–58]. Together with other factors this extended subclinical phase could result in a delayed or false negative diagnosis [59]. Therefore, our results advocate that chronic and undiagnosed, or even latent, *Mtb* infection interferes with the immune response elicited by HIV vaccine candidates and should be taken into account during vaccine design and in clinical trials.

Materials and Methods

Mtb Infection

Mtb Harlingen strain was prepared as described earlier [60]. Six wk-old female C57BL/6 mice were infected aerogenically with low dose of *Mtb* (50–100 bacteria/lung) using a nose-only aerosol exposure apparatus (In-Tox Products, Moriarty, NM, USA) as previously described [61].

Lung inoculum was verified by agar plating 24 h after infection. Lungs for all time points were homogenized in PBS with 0.02%

Tween 80 and serial dilutions of lung homogenates were plated onto Middlebrook 7H10 agar. Colonies were counted after 2 to 3 wk incubation at 37°C. All work with *Mtb* and *Mtb*-infected animals was conducted in a BSL-3 containment laboratory. The local committee on animal ethics and the Swedish Board of Agriculture approved all animal experiments.

HIV Vaccine and Immunization

Seven wk post-*Mtb* infection groups of mice (6–8 animals/group) were immunized i.n. or i.m. with 10 µg of plasmids encoding HIV-1 subtype B gp160Env, p37Gag, Nef, Tat, and Rev (MultiHIV DNA vaccine) [24] formulated in N3 adjuvant (2% lipid) and subsequently boosted twice (4 and 6 wk post-DNA vaccination) with 5 µg of recombinant gp160Env, p24Gag, Tat and Nef formulated in L3 adjuvant (2% lipid) [62,63]. Control groups were sham-vaccinated with saline.

Sample Collection

Two wk after the last HIV boost vaccination tail blood and vaginal wash samples were collected for IgG and IgA assays and frozen until the time of analysis. Four wk post-vaccination the mice were sacrificed and blood, vaginal washes, spleens and lungs were collected.

In Vitro Stimulation and Intracellular Cytokine Staining

A single cell suspension of splenocytes was obtained by grinding the spleen and passing the obtained cell suspension through a 70 µm strainer (BD Falcon) into DMEM (BD Bioscience) supplemented with 10% inactivated FBS, penicillin/streptomycin, L-glutamine, sodium-pyruvate (Invitrogen). Erythrocytes were lysed with NH₄Cl and the remaining splenocytes (1×10^6 /well) from individual animals were stimulated for 6 h in the presence of peptide pools (15-mers overlapping by 10 amino acids, Thermo-Hybaid, Germany, 1.25 µg/ml each peptide) covering either gp160Env or p24Gag proteins dissolved in complete DMEM medium, in the presence of brefeldin A (10 µg/mL, eBioscience). Medium alone was used as a negative control and PMA/Ionomycin (at 25 ng/mL and 1 µg/mL, Sigma-Aldrich) was used as positive control. After stimulation the cells were washed with FACS buffer (PBS with 1% FBS) and incubated with purified anti-mouse CD16/CD32 (2.4G2, BD Bioscience) at 20 µg/mL for 15 min at 4°C to block nonspecific binding (Fc block). The cells were washed and incubated 15 min at 4°C with primary antibodies specific for surface markers (anti-CD3 17A2, anti-CD4 GK1.5, and anti-CD8α 53-6.7, all from eBioscience), or appropriate isotype controls, diluted in FACS buffer. After washing, cells were fixed with 2% paraformaldehyde, permeabilized using permeabilization buffer (eBioscience) and incubated for 20 min at 20°C with antibodies specific for intracellular cytokines; anti-IL-2 JE56-5H4, anti-IFN-γ XMG1.2, and anti-TNF-α MP6-XT22, all from eBioscience. The cells were washed with permeabilization buffer and then with FACS buffer, resuspended and analyzed by flow cytometry using BD FACSCanto II flow cytometer (BD Biosciences). Data analysis was performed using FlowJo software.

IgG and IgA ELISA

Vaginal washes were obtained and analyzed as previously described [64–66]. 96-well plates (Nunc Maxisorp) were coated with the recombinant HIV-1 proteins p24Gag (0.5 µg/mL, Aalto Bio Reagents), gp160Env (0.5 µg/mL, BioSciences Int), Nef (0.5 µg/mL, kindly provided by V. Erfle, GSF, Munich, Germany), and Tat (1 µg/mL, kindly provided by C. Svanholm, KI, Stockholm). ELISA was carried out essentially as previously described [67].

Neutralization Assay

Immune mouse sera were pooled within each experimental group and were tested for the presence of neutralizing activity. Sera were heat-inactivated (56°C for 30 min) and serially diluted at 3-fold dilutions, starting at 1/20. Neutralization assay was performed as described earlier using replication of HIV-1 SF2 strain and the primary NSI/CCR5 tropic clade B isolate 6920 in PBMCs as readout system [65]. Virus production was measured in a p24Gag antigen capture ELISA [25]. An HIV-1-positive serum pool (HIVIG) and the human mAb 2F5, specific for the gp41 ELDKWS epitope, were used as a positive control. Neutralization was defined as the sample titer resulting in 50% reduction (NT₅₀) of p24Gag antigen in the supernatant compared with p24Env antigen content when the virus was incubated in the presence of HIV Ab from negative serum. All assays were repeated at least twice.

Statistical Analysis

The statistical significance of differences between groups was calculated by the one-way nonparametric Kruskal-Wallis test followed by Dunn's multiple comparison posttest IgG1/IgG2a ratios were compared using a two-tailed Student *t* test. Statistical analysis was performed using GraphPad PRISM software version 5.0 (GraphPad Software, Inc). P-values were considered to be significant if less than 0.05. Experiments were repeated twice.

Supporting Information

Figure S1 Effect of *Mtb* infection on HIV-specific serum IgG titers induced in mice by MultiHIV DNA vaccination followed by protein boost. Uninfected or *Mtb*-infected C57BL/6 mice were immunized and boosted with MultiHIV DNA/protein, as described in Materials and Methods. 4 wk post-vaccination HIV-specific serum IgG levels were assayed with HIV antigen-ELISA using Tat and Nef as coating antigens, as described in Materials and Methods. Median endpoint titer of 6–8 mice/group from one individual experiment is shown as a solid line. The box defines the 75th and 25th percentiles and the whiskers define the maximum and minimum values. Dashed line indicates the ELISA sensitivity threshold. HIV-specific serum IgG levels were assayed in two separate experiments. (TIF)

Figure S2 Bacterial loads in lungs of mice 17 wk post-infection with *Mtb*. C57BL/6 mice aerogenically infected with low dose *Mtb* (50–100 bacteria/lung) were, 7 wk later, vaccinated i.n. or i.m. with MultiHIV DNA in N3 adjuvant followed by two booster inoculations of HIV proteins in L3 adjuvant (details in Materials and Methods). Control group of mice was left unvaccinated. Lung homogenates from mice sacrificed 17 wk post-infection were plated on Middlebrook agar and bacterial CFU were enumerated as described in Materials and Methods. Median lung CFU value of 6–8 mice/group from individual experiment is shown as a solid line. The box defines the 75th and 25th percentiles and the whiskers define the maximum and minimum values. The bacterial load was determined in two separate experiments. (TIF)

Author Contributions

Conceived and designed the experiments: LI AP JH GK. Performed the experiments: LI JM AP MS CL. Analyzed the data: LI AP JM. Contributed reagents/materials/analysis tools: JH MS. Wrote the paper: AP LI GK MS.

References

1. AIDS epidemic update November 2009, UNAIDS, WHO (http://data.unaids.org/80/pub/Report/2009/JC1700_Epi_Update_2009_en.pdf).
2. Talbot HK, Libster R, Edwards K (2012) Influenza vaccination for older adults. *Hum Vaccin Immunother* 8: [Epub ahead of print].
3. Iyer SS, Chatraw JH, Tan WG, Wherry EJ, Becker TC, et al. (2012) Protein energy malnutrition impairs homeostatic proliferation of memory CD8 T cells. *J Immunol* 188: 77–84.
4. Whittle HC, Bradley-Moore A, Fleming A, Greenwood BM (1973) Effects of measles on the immune response of Nigerian children. *Arch Dis Child* 48: 753–756.
5. Williamson WA, Greenwood BM (1978) Impairment of the immune response to vaccination after acute malaria. *Lancet* 1: 1328–1329.
6. Cunningham AJ, Riley EM (2010) Suppression of vaccine responses by malaria: insignificant or overlooked? *Expert Rev Vaccines* 9: 409–429.
7. Usen S, Milligan P, Etchevarenaux C, Greenwood B, Mulholland K (2000) Effect of fever on the serum antibody response of Gambian children to *Haemophilus influenzae* type b conjugate vaccine. *Pediatr Infect Dis J* 19: 444–449.
8. Dauby N, Alonso-Vega C, Suarez E, Flores A, Hermann E, et al. (2009) Maternal infection with *Trypanosoma cruzi* and congenital Chagas disease induce a trend to a type 1 polarization of infant immune responses to vaccines. *PLoS Negl Trop Dis* 3: e571.
9. Urban JF Jr, Steenhard NR, Solano-Aguilar GI, Dawson HD, Iweala OI, et al. (2007) Infection with parasitic nematodes confounds vaccination efficacy. *Vet Parasitol* 148: 14–20.
10. Harries AD, Zachariah R, Corbett EL, Lawn SD, Santos-Filho ET, et al. (2010) The HIV-associated tuberculosis epidemic-when will we act? *Lancet* 375: 1906–1919.
11. Pawlowski A, Jansson M, Sköld M, Rottenberg ME, Källenius G (2012) Tuberculosis and HIV co-infection. *PLoS Pathog* 8: e1002464.
12. Diedrich CR, Flynn JL (2011) HIV/*M. tuberculosis* co-infection immunology: How does HIV exacerbate TB? *Infect Immun* 79: 1407–1417.
13. Lawn SD, Butera ST, Folks TM (2001) Contribution of immune activation to the pathogenesis and transmission of human immunodeficiency virus type 1 infection. *Clin Microbiol Rev* 14: 753–777.
14. Cingolani A, Cozzi Lepri A, Castagna A, Goletti D, De Luca A, et al. (2012) Impaired CD4 T-cell count response to combined antiretroviral therapy in antiretroviral-naïve HIV-infected patients presenting with tuberculosis as AIDS-defining condition. *Clin Infect Dis* 54: 853–861.
15. Poropatich K, Sullivan DJ Jr. (2011) Human immunodeficiency virus type 1 long-term non-progressors: the viral, genetic and immunological basis for disease non-progression. *J Gen Virol* 92: 247–268.
16. Masopust D (2009) Developing an HIV cytotoxic T-lymphocyte vaccine: issues of CD8 T-cell quantity, quality and location. *J Intern Med* 265: 125–137.
17. Owen RE, Heitman JW, Hirschhorn DF, Lanteri MC, Biswas HH, et al. (2010) HIV+ elite controllers have low HIV-specific T-cell activation yet maintain strong, multifunctional T-cell responses. *AIDS* 24: 1095–1105.
18. Tomaras GD, Haynes BF (2010) Strategies for eliciting HIV-1 inhibitory antibodies. *Curr Opin HIV AIDS* 5: 421–427.
19. Mikell I, Sather DN, Kalam SA, Altfield M, Alter G, et al. (2011) Characteristics of the earliest cross-neutralizing antibody response to HIV-1. *PLoS Pathog* 7: e1001251.
20. Belyakov IM, Ahlers JD (2012) Mucosal immunity and HIV-1 infection: applications for mucosal AIDS vaccine development. *Curr Top Microbiol Immunol* 354: 157–179.
21. Perrin H, Canderan G, Sékaly RP, Trautmann L (2010) New approaches to design HIV-1 T-cell vaccines. *Curr Opin HIV AIDS* 5: 368–376.
22. Kim JH, Rerks-Ngarm S, Excler JL, Michael NL (2010) HIV vaccines: lessons learned and the way forward. *Curr Opin HIV AIDS* 5: 428–434.
23. Rerks-Ngarm S, Pitisuttithan P, Nitayaphan S, Kaewkungwal J, Chiu J, et al. (2009) Vaccination with ALVAC and AIDSVAX to prevent HIV-1 infection in Thailand. *N Engl J Med* 361: 2209–2220.
24. Sandström E, Nilsson C, Hejdeman B, Bråve A, Bratt G, et al. (2008) Broad immunogenicity of a multigene, multiclade HIV-1 DNA vaccine boosted with heterologous HIV-1 recombinant modified vaccinia virus Ankara. *J Infect Dis* 198: 1482–1490.
25. Foulds KE, Wu CY, Seder RA (2006) Th1 memory: implications for vaccine development. *Immunol Rev* 211: 58–66.
26. Haynes BF, Liao HX, Tomaras GD. Is developing an HIV-1 vaccine possible? (2010) *Curr Opin HIV AIDS* 5: 362–367.
27. Gizurason S, Sigurdardóttir M, Stanzeit B (1998) Selective augmentation of antibodies in various mucosal regions, after intranasal immunization with diphtheria in mice. *J Pharm Sci* 87: 1267126–9.
28. Burgers WA, Chege GK, Müller TL, van Harmelen JH, Khoury G, et al. (2009) Broad, high-magnitude and multifunctional CD4+ and CD8+ T-cell responses elicited by a DNA and modified vaccinia Ankara vaccine containing human immunodeficiency virus type 1 subtype C genes in baboons. *J Gen Virol* 90: 468–480.
29. Dubos RJ, Schaedler RW (1957) Effects of cellular constituents of mycobacteria on the resistance of mice to heterologous infections I. Protective effects. *J Exp Med* 106: 703–717.
30. Schaedler RW, Dubos RJ (1957) Effects of cellular constituents of mycobacteria on the resistance of mice to heterologous infections. II. Enhancement of infection. *J Exp Med* 106: 719–726.
31. Nookala S, Srinivasan S, Kaliraj P, Narayanan RB, Nutman TB (2004) Impairment of tetanus-specific cellular and humoral responses following tetanus vaccination in human lymphatic filariasis. *Infect Immun* 72: 2598–2604.
32. Elias D, Akuffo H, Pawlowski A, Haile M, Schön T, et al. (2005) *Schistosoma mansoni* infection reduces the protective efficacy of BCG vaccination against virulent *Mycobacterium tuberculosis*. *Vaccine* 23: 1326–1334.
33. Greenwood BM, Bradley AK, Blakebrough IS, Whittle HC, Marshall TF, et al. (1980) The immune response to a meningococcal polysaccharide vaccine in an African village. *Trans R Soc Trop Med Hyg* 74: 340–346.
34. Bradley-Moore AM, Greenwood BM, Bradley AK, Bartlett A, Bidwell DE, et al. (1985) Malaria chemoprophylaxis with chloroquine in young Nigerian children. II. Effect on the immune response to vaccination. *Ann Trop Med Parasitol* 79: 563–573.
35. McGregor IA, Barr M (1962) Antibody response to tetanus toxoid inoculation in malarious and non-malarious Gambian children. *Trans R Soc Trop Med Hyg* 56: 364–367.
36. Bassat Q, Guinovart C, Sigaube B, Mandomando I, Aide P, et al. (2009) Severe malaria and concomitant bacteraemia in children admitted to a rural Mozambican hospital. *Trop Med Int Health* 14: 1011–1019.
37. Kublin JG, Patnaik P, Jere CS, Miller WC, Hoffman IF, et al. (2005) Effect of *Plasmodium falciparum* malaria on concentration of HIV-1-RNA in the blood of adults in rural Malawi: a prospective cohort study. *Lancet* 365: 233–240.
38. Sartono E, Lisse IM, Terveer EM, van de Sande PJ, Whittle H, et al. (2010) Oral polio vaccine influences the immune response to BCG vaccination. A natural experiment. *PLoS One* 5: e10328.
39. Slika MK, Homann D, Tishon A, Pagarigan R, Oldstone MB (2003) Measles virus infection results in suppression of both innate and adaptive immune responses to secondary bacterial infection. *J Clin Invest* 111: 805–810.
40. Elias D, Akuffo H, Thors C, Pawlowski A, Britton S (2005) Low dose chronic *Schistosoma mansoni* infection increases susceptibility to *Mycobacterium bovis* BCG infection in mice. *Clin Exp Immunol* 139: 398–404.
41. Hartgers FC, Yazdanbakhsh M (2006) Co-infection of helminths and malaria: modulation of the immune responses to malaria. *Parasite Immunol* 28: 497–506.
42. Cooper PJ, Chico M, Sandoval C, Espinel I, Guevara A, et al. (2001) Human infection with *Ascaris lumbricoides* is associated with suppression of the interleukin-2 response to recombinant cholera toxin B subunit following vaccination with the live oral cholera vaccine CVD 103-HgR. *Infect Immun* 69: 1574–1580.
43. Subbramanian RA, Xu J, Toma E, Morriset R, Cohen EA, et al. (2002) Comparison of human immunodeficiency virus (HIV)-specific infection-enhancing and -inhibiting antibodies in AIDS patients. *J Clin Microbiol* 40: 2141–2146.
44. Thornton AM, Shevach EM (2000) Suppressor effector function of CD4+CD25+ immunoregulatory T cells is antigen nonspecific. *J Immunol* 164: 183–190.
45. von Boehmer H (2005) Mechanisms of suppression by suppressor T cells. *Nat Immunol* 6: 338–344.
46. Hu G, Liu Z, Zheng C, Zheng SG (2010) Antigen-non-specific regulation centered on CD25+Foxp3+ Treg cells. *Cell Mol Immunol* 7: 414–418.
47. Marin ND, Paris SC, Vélez VM, Rojas CA, Rojas M, et al. (2010) Regulatory T cell frequency and modulation of IFN-gamma and IL-17 in active and latent tuberculosis. *Tuberculosis (Edinb)* 90: 252–261.
48. Kursar M, Koch M, Mitrücker HW, Nouailles G, Bonhagen K, et al. (2007) Cutting Edge: Regulatory T cells prevent efficient clearance of *Mycobacterium tuberculosis*. *J Immunol* 178: 2661–2665.
49. Chen X, Zhou B, Li M, Deng Q, Wu X, et al. (2007) CD4+CD25+FoxP3(+) regulatory T cells suppress *Mycobacterium tuberculosis* immunity in patients with active disease. *Clin Immunol* 123: 50–59.
50. Balmelli C, Demotz S, Acha-Orbea H, De Grandi P, Nardelli-Haeffliger D (2002) Trachea, lung, and tracheobronchial lymph nodes are the major sites where antigen-presenting cells are detected after nasal vaccination of mice with human papillomavirus type 16 virus-like particles. *J Virol* 76: 12596–12602.
51. World Health Organization (2009) Global tuberculosis control: a short update to the 2009 report. Geneva: World Health Organization. vi, 39 p.
52. Lin PL, Flynn JL (2010) Understanding latent tuberculosis: a moving target. *J Immunol* 185: 15–22.
53. Sherman DR, Gagneux S (2011) Estimating the mutation rate of *Mycobacterium tuberculosis* during infection. *Nat Genet* 43: 400–401.
54. Ford CB, Lin PL, Chase MR, Shah RR, Iartchouk O, et al. (2011) Use of whole genome sequencing to estimate the mutation rate of *Mycobacterium tuberculosis* during latent infection. *Nat Genet* 43: 482–486.
55. Cardona PJ (2009) A dynamic reinfection hypothesis of latent tuberculosis infection. *Infection* 37: 80–86.
56. Capuano SV, Croix DA, Pawar S, Zinovik A, Myers A, et al. (2003) Experimental *Mycobacterium tuberculosis* infection of cynomolgus macaques closely resembles the various manifestations of human *M. tuberculosis* infection. *Infect Immun* 71: 5831–5844.

57. Lin PL, Rodgers M, Smith L, Bigbee M, Myers A, et al. (2009) Quantitative comparison of active and latent tuberculosis in the cynomolgus macaque model. *Infect Immun* 77: 4631–4642.
58. Mtei L., Matee M., Herfort O., Bakari M., Horsburgh, C R., Waddell R., Cole, B F., et al. (2005) High rates of clinical and subclinical tuberculosis among HIV-infected ambulatory subjects in Tanzania. *Clin Infect Dis* 40: 1500–1507.
59. Cunningham J, Perkins M (2006) Diagnostics for tuberculosis: global demand and market potential. WHO. Geneva, Switzerland. http://whqlibdoc.who.int/publications/2006/9241563303_eng.pdf.
60. Hamasur B, Haile M, Pawlowski A, Schröder U, Williams A, et al. (2003) *Mycobacterium tuberculosis* arabinomannan-protein conjugates protect against tuberculosis. *Vaccine* 21: 4081–4093.
61. Leepiyasakulchai C, Ignatowicz L, Pawlowski A, Källenius G, Sköld M (2012) Failure to recruit anti-inflammatory CD103+ dendritic cells and a diminished CD4+ Foxp3+ regulatory T cell pool in mice that display excessive lung inflammation and increased susceptibility to *Mycobacterium tuberculosis*. *Infect Immun* 80: 1128–1139.
62. Hinkula J, Devito C, Zuber B, Benthin R, Ferreira D, et al. (2006) A novel DNA adjuvant, N3, enhances mucosal and systemic immune responses induced by HIV-1 DNA and peptide immunizations. *Vaccine* 24: 4494–4497.
63. Bråve A, Johansen K, Palma P, Benthin R, Hinkula J (2008) Maternal immune status influences HIV-specific immune responses in pups after DNA prime protein boost using mucosal adjuvant. *Vaccine* 26: 5957–5966.
64. Asakura Y, Lundholm P, Kjerrström A, Benthin R, Lucht E, et al. (1999) DNA-plasmids of HIV-1 induce systemic and mucosal immune responses. *Biol Chem* 380: 375–379.
65. Lundholm P, Asakura Y, Hinkula J, Lucht E, Wahren B (1999) Induction of mucosal IgA by a novel jet delivery technique for HIV-1 DNA. *Vaccine* 17: 2036–2042.
66. Devito C, Levi M, Broliden K, Hinkula J (2000) Mapping of B-cell epitopes in rabbits immunised with various gag antigens for the production of HIV-1 gag capture ELISA reagents. *J Immunol Methods* 238: 69–80.
67. Devito C, Zuber B, Schröder U, Benthin R, Okuda K, et al. (2004) Intranasal HIV-1-gp160-DNA/gp41 peptide prime-boost immunization regimen in mice results in long-term HIV-1 neutralizing humoral mucosal and systemic immunity. *J Immunol* 173: 7078–7089.

IV

**A murine model of *Mycobacterium tuberculosis*/HIV-1 co-infection for
studies on pathogen-specific T cell responses in vivo**

Running title: A murine model of *M. tuberculosis*/HIV-1 co-infection

Chaniya Leepiyasakulchai¹, Lech Ignatowicz¹, Lalit Rane¹ and Markus Sköld^{1*}

¹Department of Microbiology, Tumor and Cell Biology, Karolinska Institutet, Stockholm, Sweden

*Corresponding author. Mailing address: Department of Microbiology, Tumor and Cell Biology, Karolinska Institutet, Nobels väg 16, Box 280, 171 77 Stockholm, Sweden, Phone: +46-(0)8-524-85989, Fax: +46-(0)8-31-1101, E-mail: markus.skold@ki.se

Abstract

Mycobacterium tuberculosis (Mtb), the causative agent of pulmonary tuberculosis (TB), is the biggest killer of people with HIV-1/AIDS. In the present study, we took advantage of the chimeric virus EcoNDK, which is a HIV-1-like virus that infects immunocompetent wild-type mice, to establish a murine model of Mtb/HIV-1 co-infection. This model system enabled us to study how Mtb-specific CD8⁺ T cell responses are affected during co-infection in vivo. Since most co-infected individuals first encounter Mtb before they are exposed to HIV-1, we decided to first infect BALB/c or DBA/2 mice with a low dose of virulent Mtb via the respiratory route. Three weeks post infection; the animals were injected with a single dose of the virus intraperitoneally to establish Mtb/EcoNDK co-infection. After an additional two weeks, we examined viral replication and found a significantly higher viral load in Mtb/EcoNDK co-infected mice compared to animals that were infected with EcoNDK alone. We show that during pulmonary TB, the number of TB10.4-specific CD8⁺ T cells is significantly higher in resistant BALB/c mice than in susceptible DBA/2 mice. In the context of co-infection, we observed an increased number of TB10.4-specific CD8⁺ T cells in co-infected mice, suggesting that viral replication was affecting Mtb-specific T cell responses. Furthermore, irrespective of the virus, programmed-death 1 (PD1) and T cell immunoglobulin and mucin domain 3 (Tim3) are differently expressed on CD4⁺ and CD8⁺ T cells during pulmonary TB. Also, antigen-specific CD8⁺ T cells were enriched for Tim3-expressing cells, especially in the Mtb-infected lungs. Finally, Tim3⁺ TB10.4-reactive CD8⁺ T cells in Mtb-infected and in Mtb/EcoNDK-infected mice contained a high frequency of TNF- and IFN- γ -producing cells. Even though we did not detect signs of immuno-deficiency in co-infected animals, the murine model may provide a useful tool to better understand how host immune responses are affected during the early stage of Mtb/EcoNDK co-infection.

Introduction

Mycobacterium tuberculosis (Mtb), the causative agent of pulmonary tuberculosis (TB), kills nearly 2 million people annually and is one of the leading causes of death from infectious disease in the world. The emergence of multi-drug resistant and extensively drug-resistant strains of the bacterium in eastern European countries and elsewhere, and the high mortality among human immunodeficiency virus-1⁺ (HIV-1⁺) patients co-infected with Mtb, demonstrate the urgent need for new efficient vaccines and treatment regimens. The failure of current vaccine strategies clearly shows that we do not fully understand what constitutes protective immunity against Mtb or HIV-1, and how co-infection exacerbates disease progression. As a result, Mtb remains the largest killer of HIV-1-infected individuals and a threat to global health (reviewed in (1)).

Dendritic cells are important antigen presenting cells and initiate the adaptive immune response by priming T lymphocytes in the pulmonary lymph nodes (PLN) draining the lung tissue (2). Activated Mtb-specific T cells are essential for control of Mtb growth and are recruited to the infected lungs where they help reduce bacterial replication via lysis of infected cells, or indirectly via production of pro-inflammatory cytokines that activate infected macrophages. Despite a seemingly robust immune response, Mtb causes chronic infection. In fact, both Mtb and HIV-1 cause chronic infection and chronic immune activation. During HIV-1 infection, B- and T cells have an activated phenotype, including polyclonal B cell expansion and increased T cell turnover as well as increased serum levels of pro-inflammatory mediators in HIV-1⁺ patients (reviewed in (3)). Chronic immune activation and misdirected host immune reactions in response to Mtb and HIV-1 are contributing factors to the pathogenesis in humans and in animal models.

Constant antigenic stimulation can result in T cell exhaustion, which is characterized by a persistent, but dysfunctional, effector T cell population displaying loss of functional potential, i.e. cytokine production and cytotoxic activity, and proliferative ability in response to antigen stimulation. Programmed-death 1 (PD1) and T cell immunoglobulin and mucin domain 3 (Tim3) are two examples of markers of T cell exhaustion in HIV-1⁺ patients (4-6). Both molecules are involved in downregulating host immune responses and play a role in maintaining T cell tolerance. Interestingly, even though Tim3 was first identified as a cell surface marker for IFN- γ -producing CD4⁺ and CD8⁺ T cells, it has recently been used as an exhaustion marker for virus-specific CD8⁺ T cells in patients with chronic progressive HIV-1 infection (6, 7). It has also been reported that Tim-3 is upregulated on Mtb-specific CD8⁺ T cells in TB patients (8). Similar inhibitory receptor/ligand interactions may therefore play a role in modulating host immunity to both HIV-1 and Mtb in humans.

To be able to study how Mtb/HIV-1 co-infection influences Mtb-specific T cell responses *in vivo*, we took advantage of the murine model of pulmonary TB and the modified virus EcoNDK (clade D NDK backbone) published by Potash and colleagues (9). EcoNDK enables

infection of immuno-competent wild-type (WT) mice with a chimeric virus similar to HIV-1 and only have one HIV-1 protein (gp120) replaced with gp80 from ecotropic murine leukemia virus. Importantly, the chimeric virus model reproduces many aspects of HIV-1 infection in humans (9). Here, we confirm that EcoNDK can infect primary murine cells in vitro and that the virus establishes infection in BALB/c and DBA/2 mice. Interestingly, even though the virus did not influence bacterial replication, or exacerbated disease progression, we detected significantly higher amounts of viral DNA in animals co-infected with Mtb. During the early stage of Mtb/EcoNDK co-infection, our results suggests that the Mtb-specific CD8⁺ T cell population was increased in co-infected mice compared to animals infected with Mtb alone. Also, we found that the cell surface expression profile of PD1 and Tim3 differed between CD4⁺ and CD8⁺ T cells and that both markers were enriched on TB10.4-specific CD8⁺ T cells. Finally, Tim3 expression identifies TB10.4-reactive CD8⁺ T cells enriched for IFN- γ and TNF producers in both Mtb-infected and in Mtb/EcoNDK co-infected animals.

Materials and Methods

Bacteria and Virus preparation

Mtb (Harlingen strain) was prepared as previously described (10). In brief, bacteria were grown to mid-log phase in Sauton media supplemented with eight mg/ml polymyxin B and five mg/ml Fungizol at 37°C, aliquoted and stored in media containing 10% glycerol at -80°C. Virus stocks were prepared as described by Potash et al (9). *E. coli* DH5a containing the EcoNDK-coding plasmid (kindly provided by David Volsky, Columbia University, New York, NY, USA) was grown in LB media supplemented with 100 µg/ml Ampicillin (Sigma-Aldrich) and incubated in 37°C until an OD of 0.7 was reached. Plasmid DNA was isolated from pelleted bacteria using a Qiagen Mega Plasmid kit according to the manufacturer's instructions. 293T cells grown in DMEM supplemented with 10% inactivated fetal bovine serum, penicillin/streptomycin, L-glutamine, sodium-pyruvate (Invitrogen) were transfected with plasmid DNA, using (Polyscience, USA) as a transfection enhancing agent in 1:2 w/w ratio. Supernatants containing viral particles were collected after 48 and 72 h, concentrated by centrifugation (10,000 × g) and titrated for p24 content by ELISA (Biomérieux). Generation of the chimeric virus was performed in the BSL-3 facility at the Department of Microbiology, Tumor and Cell Biology (MTC), Karolinska Institutet.

Animal infections

Six-week-old female C57BL/6, BALB/c or DBA/2 mice were obtained from the breeding facility at MTC, or from Charles River (Germany). The animals were infected aerogenically with a low dose of Mtb (50-100 CFU/lung) using a nose-only aerosol exposure apparatus (In-Tox Products, Moriarty, NM) as previously described (10). The lung inoculum was verified by agar plating of total lung homogenates 24 h after infection.

For EcoNDK infection, groups of mice were injected intraperitoneally (IP) with 0.2 µg EcoNDK virus suspension (measured as amount of p24 protein) in sterile PBS. Work with Mtb- and Mtb/EcoNDK co-infected animals was conducted in a BSL-3 containment laboratory at the Astrid Fagraeus laboratory, Karolinska Institutet. All animal experiments were approved by the local animal ethics committee and the Swedish Board of Agriculture (permit number N313/09). The health status of the animals was monitored daily by Animal Care Technicians and the animals weight was recorded to ensure humane treatment.

Organ collection and sample preparation

At the indicated time points, lung homogenates, or single-cell suspensions were prepared from lungs and spleen. The mice were euthanized and blood removed from the lung tissue by perfusing the heart with sterile PBS. The organs were aseptically removed and placed in RPMI 1640 medium. The lungs were cut into small pieces and incubated in complete RPMI 1640 medium (supplemented with 10% fetal calf serum, penicillin/streptomycin, L-glutamine,

sodium-pyruvate, β -mercaptoethanol and HEPES buffer, all from Sigma-Aldrich) containing 140 U/ml collagenase type IV (Sigma-Aldrich). The digested lung tissue was passed through a steel mesh cup sieve (Sigma-Aldrich). Any remaining erythrocytes were lysed using a lysis buffer (0.15 M NH_4Cl , 1 mM KHCO_3 , 0.1 mM NaEDTA, pH 7.2-7.4), washed and re-suspended in RPMI 1640 medium. The cell suspension was passed through a 70 μm cell strainer (BD Falcon), washed and re-suspended in complete RPMI 1640 medium. Single-cell suspensions of total spleens were obtained using the frosted ends of two glass slides. Erythrocytes were lysed with lysis buffer and the cells were washed with PBS and re-suspended in complete DMEM. Total viable cells were enumerated using a hemocytometer and trypan blue exclusion of dead cells. For CFU determination, the right lobe of the lungs was homogenized in PBS with 0.02% Tween 80 and serial dilutions of lung homogenates were plated onto Middlebrook 7H11 agar plates. For day one timepoints, the total lung tissue was used to determine the CFU. Colonies were counted after a two to three week incubation at 37°C.

Cell stimulation and flow cytometry

For determination of cytokine- or p24 production, single cell suspensions were kept in complete DMEM medium, or were stimulated with a TB10.3/10.4₂₀₋₂₈-peptide (1 $\mu\text{g}/\text{ml}$), or with 50 ng/ml phorbol 12-myristate 13-acetate (PMA) (Sigma-Aldrich) and 100 ng/ml ionomycin (Sigma-Aldrich) in the presence of 10 $\mu\text{g}/\text{ml}$ Brefeldin A for 4 h at 37°C, 5% CO_2 . After incubation, the cells were washed with FACS buffer (PBS, 1% fetal bovine serum, 2 mM NaN_3) and incubated with purified anti-mouse CD16/CD32 (2.4G2, BD Bioscience) at 20 $\mu\text{g}/\text{ml}$ for 15 min at 4°C to block nonspecific binding (Fc block). The cells were washed and incubated 15 min at 4°C with primary antibodies specific for surface makers, or appropriate isotype controls, diluted in FACS buffer. A FITC-labeled anti-p24 monoclonal antibody (mAb) (KC57) and an isotype control mAb were obtained from Beckman Coulter. PerCP- or PE-Cy7-conjugated anti-CD8 α (53-6.7), anti-CD3 ϵ (145.2C11) and isotype controls were purchased from BD Pharmingen. Anti-TNF-FITC (MP6-XT22), anti-IFN- γ -PE-Cy7 (XMG1.2), anti-CD19-Alexa Fluor 450 (1D3), anti-Tim3-Alexa Fluor 647 (B8.2CL2), anti-Alexa Fluor 780 (L3T4) and isotype control mAbs were purchased from eBioscience.

For TB10.4 antigen-specific staining, cells were additionally stained with TB10.3/10.4₂₀₋₂₈-loaded H-2K^d multimer-PE reagent (ProImmune, Oxford, UK, or from the NIH Tetramer Facility) according to manufacturer's instructions. After washing, cells were fixed with 2% paraformaldehyde. For intracellular staining, the cells were permeabilized using a permeabilization buffer (eBioscience) and incubated for 20 min at 20°C with antibodies specific for intracellular cytokines or relevant isotype control mAbs. The cells were washed twice with permeabilization buffer and once with FACS buffer, re-suspended and analyzed by flow cytometry using a BD FACSCanto or a BD LSR II flow cytometer (BD Biosciences).

Data analysis was performed using the FlowJo software (version 8.8.6, Tree Star). All mice were analyzed individually.

Virus infection in vitro

Spleen cells were collected as describe before and cultured in full DMEM media supplemented with recombinant IL-2 (10 µg/ml) and stimulated with Concanavalin-A (ConA, 5 µg/ml) for four to five days. Activated cells, or human CEM T cells, were then washed and infected directly with purified EcoNDK virus (10 ng/ml). Alternatively, activated murine cells were co-cultured directly with transfected 293T cells or with transfected 293T cells separated by porous (0.45 µm) insert (Millipore). Cells were incubated in complete DMEM media at 37°C, 5% CO₂. After 48-72 h, the cells were harvested and stained for intracellular p24 as described before.

Quantitative PCR (QPCR)

The presence of EcoNDK DNA was analyzed in infected spleen and lung cells isolated using DNAzol (Invitrogen) according to manufacturer's instructions. QPCR amplification was carried out with primers EcoHIVF (5'-ATGATCTGTAGTGCTGCGCGTTCAACG-3') and EcoNDKR (5'-GAGCCGGGCGAAGCAGTACTGACCCCTC-3') and Taqman Sybr green (Sigma Aldrich). Values were normalized to GAPDH gene copy number and calculated as copies per million cells (9).

Results

Productive viral infection of primary murine cells in vitro

Modeling HIV-1 infection in rodents presents numerous obstacles. Due to the inability of HIV-1 to infect other species than primates, two main strategies to create working model systems have been developed. One is to modify, or replace, components of the murine immune system with human molecules or cells. Another is to modify the virus itself, such as the chimeric EcoHIV and EcoNDK viruses, allowing for productive viral infection of immunocompetent WT mice (9, 11). In this study, we utilized the EcoNDK virus to establish a unique small animal model of Mtb/HIV-1 co-infection.

First, we set up an in vitro assay to determine the scale of infectivity of in vitro generated viral particles. Splenic T cells from naïve BALB/c mice were activated in vitro using ConA and IL-2. The activated cells were then exposed to concentrated EcoNDK virus. Alternatively, the cells were co-cultured either directly with transfected 293T cells, or co-cultured with transfected 293T cells separated by a porous membrane that allowed newly formed viral particles to pass through. The cells were harvested after 48 or 72 h and analyzed for intracellular p24 expression to determine the frequency of infected cells.

Infection of activated splenocytes using concentrated virus resulted in the lowest frequency of infected murine cells. Approximately 0,5% of the target cells stained positive for p24 (figure 1A). By culturing the murine cells with transfected 293T cells that were separated by a porous insert, we increased the infection rate to ~1%. In the cultures where transfected 293T cells were co-cultured directly with activated splenocytes, we also analyzed infected T cell subsets (figure 1B). Interestingly, only 2.1% of the CD8⁺ T cells were producing detectable levels of p24, whereas almost 10% of the CD4⁺ T cells were p24⁺. As expected, EcoNDK did not infect the HIV-1 permissive human CEM T cell line that remained p24-negative (data not shown) (9, 12). In conclusion, despite the reduced ability of murine cells to produce HIV-1 viral particles, we confirm previous observations made by Potash et al and showed the chimeric EcoNDK virus is able to establish productive infection of primary murine cells in vitro (9, 13-17).

No difference in body weight or in bacterial burden between Mtb-infected and Mtb/EcoNDK co-infected mice

Low-dose Mtb aerosol infection of mice mimics the natural route of Mtb infection in humans. As a result, the bacteria initially replicate in the lungs of infected animals and then first disseminates to the PLN draining the lung tissue and to other organs. To better understand protective host immune responses against Mtb, inbred mouse strains that are resistant or susceptible to pulmonary TB are commonly used. To determine if Mtb/EcoNDK co-infection accelerates disease progression in Mtb-susceptible DBA/2 mice compared to resistant BALB/c mice, we first infected groups of mice with Mtb (Harlingen strain) via the

respiratory route (figure 2). Three weeks later, groups of mice were co-infected with EcoNDK IP. Disease progression was monitored by weighing the animals (figure 2A) and by determining the bacterial burden in the lungs two weeks after Mtb/EcoNDK co-infection (figure 2B). During the course of the experiment, both BALB/c and DBA/2 mice steadily gained weight. In addition, we did not detect any significant differences in body weight between Mtb-infected and Mtb/EcoNDK co-infected animals (figure 2A).

To assess the impact of EcoNDK on the ability to control bacterial replication in the lungs at an early stage of Mtb/EcoNDK co-infection, groups of mice were sacrificed two weeks after virus inoculation and lung homogenates were plated on Middlebrook 7H11 agar plates (Figure 2B). Similar to the body weight, we did not detect any significant differences between co-infected and Mtb-infected animals, or between BALB/c and DBA/2 mice.

In summary, we have demonstrated that early after Mtb/EcoNDK co-infection, the virus does not interfere with the ability of the animals to control the bacterial burden in the lungs and it does not negatively influence the general health status of the animals as determined by body weight in Mtb-susceptible and resistant mouse strains.

Reduced numbers of antigen-specific CD8⁺ T cells in lungs of Mtb-susceptible DBA/2 mice

Mice lacking CD8⁺ T cells succumb prematurely after Mtb infection, showing that MHC class I-restricted CD8⁺ T cell responses are required for optimal protection during pulmonary TB (18, 19). TB10.4 is an immunogenic protein secreted by Mtb and elicits MHC-restricted T cell responses in both humans and in mice (20-22). Because both resistant BALB/c mice and susceptible DBA/2 mice express MHC class I of H-2^d, we were able to use the same MHC class I-multimer (H-2K^d) loaded with the same Mtb-derived peptide (TB10.4₂₀₋₂₈) to examine the antigen-specific CD8⁺ T cell compartment in infected lung tissue (figure 3). Three weeks post Mtb aerosol infection, the absolute number of TB10.4-specific CD8⁺ T cells was similar in the lungs of BALB/c and DBA/2 mice, although overall numbers of CD8 cells were higher in the infected lung tissue of BALB/c mice (figure 3B). As a negative control, the TB10.4-loaded H-2K^d-multimer reagent did not detect TB10.4-reactive CD8⁺ T cells in H-2^b-expressing C57BL/6 mice, or in uninfected BALB/c mice (figure 3A and data not shown). After week three post infection (pi), there was a dramatic difference in the number of TB10.4-specific CD8⁺ T cells in resistant BALB/c mice compared to susceptible DBA/2 mice. While the number of antigen-specific CD8⁺ T cells remained essentially unchanged in DBA/2 mice, the number of antigen-specific CD8⁺ T cells increased approximately 8-fold by week six pi in infected BALB/c lungs.

Delayed T cell priming may explain the late appearance of antigen-specific T cells after Mtb infection. However, this does not explain why the number of Mtb-specific CD8⁺ T cells failed to increase in infected DBA/2 at later timepoints. Perhaps one of the underlying causes

of the increased Mtb-susceptibility of DBA/2 mice is insufficient numbers of Mtb-specific CD8⁺ cells in the infected lungs.

Increased number of TB10.4-specific CD8⁺ T cells in the lungs and in the spleen of Mtb/EcoNDK co-infected animals

To investigate the possible impact that EcoNDK infection may have on the early Mtb-specific CD8⁺ T cell response in peripheral tissues and secondary lymphoid organs of BALB/c mice, we identified TB10.4-specific CD8⁺ T cells, as well as the total CD4⁺- and CD8⁺ T cell populations in Mtb-infected and in Mtb/EcoNDK co-infected lungs and spleens (figure 4). Two weeks post EcoNDK infection, the total number of CD4⁺ T cells and CD8⁺ T cells in the lungs and in the spleen was not significantly different in Mtb-infected mice compared to Mtb/EcoNDK co-infected animals (figure 4A). Furthermore, TB10.4-specific cells were identified in the CD8⁺ T cell compartment (figure 4B-C). Even though we observed a trend towards an increased percentage and absolute number of Mtb-specific CD8⁺ T cells in the co-infected lung tissue, the differences did not reach statistical significance (figure 4B). In the spleen, the percentage and the absolute number of TB10.4-specific CD8⁺ T cells was doubled in the Mtb/EcoNDK co-infected group of mice compared to the animals that were infected with Mtb alone. Both the difference in percentage and in absolute numbers reached statistical significance (figure 4B). It is worth pointing out that the frequency of TB10.4-specific CD8⁺ T cells in the spleen was 10-fold lower than in the infected lungs (figure 4B).

Surprisingly, we observed that in the lungs, but not in the spleen, the H-2K^d/TB10.4-multimer reagent stained CD8⁺ T cells in co-infected animals significantly brighter than in Mtb-infected mice (figure 4C). This finding suggests that Mtb-specific CD8⁺ T cells in co-infected lungs express higher cell surface levels of the $\alpha\beta$ T cell receptor ($\alpha\beta$ -TCR).

We have shown that EcoNDK infection does not negatively influence the number of total T cells in the lungs and in the spleen at an early stage of co-infection. Still, a more careful analysis of the Mtb-specific CD8⁺ T cell response revealed that during early co-infection, EcoNDK seems to influence the adaptive T cell response directed against the bacterium. This conclusion is based on the increased Mtb-specific CD8⁺ T cell population, and the higher cell surface expression of the $\alpha\beta$ -TCR on Mtb-specific CD8⁺ T cells, in co-infected mice. Importantly, this observation was dependent on the presence of viral DNA in the co-infected mice. Animals that were injected with the virus, but failed to establish a productive viral infection, did not display the observed changes in the CD8⁺ T cell compartment. Therefore, we continued by focusing on the functional potential of Mtb-specific CD8⁺ T cells in Mtb-infected and Mtb/EcoNDK co-infected animals.

Similar Tim3 and PD1 cell surface expression profiles on T cell subsets in Mtb-infected and Mtb/EcoNDK co-infected mice

PD1 and Tim3 are two examples of markers of T cell exhaustion in HIV-1⁺ patients. Both molecules are involved in downregulating host immune responses and play a role in maintaining T cell tolerance. For example, PD1 is expressed on a significant fraction of CD4⁺ and CD8⁺ T cells in healthy individuals (23). We compared the Tim3 and PD1 cell surface profiles on CD4⁺- and CD8⁺ T cell subsets in Mtb-infected- and in co-infected mice in order to determine if Mtb/EcoNDK co-infection influences the expression patterns in our murine model (figure 5).

Representative pseudo-color plots from one representative experiment are shown in figure 5A. Although we did not observe any significant differences between Mtb-infected- and Mtb/EcoNDK co-infected mice, the differences in Tim3 and PD1 expression between the T cell subsets in the lungs or in the spleen were apparent. We found that most CD4⁺ T cells in the lungs and in the spleen do not express Tim3 (5% or less), and not more than 15% of the lung CD4⁺ T cells and less than 10% of the spleen CD4⁺ T cells express PD1 (figure 5B-C). By staining for Tim3 and PD1 simultaneously, we were able to show that most CD4⁺ T cells in the lung that expressed Tim3 co-expressed PD1 (Figure 5A), and that this staining pattern was essentially reversed in the spleen.

Within the total lung CD8⁺ T cell population, around 10% expressed Tim3 or PD1. Similar to the CD4⁺ T cells in the lungs, most Tim3⁺CD8⁺ T cells were also PD1⁺. Because infection with EcoNDK seem to promote an increased number of TB10.4-specific CD8⁺ T cells, we investigated the PD1 and Tim3 profile on H-2K^d/TB10.4-multimer-positive and H-2K^d/TB10.4-multimer-negative CD8⁺ T cells. Strikingly, TB10.4-specific CD8⁺ T cells in the lungs are enriched for Tim3⁺ (~40%) or PD1⁺ cells (~20%) compared to CD8⁺ T cells that stained negative for the H-2K^d/TB10.4-multimer reagent (figure 5). Also, TB10.4-specific CD8⁺ T cells that were Tim3⁺ to a large extent co-expressed PD1 (figure 5A).

The cell surface expression profile of Tim3 on CD8⁺ T cells in the spleen was different from the lungs (figure 5). Tim3 expression on total CD8⁺ T cells was lower in the spleen, similar to the expression profile we found on total splenic CD4⁺ T cells. Still, we did observe increased Tim3 expression on TB10.4-specific CD8⁺ T cells, even though the number was lower than in the infected lung tissue.

In summary, Mtb-specific CD8⁺ T cells in the infected lungs contain the highest frequency of Tim3⁺ cells and a high percentage of PD1⁺ cells. Near 70% of the antigen-specific CD8⁺ T cells in the lungs expressed Tim3 or PD1 during pulmonary TB, or during the early stage of Mtb/EcoNDK co-infection.

Mtb-specific CD8⁺Tim3⁺ T cells in the lungs are enriched for cytokine producing cells during pulmonary TB and during the early stage of Mtb/EcoNDK co-infection

The pro-inflammatory cytokines TNF and IFN- γ are required for control of mycobacterial growth in humans and in animal models (24-29). Constant antigenic stimulation caused by chronic infections, such as TB and HIV-1/AIDS, can result in T cell exhaustion, which is characterized by a persistent, but dysfunctional, effector T cell population displaying loss of functional potential, i.e. cytokine production and cytotoxic activity, and proliferative ability in response to antigen stimulation. T cell exhaustion may therefore help explain the failure of the immune system to eradicate chronic infections. We analyzed the cytokine profile in our experimental model systems to determine if we would detect signs of antigen-specific T cell exhaustion at an early stage of Mtb/EcoNDK co-infection (five weeks after Mtb infection and two weeks after EcoNDK infection) compared to the T cell activity in animals infected with Mtb alone (week five pi). Similar to the PD1 and Tim3 cell surface expression profiles, we did not detect any significant differences in cytokine production by T cells isolated from Mtb-infected mice or Mtb/EcoNDK co-infected mice (figure 6).

After polyclonal stimulation, around 20% of Tim3⁺CD4⁺ T cells produced both TNF and IFN- γ , and approximately 10% of the Tim3⁺CD4⁺ T cells produced one of the cytokines (figure 6A-B). Among Tim3⁻CD4⁺ T cells, the majority produced only TNF and 10% of the cells were able to produce both TNF and IFN- γ (figure 6A-B). Within the Tim3⁺CD8⁺ T cell subset, ~40% of the cells producing both TNF and IFN- γ after polyclonal stimulation. Approximately 30% of the Tim3⁺CD8⁺ T cells produced IFN- γ only and essentially no cells were TNF single-producers (figure 6A, C).

Even though PMA and ionomycin stimulation will reveal the functional potential of the T cell subsets, antigen-specific stimulation is more physiologically relevant (figure 6D-E). We used the same TB10.4 peptide for restimulation of the CD8⁺ T cells in vitro that was loaded onto the MHC class I-multimers for detection of Mtb-specific CD8⁺ T cells in infected organs (figures 3-5). Antigen-specific stimulation of CD8⁺ T cells isolated from the lungs of Mtb-infected mice, or from Mtb/EcoNDK co-infected animals, revealed that the Tim3⁺ subset was enriched for cells producing pro-inflammatory cytokines (figure 6D-E). It is noteworthy that ~45% of the Tim3⁺CD8⁺ T cells expressed both TNF and IFN- γ , while only ~10% of the Tim3⁻CD8⁺ cells expressed both cytokines. Irrespective of Tim3 expression, TB10.4-peptide stimulated cells contained few single-producers compared to the CD8⁺ T cells that were polyclonally activated (compare figure 6C and figure 6E).

We determined the cytokine profile among TB10.4-reactive CD8⁺ T cells in the lungs of co-infected mice and found that at the early stage of Mtb/EcoNDK co-infection, the Tim3 cell surface marker identifies CD8⁺ T cells that are enriched for both TNF- and IFN- γ -producing cells.

Increased viral load in peripheral tissues and secondary lymphoid organs of Mtb/EcoNDK co-infected mice compared to EcoNDK-infected animals

Mtb infection leads to increased viral replication in Mtb/HIV-1 co-infected patients, including in the lungs. Therefore, we determined if there was a difference in the amount of provirus in peripheral tissues and secondary lymphoid organs during EcoNDK infection and during Mtb/EcoNDK co-infection. We isolated genomic DNA from lungs and spleen of BALB/c mice and performed QPCR amplification of an EcoNDK-specific region of the gag gene using the GAPDH gene as a reference (figure 7). Similar to what has been published by other investigators, approximately 80% of the mice that were inoculated with the virus were positive for the gag gene specific for the chimeric virus in the lungs and in the spleen (9). Animals that were negative for the PCR product were excluded from the study.

EcoNDK established a productive infection both in the spleen and in the lungs, with levels averaging 600-650 infected cells/ 10^6 total cells in the spleen and 150-250 infected cells/ 10^6 total cells in the lungs. In mice infected with Mtb prior to EcoNDK inoculation, the overall levels of proviral DNA was significantly higher in both organs. The amount of viral DNA in the spleens of co-infected animals was 1.5 times higher than in EcoNDK-infected animals while in the lungs, the difference was almost double.

The total number of cells increases dramatically in peripheral tissues and secondary lymphoid organs during pulmonary TB due to proliferation and influx of recruited myeloid and lymphoid cells. Recruitment of EcoNDK-infected cells, or increased viral replication in already infected tissue-resident cells, may help explain the increased viral load we observed in our Mtb/EcoNDK co-infection model.

Discussion

Mtb/HIV-1 co-infection poses an immense public health problem and involves two deadly pathogens for which there are no efficient vaccines available. For successful vaccine development, we need to understand what constitutes protective host immunity so that we can induce it in healthy individuals. Clearly, there are gaps in our knowledge of how the immune system can control Mtb- and HIV-1 infections, and even more to elucidate when it comes to controlling Mtb/HIV-1 co-infection.

A small animal model of Mtb/HIV-1 co-infection would be a useful tool to investigate innate and adaptive immune responses *in vivo*. However, mice are not natural hosts for Mtb or HIV-1 and there are several arguments against a successful rodent model of co-infection. Even though cell surface expression of human CD4 molecules and an additional co-receptor will enable HIV-1 to enter non-human cells, additional factors that are missing in murine cells are needed for efficient production of infectious viral particles (13-17). One example is the cyclin T1 protein that supports HIV-1 Tat function and viral transcription. Murine cyclin T1 does not mediate Tat function, which reduces the ability of murine cells to produce the virus (30-32). Additional post-transcriptional defects and a block in viral assembly have been suggested to further reduce the yield of HIV-1 production in murine cells (13, 33, 34). Despite these limitations, a murine model of HIV-1 infection has been described. Potash et al reported that the chimeric viruses EcoHIV and EcoNDK infect T cells and macrophages in naïve WT mice and that a single injection of the viruses causes systemic and persistent infection, for example neuroinvasiveness. Also, the virus is immunogenic and a humoral immune response is mounted towards viral proteins, including the formation of Gag- and Tat-specific antibodies, and it induces gene expression of the complement component C3, IL-1, MCP-1, and STAT-1 (9). The chimeric virus may be useful in translational research and has been used in HIV-1 vaccine challenge studies and for preclinical evaluation of anti-retroviral drugs (35, 36). Therefore, we combined EcoNDK with the murine model of pulmonary TB to establish Mtb/EcoNDK co-infection that enabled us to start addressing basic immunological questions regarding the Mtb-specific T cell response in an *in vivo* setting (10).

In contrast to Mtb/HIV-1 co-infected patients, an advantage with the animal model is that we exactly know when co-infection was established. This allowed us to investigate the PD-1/Tim3 expression profile and the functional potential of TB10.4-specific CD8⁺ T cell at an early stage of co-infection (figures 5-6). During pulmonary TB, cross-linking of the Tim3 ligand galectin-9 (Gal9) *in vivo*, and on Mtb-infected macrophages *in vitro*, reduce Mtb growth in a murine model (37). From these observations, Tim3 has been suggested to activate Mtb-infected macrophages via interaction with Gal9 and at the same time inhibit T cell function to prevent excessive Th1-mediated inflammation and prevent immunopathology in the infected lungs (37). Similarly, PD1 inhibits T cell function, and Mtb-infected PD1-deficient mice display exacerbated disease progression, including increased levels of pro-

inflammatory cytokines in the infected lungs, inability to control bacterial growth and premature death (38, 39). As markers of exhaustion, PD1 and Tim3 are expressed by essentially non-overlapping T cell subsets in HIV-1-infected patients, suggesting that multiple mechanisms are responsible for T cell exhaustion during HIV-1/AIDS (4-6). Regulation of host immune responses during chronic infections via inhibitory receptor/ligand interactions illustrates the delicate balance between pro-inflammatory effector functions that will reduce microbial replication, and tolerogenic mechanisms needed to prevent tissue damage and loss of function of the affected organs, such as the lung tissue.

Disease progression in low-dose Mtb aerosol-infected mice is in many important respects similar to human disease. For example, lung pathology progresses gradually over time similar, the bacteria disseminate from the lung tissue, but the pathology in other infected organs is not as dramatic, and in both immuno-compromised humans and mice disease progress much faster. Susceptibility to Mtb in inbred WT mice is characterized by excessive lung inflammation. The murine model of pulmonary TB has been used by us to study the immune response against Mtb and to increase our understanding of what constitutes protective immunity in resistant mouse strains (C57BL/6 and BALB/c) compared to highly susceptible mice (DBA/2) (10). We found that lymphoid and myeloid cells that may be important in controlling the inflammatory response during pulmonary TB are markedly reduced, or even missing, in the lungs of susceptible animals (10). Figure 6 shows IFN- γ and TNF production by Tim-3⁻ and Tim-3⁺CD8⁺ T cells isolated from the lungs of Mtb-infected, or co-infected mice. TB10.4-stimulated Tim-3⁺CD8⁺ T cells were clearly enriched for cytokine-producing cells during this early stage of Mtb/EcoNDK co-infection. In addition, co-infected mice seemed to contain an elevated frequency of TB10.4-reactive CD8⁺ T cells in the lungs compared to mice infected with Mtb alone (figure 4), and Mtb-specific CD8⁺ T cells were enriched for Tim-3 expressing cells (figure 5). Taken together, the results implied increased immune activation during the early stage of Mtb/EcoNDK co-infection in our murine model. Therefore, we tested if EcoNDK would accelerate disease progression in Mtb-susceptible DBA/2 mice (figure 2). Even though co-infected DBA/2 mice did not display weight loss within the study period, and were not less able to control bacterial replication, we did observe a qualitative difference in the cytokine profile of TB10.4-reactive CD8⁺ T cells. TB10.4-reactive CD8⁺ T cells in DBA/2 lungs contained a lower frequency of TNF⁺IFN- γ ⁺ cells than TB10.4-reactive CD8⁺ T cells isolated from the lungs of BALB/c mice. However, this observation was not dependent on the presence of the chimeric virus and was also seen in Mtb-infected animals (data not shown).

An important aspect of HIV-1 infection is T cell exhaustion. Further investigations during later stages of co-infection are needed to determine if Mtb- or EcoNDK-specific T cells acquire an exhausted phenotype in our murine model. Also, we report increased viral replication in animals co-infected with Mtb (figure 7). How viral-specific host immune responses are affected during Mtb/EcoNDK co-infection also needs to be determined.

Acknowledgments

MS was supported by grants from The Swedish Research Council, The Swedish Heart-Lung Foundation, Stiftelsen Clas Groschinskys Minnesfond and Karolinska Institutet. CL was supported by a scholarship from the Royal Thai Government and LI was the recipient of a Marie-Curie Host Fellowship for Early Stage Researchers Training grant. CL and LI also received support from Stiftelsen Sigurd och Elsa Goljes Minne.

We are grateful to Dr. Markus Maeurer and Lalit Rane, Karolinska Institutet, and the staff of the Astrid Fagraeus Laboratory, Karolinska Institutet, for their help in facilitating these experiments, and to Dr. David J. Volsky, Columbia University, New York, NY, for his help in establishing the Mtb/EcoNDK co-infection model.

References

1. A. Pawlowski, M. Jansson, M. Skold, M. E. Rottenberg, G. Kallenius, Tuberculosis and HIV Co-Infection. *PLoS Pathog* **8**, e1002464 (Feb, 2012).
2. T. Tian, J. Woodworth, M. Skold, S. M. Behar, In vivo depletion of CD11c+ cells delays the CD4+ T cell response to Mycobacterium tuberculosis and exacerbates the outcome of infection. *J Immunol* **175**, 3268 (Sep 1, 2005).
3. A. Khaitan, D. Unutmaz, Revisiting immune exhaustion during HIV infection. *Curr HIV/AIDS Rep* **8**, 4 (Mar, 2011).
4. C. L. Day *et al.*, PD-1 expression on HIV-specific T cells is associated with T-cell exhaustion and disease progression. *Nature* **443**, 350 (Sep 21, 2006).
5. L. Trautmann *et al.*, Upregulation of PD-1 expression on HIV-specific CD8+ T cells leads to reversible immune dysfunction. *Nat Med* **12**, 1198 (Oct, 2006).
6. R. B. Jones *et al.*, Tim-3 expression defines a novel population of dysfunctional T cells with highly elevated frequencies in progressive HIV-1 infection. *J Exp Med* **205**, 2763 (Nov 24, 2008).
7. L. Monney *et al.*, Th1-specific cell surface protein Tim-3 regulates macrophage activation and severity of an autoimmune disease. *Nature* **415**, 536 (Jan 31, 2002).
8. X. Wang *et al.*, Elevated expression of Tim-3 on CD8 T cells correlates with disease severity of pulmonary tuberculosis. *J Infect* **62**, 292 (Apr, 2011).
9. M. J. Potash *et al.*, A mouse model for study of systemic HIV-1 infection, antiviral immune responses, and neuroinvasiveness. *Proc Natl Acad Sci U S A* **102**, 3760 (Mar 8, 2005).
10. C. Leepiyasakulchai, L. Ignatowicz, A. Pawlowski, G. Kallenius, M. Skold, Failure To Recruit Anti-Inflammatory CD103+ Dendritic Cells and a Diminished CD4+ Foxp3+ Regulatory T Cell Pool in Mice That Display Excessive Lung Inflammation and Increased Susceptibility to Mycobacterium tuberculosis. *Infect Immun* **80**, 1128 (Mar, 2012).
11. A. Boberg *et al.*, Murine models for HIV vaccination and challenge. *Expert review of vaccines* **7**, 117 (Feb, 2008).
12. J. Nitkiewicz *et al.*, Productive infection of primary murine astrocytes, lymphocytes, and macrophages by human immunodeficiency virus type 1 in culture. *Journal of neurovirology* **10**, 400 (Dec, 2004).
13. P. D. Bieniasz, B. R. Cullen, Multiple blocks to human immunodeficiency virus type 1 replication in rodent cells. *J Virol* **74**, 9868 (Nov, 2000).
14. H. Choe *et al.*, The beta-chemokine receptors CCR3 and CCR5 facilitate infection by primary HIV-1 isolates. *Cell* **85**, 1135 (Jun 28, 1996).

15. B. J. Doranz *et al.*, A dual-tropic primary HIV-1 isolate that uses fusin and the beta-chemokine receptors CKR-5, CKR-3, and CKR-2b as fusion cofactors. *Cell* **85**, 1149 (Jun 28, 1996).
16. H. Deng *et al.*, Identification of a major co-receptor for primary isolates of HIV-1. *Nature* **381**, 661 (Jun 20, 1996).
17. T. Dragic *et al.*, HIV-1 entry into CD4+ cells is mediated by the chemokine receptor CC-CKR-5. *Nature* **381**, 667 (Jun 20, 1996).
18. J. L. Flynn, M. M. Goldstein, K. J. Triebold, B. Koller, B. R. Bloom, Major histocompatibility complex class I-restricted T cells are required for resistance to Mycobacterium tuberculosis infection. *Proc Natl Acad Sci U S A* **89**, 12013 (Dec 15, 1992).
19. S. M. Behar, C. C. Dascher, M. J. Grusby, C. R. Wang, M. B. Brenner, Susceptibility of mice deficient in CD1D or TAP1 to infection with Mycobacterium tuberculosis. *J Exp Med* **189**, 1973 (1999).
20. L. Majlessi, M. J. Rojas, P. Brodin, C. Leclerc, CD8+-T-cell responses of Mycobacterium-infected mice to a newly identified major histocompatibility complex class I-restricted epitope shared by proteins of the ESAT-6 family. *Infect Immun* **71**, 7173 (Dec, 2003).
21. R. L. Skjot *et al.*, Comparative evaluation of low-molecular-mass proteins from Mycobacterium tuberculosis identifies members of the ESAT-6 family as immunodominant T-cell antigens. *Infect Immun* **68**, 214 (Jan, 2000).
22. A. Kamath, J. S. Woodworth, S. M. Behar, Antigen-specific CD8+ T cells and the development of central memory during Mycobacterium tuberculosis infection. *J Immunol* **177**, 6361 (Nov 1, 2006).
23. J. Duraiswamy *et al.*, Phenotype, function, and gene expression profiles of programmed death-1(hi) CD8 T cells in healthy human adults. *J Immunol* **186**, 4200 (Apr 1, 2011).
24. A. M. Cooper *et al.*, Disseminated tuberculosis in interferon gamma gene-disrupted mice. *J Exp Med* **178**, 2243 (Dec 1, 1993).
25. J. L. Flynn *et al.*, An essential role for interferon gamma in resistance to Mycobacterium tuberculosis infection. *J Exp Med* **178**, 2249 (Dec 1, 1993).
26. J. L. Flynn *et al.*, Tumor necrosis factor-alpha is required in the protective immune response against Mycobacterium tuberculosis in mice. *Immunity* **2**, 561 (Jun, 1995).
27. J. Keane *et al.*, Tuberculosis associated with infliximab, a tumor necrosis factor alpha-neutralizing agent. *N Engl J Med* **345**, 1098 (Oct 11, 2001).
28. D. Lopez-Maderuelo *et al.*, Interferon-gamma and interleukin-10 gene polymorphisms in pulmonary tuberculosis. *Am J Respir Crit Care Med* **167**, 970 (Apr 1, 2003).
29. M. J. Newport *et al.*, A mutation in the interferon-gamma-receptor gene and susceptibility to mycobacterial infection. *N Engl J Med* **335**, 1941 (Dec 26, 1996).

30. P. D. Bieniasz, T. A. Grdina, H. P. Bogerd, B. R. Cullen, Recruitment of a protein complex containing Tat and cyclin T1 to TAR governs the species specificity of HIV-1 Tat. *The EMBO journal* **17**, 7056 (Dec 1, 1998).
31. K. Fujinaga, R. Taube, J. Wimmer, T. P. Cujec, B. M. Peterlin, Interactions between human cyclin T, Tat, and the transactivation response element (TAR) are disrupted by a cysteine to tyrosine substitution found in mouse cyclin T. *Proc Natl Acad Sci U S A* **96**, 1285 (Feb 16, 1999).
32. M. E. Garber *et al.*, The interaction between HIV-1 Tat and human cyclin T1 requires zinc and a critical cysteine residue that is not conserved in the murine CycT1 protein. *Genes & development* **12**, 3512 (Nov 15, 1998).
33. R. Mariani *et al.*, A block to human immunodeficiency virus type 1 assembly in murine cells. *J Virol* **74**, 3859 (Apr, 2000).
34. J. X. Zhang, G. E. Diehl, D. R. Littman, Relief of preintegration inhibition and characterization of additional blocks for HIV replication in primary mouse T cells. *PLoS One* **3**, e2035 (2008).
35. E. Hadas *et al.*, Testing antiretroviral drug efficacy in conventional mice infected with chimeric HIV-1. *Aids* **21**, 905 (May 11, 2007).
36. Y. Roshorm *et al.*, Novel HIV-1 clade B candidate vaccines designed for HLA-B*5101(+) patients protected mice against chimaeric ecotropic HIV-1 challenge. *Eur J Immunol* **39**, 1831 (Jul, 2009).
37. P. Jayaraman *et al.*, Tim3 binding to galectin-9 stimulates antimicrobial immunity. *J Exp Med* **207**, 2343 (Oct 25, 2010).
38. E. Lazar-Molnar *et al.*, Programmed death-1 (PD-1)-deficient mice are extraordinarily sensitive to tuberculosis. *Proc Natl Acad Sci U S A* **107**, 13402 (Jul 27, 2010).
39. S. Tousif *et al.*, T cells from Programmed Death-1 deficient mice respond poorly to *Mycobacterium tuberculosis* infection. *PLoS One* **6**, e19864 (2011).

Figure legends

Figure 1. EcoNDK infects primary murine cells in vitro. Murine splenocytes were stimulated with ConA and IL-2 for 4-5 days and then infected with the EcoNDK virus as outlined below. The cells were harvested after 72 h and analyzed for specific cell surface markers and intracellular p24 protein. (A) Stimulated cells were infected directly with concentrated EcoNDK virus, or co-cultured with transfected 293T cells separated by a 0.45 μm filter. (B) The stimulated spleen cells were co-cultured directly together with non-transfected (upper left panel) or transfected 293T cells (upper right panel and lower panels). The lower panels show p24 expression on gated $\text{CD45.2}^+\text{CD19}^-$ cells. (C) The left panel shows p24 expression in transfected 293T cells and a representative isotype control staining is displayed in the right panel. Representative plots of two independent experiments are shown. The gates were set after relevant isotype control mAbs.

Figure 2. Change in body mass and bacterial load during pulmonary TB and during Mtb/EcoNDK co-infection. BALB/c and DBA/2 mice were infected with a low dose of Mtb via the respiratory route. Three weeks later, groups of mice were co-infected with EcoNDK IP (dashed line). The weight of the mice was determined weekly over the course of the experiment. The mean percent change of body weight ($\pm\text{SEM}$) is shown in (A). Groups of mice were sacrificed two weeks after virus injection and the bacterial load was enumerated in lung homogenates (B). The bacterial load in the lungs of individual mice is shown with mean lung CFU values shown as a solid line in. Statistical significant differences between the groups were calculated using non-paired *t*-test.

Figure 3. Mtb-specific CD8^+ T cells in Mtb-infected susceptible and resistant mice. (A) CD8^+ T cells specific for an Mtb-derived TB10.4-peptide presented by H-2K^d were identified in uninfected and Mtb-infected lung tissue. H-2K^d/TB10.4-specific CD8^+ T cells were not detected in naïve BALB/c or DBA/2 mice (data not shown), or in Mtb-infected H-2^b-expressing C57BL/6 mice. (B) The absolute number of TB10.4-specific CD8^+ T cells was reduced in the lungs of susceptible DBA/2 mice compared to resistant BALB/c mice 4 to 12 pi. The graphs display mean \pm SEM. Mtb-specific CD8^+ T cells were enumerated and characterized in five separate experiments with 2-3 mice per group in each experiment.

Figure 4. Increased levels of Mtb-specific CD8⁺ T cells in the lungs and in the spleen of Mtb/EcoNDK co-infected BALB/c mice. Using the same gating strategy as in figure 3, total CD4⁺ T cells, total CD8⁺ T cells and TB10.4-specific CD8⁺ T cells were identified in the lungs and in the spleen two weeks post EcoNDK infection (week five post Mtb infection). (A) The graphs display the absolute number of CD4⁺- and CD8⁺ T cells in the lungs (left panel) and in the spleen (right panel) of Mtb/EcoNDK co-infected and Mtb-infected animals. (B) The graphs show the percentage and absolute number of TB10.4-specific CD8⁺ T cells in the lungs (left panel) and in the spleen (right panel) of Mtb/EcoNDK co-infected and Mtb-infected animals. (C) The bar graph display the mean fluorescence intensity of the H-2K^d/TB10.4-multimer cell surface staining on CD8⁺ T cells in the lungs and spleen of Mtb/EcoNDK co-infected and Mtb-infected mice. The graphs display mean \pm SEM. A *t*-test was used to determine statistical difference between Mtb-infected and Mtb/EcoNDK co-infected animals (*, *p* < 0.05). Filled bars = EcoNDK/Mtb co-infected animals; open bars = Mtb-infected animals.

Figure 5. Different Tim3 and PD1 expression profiles on CD4⁺ and CD8⁺ T cell subsets in infected BALB/c mice. To examine the Tim3 and PD1 expression profiles on T cell subsets, total lung- and spleen cells were prepared from Mtb-infected and Mtb/EcoNDK co-infected BALB/c mice two weeks post EcoNDK infection (week five post Mtb infection). (A) The pseudo-color contour plots show representative Tim3 and PD1 cell surface stainings on gated total CD4⁺ T cells, total CD8⁺ T cells and CD8⁺ T cells divided into the H-2K^d/TB10.4-multimer-positive and H-2K^d/TB10.4-multimer-negative subsets from a Mtb/EcoNDK co-infected mouse. (B-C) The graphs illustrate the percentage and absolute number of gated T cells that express Tim3, PD1 or both Tim3 and PD1 in the lungs (B) and in the spleen (C). Graphs display mean \pm SEM. Mtb-infected mice are represented by open bars and Mtb/EcoNDK co-infected mice by filled bars.

Figure 6. Cytokine production by antigen-specific Tim3⁻ and Tim3⁺ CD8⁺ T cells during pulmonary TB and during the early stage of Mtb/EcoHIV co-infection. BALB/c mice were infected with Mtb via the respiratory route. Three weeks pi, groups of mice were injected with EcoNDK IP. Lung cells were analyzed after an addition two weeks. The cytokine profile of Mtb-specific Tim3⁻ and Tim3⁺ CD8⁺ T cells in the lungs was analyzed after TB10.4-peptide stimulation in vitro (D-E). For comparison, the cytokine profile of polyclonally stimulated CD4⁺ and CD8⁺ T cells in the lungs was included in the analysis (A-C). (A) The pseudo-color plots show identification of Tim3⁺ and Tim3⁻ cells on pre-gated CD4⁺- and CD8⁺ T cells from a Mtb/EcoNDK co-infected mouse (left panels). The middle panels display intracellular TNF and IFN- γ production by Tim3⁺ and Tim3⁻ cells after PMA

and ionomycin stimulation. Cytokine production by cells kept in media alone is shown in the right panels. All gates were set after relevant isotype control mAbs (data not shown). (B-C) The graphs show the percentage of cytokine producing CD4⁺ (B) and CD8⁺ T cells (C) after polyclonal stimulation. The T cell populations were further divided into Tim3⁻ and Tim3⁺ cells as indicated. (D) The plot shows identification of Tim3⁻ and Tim3⁺ cells on pre-gated CD8⁺ T cells from a Mtb/EcoNDK co-infected mouse (left panel). Intracellular TNF and IFN- γ production by Tim3⁺ and Tim3⁻ cells are shown in the middle panels. The cells were stimulated with a TB10.4-peptide or kept in media alone as indicated. The right panels show isotype control stainings for the anti-TNF and anti-IFN- γ mAbs. (E) The graphs display the cytokine profile of Tim3⁺CD8⁺ T cells (left panel) and Tim3⁻CD8⁺ T cells (right panel) after TB10.4-peptide stimulation. The graphs display mean \pm SEM. Filled bars = EcoNDK/Mtb co-infected mice; open bars = Mtb-infected mice.

Figure 7. Increased viral load in Mtb/EcoNDK co-infected mice. Three weeks post Mtb aerosol infection, groups of BALB/c mice were injected once IP with EcoNDK. For comparison, naïve mice were infected with ecoNDK alone. DNA from the lungs and spleen was isolated two weeks after virus infection and the number of EcoNDK gag gene copies in relation to the GAPDH gene was enumerated by QPCR as described in Materials and Methods. The results presented in the graphs have been pooled from five separate co-infection experiments and from two separate experiments where the mice were infected with EcoNDK alone. Animals that were injected with the virus, but displayed the same, or lower EcoNDK DNA levels than the negative controls, i.e. Mtb-infected mice, naïve mice and blank samples, were considered EcoNDK non-infected and excluded from the study. Statistical significance was determined using a non-paired *t*-test (*, $p < 0.05$).

Figure 1

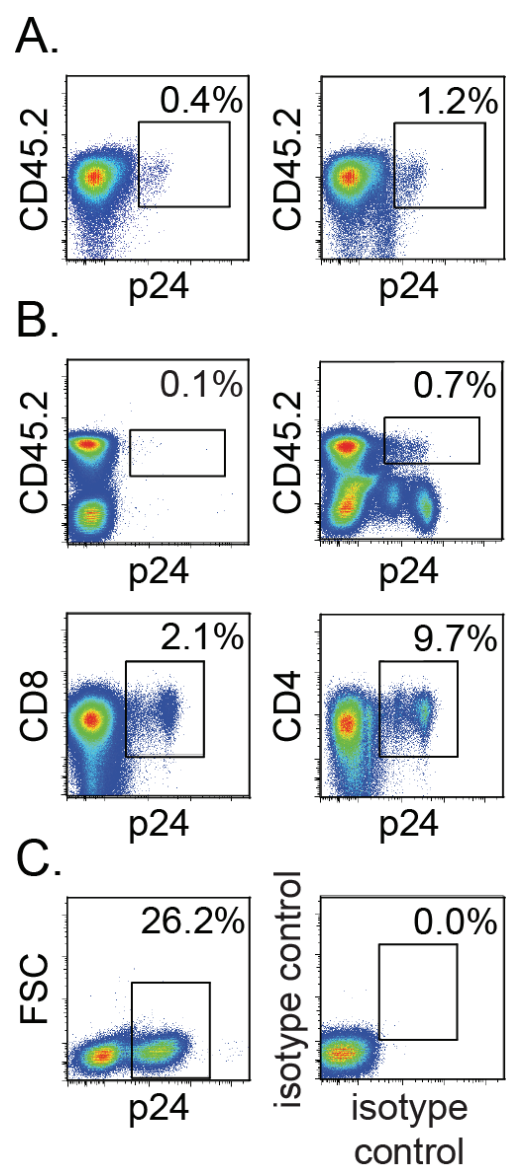


Figure 2

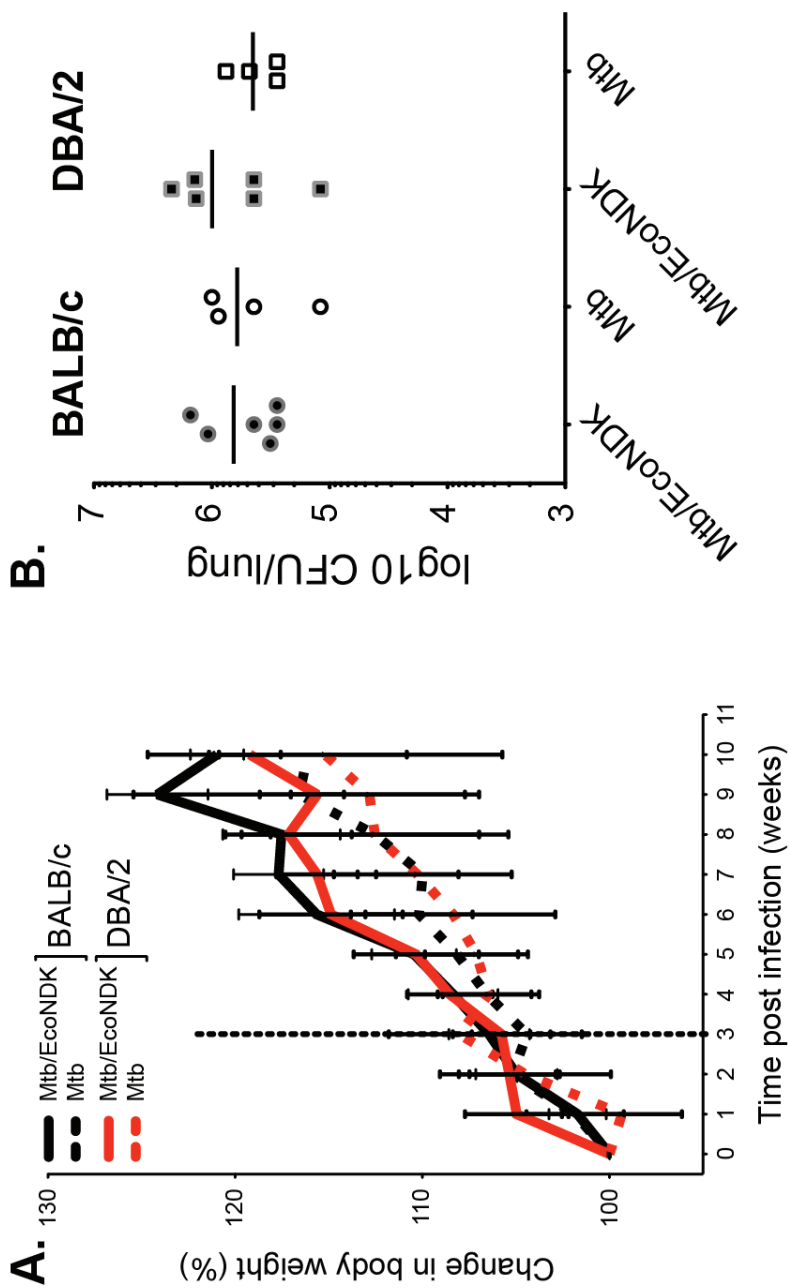


Figure 3

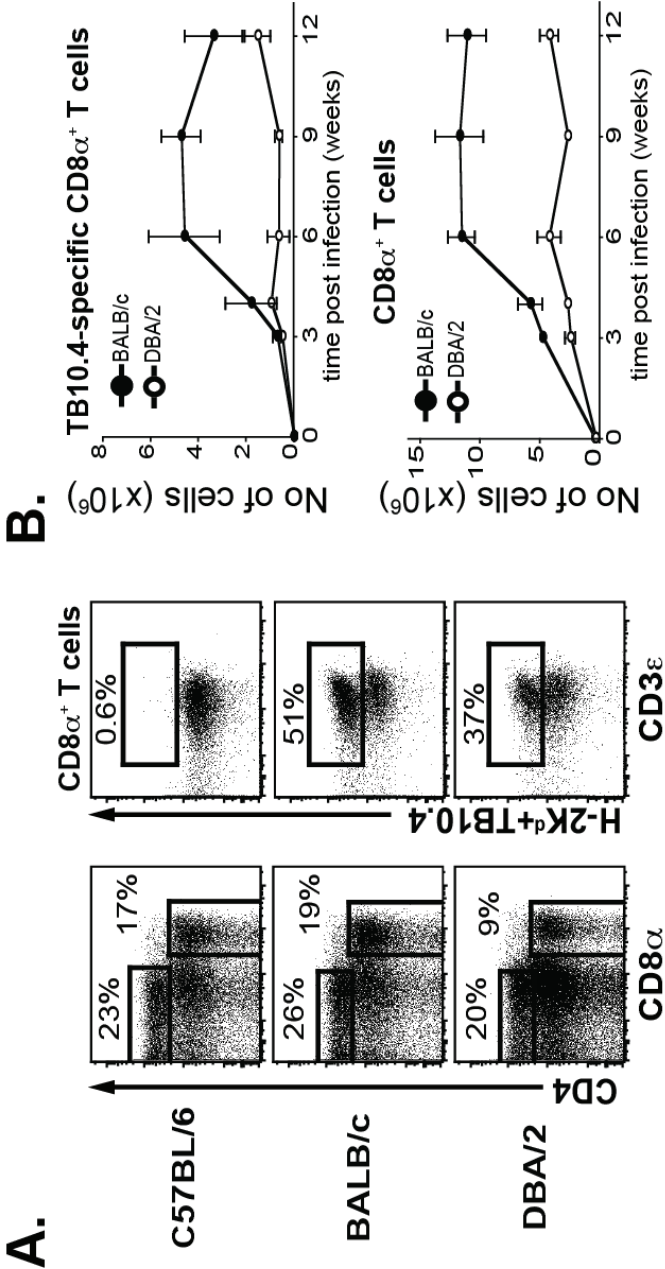


Figure 4

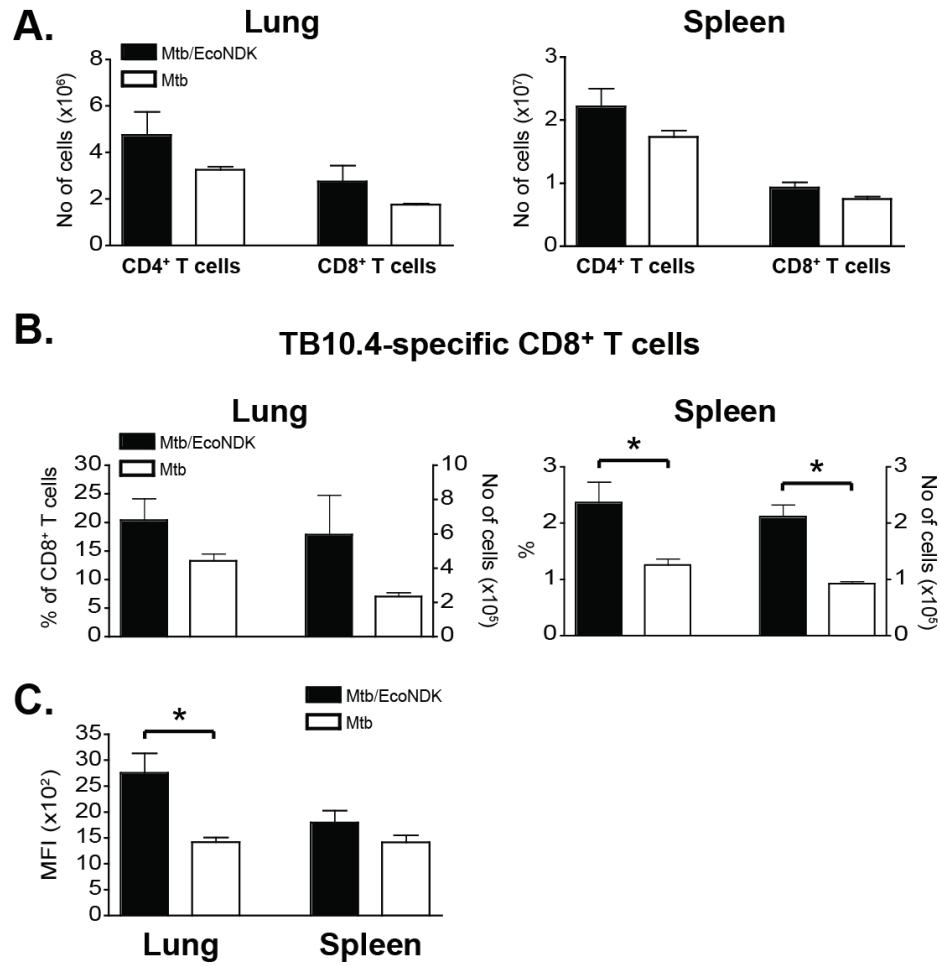


Figure 5

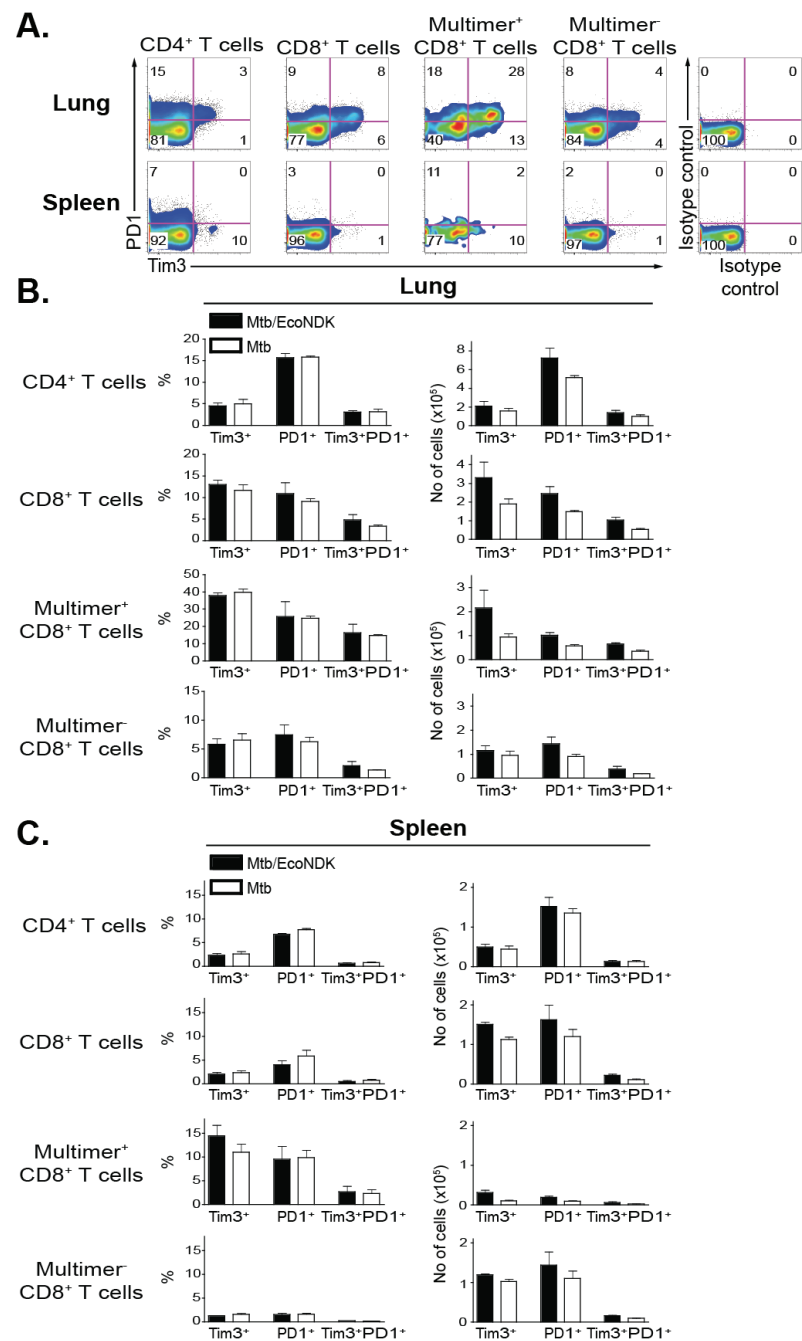


Figure 6

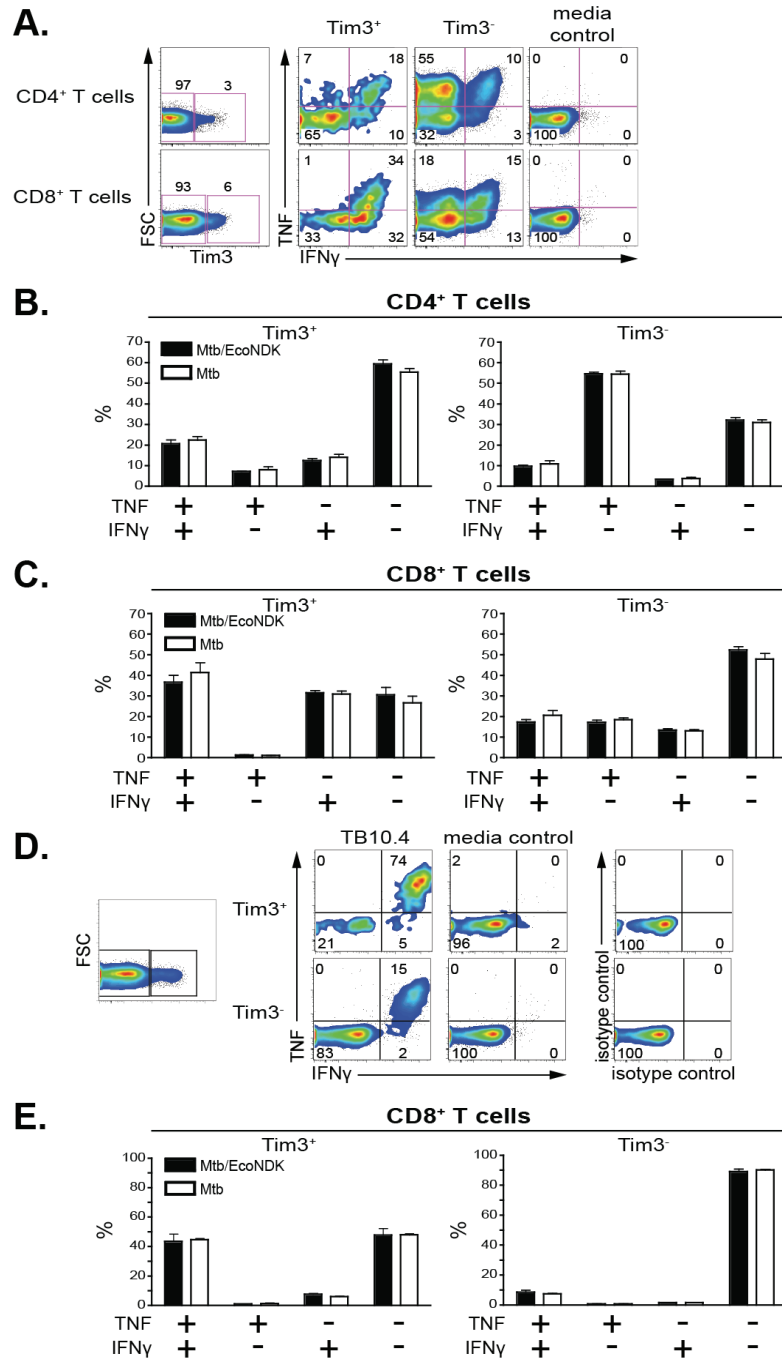
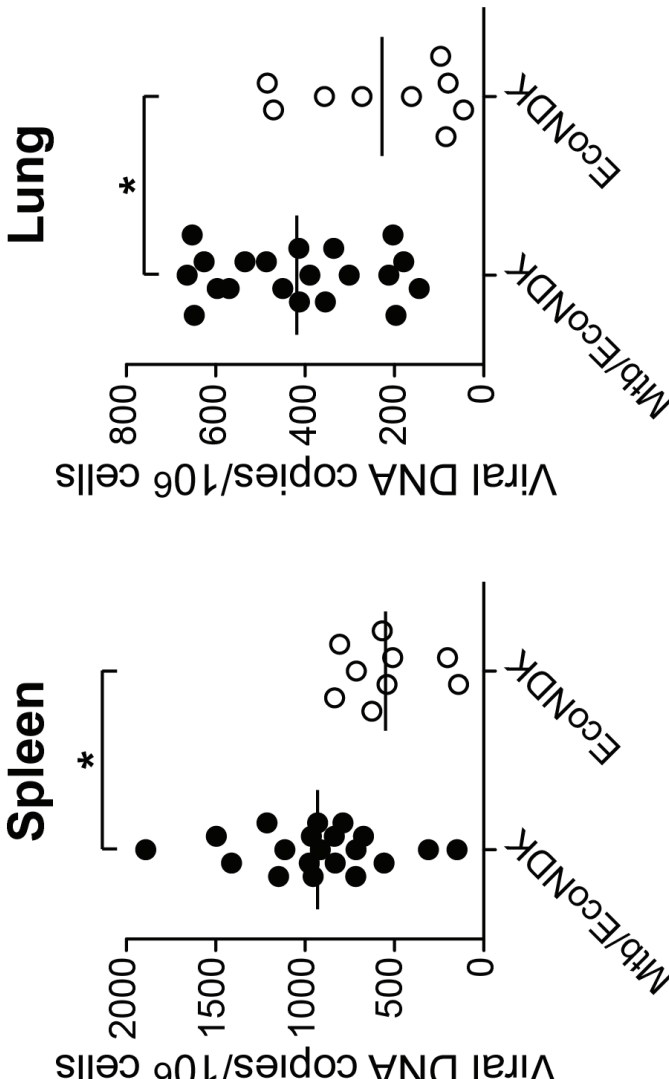


Figure 7





Department of Microbiology, Tumor and Cell Biology

Immune regulation during pulmonary TB and during M. tuberculosis/HIV-1 co-infection

AKADEMISK AVHANDLING

som för avläggande av medicine doktorsexamen vid
Karolinska Institutet offentligen försvaras i
Petrén, Nobels väg 12B, Solna

Torsdag den 26 september, 2013, kl 09.00

av

Chaniya Leepiyasakulchai, M.Sc.

Huvudhandledare:

Markus Sköld, PhD
Karolinska Institutet
Department of Microbiology, Tumor and Cell
Biology

Bihandledare:

Prof. Markus Maeurer, MD, PhD
Karolinska Institutet
Therapeutic Immunology (TIM)
Department of Laboratory Medicine

Prof. Hans Wigzell, MD, PhD
Karolinska Institutet
Department of Microbiology, Tumor and Cell
Biology

Fakultetsopponent:

Prof. T. Mark Doherty, PhD
University of Bergen, Norway
Institute for International Health
Faculty of Medicine

Betygsnämnd:

Prof. Anders Lindén, MD, PhD
Karolinska Institutet
The Institute of Environmental Medicine

Docent Benedict Chambers, PhD
Karolinska Institutet
Center of Infectious Medicine (CIM)
Department of Medicine

Docent Helena Aro, PhD
Stockholm University,
Department of Genetics, Microbiology and
Toxicology

Stockholm 2013

ABSTRACT

Individually, tuberculosis (TB) and acquired immunodeficiency syndrome (AIDS) pose major global health problems and together, they form a deadly liaison. Preventive vaccines for any of the diseases are not yet available. Therefore, better understanding of protective immunity to each pathogen that cause the diseases and how co-infection influences host immune responses are urgently needed. The overall aim of this thesis was to increase our understanding of immune regulation and protective immune responses during pulmonary TB and during *Mycobacterium tuberculosis* (Mtb)/ human immunodeficiency virus-1 (HIV-1) co-infection in the mouse model.

In **study I**, we explored CD103⁺ dendritic cell (α E-DC) and CD4⁺Foxp3⁺ regulatory T (Treg) cell function during pulmonary TB. We showed that in mice resistant to Mtb infection the number of α E-DCs increased dramatically in response to Mtb infection. In contrast, highly susceptible mice failed to recruit α E-DCs even during chronic infection. Instead of producing TNF α , α E-DCs preferentially produced TGF β . In contrast to resistant mice, the Treg cell population was diminished in the lungs, but not in the draining pulmonary lymph node (PLN) of highly susceptible DBA/2 mice during chronic infection. Further, we showed that Treg cells produced IFN γ in response to infection with a virulent clinical Mtb isolate. The reduced number of lung α E-DCs and Treg cells in susceptible mice coincided with severe lung inflammation and increased bacterial burden. Our results indicated that α E-DCs and Treg cells may play a role in regulating the host immune response during pulmonary TB.

In **study II**, we further investigated the origin, tissue localization, infection rate and cytokine profile of α E-DCs during pulmonary TB. We showed that alveolar epithelial cells support monocyte survival and differentiation *in vitro*. We demonstrated that bone marrow-derived monocytes were precursors of α E-DCs in the lungs and PLN during pulmonary TB. We confirmed the localization of α E-DCs beneath the bronchial epithelial cell layer and near the vascular wall during steady state conditions, and showed that α E-DCs had a similar localization in the lungs during pulmonary TB. In addition, α E-DCs were detected in the bronchoalveolar lavage during the infection. In contrast to other DC subsets, we found that only a minor fraction of lung α E-DCs was infected with the bacterium. We also showed that virulent Mtb did not significantly alter the cell surface expression level of MHC II on infected cells *in vivo* and that α E-DCs contain the highest frequency of IL-12p40⁺ cells among the myeloid cell subsets in infected lungs. Our results support a model in which inflammatory monocytes are recruited into the Mtb-infected lung tissue and, depending on which non-hematopoietic cells they interact with, differentiate along different paths to give rise to multiple monocyte-derived cells, including DC with a distinctive α E-DCs phenotype.

In **study III**, we determined the impact of chronic Mtb infection on the immunogenicity of a HIV vaccine candidate. We found that, depending on the vaccination route, Mtb-infected mice displayed impairment in both the magnitude and in the quality of both antibody- and T cell responses to the vaccine components p24Gag and gp160Env. Mtb-infected and HIV-vaccinated mice exhibited reduced p24Gag-specific serum IgG and IgA titers, and suppressed gp160Env-specific serum IgG titers compared to uninfected HIV-1-vaccinated controls. Importantly, the virus neutralizing activity in serum of intramuscular HIV-vaccinated Mtb-infected mice was significantly decreased relative to the uninfected controls. In addition mice concurrently infected with Mtb had fewer p24Gag-specific IFN γ -expressing T cells and multifunctional T cells in the spleen. These results suggested that Mtb infection may interfere with the effectiveness of HIV vaccines in humans.

In **study IV**, we established a mouse model for Mtb/HIV-1 co-infection by utilizing the chimeric EcoNDK virus. During the time-course of the experiment, we did not detect signs of immunodeficiency. However, we confirmed that the virus was present in Mtb/EcoNDK co-infected mice at least 14 days after a single injection of the virus. In fact, the viral load was significantly higher in the lungs and in the spleen of Mtb/EcoNDK co-infected mice compared to animals infected with the virus alone. We showed that EcoNDK influence the adaptive T cell response directed towards the bacterium. We observed that the number of Mtb-specific CD8⁺ T cells was significantly increased in the spleen compared to Mtb-infected animals. Furthermore, we characterized the cell surface expression profile of T cell immunoglobulin and mucin domain-3 (Tim-3) and Program Death 1 (PD-1) on T cell subsets during TB and during Mtb/EcoNDK co-infection. Even though we did not detect any significant difference between Mtb-infected and co-infected mice, we did find that Tim-3 and PD-1 were utilized differently by CD4⁺ T cells and CD8⁺ T cell subsets. Finally, we showed that TB10.4-specific CD8⁺Tim-3⁺ T cells were enriched for both TNF α - and IFN γ -producing cells. Our murine co-infection model may be a useful tool to elucidate why pulmonary TB is such a problem in patients with HIV-1/AIDS.

© Chaniya Leepiyasakulchai, 2013

ISBN 978-91-7549-276-6